FINAL REPORT

DC Microgrid Building Energy Management Platform for Improved Energy Efficiency, Energy Security, and Operating Costs

ESTCP Project EW-201352

DECEMBER 2019

John Saussele
Bosch Building Grid Technologies

ESTCP

Page Intentionally Left Blank

Page Intentionally Left Blank

REPORT DOCUMENTATION PAGE

Form Approved
OMB No. 0704-0188

1. REPORT DATE *(DD-MM-YYYY)*	2. REPORT TYPE	3. DATES COVERED *(From - To)*
12/31/2019	ESTCP Final Report	3/7/2014 - 3/31/2018

4. TITLE AND SUBTITLE
DC Microgrid Building Energy Management Platform for Improved Energy Efficiency, Energy Security, and Operating Costs

5a. CONTRACT NUMBER
14-C-0001

5b. GRANT NUMBER

5c. PROGRAM ELEMENT NUMBER

6. AUTHOR(S)
John Saussele

5d. PROJECT NUMBER
EW-201352

5e. TASK NUMBER

5f. WORK UNIT NUMBER

7. PERFORMING ORGANIZATION NAME(S) AND ADDRESS(ES)
Bosch Building Grid Technologies
38000 Hills Tech Drive
Farmington Hills, MI 48331

8. PERFORMING ORGANIZATION REPORT NUMBER
EW-201352

9. SPONSORING/MONITORING AGENCY NAME(S) AND ADDRESS(ES)
Environmental Security Technology Certification Program
4800 Mark Center Drive, Suite 17D03
Alexandria, VA 22350-3605

10. SPONSOR/MONITOR'S ACRONYM(S)
ESTCP

11. SPONSOR/MONITOR'S REPORT NUMBER(S)
EW-201352

12. DISTRIBUTION/AVAILABILITY STATEMENT
DISTRIBUTION STATEMENT A. Approved for public release: distribution unlimited.

13. SUPPLEMENTARY NOTES

14. ABSTRACT
In this project, a building-scale DC microgrid was installed containing rooftop solar PV, commercial high-bay lighting, industrial ceiling fans, and battery energy storage. By avoiding conversions from DC to AC in the sources which create the electrical energy (solar) as well as from AC back to DC in the electrical load devices which utilize the energy (lights and fans), the objective of the project was to demonstrate improvements in efficiency, reliability, resiliency, and cost.

15. SUBJECT TERMS
DC Microgrid, Building Energy Management Platform, Energy Efficiency, Energy Security, Operating Costs

16. SECURITY CLASSIFICATION OF:			17. LIMITATION OF ABSTRACT	18. NUMBER OF PAGES	19a. NAME OF RESPONSIBLE PERSON
a. REPORT	b. ABSTRACT	c. THIS PAGE			John Saussele
UNCLASS	UNCLASS	UNCLASS	UNCLASS	285	19b. TELEPHONE NUMBER *(Include area code)* 704-799-0127

Page Intentionally Left Blank

FINAL REPORT
Project: EW-201352

TABLE OF CONTENTS

TABLE OF CONTENTS (Continued)

LIST OF FIGURES

Page

LIST OF TABLES

Page

ACRONYMS AND ABBREVIATIONS

AC	Alternating Current
BESS	Battery Energy Storage System
CALCE	Center for Advance Life Cycle Engineering
CAPEX	Capital Expenditure
DC	Direct Current
DCMG	Direct Current Microgrid
DoD	Department of Defense
DOE	Department of Energy
ESCO	Energy Services Company
ESTCP	Environmental Security Technology Certification Program
HID	High Intensity Discharge
kVA	Kilovolt-Ampere
kW	Kilowatts
kWh	Kilowatt-Hours
LED	Light Emitting Diode
MPPT	Maximum Power Point Tracking
MWh	Megawatt-Hours
NEC	National Electrical Code
NGLIA	Next Generation Lighting Industry Alliance
NREL	National Renewable Energy Labs
OPEX	Operational Expenditure
PLC	Power Line Communications
POE	Power Over Ethernet
PV	Photovoltaic
SSL	Solid State Lighting
VFD	Variable Frequency Drive
W	Watts

Page Intentionally Left Blank

ACKNOWLEDGEMENTS

The author would like to thank the ESTCP for the funding and support of this project as well the Fort Bragg Army Base for hosting the building-scale demonstration. Completion of this project represents a major step forward in validating the advantages of DC microgrids in terms of resiliency, energy efficiency, reliability, and cost. The Fort Bragg demonstration site was also the first of its kind to utilized existing building wiring, whereby outdated AC lighting fixtures were replaced one-for-one on standard lighting circuits with DC lighting fixtures in the same manner as a routine lighting upgrade, proving the viability of DC microgrids in phased retrofit as well as new construction applications. Without the support of the ESTCP and Fort Bragg, this important progress toward commercialization of DC building technologies would not have been possible.

Page Intentionally Left Blank

1.0 INTRODUCTION

1.1 BACKGROUND

Commercial and residential buildings account for approximately 40% of the nation's total energy demand [1] and 75% of electricity use [2], resulting in an annual national energy bill totaling roughly $415 billion [3]. In addition, the U.S. Department of Energy estimates that on average, power outages result in $80 billion per year in economic losses [4]. With 568,383 facilities and over 2.2 billion square feet of building space [5], the DoD is one of the largest real estate owners in the US. Any technology which improves DoD building energy efficiency while simultaneously increases resiliency to power outages can have a significant financial impact when applied over such a large portfolio, while simultaneously increasing national security. This project demonstrates the use of Direct Current (DC) technology for power distribution within commercial buildings, which increases energy efficiency while improving resiliency and also has significant reliability advantages, all of which contribute to overall lifetime cost savings when compared to conventional Alternating Current (AC) technology.

Requirements for electrical devices in buildings to operate on AC is largely historic, and results in wasted energy through many unnecessary conversions back and forth to DC within a building, as well as inherent resiliency and reliability limitations due to the additional conversion/switching devices needed to interoperate with the AC supplied from the utility grid. In addition, conventional rooftop solar photovoltaic (PV) systems all generate DC and incorporate utility grid connected DC to AC solar PV inverters which shut off during a power outage, eliminating the ability of the solar power to be utilized to improve resiliency during an emergency blackout situation. The use of DC power distribution within a building can result in significant lifetime cost savings in terms of increased energy efficiency, reduced maintenance costs by eliminating conversion electronics failures, as well as increased resiliency with the added ability to use the power generated from rooftop solar PV arrays during a power outage.

DC power technology has been available for more than a century, but was not practical or efficient for the nationwide utility grid architecture since there was a desire to transmit power at high voltage over long distances from large, centralized power plants. AC was ultimately chosen for this purpose due to the ability to step-up and step-down the voltage using simple wire-wound magnetic transformers, which was the only available technology at the time and required AC. However, when looking at the present electrical power profile within a building, several things now warrant revisiting DC on a local level: 1) the aggressive adoption of on-site DC generation sources such as rooftop solar PV; 2) advanced high-capacity batteries (inherently DC) being available in stationary energy storage systems; and 3) major technology changes in the typical devices which use electricity in a building, i.e. a transition to light-emitting diode (LED) lighting technology, motors operating with variable frequency drives (VFD), chargers for battery-operated devices/vehicles, and the ever-increasing use of servers and other information technology equipment, all of which natively operate on DC power. It is fair to say that all modern and efficient devices using electricity in a building are internally converting from AC to DC, and that all modern and efficient devices generating or storing electricity at a building level (solar arrays, batteries, rotational generators, fuel cells, etc.) utilize DC internally which is then converted to AC.

With the tremendous nationwide utility infrastructure investments made in the past, it can be assumed that that the transmission grid from central power plants to buildings will remain AC for the foreseeable future. However, for power distribution *within* the building, it is now worth reconsidering the use of DC. A system which distributes electrical power from local DC sources to the DC devices using electrical power (loads) has generally been referred to as a DC microgrid, and is typically a building-scale system. Figure 1 shows a high-level graphical comparison of a hypothetical building utilizing conventional AC technology vs. a building utilizing a DC microgrid for major local sources and loads. The green colors within the AC building in this diagram illustrates the "hidden" DC which actually exists in all modern building devices, and that enables the simplicity gained by connecting these devices together via a DC electrical distribution system as shown in the DC microgrid building. In the DC microgrid, the reduced need for electronics to convert DC to AC and AC to DC has a direct impact on energy efficiency as well as reliability over lifetime. Note that for illustrative purposes the figure only shows a building with 8 lights, however a larger commercial building could have hundreds or even thousands of lights, each having its own internal AC to DC converter in a conventional AC architecture.

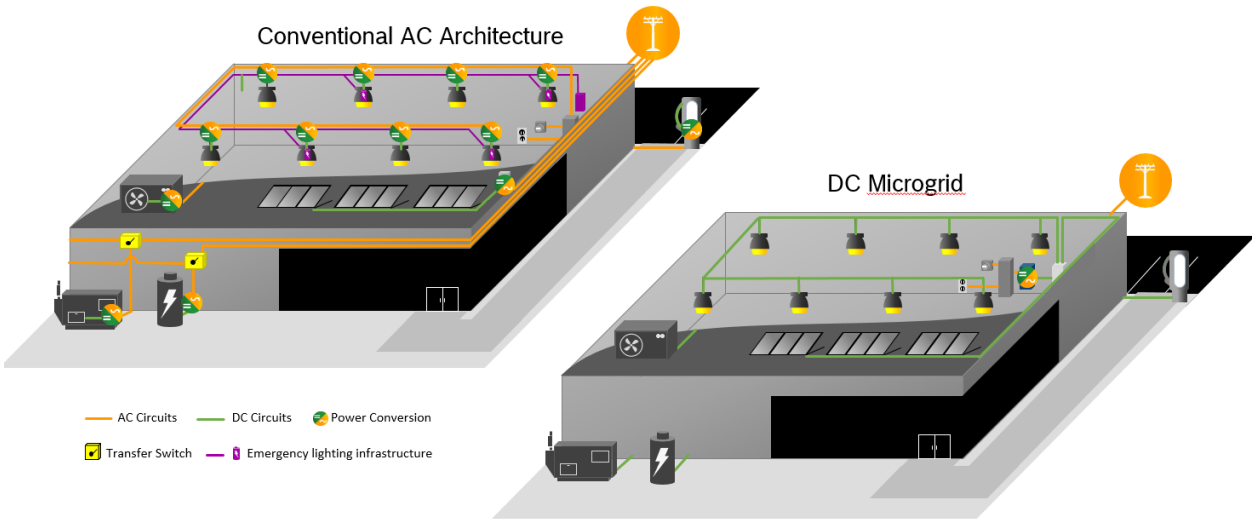

Figure 1. AC Complexity vs. DC Simplicity

1.2 OBJECTIVE OF THE DEMONSTRATION

In this project, a building-scale DC microgrid was installed containing rooftop solar PV, commercial high-bay lighting, industrial ceiling fans, and battery energy storage. By avoiding conversions from DC to AC in the sources which create the electrical energy (solar) as well as from AC back to DC in the electrical load devices which utilize the energy (lights and fans), the objective of the project was to demonstrate improvements in efficiency, reliability, resiliency, and cost. Beyond the single building demonstration, the overarching objective was to prove that building-scale DC microgrids not only have many advantages over traditional AC technology, but can also be implemented cost effectively as a phased retrofit as well as in new construction. A phased retrofit of an existing building could especially makes sense when coordinated with other building energy upgrades such as the transition to LED lighting or the addition of rooftop solar arrays. The benefits of utilizing DC power distribution exist for all sources of power located locally at the building.

Solar PV was chosen for the demonstration since it is the fastest-growing distributed power source as well as being renewable and deployable on existing buildings. Lighting was chosen since it is a major power load in all buildings, and retrofit energy efficient lighting upgrades are constantly occurring in older buildings, offering the perfect opportunity to consider DC lighting as an alternative. Industrial ceiling fans were chosen primarily to prove that DC can also be effectively utilized in motor loads.

1.3 REGULATORY DRIVERS

Large-scale deployment of distributed energy generation such as commercial rooftop solar PV can only be achieved when these building assets provide attractive returns to their owners while also allowing utilities the capability to safely and reliably mitigate the impact of intermittency on the distribution infrastructure. This is due to the fact that conventional solar PV systems are AC connected and designed to feed excess solar energy into the utility grid, which it was not originally designed to handle. To compound this stress on the grid infrastructure, peak solar power will typically hit a group of buildings in one area at the same time. According to the National Renewable Energy Laboratory (NREL), most US jurisdictions limit solar PV penetration to 15% of peak load, after which utility grid interconnections are either strictly limited or only allowed after an expensive impact study. Since Hawaii cannot share excess power with neighboring states, this limit is already manifesting itself and Hawaii is severely restricting AC grid-connected solar installations. With its very high adoption of solar energy, California is also beginning to restrict solar PV interconnections.

Per 10 U.S. Code 2911, DoD Energy Policy, DoD has a goal of procuring or producing 25% of facility energy from renewable sources by 2025. Similarly, many states have aggressive goals related to renewable energy, such as California's requirement that future buildings be zero net energy designs. Currently, 16 states are also actively working on plans to enhance resiliency against grid power outages, since the risk and impact of such emergencies is increasing due to climate change and aging infrastructure. Rooftop solar PV is a critical enabling technology to meet these future energy and resiliency objectives. However, meeting these goals while also staying under the permitted limits of distributed solar energy on the utility grid presents a significant challenge for conventional AC-connected systems. Since DC systems are inherently designed to maximize the flow of DC power locally from source to load in order to minimize conversions to AC, such a configuration inherently reduces interaction with the utility grid and therefore allows significantly higher levels of solar penetration to occur while also increasing resiliency. As illustrated in this report, DC microgrids represent the most energy efficient, reliable, and resilient way to implement distributed energy resources at a building level while also having significantly lower lifetime cost when compared to conventional AC alternatives.

Page Intentionally Left Blank

2.0 TECHNOLOGY DESCRIPTION

2.1 TECHNOLOGY OVERVIEW

In order to better understand the advantages of a DC microgrid, one must first understand the limitations of conventional AC electrical distribution systems in buildings, as illustrated in Figure 2.

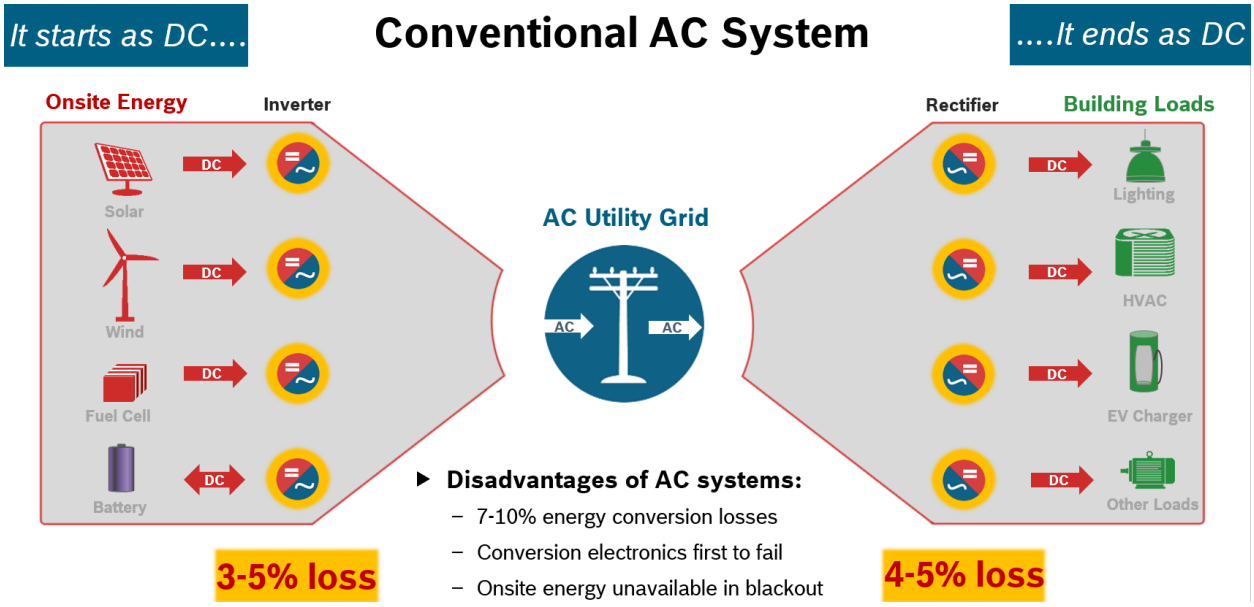

Figure 2. Disadvantages of Conventional AC Systems

As show on the left side Figure 2, all modern sources of onsite electrical power, as well as energy storage technologies such as batteries, internally utilize DC. These power sources must incorporate DC to AC inverters in order to supply power to the devices using electricity within the building, since these loads were specifically designed to utilize AC power from the utility grid. However, all modern an efficient building loads internally also utilize DC, and therefore need additional AC to DC conversion electronics. In most cases these conversion electronics are hidden within the device itself, but most people are familiar with the "power brick" which connects a laptop computer to a wall outlet, which is a more visible example of AC to DC converter electronics. For onsite sources of power and storage, such as rooftop solar PV and batteries, the DC to AC conversion losses are typically 3-5%. Navigant Research's 2013 study on DC Power for Commercial Buildings states that the typical AC to DC conversion losses for building loads ranges between 4-25% depending on the load. For more efficient, higher power loads, this report assumes a more conservative range of 4-5% as shown in the figure, so total energy loss due to conversions in a conventional AC system would be in the range of 7-10% from source to load.

In addition to the energy losses due to conversions back-and-forth between DC and AC, Figure 2 can be used to illustrate the other two key disadvantages of conventional AC systems: 1) the additional electronics required for such conversions are a significant point of failure in every building device and therefore increases lifetime maintenance costs; and 2) having the utility grid effectively in the middle of the power flow chain even for local sources of power such as a rooftop solar array is the main reason why such local sources are disabled and cannot easily be utilized in loads for backup during a power outage in a typical AC configuration.

All modern and efficient building devices could benefit from DC distribution. For this project, a demonstration using solar and lighting in a commercial building application was chosen as the focus for the following reasons:

1. The rooftop solar PV panels (modules) and LED lighting elements themselves have very long lifetimes. In these cases, the DC to AC and AC to DC conversion electronics are by far the weak link in terms of reliability, and lead to higher system maintenance costs over lifetime. These costs can be particularly significant for commercial high-bay lighting as used in the demonstration, since the lights are typically located 25 feet or more above the floor requiring significant equipment and safety procedures to maintain, leading to high labor maintenance cost over the lifetime of the building.
2. Commercial lighting is typically wired on separate power circuits and circuit breaker panels from the rest of the AC building power distribution. Since the same wires can carry either AC or DC, the DC microgrid can be retrofit to an existing commercial building by sending power from DC sources just through the separate lighting circuits to the retrofit DC lights, while keeping the rest of the building circuits as AC.
3. The market for commercial solar installations is constantly increasing year over year, and complete lighting retrofits typically occur several times over the lifetime of every commercial building. The DC microgrid installation can be timed to coincide with a needed lighting upgrade, as was the case with the demonstration project. The solar PV array may be added at the same time as the lighting, but could also be added anytime in the future, since the maintenance advantage of the DC lighting would exist even before the solar PV was added to the system. This allows a phased approach to installing the DC microgrid based on budget or other limitations.
4. Lighting represents a significant energy user in almost every building type – typically 30% or more of overall power consumption in commercial buildings.
5. Most commercial buildings are primarily used during the daytime, meaning DC lighting is typically turned on when solar PV is generating power, maximizing the amount of power which can be transferred as DC directly from solar PV to lighting without conversion.

As a very simple example to illustrate the benefits of a DC microgrid, Figure 3 compares the extremely efficient power flow from solar to lighting in a DC configuration, as opposed to the power flow in a conventional building, where two AC power conversions must occur with associated losses. Note that for efficient lighting technologies, some electronics are still required in a DC light to properly drive the lighting elements (i.e. LED, fluorescent or induction tubes) in order to enable dimming and other lighting control features. However, these DC lighting driver electronics can be designed to have only 2-3% loss (depending on sophistication of control features) and will not exhibit the lifetime reliability issues associated with AC lighting drivers.

Also note that the utility grid is no longer in the middle of the power flow in the DC microgrid, making it inherently more resilient to a power outage.

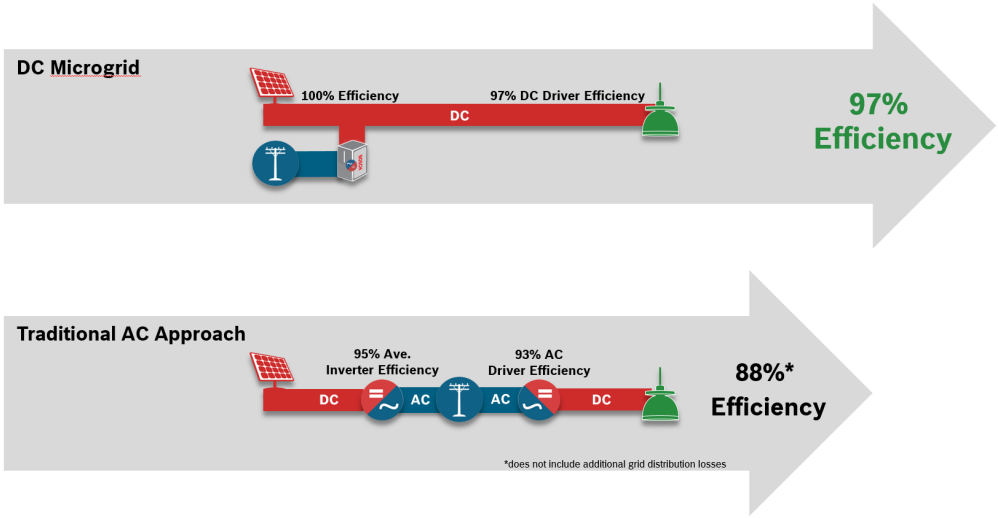

Figure 3. Power Flow Comparison – Solar PV to Lighting

The DC microgrid demonstration was performed at the Hercules Fitness Center building, located in Fort Bragg, NC. The primary focus for the project was to maximize the utilization of solar PV energy in the lighting, with a total of 44 high-bay ceiling lights in two rooms (a basketball court gymnasium and a large weight room) replaced with DC versions. Other goals of the project were to show the resiliency and reliability advantages of DC architectures. Figure 4 is an overview of the project.

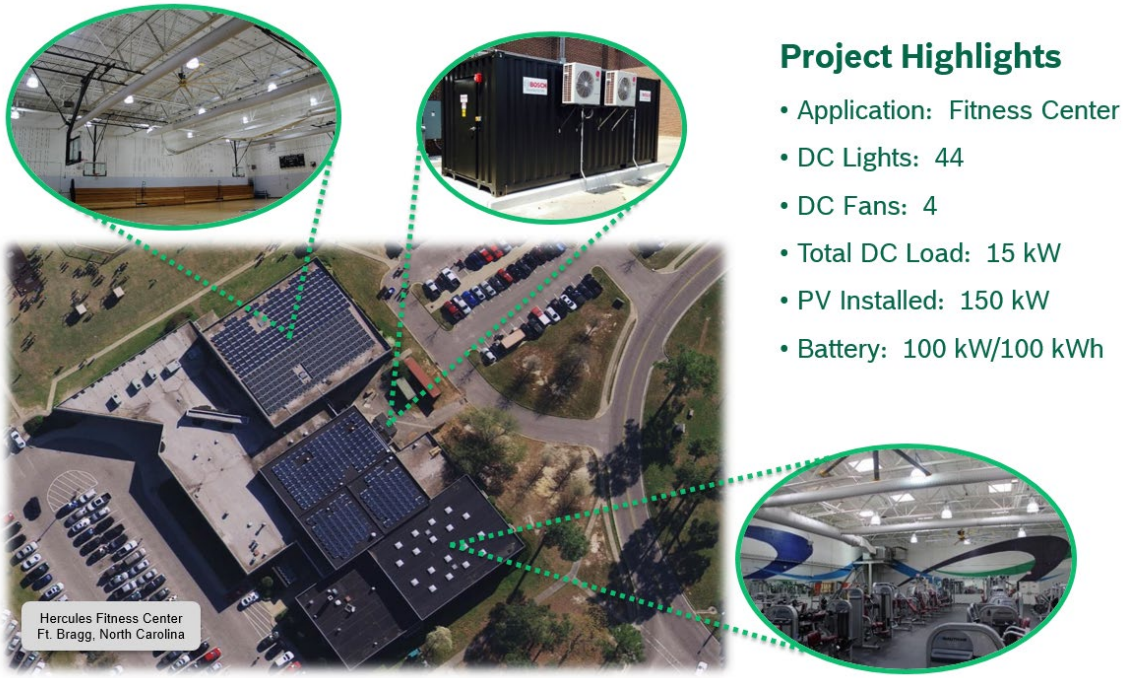

Figure 4. Project Overview

In addition to the DC lighting, four 18-foot DC industrial ceiling fans were also added to the two test rooms primarily to demonstrate that DC could also be utilized effectively in motor loads and is not limited to just lighting applications. The energy usage of industrial ceiling fans is far less than the lighting (one fan typically used the energy of only two lights), and there were no ceiling fans previously in the demonstration building for A/B comparisons, so the fans were simply used as confirmation that motor loads could be driven by DC, while supplying some additional needed ventilation and comfort to the fitness center occupants. The demonstration was constructed in two phases as shown in Figure 5.

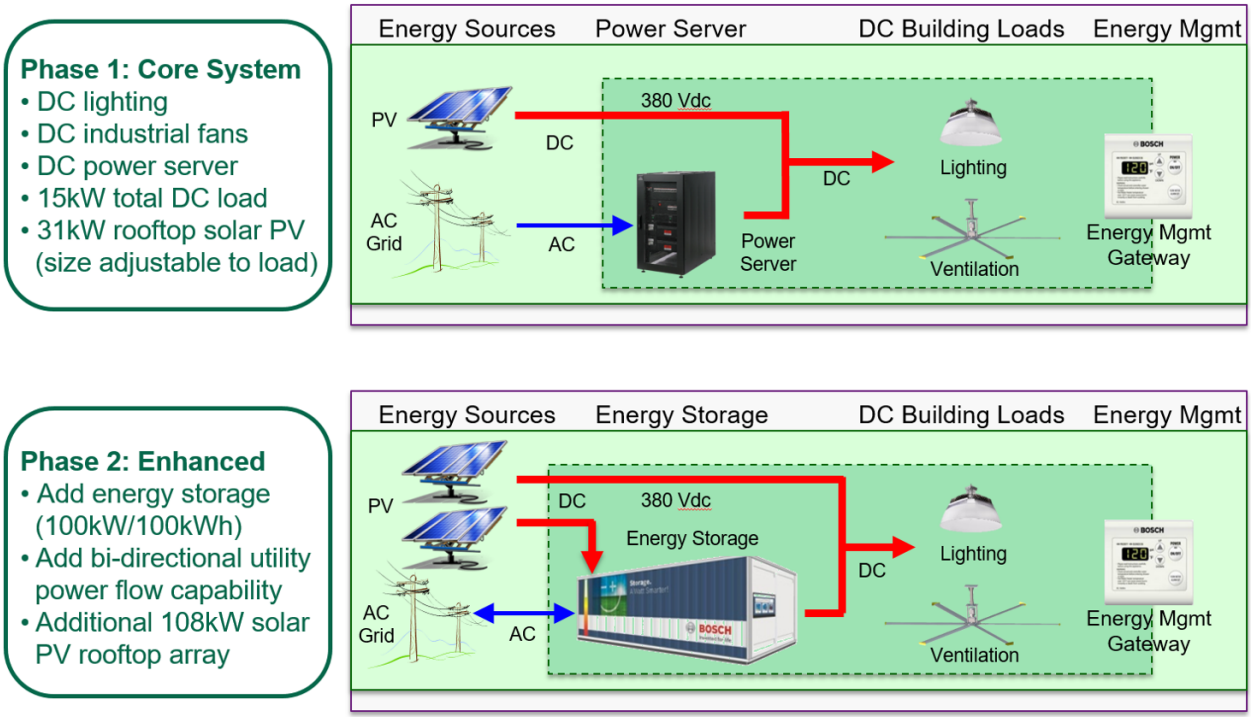

Figure 5. Content of the Project Phases

In Phase 1, the goal was to install the DC lights and DC ceiling fans in addition to enough rooftop solar PV to drive the DC loads. Since a major cost of a solar installation is the labor to mobilizing the rooftop crews, one complete section of the rooftop was filled with a solar array during Phase 1, resulting in some additional capacity to allow flexibility in testing higher DC load levels. However, the array was wired in such a way that it could be adjusted to provide a maximum 15kW to match the total DC load by simply disconnecting some of the panels or strings of panels, as was done during the Phase 1 testing.

The chosen configuration of the DC microgrid always prioritizes the utilization of solar PV energy, since the solar PV effectively has a straight connection to the DC loads. Only when there is not sufficient power available from solar PV does the utility grid fill-in the additional power needed via the power server, the only AC to DC converter in this core system. This configuration also has a basic level of resiliency automatically built-in, such that the DC loads can be powered by solar in the absence of utility power. It is worth noting that this low level resiliency comes at no cost in a simple DC configuration, and may be useful for loads which do not have the necessity to be powered continuously to perform the intended function, such as air conditioning or electric vehicle charging.

However, this simple configuration is not practical for lighting systems, since the variability of solar power due to weather conditions (e.g. clouds passing by) is significant and would immediately affect the lighting brightness during a power outage.

The DC microgrid system was designed to be applicable to retrofit installations as well as new construction. Key to this consideration is the use of 380 volts DC as the nominal voltage, which enables the re-use of existing building wiring. This allows the DC lighting to be installed in the same way as at typical AC lighting upgrade (simply replace old AC light fixtures with new DC light fixtures), and makes the DC microgrid a valid option to consider during a normal building energy efficiency lighting upgrade cycle.

Phase 2 was designed to significantly enhance the resiliency of the project, by adding a 100kWh battery energy storage system (BESS) along with the ability to import and export power through a 100kW bi-directional connection to the utility grid. The BESS components were housed in a 20 ft. container located behind the building, allowing most of the system to be built and tested offsite and delivered as a subsystem (see Figure 6).

Figure 6. Battery Energy Storage System (BESS)

Additional full sections of the rooftop were filled with solar arrays in Phase 2, resulting in 108kW of added power generation capacity dedicated to the BESS. With this configuration, the BESS prioritizes charging from solar PV power, and the stored energy is then available to back-up the DC loads in case of a power outage. Since the amount of solar PV power is far greater than the DC loads, the system can also continuously charge the BESS during the day while still suppling power to the DC loads as well as power the DC loads throughout the night at a lower emergency level.

This configuration allows an extended timeframe of emergency backup without the need for other power sources. The bi-directional connection to the utility grid was added to allow other modes of operation which improve the long-term economics of the storage system: In the case where the BESS has been fully charged from solar PV power, the excess solar PV power can then be exported to the utility for credit through normal net-metering or power purchase agreement mechanisms available from the utility for conventional solar PV systems. Also, since utilities typically charge commercial customers higher electricity rates during daytime hours of peak energy demand and lower rates at night when energy demand is less, the BESS can charge during nighttime and discharge during the daytime to further improve the payback of the system.

In order to provide an A/B comparison between the performance of the DC microgrid with respect to a conventional AC system, a small reference system was added to the building as shown in Figure 7.

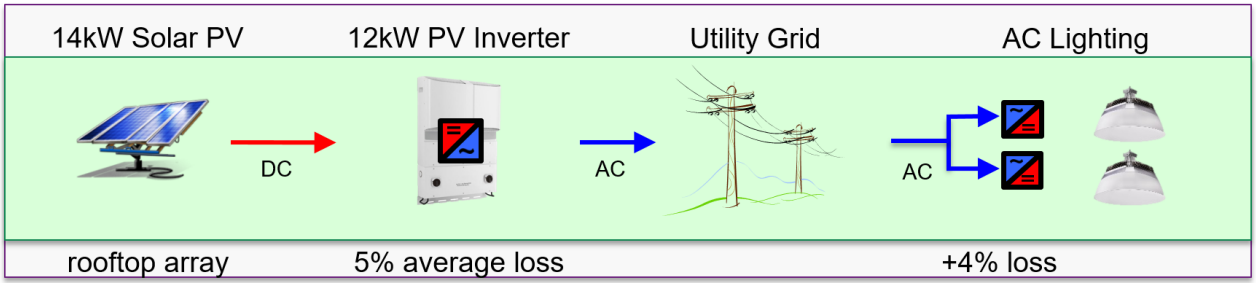

Figure 7. AC Reference System

The AC reference system consisted of a 14kW solar PV array with identical roof orientation and components as the Phase 1 DC array, a 12kW PV inverter (typical industry practice is to have 15%-20% more array capacity than inverter capacity in order to reduce the cost of the inverter and optimize system economics), and standard AC lights which are the same exact model as the DC lights. In an AC system, the quantity of lights do not need to match the size of the solar PV array, since the utility grid is effectively in the middle of the power flow, so only 4 AC lights were installed to maximize the number of DC lights in the demonstration. Figure 7 includes values for the *additional* conversion losses in an AC system when compared to a DC system, to further clarify the efficiency differences shown in Figure 3.

Figure 8 is an overview of the solar arrays installed in each Phase. Note that the Phase 1 array contains both the 14kW reference array as well as the 31kW DC microgrid array. These arrays were built on the same rooftop within an identical orientation to facilitate the A/B comparison. Although they appear to be one 45kW rooftop array, they are electrically subdivided between the separate AC and DC systems.

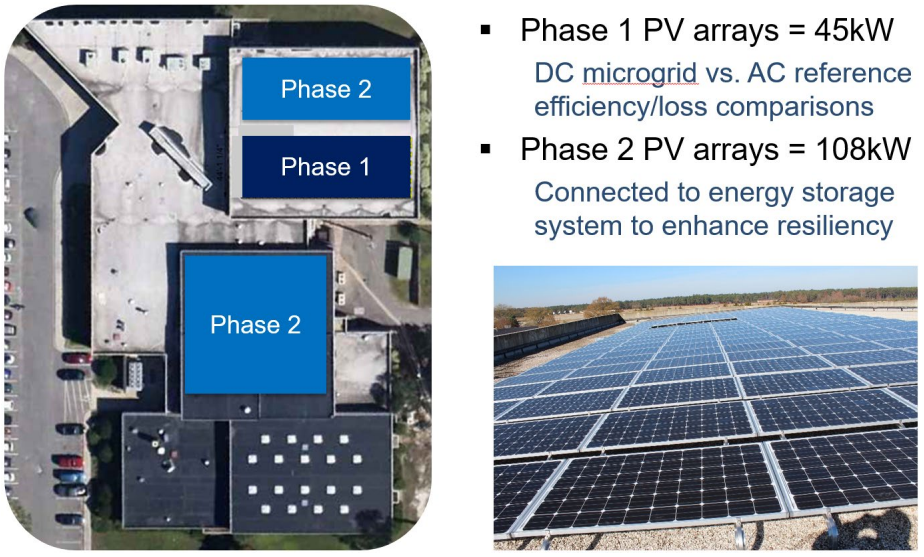

Figure 8. Solar PV Installation Phases

2.2 TECHNOLOGY DEVELOPMENT

The previous technology overview section is a concise explanation as to the rational for inclusion and sizing of the various subcomponents of the system. Actual implementation of a functional design into a building required detailed design work, electrical drawings and documentation. The following sections explain some key design elements of the system, and give reference to appendices containing detailed documentation.

The electrical construction drawings for the overall system are included in Appendix B. As explained in previous sections, the installed PV solar arrays can be categorized into three basic subarrays. In Phase 1, a 31kW array was installed (Array A) as well as a 14kW array (Array B). These two arrays were installed on the same area of the roof, with the same south-facing orientation, and using the same exact components in order to allow for a normalized A/B comparison between the core DC microgrid and a conventional AC reference system. These first arrays were constructed in early 2015 and utilized Suniva OPT270-60-4-100 PV modules (panels). In Phase 2, a combined 108kW of additional solar PV was installed on other roof sections (referenced in the construction drawings as Array C = 45kW, Array D = 33kW, Array E = 30kW) and dedicated to the Phase 2 BESS enhancement. The Phase 2 arrays were added in early 2016 and utilized Canadian Solar CS6P-250 PV modules. Note that the solar installation was re-quoted for Phase 2 and a different vendor was selected which used different PV modules. However, the Phase 2 array was not part of the A/B comparison, so the use of different components did not affect any comparison results. The datasheets for the solar PV modules used in the two phases are included in Appendix C.

The power server shown in Figure 5 is a key component of the DC microgrid. It supplies any incremental fill-in DC power needed by the loads in case solar power is insufficient, as well as supplying power that may be needed late at night or early morning, depending on the building operating hours. In the demonstration building, power server usage was limited since the

building was not open overnight. The system could also operate from the BESS during these times, however utility grid energy is inexpensive at these non-peak hours, so the system was designed to use utility grid power during nighttime (if needed) and to save the BESS power for emergency and peak-power needs. The power server selected for the demonstration was an Emerson NetSure 4015. This is a modular device designed for the data center market, so its design is well suited for extended use in critical power applications. It utilizes 15kW plug-in rectifier modules, allowing scalable power levels in 15kW increments as well as redundancy. For this project, two 15kW rectifier modules were utilized for redundancy, since only one meets the needs of the maximum DC load in the building. Another important feature of the NetSure 4015 is the ability to adjust the operating voltage within a limited range. The DC microgrid operates at a nominal voltage of 380 volts DC. The ability to dynamically adjust the voltage of the power server within a limited range allows the Energy Management Gateway to optimize the system voltage in order to keep the solar PV array operating at its maximum power point. This maximum power point tracking (MPPT) function is normally performed by the solar inverter in a conventional AC installation. Since there is no inverter between the solar array and the DC loads in a DC micrigrid, the MPPT function was performed in this alternate way. The algorithms for performing MPPT are available from a variety of open sources, so explanation is beyond the scope of this report and not critical to understand the operation. The efficiency of the selected power server is 97%, allowing the DC lighting to operate slightly more efficient than AC lighting from the grid during the limited nighttime hours. However, the power server is not in the path of the solar energy to the lighting, so this efficiency has no effect on the primary goal of better utilization of solar energy.

Although not a component of the DC microgrid, the solar PV inverter included in the reference system of Figure 7 plays an important role in the A/B performance comparison between the DC system and a conventional AC system. To keep the budget low for the reference system while also ensuring the system is representative of a larger rooftop commercial installation, an ABB PVI-12.0-I solar PV inverter was selected, as a 12kW inverter would be a typical size selected for a 14kW array as well as it having a 3-phase commercial power AC connection. The datasheets for the power server and reference solar PV inverter are included in Appendix C.

The initial DC light tested in the demonstration project was a 250W high-bay induction light with a modified electronic ballast allowing DC operation. These lights operated in the project for approximately 3 years from 2015 to 2018. As a product targeted for larger commercial market use, Bosch developed a DC lighting LED driver which allowed LED high-bay lights to run in a DC microgrid configuration simply by changing the driver electronics. The energy efficiency gained by operating on DC was nearly identical for the induction lights as it was for the LED lights. Since the DC induction light never became a commercial product, and since Fort Bragg desired to keep the DC lighting system running after the completion of the demonstration, the DC induction lights were changed to DC LED lights at the end of 2018. Even though the DC LED lighting was only installed at the end of the project, substantial lab data existed for the LED driver since it was being developed as a commercial product, so results presented in the performance assessment primary focus on the LED driver data. Datasheets for the induction light fixtures, LED light fixtures, and DC LED driver electronics are included in Appendix C.

The high-level purpose and function of the BESS system added in Phase 2 was explained in previous sections, and the detailed design theory, diagrams, and operation is well documented in the BESS operation manual, which is included in Appendix D.

2.3 ADVANTAGES AND LIMITATIONS OF THE TECHNOLOGY

Alternative DC-based lighting systems exist, such as power-over-ethernet (POE) which utilizes Ethernet wiring normally associated with data transmission to also provide power to the lighting. POE uses low voltages, typically 48 volts or less. Still other DC lighting system have been developed with utilize low voltage DC, such as 24 volts. Since the required current equals the lighting power divided by the voltage, over 10 amps of current would be required to power a 250W industrial high-bay light at 24 volts, as opposed to only 2/3 amp at 380 volts. The diameter of the wire needed increases with the current draw. Therefore, a system utilizing thin wiring designed for data is not practical to use with high-wattage lighting without exhibiting very high losses in the wiring. If the wiring were changed to accommodate the high current needs, the cost would be prohibitively expensive due to the large diameter and associated copper needed. A key advantage of the 380 volt DC lighting used in this demonstration is its ability to be retrofit to an older building with existing wiring as well as be implemented in new construction projects using standard wire and components. Typical commercial building projects select the wire assuming 277 volts or 120 volt is used for lighting circuits (one phase of 480 volt or 208 volt 3-phase AC, depending on the electrical service from the utility), and standard wiring insulation rating is 600 volts maximum AC or DC. In both cases, 380 volts DC falls between these values, meaning the current will be lower for the DC lighting than it would be for AC lighting on the same wiring, and the insulation rating will not be exceeded. Using standard or existing wiring represents a significant labor savings over low-voltage DC lighting systems requiring special wiring, especially with respect to the substantial wiring effort involved when installing commercial lighting systems in very large buildings with thousands of lights.

One consideration in implementing a DC system versus a conventional AC system is that the power requirements of the loads should ideally be matched to the power capability of the sources, since the utility grid cannot act as a "buffer" between the two systems. This is one potential advantage of a simple AC system involving just solar PV and lighting. Take for example the conventional AC reference system shown in Figure 7. It is not necessary for the lighting load to match the solar PV power generation, since all the power effectively flows through the utility grid. However, as soon as a battery is included in an AC system for backup purposes, the exact same size considerations come into play (i.e. which AC loads will be backed-up by the battery and how long will the energy storage last when powering those loads), so this advantage would only exist in simple AC systems without batteries, and would not outweigh the efficiency, reliability, and resiliency advantages which exist even in simple DC systems. A practical way to manage the optimum balance in DC microgrids is to plan a phase-in of DC sources and storage *after* the DC loads are added. For example, DC lighting could be added with a matching power server to gain the reliability advantages, followed by a DC solar PV system installed at a later date matched to the lighting load. In other words, the limitation in this example is that a DC solar PV system could not be added first without a DC load, since there would be nothing to utilize the DC power. As long as a strategy of balancing DC sources with DC loads is followed when planning a DC microgrid, this limitation is of minimal concern.

Page Intentionally Left Blank

3.0 PERFORMANCE OBJECTIVES

Table 1 summarizes the performance objectives and results of the demonstration project:

Table 1. Summary of Project Objectives and Results

Performance Objective	Metric	Data Requirements	Success Criteria	Results
Quantitative Performance Objectives				
Increase energy efficiency	Improved utilization of solar PV energy through reduced power conversion losses	AC and DC device efficiency/loss measurements using power analyzer	> 5% improvement in utilization of solar PV energy vs. conventional system	9% improvement demonstrated
Demonstrate load-leveling	Ability to offset full power level of DC loads for a set period in all seasonal conditions	Measure power and energy flow into utility grid during battery discharge	Offset complete DC lighting load during a set period for 365 cycles w/ test > 1yr.	382 cycles completed during 18 month test
Improve system reliability	Reduced failure rate of DC components vs. AC components	Record component failures, research field data/studies, seek expert opinion	> 50% improvement in lifetime maintenance costs DC microgrid vs. conventional AC system	No component failures in DC system; 100% improvement predicted
Cost effective commercial system	Lifetime costs DC system vs. conventional AC system	Commercial costs estimates at scale	>10% improvement in cost vs. conventional system	15%-30% cost improvement modeled
Qualitative and Go/No-Go Quantitative Performance Objective				
Add resiliency	Ability to provide backup power to DC loads during power outage	Evaluate adequacy of lighting & ventilation level during power outage	Satisfactory power for lighting and ventilation available day/night	More than sufficient power available

Additional discussion and details on each performance objective follows:

Increase Energy Efficiency: The primary objective of the demonstration was to prove that local sources of building power (rooftop solar PV), when connected via DC power distribution to devices using this power in the building (DC lighting), would be more energy efficient than conventional AC systems. The DC microgrid system exhibits higher energy utilization through the efficiency gains made by avoiding the DC to AC conversion losses which occur in conventional solar PV systems, as well as by avoiding the AC to DC conversion losses which occur in conventional AC building devices such as lighting. Solar arrays are a long-term asset, with modules typically warranted for 25 years. Even modest gains in efficiency can have substantial impact over the long life of the system. Therefore, a gain of 5% or more in the utilization of solar PV energy in the building lighting would be significant and was chosen as the success criteria. In order to evaluate the improvement made by the DC microgrid, a smaller AC reference system was constructed on the same building using conventional techniques (solar included DC/AC inverter and lights included AC/DC lighting electronics) while using identical solar panels and lighting fixtures.

Comparing the lighting efficiencies between AC vs. DC lighting electronics is a straightforward static measurement and can be done using a high-accuracy meter designed to measure input power and output power and calculate efficiency in real time. Since the DC microgrid has no solar PV inverter, conversion energy losses are effectively zero. Measuring the energy losses in a conventional AC solar PV inverter is more complicated since this is a dynamic value which changes depending on weather conditions, time of day, seasons, etc. This value was determined through long-term measurement of the reference inverter losses. Overall, the efficiency gain of the DC microgrid vs. a conventional AC system was found to be 9% in the demonstration project. The efficiency gain of DC lighting over the best-in-class AC lighting accounts for 4% of this, and the efficiency gained by having no PV inverter accounts for 5% of the total.

Demonstrate Load-Leveling: Battery energy storage added to a building electrical system purely for the purpose of backup power can be difficult to monetize, even though there is a high intrinsic value to having critical buildings that can continue to operate in an emergency mode during a utility grid power outage. One mechanism to potentially payback some of the upfront costs of a BESS system is through "load-leveling" or "peak-shaving". Electrical utilities often have challenges to meet power demand at certain times of the day under certain conditions. For example, late afternoon in the summertime when air-conditioning demand is high due to all buildings in a region heating up from sun load. The traditional way for utilities to handle this demand is to temporarily activate utility-owned "peaker plants" as needed, typically running on natural gas. However, in some cases these peaker plants may only run a few hours a year, and in other cases the peak demand is increasing year-over-year in a region, forcing the utilities to plan future construction of new peaker plants. In order to incentivize commercial customers to help manage the peak load problem, the utilities will raise the cost of peak power. Common ways for the utilities to implement this strategy is through different time-of-day electricity rates, and by implementing demand charges – typically a penalty for the maximum kW power drawn during any 15-minute period during the month. Depending on the building power profile, this 15-minute demand charge cost can be a similar magnitude on the electricity bill as the kWh energy usage charge for the entire month. To show how this feature could be implemented in the DC microgrid configuration, the BESS system was regularly discharged to completely offset the maximum DC load of 15kW. The success criteria chosen was to demonstrate 365 discharge cycles over several seasons, which could correspond to a utility time-of-day rate or peak demand time per day, for example. The system actually demonstrated 382 cycles between August 2015 and January 2017, fully meeting the criteria.

Improve System Reliability: In solar PV systems, the rooftop panels have a very long life with typical warranties being 25 years. However, the PV inverters required in conventional systems to perform the DC to AC conversion are normally repaired or replaced 2 to 4 times during the lifetime of the PV system. In LED lighting, the LEDs elements themselves have a very long life of 100,000 hours or more. However, the lighting driver electronics typically have a warranty of only 5 years with the stages associated with AC to DC conversion having a wear mechanism making them the weak link. The 3 year timeframe of the demonstration was not long enough to fully illustrate the reliability advantages of the DC system vs. an AC system. No DC or reference AC lights failed during the demonstration period, but this would not be expected in such a short timeframe. However, the solar PV inverter on the reference AC system did exhibit a complete failure in the middle of the demonstration period and needed replacement. A much longer timeframe would be needed with a much larger sample size to statistically quantify the advantage from field data. Some useful studies exist which help clarify the advantage.

The DOE recently studied the failure mechanism for lighting electronics and found the components associate with AC the most likely to fail. Also, outside if the ESTCP funding, Bosch contracted an expert organization which very conservatively estimated the life of DC lighting electronics as twice that of comparable AC lighting electronics. For the success criteria, an improvement greater than 50% in lifetime costs related to reliability failures was assumed to be significant. Since the DC microgrid has no solar PV inverter to fail (and the AC reference inverter did in fact fail during the demonstration), and based on the DOE study and expert opinion, a 100% improvement in reliability is conservatively assumed, meeting the success criteria. A longer-term study would be recommended to further refine this assessment.

Cost Effectiveness of Commercial System: As illustrated, the key benefits of a DC microgrid vs. a conventional AC system are increased energy efficiency, added resiliency, and improved reliability. Secondary benefits are the ability to use the BESS for load leveling, and the potential for significantly reduced lighting controls wiring. The cost impact of these benefits are best modeled over the system lifetime (assumed for calculation purposes to be 25 years based on the solar PV module warranty period) in order for the reliability advantages to become apparent as well as for the improved solar PV energy utilization to accumulate. For the success criteria, it is assumed that a DC system would need to exhibit >10% lifetime cost savings compared to an equivalent AC system in addition to the inherent resiliency advantages to gain commercial traction. An example commercial cost comparison with a detailed breakdown follows later in this report, showing a 15%-30% lifetime cost advantage of the DC system depending on whether secondary benefits are assumed or not.

Add Resiliency: Another objective of the demonstration was to prove that the DC microgrid system could be enhanced by adding a battery energy storage system and additional rooftop solar PV in a second phase, thereby increasing the resiliency of the system. The Phase 2 system added a container-sized 100kWh storage system as well as an additional 108kW of solar PV to the rooftop dedicated to the BESS. The overall objective was to create a system which would provide a useful level of resiliency, with the metric being both go/no-go quantitative (could the lights and fans stay on during a power outage) and qualitative (would there be an adequate level of light and ventilation overnight from the battery alone). Although the peak DC load of the building was in the range of 15kW with DC lighting at maximum brightness and DC fans running full speed, it was found that substantially lower power levels are needed for emergency operation. For example, 2kW or less are needed at nighttime for rooms used as an emergency shelter for sleeping, since it is desired that the lights be dimmed to very low levels. In the demonstration project, the large solar array combined with 100kWh of battery storage was more than adequate to meet the success criteria.

Page Intentionally Left Blank

4.0 FACILITY/SITE DESCRIPTION

4.1 FACILITY/SITE LOCATION AND OPERATIONS

In coordination with Fort Bragg personnel, the location selected for the demonstration was building A-402, the Hercules Fitness Center on Pope Field, located at 763 Armistead Street, Fort Bragg, NC. The specific rooms used were the gymnasium basketball court and the large, high-ceiling weight room. The DC microgrid is a scalable system, but specifically targeted at large commercial buildings. Using the two high-ceiling (high-bay) rooms at this fitness center allowed demonstration of the smallest representative DC microgrid system using only 44 DC lights, compared to the several hundred that would be needed for a warehouse demonstration, for example.

The following criteria were used to select the ideal demonstration site:

- The site should be a large, high-ceiling building (e.g., warehouse, gymnasium, commissary, vehicle maintenance garage, or aircraft hangar) with a flat roof that can accommodate a solar PV array and high-bay lighting. Fort Bragg previously studied which buildings could accommodate solar PV in the future, and the Hercules Fitness Center was on that list.
- The building should have seven-day operation, and an electrical consumption pattern generally aligned with the solar PV system's energy generation. Daytime operation is critical because the core system solar array is sized to directly power the lights, eliminating the need for a grid-tied inverter to feed power back into the grid. For this reason, a residential building which is unoccupied during the daytime would not be a good candidate for a DC microgrid. The Hercules Fitness Center has daytime operating hours weekdays and weekends year-round.
- Since the AC lighting would be replaced with DC lighting, it was desired that the rooms being retrofitted should be in need of a lighting upgrade. The two rooms selected at the Hercules Fitness Center had very old and inefficient metal-halide lighting.
- Ideally, the rooms used for the demonstration could be used as emergency shelters, since the DC microgrid can continue to operate in an emergency mode during power outages. Fort Bragg may utilize the gymnasium-type rooms as emergency shelters for the on-base housing during critical situations.
- Note that the DC microgrid configuration described provides advantages in all climate zones. Thus, the geographic location of the demonstration site was not critical. A site in North Carolina was desired since the Bosch personnel working on the project were located in that state, which led to the initial discussion with Fort Bragg.

4.2 FACILITY/SITE CONDITIONS

One downside of the selected facility is the orientation of the building. Ideally, the modules on a solar array should be mounted on a tilt rather than flat to enable rain to periodically rinse dust off the panels. The tilt should also be south-facing for maximum energy harvest over the year.

Since one of the goals of this demonstration was to perform an A/B comparison of the DC microgrid with respect to a conventional AC reference system, it was particularly important to remove any building orientation variables from the data. The Hercules Fitness Center building is oriented 45 degrees from due south with the rooftop having a peak in the middle, with 2 roof planes running SW and NE. The peak and the building orientation made it challenging to optimally place a true "due south" array for Phase 1, while also leaving space for the additional arrays planned in the Phase 2 expansion as shown in Figure 9.

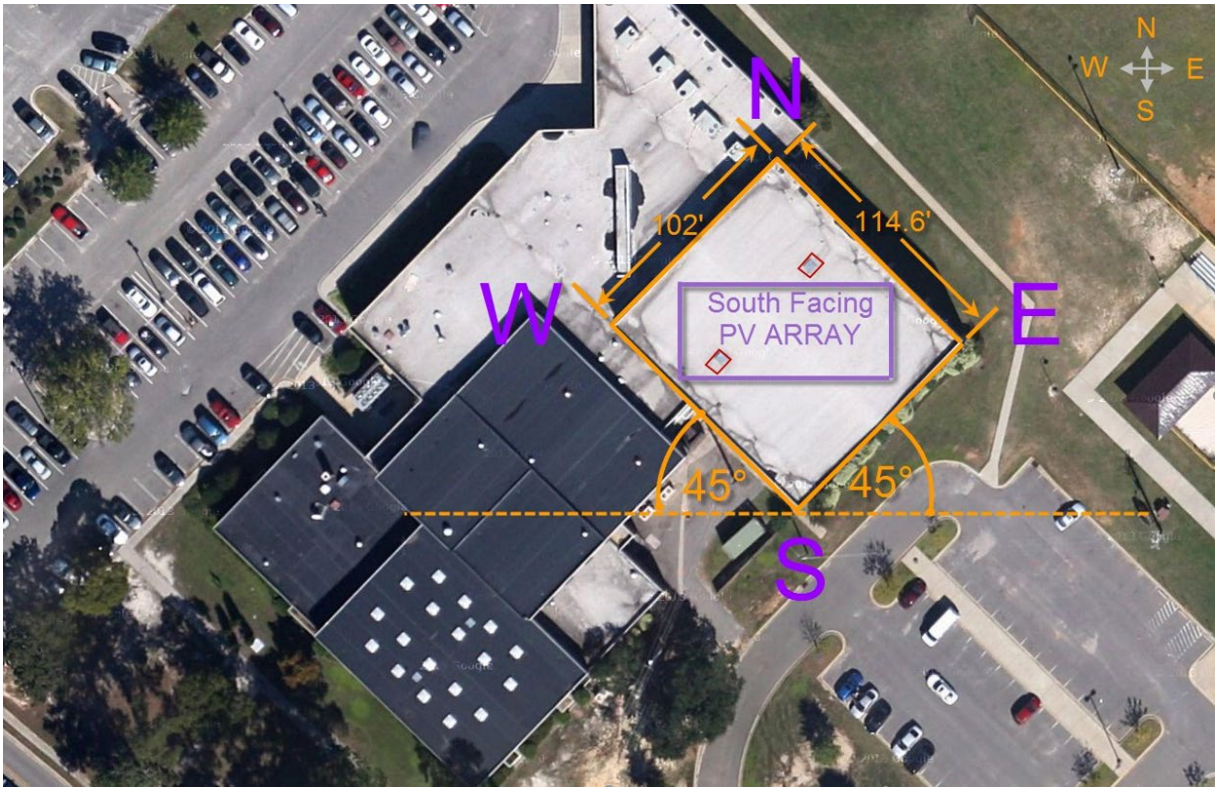

Figure 9. Demonstration Building Orientation

This issue was addressed by using a solar PV mounting system with a custom tilt angle. See Figure 10. The solar PV panel mounting system tilts the panels in the south-east direction (green arrow) at the same 2 degree angle as the normal roof pitch tilts south-west (yellow arrow), resulting in an overall tilt vector due south (red arrow). In other words, this mounting scheme results in one corner of each panel pointing south, and being the lowest point of that panel.

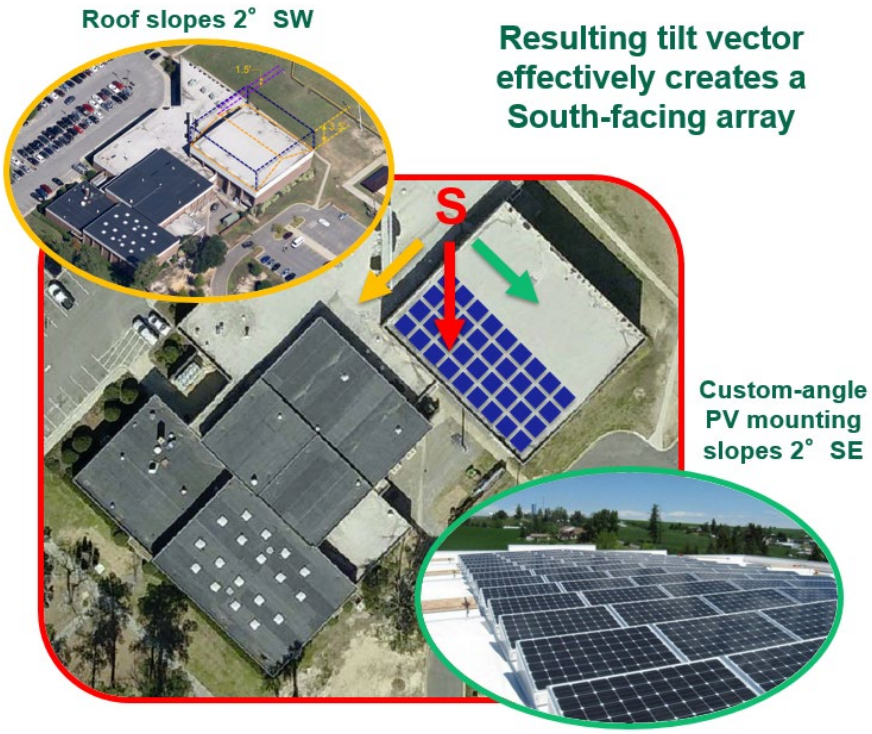

Figure 10. Creating a South Facing Solar PV Array

This precise mounting was only performed for the 14kW and 31kW Phase 1 arrays which were used for the AC and DC comparison. Note these two Phase 1 arrays are next to each other and appear as one array in Figures 4, 8, and 10. The arrays added in Phase 2 are only connected to the BESS, so the use of custom mounting tilt angles was not necessary. Details for all the solar PV arrays are included in Appendix B.

Another minor issue with the selected building was the available AC voltage. Larger and newer commercial buildings typically use 480 volt 3-phase AC as the utility power feed to the building. The Hercules Fitness Center, being a smaller and older building, utilizes 208 volt 3-phase AC from the utility. The power server selected as well as the BESS required the more common 480 volt AC power, and it was desired to develop a system which would work with this more modern standard. This issue was resolved by simply installing a 150kVA 3-phase transformer at the site to convert enough 208 volt AC to 480 volt AC for use by the DC microgrid components. Similar utility service mismatches often exist with AC equipment installations in buildings, so these transformers are commonly available and this was not seen as a critical issue.

Page Intentionally Left Blank

5.0 TEST DESIGN

5.1 CONCEPTUAL TEST DESIGN

The systems installed in Phase 1 were designed to enable a side-by-side A/B efficiency comparison between conventional AC building technology and a DC microgrid. The conventional AC system consists of AC high-bay lights as the load and a solar PV array with an AC utility grid-connected inverter (Figure 7). The core DC microgrid consists of a DC version of the same high-bay lights and a solar PV array without inverter (system shown at the top of Figure 5). As explained in previous sections, the solar PV arrays use identical components and have identical orientations. The DC microgrid contains 44 DC lights, and 4 identical AC lights were added to the gymnasium room as reference. Since percent efficiency measurements were used for the comparison, the results are automatically normalized and differences in the quantity of lights and solar array sizes do not affect the results.

The Phase 2 system was designed to add resiliency to the system by adding energy storage in the form of a container-size battery system. The ability to backup DC loads during a power outage could be demonstrated by simply cutting-off the AC power to the system through the circuit breaker panels. Another feature of the energy storage was to provide load-leveling, where the battery is discharged into the utility grid at prescribed periods, for example when utility power is expensive. Although not a resiliency feature, load-leveling can help to pay back the additional investment made in an energy storage system. The BESS was instrumented to allow long-term demonstration of the load-leveling feature.

5.2 BASELINE CHARACTERIZATION

The two rooms of the Hercules Fitness Center where the demonstration took place previously had very old and inefficient metal halide lights, also known as high intensity discharge (HID) lights. There were 44 HID lights required 452W of power each, for a total lighting power consumption of 19.9kW. Because these lights were so old, they had lost brightness and exhibited color shift, common problems with aging HID fixtures. For the demonstration the rooms were retrofit with 44 DC induction high-bay lights using only 250W each, immediately reducing the lighting power consumption by 45% to 11kW while drastically improving brightness and lighting color. Figure 11 shows the 1-for-1 retrofit of the existing lights, as well as the installation of the new DC fans.

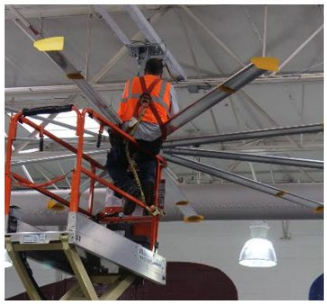

Installing 18' dia. DC ceiling fans

Replacing AC HID Lights

Completed weight room with 20 DC lights and 2 DC ceiling fans

Figure 11. Retrofitting DC System to Existing Rooms

There were previously no ceiling fans in the basketball court gymnasium and weight room. DC fans use very little power, and were added to the demonstration project primarily to show that motor loads could also effectively utilize DC. It was originally thought that adding the fans may reduce the need for air conditioning and also save energy in this way (a common use of ceiling fans, and not specific to DC). However, being a fitness center, the comfort levels of the rooms were drastically improved by the added ventilation, so no attempt was made to cut back on air conditioning use, since proof of energy savings through ceiling fan use was not primarily related to the DC demonstration.

Since the previous lights in the test rooms were very old technology, and the rooms did not previously contain ceiling fans, focus was not given to detailed baselining of the existing infrastructure. Instead, comparisons were made between new, state-of-the-art equivalent AC lights installed at the same time as the DC lights as a more meaningful and fair comparison between the DC microgrid and modern AC approaches. As part of a marketing handout preparation and independent of the ESTCP project, a simple case study (see Appendix F) was prepared using the old technology lights at the Hercules Fitness Center as a baseline, but the rest of the analysis in this report assumes new, equivalent technology lights as the AC reference.

5.3 DESIGN AND LAYOUT OF TECHNOLOGY COMPONENTS

Figure 12 illustrates the layout of the DC loads within the demonstration building. Figure 4 and 8 showed the layout of the sources and storage elements. Detailed design drawings are included in Appendix B with datasheets for key components in Appendix C.

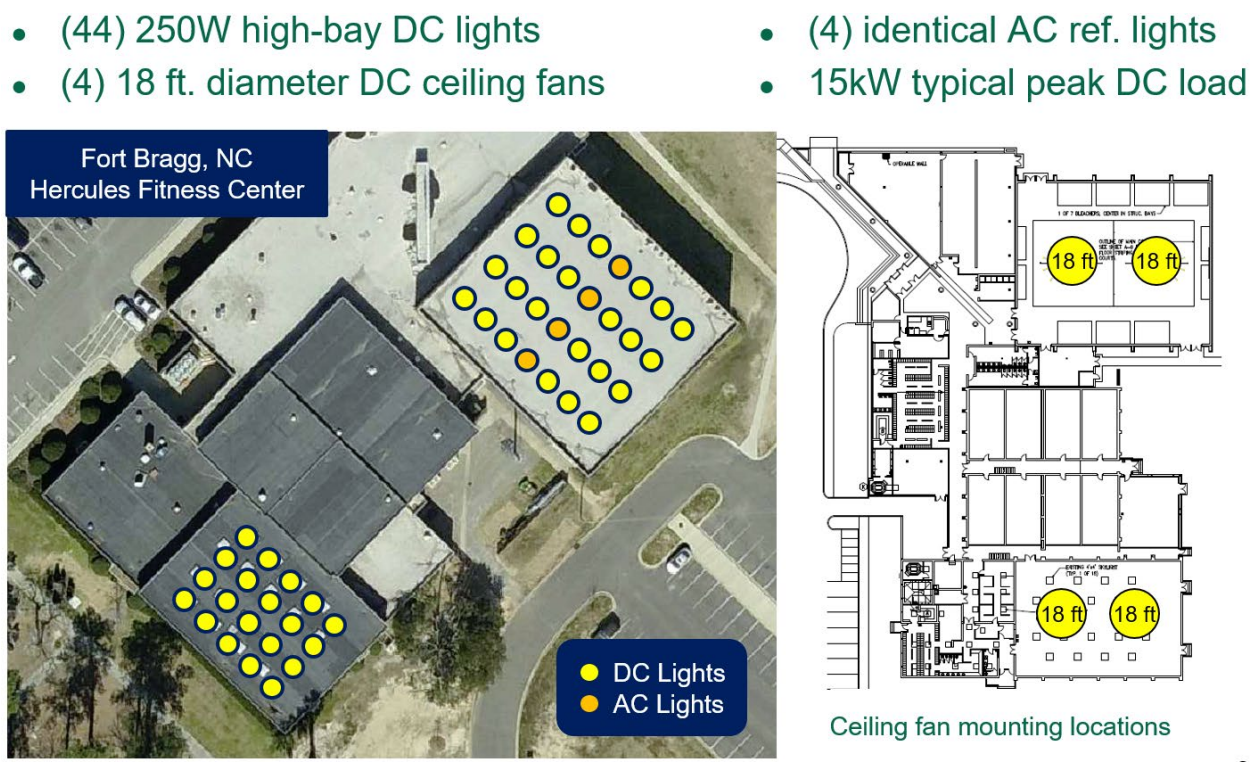

Figure 12. Layout of DC Loads

5.4 OPERATIONAL TESTING

Table 12 summarizes the operational phases discussed in other sections of this report, with references to appropriate appendices with detailed information. Note that the BESS system was removed at the end of the demonstration as part of the decommissioning, but that the core DC microgrid remained at the request of Fort Bragg, using updated DC LED lighting.

Table 2. Summary of Operational Phases

Operational Phase	Description	Timeframe	Notes
Phase 1 core DC microgrid installed	Existing AC metal halide lights replaced with DC induction lights, Power Server installed, 31kW solar PV array installed	Q2 2015	44 DC induction lights retrofit to same positions as original lights – critical validation that use of existing building wiring for retrofit DC devices is feasible
Phase 1 AC reference system installed	14kW solar PV array with 12kW solar PV inverter installed, AC induction lights used	Q2 2015	4 identical AC induction lights installed for reference in gymnasium basketball court (separate conventional AC circuit used)
Phase 2 enhanced system including BESS installed	BESS installed with interfaces to core DC microgrid and utility grid	Q3 2015	See Appendix D for detailed BESS documentation & commissioning report
Phase 2 additional solar PV arrays installed	108kW added and connected to BESS	Q1 2016	BESS gained ability to charge from solar PV as well as from utility grid
A/B comparison of AC and DC systems	Compare efficiency and losses between AC devices and DC devices	Updated through Q2 2018	Lighting efficiencies measured in lab for higher accuracy, solar PV losses measured in field to account for weather and seasons
Long-term test of BESS load-leveling capability	BESS offsets DC microgrid energy daily while grid connected and provides backup power during grid loss	Aug 2015 - Jan 2017	Monthly test reports in Appendix E
Decommission of BESS system	BESS removed and recycled	Q4 2018	108kW solar PV array connected to inverter in standard AC configuration per Fort Bragg request
DC lighting upgraded	DC induction lights replaced with DC LED lights	Q4 2018	Fort Bragg requested DC lights and power server remain – lights upgraded to Cree LED with DC drivers (see Appendix C)

5.5 SAMPLING PROTOCOL

In order to compare the conversion losses between a conventional AC system and a DC microgrid, highly accurate power meters are required. In this demonstration project, a Yokogawa WT3000E high accuracy power analyzer was utilized for critical efficiency measurements. This meter is capable of comparing the AC or DC input power to an electronic device with the AC or DC output power of the device and calculating power efficiency/loss from the difference in real time, with accuracies of 0.04%. The meter was purchased new for this project by Bosch and was calibrated at the factory.

5.6 SAMPLING RESULTS

As was illustrated in Figure 3, a key advantage of the DC microgrid is the ability to directly utilize solar power generated from a rooftop PV array at very high efficiencies in DC lighting, as opposed to a conventional AC system where conversions from DC to AC and then back to DC occur for all solar power generated. In the DC microgrid, the only element where some power loss occurs is in the DC driver electronics within the light fixture itself. This efficiency is independent of building factors, and was best measured in a lab environment. Table 3 shows lab results from measuring 5 DC light fixture samples. Although the input power and output power shows some normal variation based on differences in light fixtures, the measured efficiency of the electronics is extremely consistent and within the range of expected measurement accuracy. The lowest measurement (97.0%) was used to determine the 3% DC lighting loss value stated throughout this report.

Table 3. DC Lighting Efficiency Measurements

Bosch DC LED Driver Serial #	DC Input Voltage	DC Input Power to Fixture (Watts)	DC Output Power to LEDs (Watts)	Efficiency (%)
SN# 1f171006001	380	254.3	246.9	97.1
SN# 1f171006002	380	260.6	252.7	97.0
SN# 1f171006003	380	267.4	259.6	97.1
SN# 1f171006004	380	256.7	249.3	97.1
SN# 1f171006005	380	275.0	266.8	97.0

Prior to installing the DC driver, the original AC driver used in the lighting fixture was an Inventronics EUC-200S070DT. For comparison, the datasheet for the AC driver states an efficiency of 93% (datasheet included in Appendix C). This efficiency value was measured and validate using one reference lighting fixture in the lab, so 93% was used as the reference AC light fixture power loss, as was shown in Figure 3. This efficiency is on the high end for AC light fixtures, and represents as a good state-of-the-art reference value for AC driver efficiency.

The other device which exhibits significant energy loss in conventional AC systems is the solar inverter, which is responsible for the DC to AC conversion of PV power. Figure 13 shows the efficiency curve for the ABB PVI-12.0-I inverter used in the reference system. The datasheet for such inverters often indicate the peak efficiency, even though the efficiency changes at different power levels and voltages as can be seen from the curve. These conditions vary primarily based on time of day and weather conditions. Every solar inverter spends significant time at lower power levels during morning and evening, as well as during cloudy conditions and wintertime, when solar irradiance is lower. To obtain a suitable reference efficiency number, a lab-grade power analyzer was installed on the reference inverter at Fort Bragg and allowed to accumulate an average efficiency value over a variety of weather conditions. The efficiency value converged to 95%, a plausible value based on the efficiency graph in the datasheet. Therefore, 5% was used as the inverter loss in the AC case. One would expect this value to be slightly higher in cloudier geographies (i.e. northern climates), and slightly lower in sunnier geographies (i.e. desert climates) and to have some variation between inverter models. However, since the DC microgrid does not have solar inverter, it made sense to limit the investigation of AC devices and use 5% as a reasonable loss number for comparison.

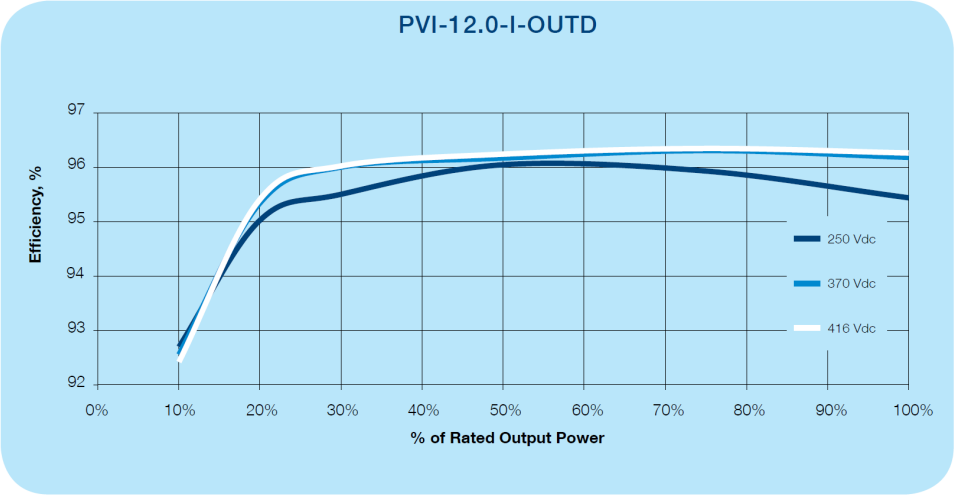

Figure 13. Reference Solar PV Inverter Efficiency Curve

After installation of the BESS system during Phase 2 of the demonstration, a long-term test period took place from August 2015 until January 2017 to demonstrate the load-leveling capability of the BESS. During this timeframe, 382 discharge cycles occurred with a total of 41.2 MWh of energy exported to the utility grid. In addition, there were five short-term events when the DC microgrid was powered by the BESS in a backup power mode. Detailed monthly reports of the BESS tests are included in Appendix E.

6.0 PERFORMANCE ASSESSMENT

Section 3.0 provides an overview summary of project objectives, selection of success criteria, and results. The paragraphs below contain additional details and discussion regarding the key objectives of improved energy efficiency, resiliency, and reliability.

Increase Energy Efficiency: As discussed previously and illustrated in Figures 3 and 7, the energy efficiency advantages of the DC microgrid are due to the additional conversion losses which occur in a conventional AC system. In the demonstration project, the additional losses are in the PV inverter and in the lighting electronics. Section 5.6 contains discussion on the 5% loss measured for the inverter connected to the solar array on the reference system as well as lab data from the DC LED lighting driver electronics. The additional losses in AC LED lighting driver electronics is the difference in efficiencies as compared to DC LED lighting driver electronics (i.e. 97% - 93% = 4%). The DC lighting fixtures which were originally installed at the beginning of the project in 2015 were 250W induction lights with DC lighting driver electronics (called ballasts for induction lights) modified to operate on DC. The DC induction lights were available for the demonstration project much earlier, but the DC version was never commercialized, since development efforts by Bosch were focused on the faster-growing LED lighting market. Nevertheless, some limited lab comparison testing was done on the AC and DC versions of the induction lights, showing a very similar advantage (96.9% efficiency for DC induction light ballast vs. 92.7% efficiency for AC induction light ballast, or 4.2% additional loss for the AC conversion). Table 4 is another summary of the results and includes the induction lights as well as LED. Since the LED lighting electronics were being commercialized by Bosch, the product and lab test data was much more mature, and therefore LED lighting is used for the comparison and discussion in this report.

Table 4. Summary of Measured AC vs. DC System Losses

Device	AC System Energy Losses	DC System Energy Losses	DC vs. AC Improvement
Lighting (LED/Induction) Lab Tested	7.0 % / 7.3%	3.0% / 3.1%	4.0% / 4.2%
Inverter Field Tested	5%	0% (no inverter)	5%
Total Improvement	9.0% / 9.2%		

In addition to the DC efficiency improvements measured in the lab and in the demonstration project at Fort Bragg, independent of ESTCP funding Bosch contracted the National Renewable Energy Lab (NREL) to simulate how the system would perform in other geographies. It was expected that the AC inverter would experience higher losses in cloudier environments, since the inverter would spend more time at lower efficiency levels as shown in Figure 13. This effect would give the DC microgrid an additional advantage in northern states. However, NREL found another significant energy efficiency advantage of the DC microgrid which was not initially anticipated. Electrical energy losses which occur in the lighting electronics turn into heat energy.

Since the light fixtures are located inside the building, these losses are effectively heating up the building. In summertime, this heat energy must be removed by the air conditioning system, requiring extra energy. In wintertime, this lost heat contributes to keeping the building warm, but represents a very expensive resistive way to heat a building (similar to baseboard heating), and offsets more efficient and cost effective heating methods such as heat pumps, natural gas, etc. The AC lighting electronics exhibit higher losses than the DC lighting electronics, and therefore contribute more heat to the building. In NREL's models, the DC system had advantage over the AC system in all climates, as shown by the blue color over the entire map in Figure 14. However, the additional savings in air conditioning energy provided by the lower lighting losses in the DC system results in even higher savings in climates with high air conditioning usage, as illustrated by the darker blue colors in Figure 14. This would also mean a smaller capacity air conditioning system could potentially be used in buildings incorporating DC lighting, resulting in further equipment cost savings. The potential air conditioning equipment costs savings was not modeled and is beyond the scope of this report, but represents an additional potential advantage of DC microgrids. The NREL study is attached in Appendix G.

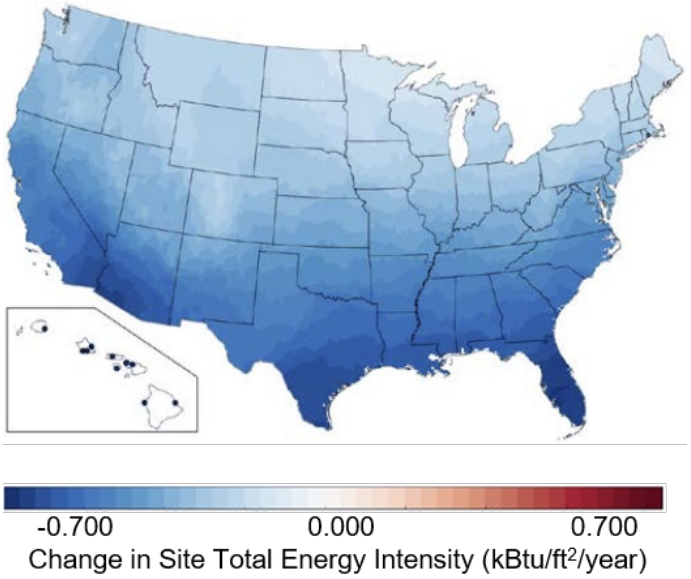

Figure 14. DC Lighting Reduces Air Conditioning Load

Demonstrate Load-Leveling: Battery energy storage added to a building electrical system purely for the purpose of backup power can be difficult to monetize, even though there is a high intrinsic value to having a building that can continue to operate in an emergency mode during a utility grid power outage. However, US fire code requires all commercial buildings to have systems providing a minimum of 90 minutes of low-level lighting in the case of power loss, to allow safe egress of occupants in an emergency blackout situation. Since all lighting in the DC microgrid is effectively backed-up by the BESS, this requirement can be met without additional dedicated emergency backup lighting systems. Using the BESS to meet the backup lighting requirements in the fire code represents one way to help justify the cost of the BESS. Another mechanism to potentially payback some of the upfront costs of the BESS system is through "load-leveling" or "peak-shaving". Electrical utilities often have challenges to meet power demand at certain times of the day under certain conditions. For example, late afternoon in the summertime when air-conditioning demand is high due to buildings heating up from sun load.

The traditional way for utilities to handle this demand is to temporarily activate utility-owned "peaker plants" as needed, typically running on natural gas. However, in some cases these peaker plants may only run a few hours a year, and in other cases the peak demand is increasing year-over-year in a region, forcing the utilities to plan future construction of new peaker plants. In order to incentivize commercial customers to help manage the peak load problem, the utilities often raise the cost of peak power. Common ways for the utilities to implement this strategy is through different time-of-day electricity rates, and by implementing demand charges – typically a penalty for the maximum kW power drawn during any 15-minute period during the month. Depending on the building power profile, this 15-minute demand charge cost can be a similar magnitude on the electricity bill as the kWh energy usage charge for the entire month. To show how this feature could be implemented in the DC microgrid configuration, the BESS system was regularly discharged for a fixed period of time to completely offset the maximum DC load of 15kW. The success criteria chosen was to demonstrate 365 discharge cycles over several seasons, which could correspond to a time-of-day rate or peak demand time per day, for example. The system actually demonstrated 382 cycles between August 2015 and January 2017, fully meeting the criteria. Detailed documentation on the BESS system design and theory of operation are included in Appendix D, and monthly reports on the BESS long-term testing are included in Appendix E.

Improve System Reliability: The 3 year timeframe of the demonstration was not long enough to fully validate the reliability advantages of the DC system vs. an AC system. No DC or reference AC lights failed during the demonstration period, but this would not be expected in such a short timeframe. The solar PV inverter on the reference AC system did exhibit a complete failure in the middle of the demonstration period and needed replacement, although this was just one data point. A much longer timeframe would be needed with a much larger sample size to statistically quantify the DC vs. AC difference simply from demonstration data. However, other useful information exists which supports the reliability advantage of DC systems. In solar PV systems, the rooftop panels have a very long life with typical warranties being 25 years, but the PV inverters required in conventional systems to perform the DC to AC conversion are normally replaced 2 to 4 times during the lifetime of the PV system. Within an LED lighting fixture, the light-producing LED elements themselves have a very long useable lifetime (often 100,000 hours or more) and the normal wear mechanism of an LED element is to slowly lose brightness over operating time, giving plenty of warning to plan a fixture replacement or upgrade. However, the AC driver electronics required to power the LED from utility power and contained in each fixture typically have warranty periods of only 5 years and are the primary cause of complete LED fixture failure requiring replacement. The shorter warranty period is well known in the lighting industry, and there is some data publically available regarding actual field failure rates. Figure 15 can be found in a report by the Next Generation Lighting Industry Alliance (NGLIA) - LED Systems Reliability Consortium [6], showing the AC driver electronics being by far the highest cause of field failure in conventional LED lighting fixtures, also called solid state lighting (SSL) luminaries.

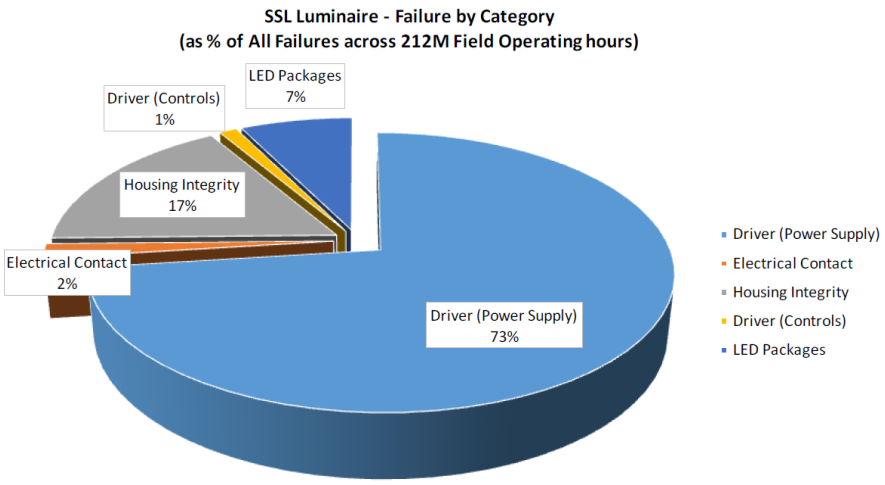

Figure 15. AC LED Lighting Fixture Failures by Category

From a wear mechanism standpoint, the weak link within the AC driver electronics is the "front end" electronics where the AC to DC conversion and AC power factor correction takes place. This fact was further validated by an independent DOE study [7], which found a majority of AC driver failures are associated with components in the AC front-end stages. These stages are only required in AC drivers and contain electrolytic capacitors having a wear mechanism associated with the constant charging and discharging required to rectify single-phase AC at 60 cycles per second to smooth DC needed by the LED elements while also correcting the power factor. On the other hand, DC driver electronics require no such rectification/power factor correction stages and therefore have no wear mechanism in the lighting driver electronics with a timeframe less than the useable lifetime of the LEDs themselves. In 2015 and outside of the ESTCP funding, Bosch contracted an expert organization in electronic reliability studies, the Center for Advanced Life Cycle Engineering (CALCE) at the University of Maryland (www.calce.umd.edu) to further validate the reliability improvement of using DC electronics for lighting. CALCE verified that there are no wear mechanisms in DC lighting electronics leading to a lifetime less than the LED lighting elements themselves, unlike in AC lighting electronics where CALCE validated that the electrolytic capacitors will wear out and limit the driver lifetime. CALCE very conservatively estimated the life of DC lighting electronics as twice that of comparable AC lighting electronics. Based on the solar inverter failure in the demonstration project (an AC conversion device), and information from DOE, NGLIA, and CALCE regarding the reliability issues with AC lighting electronics, DC lights are conservatively estimated to have half the replacement cost over an assumed system lifetime of 25 years as compared to a conventional AC system (one replacement for DC lights vs. two replacements for AC lights).

Add Resiliency: The first phase of the demonstration included 31kW of solar PV connected to the DC lighting and DC ceiling fans. Although the Phase 1 system could technically operate in the daytime during a utility grid power outage if there was enough solar power available, this configuration is not ideal from a resiliency standpoint, since the lights would abruptly dim whenever a cloud passes by because the power server could not fill-in the missing energy. In addition, no power for lighting or ventilation would be available at night in this simple configuration. The Phase 2 system added a container-sized 100kWh BESS as well as an additional 108kW of solar PV to the rooftop dedicated to the BESS (139kW total on the DC microgrid).

The overall objective was to create a system which would provide a more useful level of resiliency, with the metric being both go/no-go quantitative (could the lights stay on during a power outage) and qualitative (would there be a useable level of light overnight from the battery alone). Although the peak DC load of the building was in the range of 15kW with DC lighting at maximum brightness and DC fans running full speed, the building occupants eventually found that less than full power levels were more optimum for the application (gymnasium basketball court and weight room). Therefore, the total DC power level was always less than 10kW, even during the daytime. It was also found that very low levels of lighting are desired at night for rooms used as an emergency shelter, which lowered the power needed to 2kW or less for 8 hours or more. Since 139kW of solar PV typically generates more than 10kW during the daytime even in cloudy conditions, and 100kWh of battery energy storage capacity was more than sufficient for the nighttime load (100kWh storage could provide 2kW for 50 hours), this configuration easily met the success criteria. No actual long-term power outages occurred at Fort Bragg during the demonstration period, but the BESS did provide backup to 5 short-term power loss events, as shown in the monthly reports in Appendix E.

Page Intentionally Left Blank

7.0 COST ASSESSMENT

7.1 COST MODEL

The demonstration project at Fort Bragg is relatively small scale (only 44 DC lights), was the first of its kind, and was designed primarily to develop and demonstrate the feasibility and functions of a DC microgrid. Therefore, it is not the most representative project to use for a commercial cost model. However, in considering commercialization of the technology, Bosch studied all the costs of a marketable commercial-scale system in detail and found the lifetime savings advantage of DC technology to be up to 30% less than a comparable AC system, while also having additional resiliency advantages. The following sections explain the cost drivers and present a cost comparison for a more representative commercial project.

7.2 COST DRIVERS

The demonstration project proved the feasibility of implementing a DC microgrid in an existing building via a phased retrofit approach, starting with a standard energy efficiency lighting upgrade. The old, inefficient AC lights were first exchanged with new DC induction lights at the beginning of the project, and then again to DC LED lights at the end. Both installations were performed in the same manner as a traditional AC lighting upgrade. The rooftop solar arrays are essentially identical to conventional rooftop PV systems, but are simply connected to the DC microgrid rather than to a PV inverter as would be done in a typical solar installation. Although not specific to a DC microgrid, by far the biggest cost driver is adding large amounts of energy storage to a building in a container-sized system. Although battery prices continue to fall making the component costs of a BESS continually less, the effort to locate, electrical integrate, and properly maintain such distributed devices can be challenging. As an example, the Hercules Fitness Center had a relatively ideal location for the BESS, but Figure 16 gives an indication of some of the preparation steps that were still necessary for the demonstration project prior to the arrival of the container.

Figure 16. Site Preparation Prior to BESS Installation

Again, these challenges would exist for any container-sized storage system, and are not specific to DC microgrids. A large BESS could still make sense in areas with high utility peak electricity prices where load-leveling or peak-shaving strategies would have an attractive payback. Many other studies and tools exist to evaluate the benefits of a BESS for different utility rate structures. Since this is primarily an AC utility grid integration issue, it is beyond the scope of this report, which is focused on unique DC aspects of the system. For the cost analysis and comparison in the next section, a simpler approach is taken to adding battery energy storage to a building: As mentioned previously in this report, to meet fire code, all buildings require a means to provide a low-level of lighting for 90 minutes in case of a power outage. Since all the DC lights in a DC microgrid as well as the battery system are connected together on the same DC circuits, the minimum emergency lighting requirement can be met very cost effectively in this configuration. The traditional method for large commercial buildings to meet the emergency lighting requirement with AC distribution is to identify in advance which lights will activate in an emergency, and then connect them to dedicated circuits to a transfer switch and battery through an inverter. This method adds additional wiring costs and cannot easily be changed as a building is reconfigured. Figure 17 illustrates the differences between the typical central AC emergency lighting system used in commercial buildings and a DC microgrid approach.

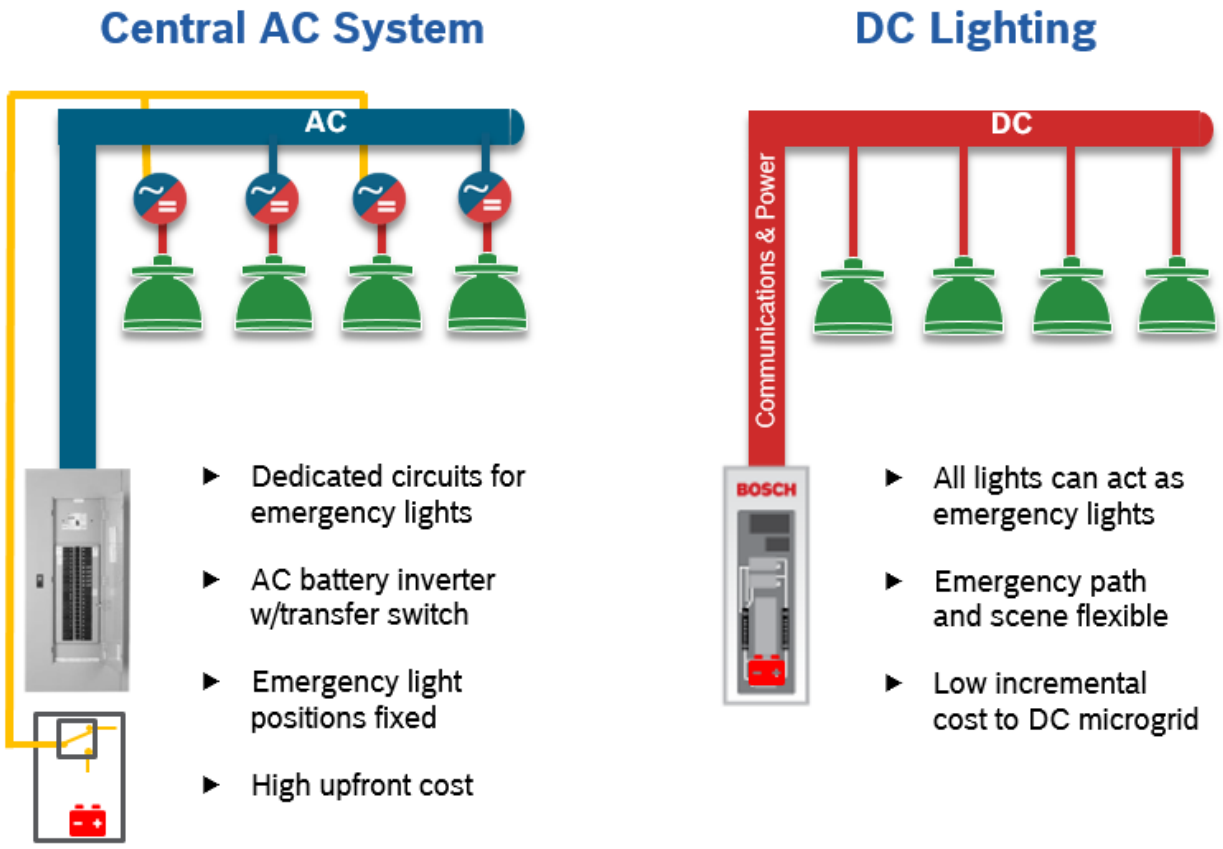

Figure 17. Conventional AC Emergency Lighting System vs. DC Microgrid

Battery energy storage in a DC microgrid architecture is completely scalable from a container-sized BESS system when utility rate structures enable reasonable payback, to small systems that allow the building to meet emergency lighting requirements. Since the latter is universal to all buildings and allows an immediate up-front savings, this simple emergency lighting system is assumed for the cost comparison in the next section.

7.3 COST ANALYSIS AND COMPARISON

The DC microgrid approach is applicable to many commercial building types, but is particularly attractive in larger buildings used 7 days per week. As an example, Table 5 is a cost comparison between a traditional AC approach and a DC microgrid when incorporated into a commercial building with 410 lights.

Table 5. Example Project Cost Comparison – AC vs. DC Approaches

		Traditional Approach	DC Microgrid	
		AC Solar & AC LED	DC Solar & DC LED	
	LED Total Wattage	27kW	27Kw	*Savings*
	PV Installed	70 kW	70 kW	
Capex	Solar	$192,500	$182,000	
	LED Lighting fixtures and installation	$460,000	$481,000	
	Lighting Controls and installation	$330,000	$68,000	
	Emergency Backup Power	$70,000	$25,000	
	Total Initial Cost	**$1,052,500**	**$756,000**	**$296,500**
Opex	LED Lighting - Replacement	$250,000	$125,000	
	Energy – 25 Years	$186,000	$166,000	
	Monitoring, Control, Management – 25 Years	$37,500	$37,500	
	Total Operational Cost - 25 Years	**$473,500**	**$328,500**	**$145,000**
Total	**Total Cost of Ownership – 25 Years**	**$1,526,000**	**$1,084,500**	**$441,500**
	Simple Payback (Yrs.)	**5**	**3**	

The assumptions for this example project are: 300,000 sq. ft. facility with 410 DC LED light fixtures @ 66 watts each on for 10 hours per day, and an electricity rate of $0.15 per kWh increasing 2% per year. Further detail on each line item follows:

LED Total Wattage and PV Installed: The same total wattage of lighting load and solar PV is assumed for each case. In reality, each DC light would consume around 4% less power as an identical AC light for the same light output since there are no energy losses due to the AC/DC conversion that takes place in each AC light. Similarly, the pure DC solar array could be 5% smaller than a traditional solar array utilizing an AC inverter (which typically loses 5% of the solar energy flowing through it) and provide the same energy benefit. To simplify the model, LED total wattage and PV installed are assumed to be the same for the DC and AC system and the efficiency advantages are reconciled in the 25 year energy cost calculation.

Solar: The DC microgrid does not require an inverter, so the upfront cost for the solar PV system is less in addition to the DC efficiency advantage over a conventional AC approach.

LED Lighting Fixtures and Installation: The LED lighting differs between the two cases only in the lighting electronics, commonly referred to as the LED driver, which is a subcomponent of the lighting fixture and determines whether the light operates on AC or DC voltage. DC lighting costs were based on a fixture utilizing the Bosch DC LED driver technology, while the AC lighting costs are based on market price. Presently, DC lighting costs are slighting higher than AC lighting costs due to two factors: 1) the economies of scale for AC lighting are much higher, since DC lighting drivers are starting at a low volume level and 2) advanced Power Line - Communications (PLC) lighting controls are implemented in the DC driver, which allows lighting command signals (on, off, dim, etc.) to be sent over the same wires as the power. Although this technology is not new, communications via PLC over dedicated DC power wires is much more reliable than AC since electrical noise levels are inherently lower and predictable on a DC bus where all devices are known and can be qualified. The savings in controls wiring (see below) far outweighs the additional cost for the option.

Lighting Controls and Installation: As mentioned above, the DC LED lighting fixtures contain PLC electronics enabling lighting control commands to be transmitted over the existing power wires, without the necessity for additional wiring dedicated for controls. For energy savings, more sophisticated lighting controls are typically desired, and mandated for all lighting retrofits and new construction in some areas such as California (CA Title 24). Traditional AC lighting requires an entire separate network of control wiring to each lighting fixture, which results in high labor costs for both retrofit and new construction. Some AC wireless lighting control schemes also exist, but are expensive and unreliable in many applications such as industrial buildings and parking structures. Different lighting control options are compared in Figure 18. For the example cost comparison, the wired controls option is used for the AC case.

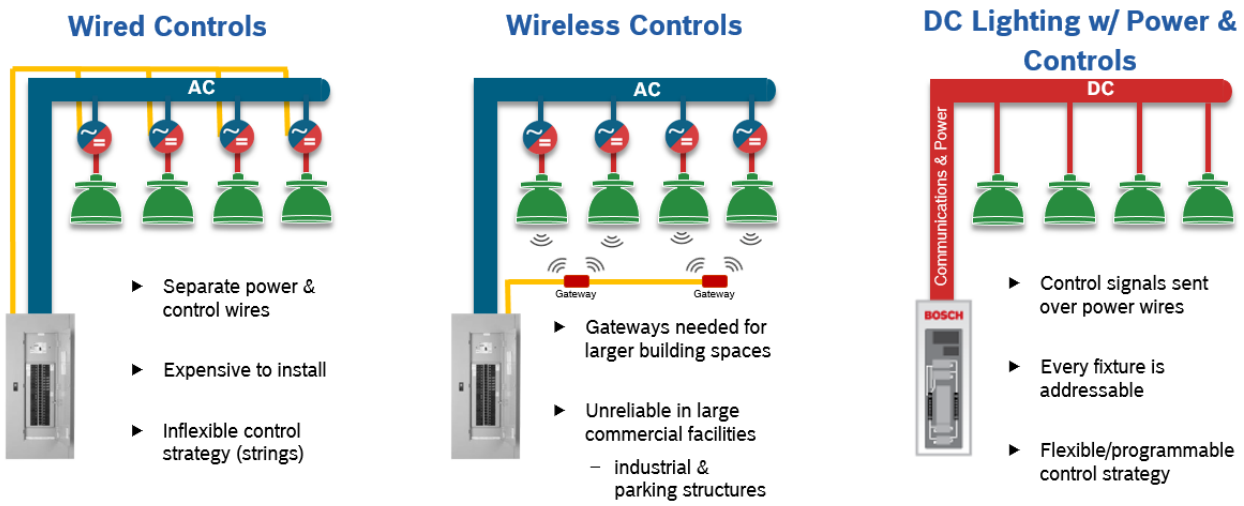

Figure 18. Comparison of Lighting Control Options

Emergency Backup Power: As a requirement of the fire code, all US buildings must have systems to provide a minimum level of emergency lighting in a building to support safe egress in case of a power outage. In traditional AC systems, this requirement is typically met through dedicated AC lighting circuits connected to a battery and a central inverter system, as discussed in section 7.2 and shown in Figure 17. DC microgrid already has battery storage with lighting connected, so the entire DC lighting network can provide emergency lighting to meet the fire code. This built-in feature results in significant savings over the dedicated emergency lighting hardware in a conventional AC installation.

LED Lighting Replacement: Within an LED lighting fixture, the light-producing LED elements themselves have a very long useable lifetime (often 100,000 hours or more) and the normal wear mechanism of an LED element is to slowly lose brightness over operating time, giving plenty of warning to plan a fixture replacement or upgrade. However, the AC driver electronics contained in each lighting fixture and required to power the LEDs from utility power typically have warranty periods of only 5 years, and are the primary cause of complete LED fixture failure requiring replacement. This is due to an unavoidable wear mechanism which exists in the AC to DC conversion stage. Industry studies by the Next Generation Lighting Industry Alliance [6] and DOE [7] further validate that the AC driver electronics are the weak link in fixture reliability. By comparison, the DC LED driver developed by Bosch was planned to be commercialized with a 10 year warranty, although no known wear mechanisms were known which would indicate a failure prior to the LED elements themselves. In the 3 year timeframe of the actual demonstration at Fort Bragg, there were no failures of the DC lights or AC reference lights, however one would not expect to see the DC advantage unless the period of the project were much longer. For the lifetime cost comparison example, DC lights are conservatively assumed to have half the replacement cost over 25 years (one replacement of the DC lights vs. two replacements for the AC lights).

Energy – 25 Years: By avoiding the DC to AC conversion which normally occurs in a solar PV inverter which is utility grid connected, as well as the AC to DC conversion which normally occurs within the lighting electronics within a typical AC lighting fixture, the DC system is assumed to avoid 9% of the losses. Since NREL found that the energy conversion losses in the lighting fixture result in heat being added to the building (requiring additional air conditioning power to remove in summer and displacing less costly heating methods in winter), an additional 3% is conservatively added to the difference calculation to accommodate these additional savings.

Monitoring, Control, Management – 25 Years: These are the typical lifetime costs for the service to remotely monitoring, control, and manage the system. Since these costs are based on software and information technology, there would be no fundamental differences between the AC and DC cases. Therefore, the costs are assumed to be the same in the example.

Lifetime savings for DC microgrids occur both upfront by requiring lower capital costs as well as over time with lower operating costs. In the example case, the DC microgrid saves almost 30% as compared to a conventional AC system. Savings will vary based on different building types and use profiles, but savings will typically be between 15% and 30%.

Page Intentionally Left Blank

8.0 IMPLEMENTATION ISSUES

No major barriers to implementation of DC microgrids in buildings were found during the demonstration project, and the building devices (lights and fans) operated identically to conventional technology, requiring no special training for the facility managers or building occupants. The following comments are intended to aid others considering implementing future projects with DC technology:

The National Electrical Code (NEC) is a building code used by state permitting and inspection agencies. DC in buildings has been allowed and addressed in the NEC for many years, since conventional rooftop solar PV arrays utilize DC up to the inverter connection. However, electricians and inspectors are not always familiar with DC microgrids or with all the various sections of the NEC where DC is addressed. A significant improvement was made in the 2017 version of the NEC, which adds article 712 "Direct Current Microgrids", which greatly simplifies the initial discussion with permitting agencies and installers regarding the code compliance of the system.

A majority of the devices used in the demonstration were commercial off-the-shelf components. Standard building wiring is rated for both AC and DC, and other components needed in the building electrical distribution systems (panels, circuit breakers, fuses, etc.) are readily available in DC versions. Bosch developed a DC LED lighting driver which could be used in production LED high-bay fixtures from several manufacturers, but chose to wind-down the Building Grid Technologies business prior to commercializing the product. However, any manufacturer currently making AC LED drivers would also be capable of producing DC LED drivers, as they represent a much simpler design.

A potential path to more widespread adoption of DC microgrids in DoD applications is through financing mechanisms offered by Energy Service Companies (ESCOs) or other similar organizations. Financing of DC microgrid projects have a couple advantages. First, DC microgrids can represent a substantial upfront investment since several building systems are involved, and the payback comes in terms of improved energy efficiency and lower maintenance costs over the long lifetime of the system when compared to conventional AC technology. The system could be installed in phases over several years to spread-out the investment, but substantial upfront investments would still need to be made, potentially posing challenges to widespread DoD deployment. Financing offers the opportunity for the energy and maintenance cost savings to offset the payments, reducing or eliminating the upfront cost hurdle. The second reason is because solar PV is a key component of the DC microgrid. Significant federal tax credits (30% of total solar PV installation costs) are available to non-government agencies. Private companies like ESCOs are able to own solar PV systems installed on DoD facilities and therefore take the tax credits, while effectively sharing tax credit savings with the DoD through better financing terms (e.g. lower payments, shorter length, better interest rate, etc.). The DoD would not be able to benefit from the 30% tax credit on the solar portion of the DC microgrid when making a direct purchase of the system.

An important consideration when implementing a DC microgrid is to balance the sources supplying DC power with the loads using DC power, in order to optimize the efficiency advantages. A good example of this is the simple core system installed in Phase 1 assuming a 15kW solar array, 15kW power server, and 15kW of DC loads (the original tested configuration). Since the chosen demonstration site has long daytime operating hours 7 days a week, all solar power available from the PV array is immediately consumed by the DC lighting and DC ceiling fans with no power loss from AC conversions. Any time there is less than 15kW of solar power available (e.g. cloudy conditions reducing solar output), or if there is a special need for lighting at nighttime, the 15kW DC power server can supply any needed make-up power up to the full 15kW required by the DC load. In order to optimize the utilization of DC sources such as solar PV, the DC loads must be sufficiently large enough to match available power. An exception to this balancing guideline is the case where resiliency takes priority, as was demonstrated in Phase 2. In this case, the additional solar array and battery storage system were much larger than the DC load. This enabled a high level of resilience, but a bi-directional connection to the AC utility grid was also added in order to export excess solar once the battery storage is fully charged. As was demonstrated, the utility grid connection could then be utilized for load-leveling to support payback of the battery investment, as with a conventional AC storage system. A high value topic for future DC microgrid demonstrations would be to add variable DC loads which could be dynamically controlled based on the availability of solar power, such as DC air conditioning and/or DC electric vehicle charging. These loads differ from lighting in that their power demand can be reduced for significant periods of time without affecting the function. For example, an air conditioner could reduce in speed while a cloud passes by and then speed up again when full sun is available, without a perceptible change in temperature for the room being cooled. Similarly, an electric vehicle could be charged at different rates during the day to match solar output while still being fully charged by the end of the day. These variable loads also have the ability to be “shed” during an emergency power outage, to prioritize the availability of power for lighting. In general, the more major building electrical loads that are available to operate directly from DC power, the more potential exists to optimize utilization of distributed energy resources through DC microgrids.

9.0 REFERENCES

1. U.S. Department of Energy, 2019, U.S. Energy Information Administration, Monthly Energy Review, Table 2.1, https://www.eia.gov/totalenergy/data/monthly/#consumption

2. U.S. Department of Energy, 2019, U.S. Energy Information Administration, Electric Power Monthly, Table 5.1, https://www.eia.gov/electricity/monthly/epm_table_grapher.php?t=epmt_5_01

3. U.S. Department of Energy, 2019, U.S. Energy Information Administration, Natural Gas Summary, http://www.eia.gov/dnav/ng/ng_sum_lsum_dcu_nus_a.htm

4. U.S. Department of Energy, 2004, Lawrence Berkeley National Laboratory, LBNL-55718 Understanding the Cost of Power Interruptions to U.S. Electricity Consumers, https://emp.lbl.gov/sites/all/files/lbnl-55718.pdf

5. U.S. Department of Defense, 2016, Deputy Under Secretary of Defense Installations and Environment, Real Property Data Fast Facts, https://www.acq.osd.mil/eie/Downloads/Fast_Facts_2016.pdf

6. Next Generation Lighting Industry Alliance - LED Systems Reliability Consortium, 2014, LED Luminaire Lifetime: Recommendations for Testing and Reporting, www.nglia.org/pdfs/led_luminaire_lifetime_guide_sept2014.pdf

7. U.S. Department of Energy, 2019, Accelerated Stress Testing Results on Single-Channel and Multichannel Drivers, www.energy.gov/eere/ssl/downloads/accelerated-stress-testing-results-single-channel-and-multichannel-drivers

Page Intentionally Left Blank

APPENDICES

Appendix A: Points of Contact

Point of Contact	Organization Address	Phone E-mail	Role in Project
John Saussele	Robert Bosch LLC 38000 Hills Tech Dr. Farmington Hills, MI 48331	+1 (248) 310-4029 mobile john.saussele@gmail.com	Principal Investigator
Kevin Shannahan	Robert Bosch LLC 38000 Hills Tech Dr. Farmington Hills, MI 48331	+1(248)876-1190 phone kevin.shannahan@us.bosch.com	Manager - Public Funds, Robert Bosch LLC

Appendix B: Electrical Design Drawings

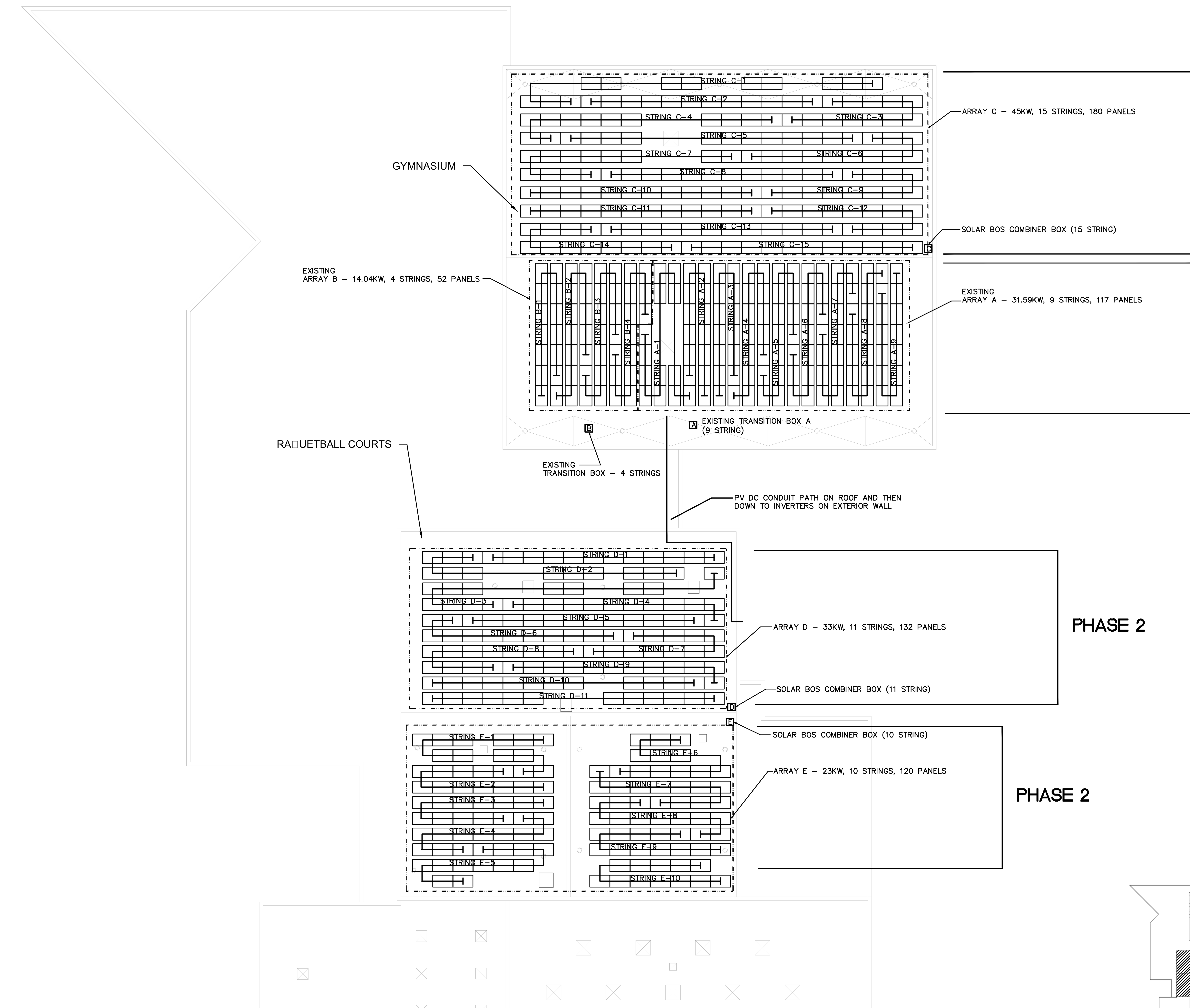

① ROOF PLAN – PV

1/16" = 1'-0"

NOTES:

1. ARRAY A & B ARE EXISTING PHASE 1. 45.63KW DC. 169 PANELS.
2. ARRAY C IS PHASE 2. 45KW DC. 180 PANELS.
3. ARRAY D IS PHASE 2. 33KW DC. 132 PANELS.
4. ARRAY E IS PHASE 2. 30KW DC. 120 PANELS.
5. SEE RACKING/BALLAST LAYOUT FOR ACTUAL PV ARRAY DIMENSIONS AND LOCATIONS.

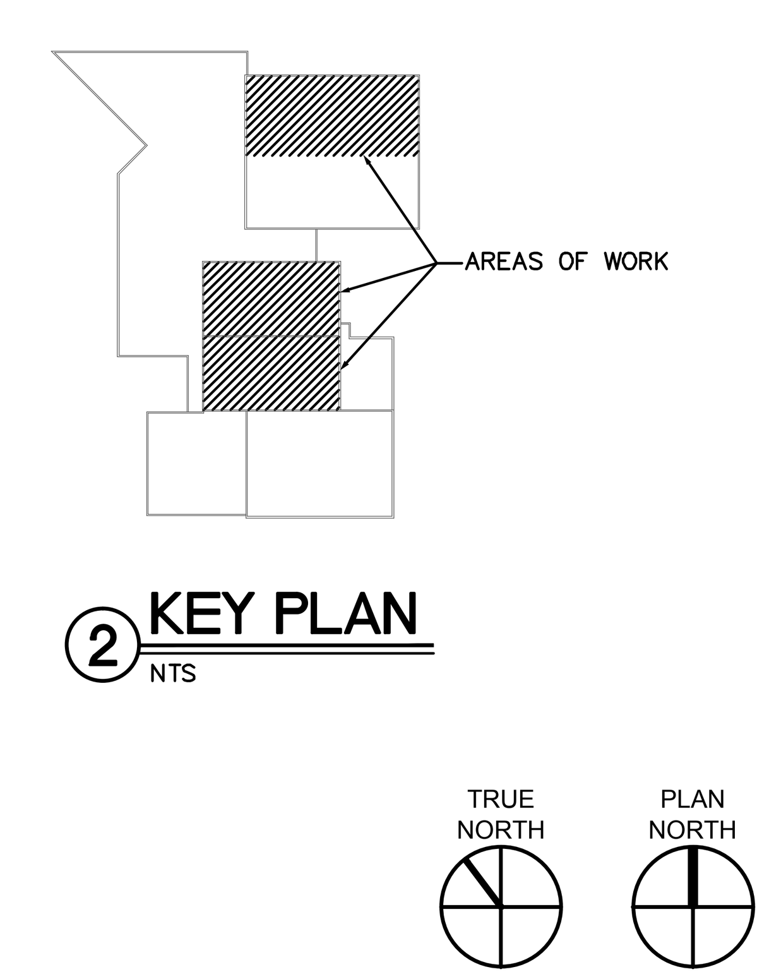

② KEY PLAN

NTS

optima engineering
1927 S   Tr   S , S   300, C   r   NC 28203
333 F   S , S   311, R   NC 27601
Phone: 704-338-1292 • www.optimaengineering.com

NORTH CAROLINA PROFESSIONAL SEAL 15   ENGINEER KEITH G. PEH 1/29/2016

SYMBOL	DESCRIPTION	DATE	BY
4	100 DESIGN SUBMITTAL (FOR CONSTRUCTION)	01/29/2016	A H
3	100 DESIGN SUBMITTAL (NOT FOR CONSTRUCTION)	10/22/2014	A H
2	65 DESIGN SUBMITTAL (NOT FOR CONSTRUCTION)	09/11/14	KGP
1	35 DESIGN SUBMITTAL (NOT FOR CONSTRUCTION)	06/1/14	A H

DESIGNED BY: OPTIMA ENGINEERING		DATE: 01/29/2016
DWN BY: A H	CKD BY: KGP	DPW FILE NO.: XXXXXX
SUBMITTED BY: XXX		ESTCP NO. 13 EB-EW1-104
FILE NAME: XEPWR.DGN		
SIZE: ANSI D	PLOT SCALE: AS SHOWN	PLOT DATE: 09/11/2014

.\NARENCO log horizontal.jpg

ZAPATA TRUST • INTEGRITY • QUALITY

HERCULES PHYSICAL FITNESS CENTER
DC MICROGRID - BLDG P-402
POPE ARMY AIRFIELD, NORTH CAROLINA

ROOF PLAN -
PV LAYOUT

PLATE REFERENCE NUMBER
PV-202
SHEET 7 OF 7
OPTIMA #: 14-0386

INVERTER STRING AND CIRCUIT CALCULATIONS

OF DESIGN: −10 DEGREES CELSIUS

STRING & CIRCUIT CALCULATIONS

STRING OVERCURRENT:

13 MODULES PER SERIES STRING = VOC (38.4V) X 13 = 499.2V
@ ISC (9.18A) PER STRING (15A OCP PER MFR)

MAX SYSTEM VOLTAGE

(38.4V + 5.543) X 13 = 557.73V AT RECORDED LOW TEMP OF −10 DEGREES C
ARRAY WIRE SIZING AND OVERCURRENT:

ISC X 9 STRINGS = (9.18 X 9) X 125% = 103.28A PER NEC 690.8(A)(1), 103.28 X 125% = 129.09A
PER 690.8(B)(1) FOR CONDUCTOR SIZING

LABEL PER NEC 690.53

RATED MAXIMUM POWER POINT CURRENT (Imp X #OF STRINGS) = 78.3A

RATED MAXIMUM POWER POINT VOLTAGE (Vmp X #OF PANELS IN SERIES−STRING) = 403VDC

MAXIMUM SYSTEM VOLTAGE (TEMP. COMPENSATED) (Voc + Tcoeff) = 557.73V

MAXIMUM SHORT CIRCUIT CURRENT (Isc X 1.25 X #OF STRINGS) = 103.28A

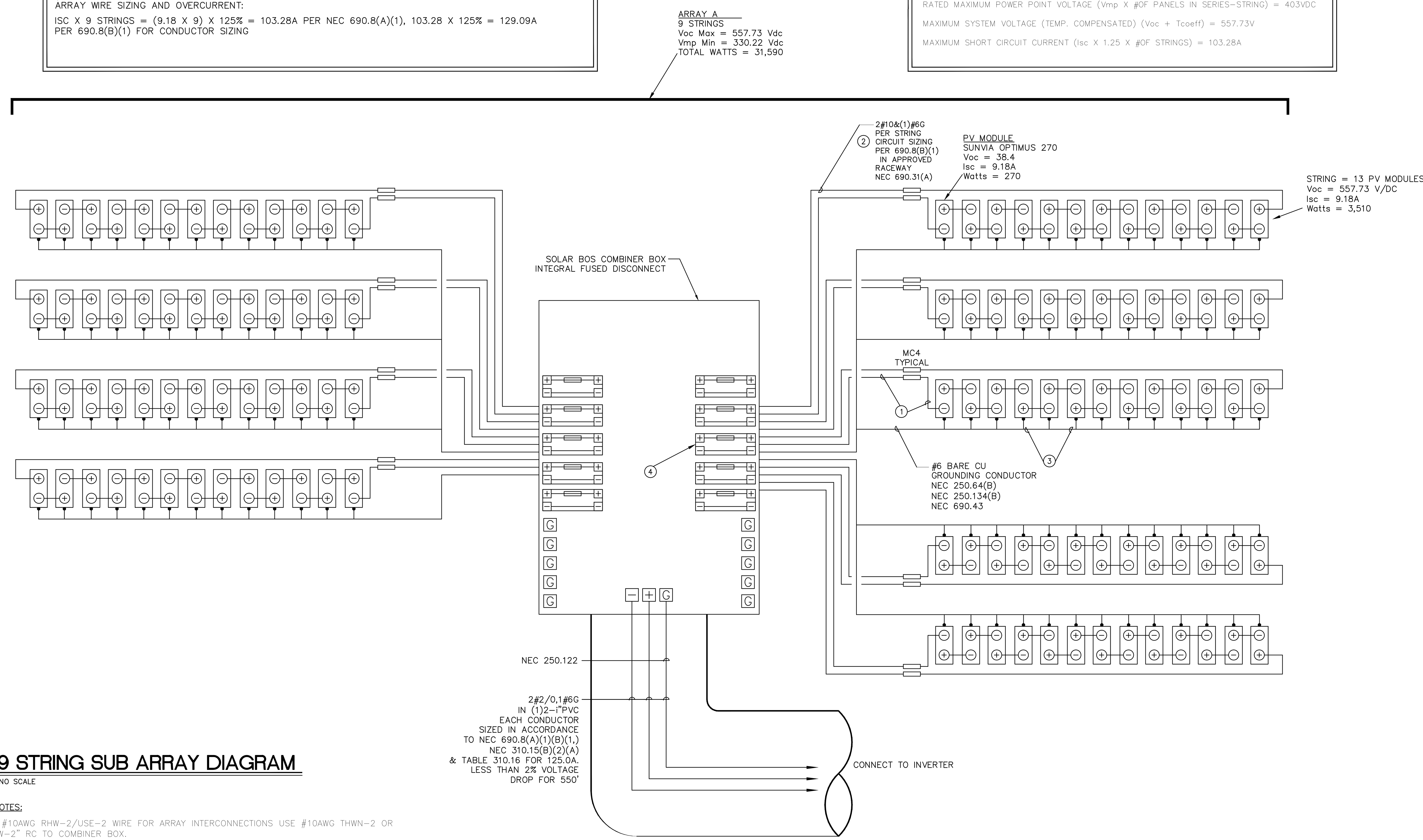

1 9 STRING SUB ARRAY DIAGRAM

NO SCALE

KEYED NOTES:

1. USE #10AWG RHW−2/USE−2 WIRE FOR ARRAY INTERCONNECTIONS USE #10AWG THWN−2 OR XHHW−2" RC TO COMBINER BOX.
2. DC CONDUCTOR SIZING BASED ON NEC 690.8(B)(1). TEMPERATURE DERATING BASED ON NEC TABLE 310.15(B)(16). CONDUCTOR DERATING BASED ON NEC 310.15(B)(2)a BASED ON NUMBER OF CURRENT CARRYING CONDUCTORS IN CONDUIT. CONDUIT SIZE BASED ON NEC ANNEX C, TABLE C9.
3. EQUIPMENT GROUNDING CONDUCTORS SMALLER THAN #6AWG SHALL BE PROTECTED FROM PHYSICAL DAMAGE BY A RACEWAY EXCEPT WHERE RUN IN HOLLOW SPACES OF WALLS OR PLENUMS, WHERE NOT SUBJECT TO PHYSICAL DAMAGE, OR WHERE PROTECTED FROM PHYSICAL DAMAGE.
4. ELECTRICAL CONTRACTOR TO VERIFY THE FUSING PLACEMENT (POLARITY) WITH PANEL MANUFACTURER BEFORE ORDERING COMBINER BOX. FUSE PLACEMENT IN COMBINER BOX MUST BE COORDINATED WITH FUSE PLACEMENT (POLARITY) IN PV MODULE.
5. ALL GROUNDING CONNECTIONS SHALL BE IN ACCORDANCE WITH NEC SECTION 250.160 DC SYSTEMS. DIRECT CURRENT SYSTEMS SHALL COMPLY WITH 250.160 AND OTHER SECTIONS OF ARTICLE 250 NOT SPECIFICALLY INTENDED FOR AC SYSTEMS.

optima engineering
Phone: 704-338-1292 • www.optimaengineering.com

SYMBOL	DESCRIPTION	DATE	BY
3	100 DESIGN SUBMITTAL (NOT FOR CONSTRUCTION)	10/22/2014	A.H
2	65 DESIGN SUBMITTAL (NOT FOR CONSTRUCTION)	09/11/14	KGP
1	35 DESIGN SUBMITTAL (NOT FOR CONSTRUCTION)	06/1/14	A.H

DESIGNED BY: OPTIMA ENGINEERING		DATE: 09/11/2014
DWN BY: A.H	CKD BY: KGP	DPW FILE NO.: XXXXXX
SUBMITTED BY: XXX		ESTCP NO. 13 EB-EW1-104
FILE NAME: XENOTE (2).DGN		
SIZE: ANSI D	PLOT SCALE: AS SHOWN	PLOT DATE: 09/11/2014

NARENCO log horizontal.jpg

ZAPATA TRUST·INTEGRITY·QUALITY

HERCULES PHYSICAL FITNESS CENTER
DC MICROGRID - BLDG P-402
POPE ARMY AIRFIELD, NORTH CAROLINA

9 STRING SUB ARRAY
DIAGRAM

PLATE REFERENCE NUMBER
PV-104
SHEET 19 OF 23

INVERTER STRING AND CIRCUIT CALCULATIONS

OF DESIGN: −10 DEGREES CELSIUS

STRING & CIRCUIT CALCULATIONS

STRING OVERCURRENT:

13 MODULES PER SERIES STRING = VOC (38.4V) X 13 = 499.2V
@ ISC (9.18A) PER STRING (15A OCP PER MFR)

MAX SYSTEM VOLTAGE

(38.4V + 5.543) X 13 = 557.73V AT RECORDED LOW TEMP OF −10 DEGREES C
ARRAY WIRE SIZING AND OVERCURRENT:

ISC X 4 STRINGS = (9.18 X 4) X 125% = 45.90A PER NEC 690.8(A)(1), 45.90 X 125% = 57.37A
PER 690.8(B)(1) FOR CONDUCTOR SIZING

LABEL PER NEC 690.53

RATED MAXIMUM POWER POINT CURRENT (Imp X #OF STRINGS) = 34.8A

RATED MAXIMUM POWER POINT VOLTAGE (Vmp X #OF PANELS IN SERIES-STRING) = 403VDC

MAXIMUM SYSTEM VOLTAGE (TEMP. COMPENSATED) (Voc + Tcoeff) = 557.73V

MAXIMUM SHORT CIRCUIT CURRENT (Isc X 1.25 X #OF STRINGS) = 45.9A

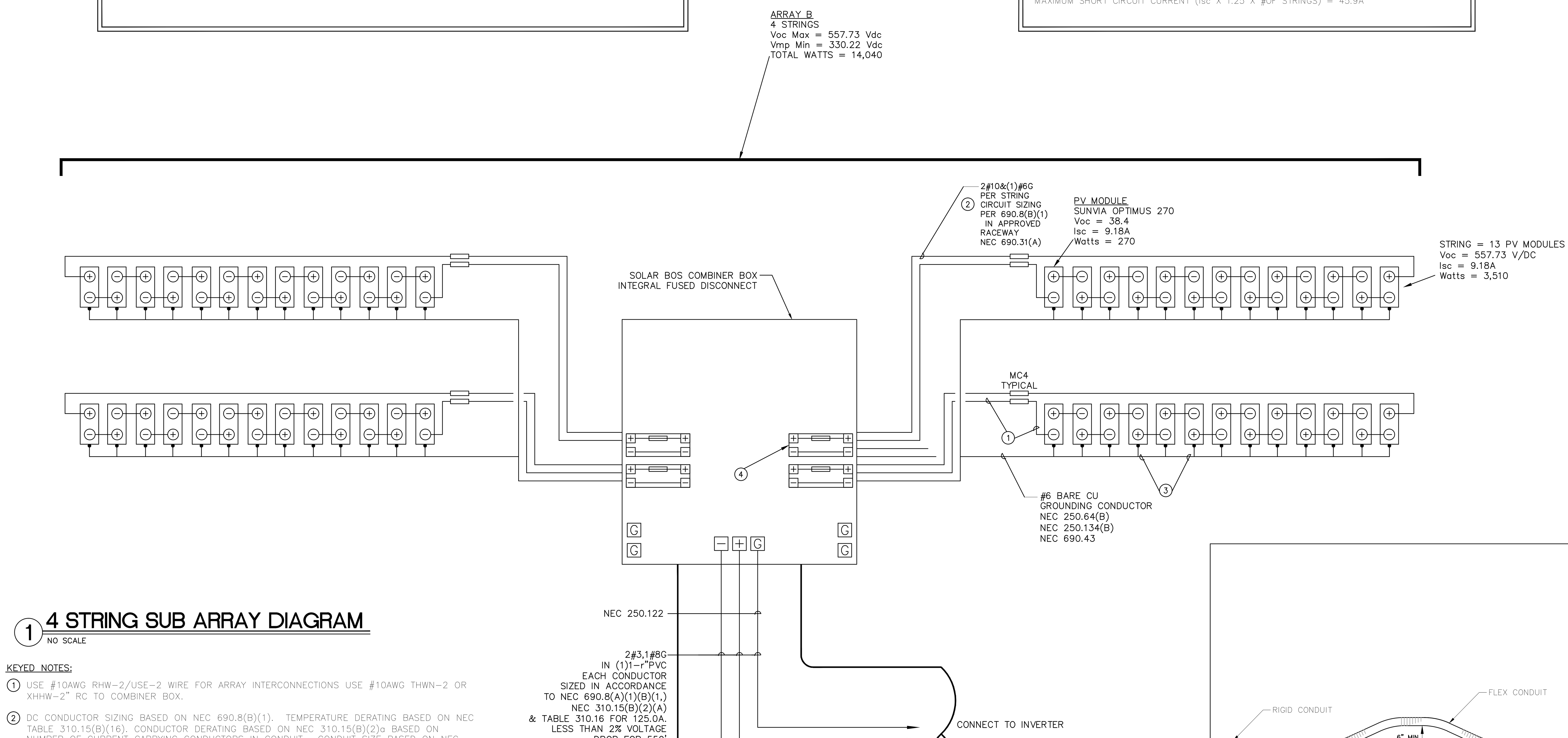

1 4 STRING SUB ARRAY DIAGRAM

NO SCALE

KEYED NOTES:

1. USE #10AWG RHW-2/USE-2 WIRE FOR ARRAY INTERCONNECTIONS USE #10AWG THWN-2 OR XHHW-2" RC TO COMBINER BOX.
2. DC CONDUCTOR SIZING BASED ON NEC 690.8(B)(1). TEMPERATURE DERATING BASED ON NEC TABLE 310.15(B)(16). CONDUCTOR DERATING BASED ON NEC 310.15(B)(2)a BASED ON NUMBER OF CURRENT CARRYING CONDUCTORS IN CONDUIT. CONDUIT SIZE BASED ON NEC ANNEX C, TABLE C9.
3. EQUIPMENT GROUNDING CONDUCTORS SMALLER THAN #6AWG SHALL BE PROTECTED FROM PHYSICAL DAMAGE BY A RACEWAY EXCEPT WHERE RUN IN HOLLOW SPACES OF WALLS OR PLENUMS, WHERE NOT SUBJECT TO PHYSICAL DAMAGE, OR WHERE PROTECTED FROM PHYSICAL DAMAGE.
4. ELECTRICAL CONTRACTOR TO VERIFY THE FUSING PLACEMENT (POLARITY) WITH PANEL MANUFACTURER BEFORE ORDERING COMBINER BOX. FUSE PLACEMENT IN COMBINER BOX MUST BE COORDINATED WITH FUSE PLACEMENT (POLARITY) IN PV MODULE.
5. ALL GROUNDING CONNECTIONS SHALL BE IN ACCORDANCE WITH NEC SECTION 250.160 DC SYSTEMS. DIRECT CURRENT SYSTEMS SHALL COMPLY WITH 250.160 AND OTHER SECTIONS OF ARTICLE 250 NOT SPECIFICALLY INTENDED FOR AC SYSTEMS.

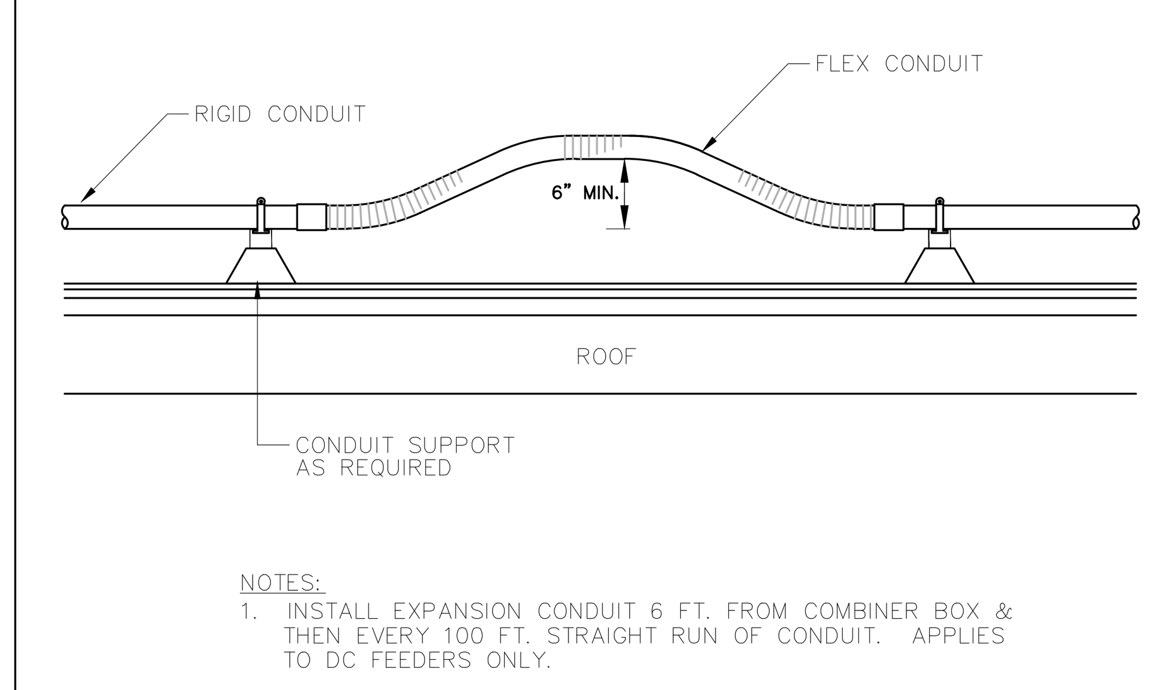

NOTES:
1. INSTALL EXPANSION CONDUIT 6 FT. FROM COMBINER BOX & THEN EVERY 100 FT. STRAIGHT RUN OF CONDUIT. APPLIES TO DC FEEDERS ONLY.

2 PV CONDUIT EXPANSION

NO SCALE

optima engineering

SYMBOL	DESCRIPTION	DATE	BY
3	100 DESIGN SUBMITTAL (NOT FOR CONSTRUCTION)	10/22/2014	A.H
2	65 DESIGN SUBMITTAL (NOT FOR CONSTRUCTION)	09/11/14	KGP
1	35 DESIGN SUBMITTAL (NOT FOR CONSTRUCTION)	06/1/14	A.H

DESIGNED BY: OPTIMA ENGINEERING	DATE: 09/11/2014
DWN BY: A.H / CKD BY: KGP	DPW FILE NO.: XXXXXX
SUBMITTED BY: XXX	ESTCP NO. 13 EB-EW1-104
FILE NAME: XENOTE (2).DGN	
SIZE: ANSI D / PLOT SCALE: AS SHOWN	PLOT DATE: 09/11/2014

NARENCO log horizontal.jpg

ZAPATA TRUST·INTEGRITY·QUALITY

HERCULES PHYSICAL FITNESS CENTER
DC MICROGRID - BLDG P-402
POPE ARMY AIRFIELD, NORTH CAROLINA

4 STRING SUB ARRAY DIAGRAM

PLATE REFERENCE NUMBER
PV-102
SHEET 17 OF 23

INVERTER STRING AND CIRCUIT CALCULATIONS

OF DESIGN: −10 DEGREES CELSIUS

STRING & CIRCUIT CALCULATIONS

STRING OVERCURRENT:

12 MODULES PER SERIES STRING = VOC (37.2V) X 12 = 446.4V
@ ISC (8.87A) PER STRING (15A OCP PER MFR)

MAX SYSTEM VOLTAGE

(37.2V + 4.426) X 12 = 499.52V AT RECORDED LOW TEMP OF −10 DEGREES C
ARRAY WIRE SIZING AND OVERCURRENT:

ISC X 15 STRINGS = (8.87 X 15) X 125% = 166.31A PER NEC 690.8(A)(1), 166.31 X 125% = 207.89A PER 690.8(B)(1) FOR CONDUCTOR SIZING

LABEL PER NEC 690.53

RATED MAXIMUM POWER POINT CURRENT (Imp X #OF STRINGS) = 124.5A

RATED MAXIMUM POWER POINT VOLTAGE (Vmp X #OF PANELS IN SERIES−STRING) = 361.2VDC

MAXIMUM SYSTEM VOLTAGE (TEMP. COMPENSATED) (Voc + Tcoeff) = 499.52V

MAXIMUM SHORT CIRCUIT CURRENT (Isc X 1.25 X #OF STRINGS) = 166.31A

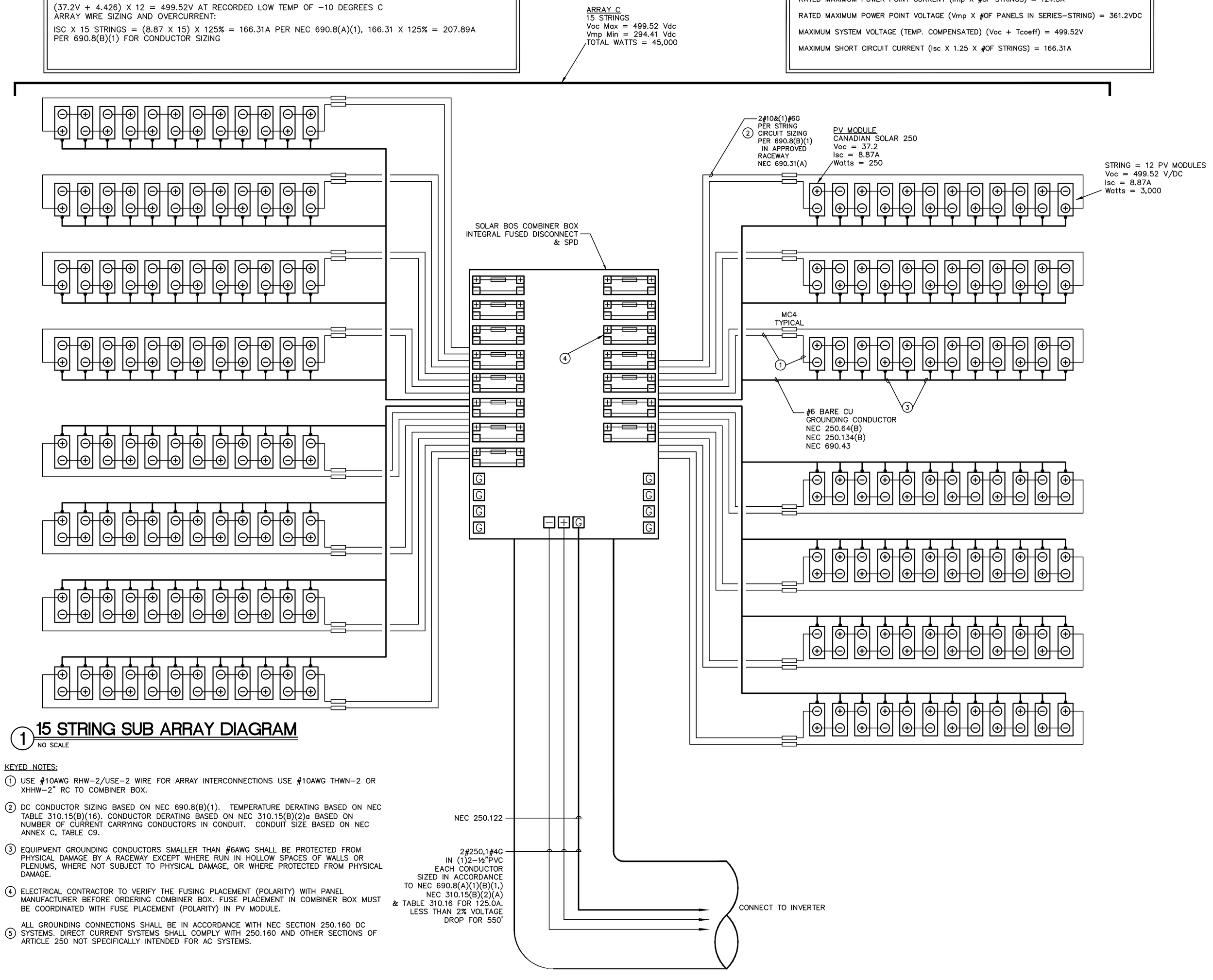

1 15 STRING SUB ARRAY DIAGRAM

NO SCALE

KEYED NOTES:

1. USE #10AWG RHW−2/USE−2 WIRE FOR ARRAY INTERCONNECTIONS USE #10AWG THWN−2 OR XHHW−2" RC TO COMBINER BOX.
2. DC CONDUCTOR SIZING BASED ON NEC 690.8(B)(1). TEMPERATURE DERATING BASED ON NEC TABLE 310.15(B)(16). CONDUCTOR DERATING BASED ON NEC 310.15(B)(2)a BASED ON NUMBER OF CURRENT CARRYING CONDUCTORS IN CONDUIT. CONDUIT SIZE BASED ON NEC ANNEX C, TABLE C9.
3. EQUIPMENT GROUNDING CONDUCTORS SMALLER THAN #6AWG SHALL BE PROTECTED FROM PHYSICAL DAMAGE BY A RACEWAY EXCEPT WHERE RUN IN HOLLOW SPACES OF WALLS OR PLENUMS, WHERE NOT SUBJECT TO PHYSICAL DAMAGE, OR WHERE PROTECTED FROM PHYSICAL DAMAGE.
4. ELECTRICAL CONTRACTOR TO VERIFY THE FUSING PLACEMENT (POLARITY) WITH PANEL MANUFACTURER BEFORE ORDERING COMBINER BOX. FUSE PLACEMENT IN COMBINER BOX MUST BE COORDINATED WITH FUSE PLACEMENT (POLARITY) IN PV MODULE.
5. ALL GROUNDING CONNECTIONS SHALL BE IN ACCORDANCE WITH NEC SECTION 250.160 DC SYSTEMS. DIRECT CURRENT SYSTEMS SHALL COMPLY WITH 250.160 AND OTHER SECTIONS OF ARTICLE 250 NOT SPECIFICALLY INTENDED FOR AC SYSTEMS.

optima engineering
1927 S[illegible] Tr[illegible] S., S[illegible] 300, C[illegible] NC 28203
333 F[illegible] S., S[illegible] 311, R[illegible] NC 27601
Phone: 704-338-1292 • www.optimaengineering.com

NORTH CAROLINA PROFESSIONAL SEAL 15427 ENGINEER KEITH G. PECH
1/29/2016

SYMBOL	DESCRIPTION	DATE	BY
4	100 DESIGN SUBMITTAL (FOR CONSTRUCTION)	01/29/2016	A.H
3	100 DESIGN SUBMITTAL (NOT FOR CONSTRUCTION)	10/22/2014	A.H
2	65 DESIGN SUBMITTAL (NOT FOR CONSTRUCTION)	09/11/14	KGP
1	35 DESIGN SUBMITTAL (NOT FOR CONSTRUCTION)	06/11/14	A.H

DESIGNED BY: OPTIMA ENGINEERING
DWN BY: A.H
CKD BY: KGP
SUBMITTED BY: XXX
FILE NAME: XREFNOTE.DGN
DATE: 01/29/2016
DPW FILE NO.: XXXXXX
ESTCP NO.: 13-EB-EWY-104
SIZE: ANSI D
PLOT SCALE: AS SHOWN
PLOT DATE: 09/11/2014

`.\WARENCO log horizontol.jpg`

ZAPATA TRUST-INTEGRITY-QUALITY
ZAPATA ENGINEERING, P.A.
4908 TOWER OAKS BLVD.
ROCKVILLE, MARYLAND 20852
PHONE: 301.984.8005
FAX: 301.984.8006
E-MAIL: ZAPATA@ZAPATAENGINEERING.COM

HERCULES PHYSICAL FITNESS CENTER
DC MICROGRID - BLDG P-402
POPE ARMY AIRFIELD, NORTH CAROLINA

15 STRING SUB ARRAY DIAGRAM

PLATE REFERENCE NUMBER
PV-104
SHEET 5 OF 7

OPTIMA #: 14-0386

INVERTER STRING AND CIRCUIT CALCULATIONS

OF DESIGN: −10 DEGREES CELSIUS

STRING & CIRCUIT CALCULATIONS

STRING OVERCURRENT:

12 MODULES PER SERIES STRING = VOC (37.2V) X 12 = 446.4V
@ ISC (8.87A) PER STRING (15A OCP PER MFR)

MAX SYSTEM VOLTAGE

(37.2V + 4.426) X 12 = 499.52V AT RECORDED LOW TEMP OF −10 DEGREES C
ARRAY WIRE SIZING AND OVERCURRENT:
ISC X 11 STRINGS = (8.87 X 11) X 125% = 121.96A PER NEC 690.8(A)(1), 121.96 X 125% = 152.45A
PER 690.8(B)(1) FOR CONDUCTOR SIZING

LABEL PER NEC 690.53

RATED MAXIMUM POWER POINT CURRENT (Imp X #OF STRINGS) = 91.3A

RATED MAXIMUM POWER POINT VOLTAGE (Vmp X #OF PANELS IN SERIES−STRING) = 361.2VDC

MAXIMUM SYSTEM VOLTAGE (TEMP. COMPENSATED) (Voc + Tcoeff) = 499.52V

MAXIMUM SHORT CIRCUIT CURRENT (Isc X 1.25 X #OF STRINGS) = 121.96A

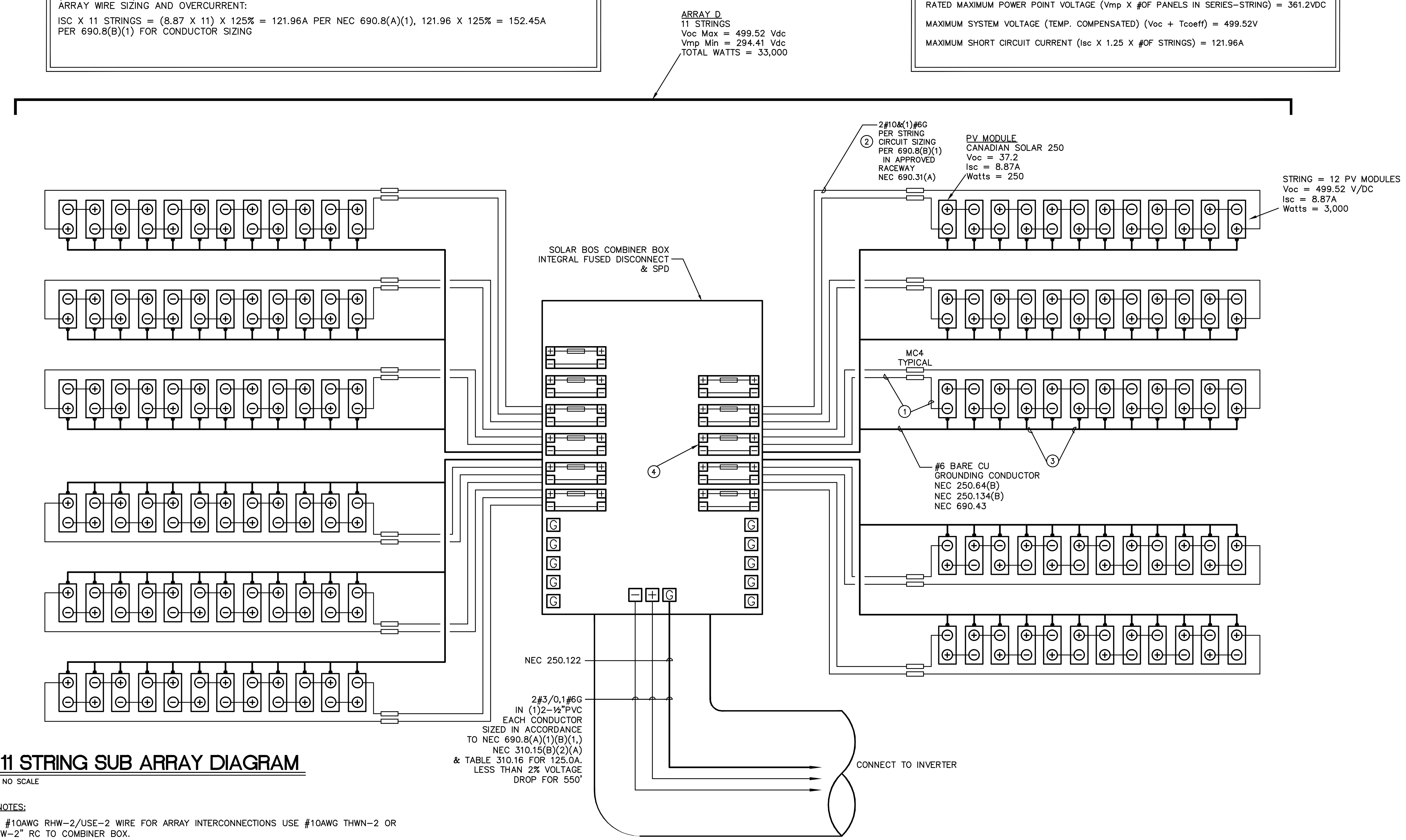

(1) 11 STRING SUB ARRAY DIAGRAM

NO SCALE

KEYED NOTES:

1. USE #10AWG RHW−2/USE−2 WIRE FOR ARRAY INTERCONNECTIONS USE #10AWG THWN−2 OR XHHW−2" RC TO COMBINER BOX.
2. DC CONDUCTOR SIZING BASED ON NEC 690.8(B)(1). TEMPERATURE DERATING BASED ON NEC TABLE 310.15(B)(16). CONDUCTOR DERATING BASED ON NEC 310.15(B)(2)a BASED ON NUMBER OF CURRENT CARRYING CONDUCTORS IN CONDUIT. CONDUIT SIZE BASED ON NEC ANNEX C, TABLE C9.
3. EQUIPMENT GROUNDING CONDUCTORS SMALLER THAN #6AWG SHALL BE PROTECTED FROM PHYSICAL DAMAGE BY A RACEWAY EXCEPT WHERE RUN IN HOLLOW SPACES OF WALLS OR PLENUMS, WHERE NOT SUBJECT TO PHYSICAL DAMAGE, OR WHERE PROTECTED FROM PHYSICAL DAMAGE.
4. ELECTRICAL CONTRACTOR TO VERIFY THE FUSING PLACEMENT (POLARITY) WITH PANEL MANUFACTURER BEFORE ORDERING COMBINER BOX. FUSE PLACEMENT IN COMBINER BOX MUST BE COORDINATED WITH FUSE PLACEMENT (POLARITY) IN PV MODULE.
5. ALL GROUNDING CONNECTIONS SHALL BE IN ACCORDANCE WITH NEC SECTION 250.160 DC SYSTEMS. DIRECT CURRENT SYSTEMS SHALL COMPLY WITH 250.160 AND OTHER SECTIONS OF ARTICLE 250 NOT SPECIFICALLY INTENDED FOR AC SYSTEMS.

optima engineering
1927 S... Tr... S..., S... 300, C... NC 28203
333 F... S..., S... 311, R... NC 27601
Phone: 704-338-1292 • www.optimaengineering.com

NORTH CAROLINA PROFESSIONAL ENGINEER SEAL 15427 KEITH G. PEHL 1/29/2016

SYMBOL	DESCRIPTION	DATE	BY
4	100% DESIGN SUBMITTAL (FOR CONSTRUCTION)	01/29/2016	A.H
3	100% DESIGN SUBMITTAL (NOT FOR CONSTRUCTION)	10/22/2014	A.H
2	65% DESIGN SUBMITTAL (NOT FOR CONSTRUCTION)	09/11/14	KGP
1	35% DESIGN SUBMITTAL (NOT FOR CONSTRUCTION)	06/1/14	A.H

DESIGNED BY: OPTIMA ENGINEERING		DATE: 01/29/2016
DWN BY: A.H	CKD BY: KGP	DPW FILE NO.: XXXXXX
SUBMITTED BY: XXX		ESTCP NO. 13 EB-EW1-104
FILE NAME: XENOTE.DGN		
SIZE: ANSI D	PLOT SCALE: AS SHOWN	PLOT DATE: 09/11/2014

.\NARENCO log horizontal.jpg

ZAPATA TRUST • INTEGRITY • QUALITY

HERCULES PHYSICAL FITNESS CENTER
DC MICROGRID - BLDG P-402
POPE ARMY AIRFIELD, NORTH CAROLINA

9 STRING SUB ARRAY
DIAGRAM

PLATE REFERENCE NUMBER
PV-103
SHEET 4 OF 7
OPTIMA #: 14-0386

INVERTER STRING AND CIRCUIT CALCULATIONS

OF DESIGN: −10 DEGREES CELSIUS

STRING & CIRCUIT CALCULATIONS

STRING OVERCURRENT:

12 MODULES PER SERIES STRING = VOC (37.2V) X 12 = 446.4V
@ ISC (8.87A) PER STRING (15A OCP PER MFR)

MAX SYSTEM VOLTAGE

(37.2V + 4.426) X 12 = 499.52V AT RECORDED LOW TEMP OF −10 DEGREES C
ARRAY WIRE SIZING AND OVERCURRENT:
ISC X 10 STRINGS = (8.87 X 10) X 125% = 110.88A PER NEC 690.8(A)(1), 110.88 X 125% = 138.59A
PER 690.8(B)(1) FOR CONDUCTOR SIZING

LABEL PER NEC 690.53

RATED MAXIMUM POWER POINT CURRENT (Imp X #OF STRINGS) = 83A

RATED MAXIMUM POWER POINT VOLTAGE (Vmp X #OF PANELS IN SERIES−STRING) = 361.2VDC

MAXIMUM SYSTEM VOLTAGE (TEMP. COMPENSATED) (Voc + Tcoeff) = 499.52V

MAXIMUM SHORT CIRCUIT CURRENT (Isc X 1.25 X #OF STRINGS) = 110.88A

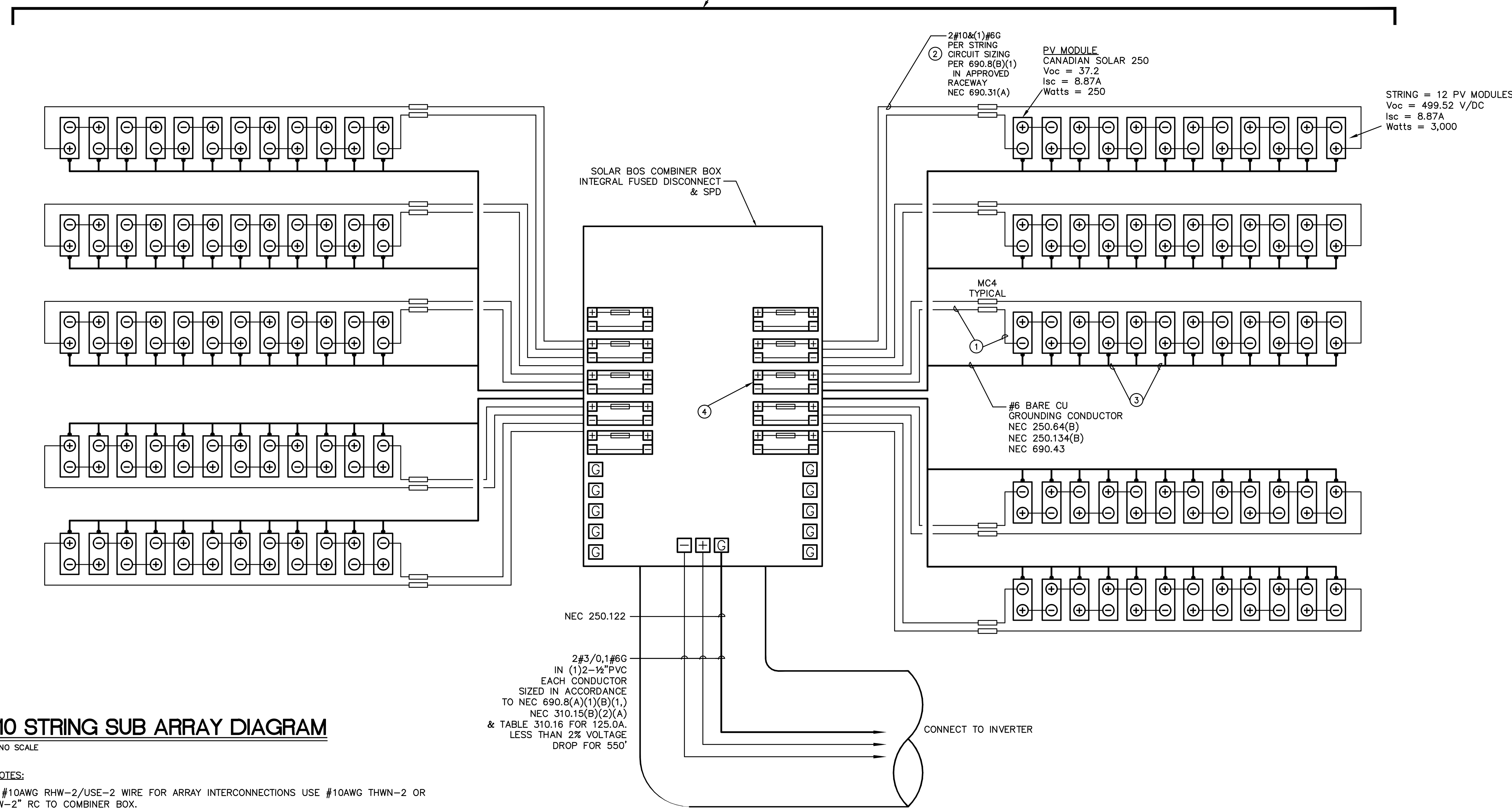

(1) 10 STRING SUB ARRAY DIAGRAM

NO SCALE

KEYED NOTES:

1. USE #10AWG RHW−2/USE−2 WIRE FOR ARRAY INTERCONNECTIONS USE #10AWG THWN−2 OR XHHW−2" RC TO COMBINER BOX.
2. DC CONDUCTOR SIZING BASED ON NEC 690.8(B)(1). TEMPERATURE DERATING BASED ON NEC TABLE 310.15(B)(16). CONDUCTOR DERATING BASED ON NEC 310.15(B)(2)a BASED ON NUMBER OF CURRENT CARRYING CONDUCTORS IN CONDUIT. CONDUIT SIZE BASED ON NEC ANNEX C, TABLE C9.
3. EQUIPMENT GROUNDING CONDUCTORS SMALLER THAN #6AWG SHALL BE PROTECTED FROM PHYSICAL DAMAGE BY A RACEWAY EXCEPT WHERE RUN IN HOLLOW SPACES OF WALLS OR PLENUMS, WHERE NOT SUBJECT TO PHYSICAL DAMAGE, OR WHERE PROTECTED FROM PHYSICAL DAMAGE.
4. ELECTRICAL CONTRACTOR TO VERIFY THE FUSING PLACEMENT (POLARITY) WITH PANEL MANUFACTURER BEFORE ORDERING COMBINER BOX. FUSE PLACEMENT IN COMBINER BOX MUST BE COORDINATED WITH FUSE PLACEMENT (POLARITY) IN PV MODULE.
5. ALL GROUNDING CONNECTIONS SHALL BE IN ACCORDANCE WITH NEC SECTION 250.160 DC SYSTEMS. DIRECT CURRENT SYSTEMS SHALL COMPLY WITH 250.160 AND OTHER SECTIONS OF ARTICLE 250 NOT SPECIFICALLY INTENDED FOR AC SYSTEMS.

optima engineering
Phone: 704-338-1292 • www.optimaengineering.com
NORTH CAROLINA PROFESSIONAL ENGINEER SEAL 15437 KEITH G. PEHL 1/29/2016

SYMBOL	DESCRIPTION	DATE	BY
4	100 DESIGN SUBMITTAL (FOR CONSTRUCTION)	01/29/2016	A.H
3	100 DESIGN SUBMITTAL (NOT FOR CONSTRUCTION)	10/22/2014	A.H
2	65 DESIGN SUBMITTAL (NOT FOR CONSTRUCTION)	09/11/14	KGP
1	35 DESIGN SUBMITTAL (NOT FOR CONSTRUCTION)	06/1/14	A.H

.\NARENCO log horizontal.jpg

ZAPATA TRUST·INTEGRITY·QUALITY

DESIGNED BY: OPTIMA ENGINEERING		DATE: 01/29/2016
DWN BY: A.H	CKD BY: KGP	DPW FILE NO.: XXXXXX
SUBMITTED BY: XXX		ESTCP NO. 13 EB-EW1-104
FILE NAME: XENOTE.DGN		
SIZE: ANSI D	PLOT SCALE: AS SHOWN	PLOT DATE: 09/11/2014

HERCULES PHYSICAL FITNESS CENTER
DC MICROGRID - BLDG P-402
POPE ARMY AIRFIELD, NORTH CAROLINA

6 STRING SUB ARRAY DIAGRAM

PLATE REFERENCE NUMBER
PV-102
SHEET 3 OF 7
OPTIMA #: 14-0386

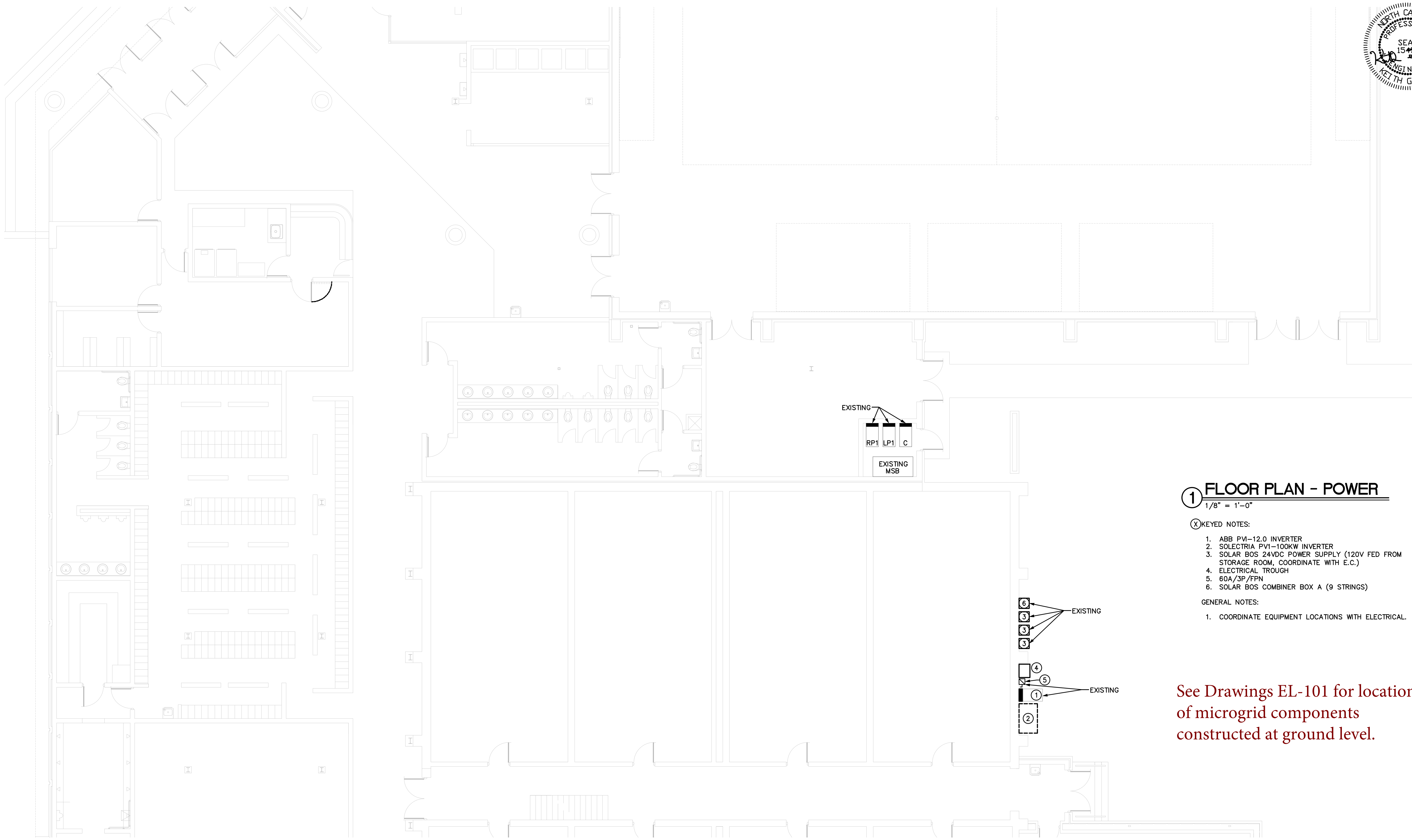

① FLOOR PLAN - POWER
1/8" = 1'-0"

ⓧ KEYED NOTES:

1. ABB PVI-12.0 INVERTER
2. SOLECTRIA PVI-100KW INVERTER
3. SOLAR BOS 24VDC POWER SUPPLY (120V FED FROM STORAGE ROOM, COORDINATE WITH E.C.)
4. ELECTRICAL TROUGH
5. 60A/3P/FPN
6. SOLAR BOS COMBINER BOX A (9 STRINGS)

GENERAL NOTES:

1. COORDINATE EQUIPMENT LOCATIONS WITH ELECTRICAL.

See Drawings EL-101 for location of microgrid components constructed at ground level.

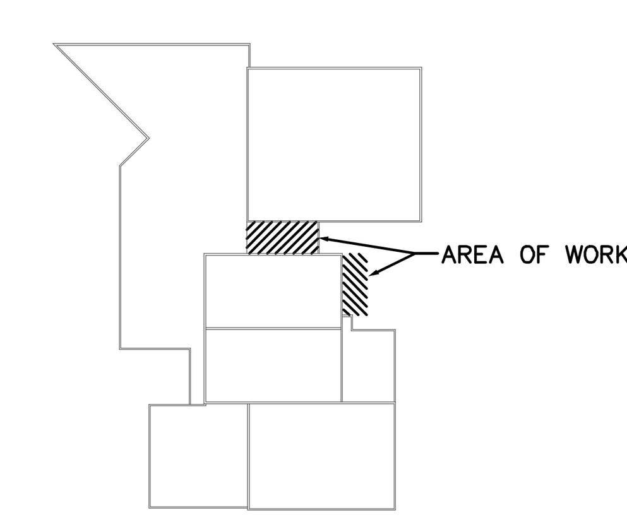

① KEY PLAN
NTS

TRUE NORTH

PLAN NORTH

optima engineering
1927 S. Tryon St., Suite 300, Charlotte, NC 28203
333 Fayetteville St., Suite 311, Raleigh, NC 27601
Phone: 704-338-1292 • www.optimaengineering.com

NORTH CAROLINA PROFESSIONAL ENGINEER SEAL 15137 KEITH G. PEHL 1/29/2016

SYMBOL	DESCRIPTION	DATE	BY
4	100 DESIGN SUBMITTAL (FOR CONSTRUCTION)	01/29/2016	A.H
3	100 DESIGN SUBMITTAL (NOT FOR CONSTRUCTION)	10/22/2014	A.H
2	65 DESIGN SUBMITTAL (NOT FOR CONSTRUCTION)	09/11/14	KGP
1	35 DESIGN SUBMITTAL (NOT FOR CONSTRUCTION)	06/1/14	A.H

DESIGNED BY: OPTIMA ENGINEERING		DATE: 01/29/2016
DWN BY: A.H	CKD BY: KGP	DPW FILE NO.: XXXXXX
SUBMITTED BY: XXX		ESTCP NO. 13 EB-EW1-104
FILE NAME: XEPWR.DGN		
SIZE: ANSI D	PLOT SCALE: AS SHOWN	PLOT DATE: 09/11/2014

.\NARENCO log horizontal.jpg

ZAPATA TRUST • INTEGRITY • QUALITY

HERCULES PHYSICAL FITNESS CENTER
DC MICROGRID - BLDG P-402
POPE ARMY AIRFIELD, NORTH CAROLINA

FLOOR PLAN - ELECTRICAL

PLATE REFERENCE NUMBER
PV-201
SHEET 6 OF 7
OPTIMA #: 14-0386

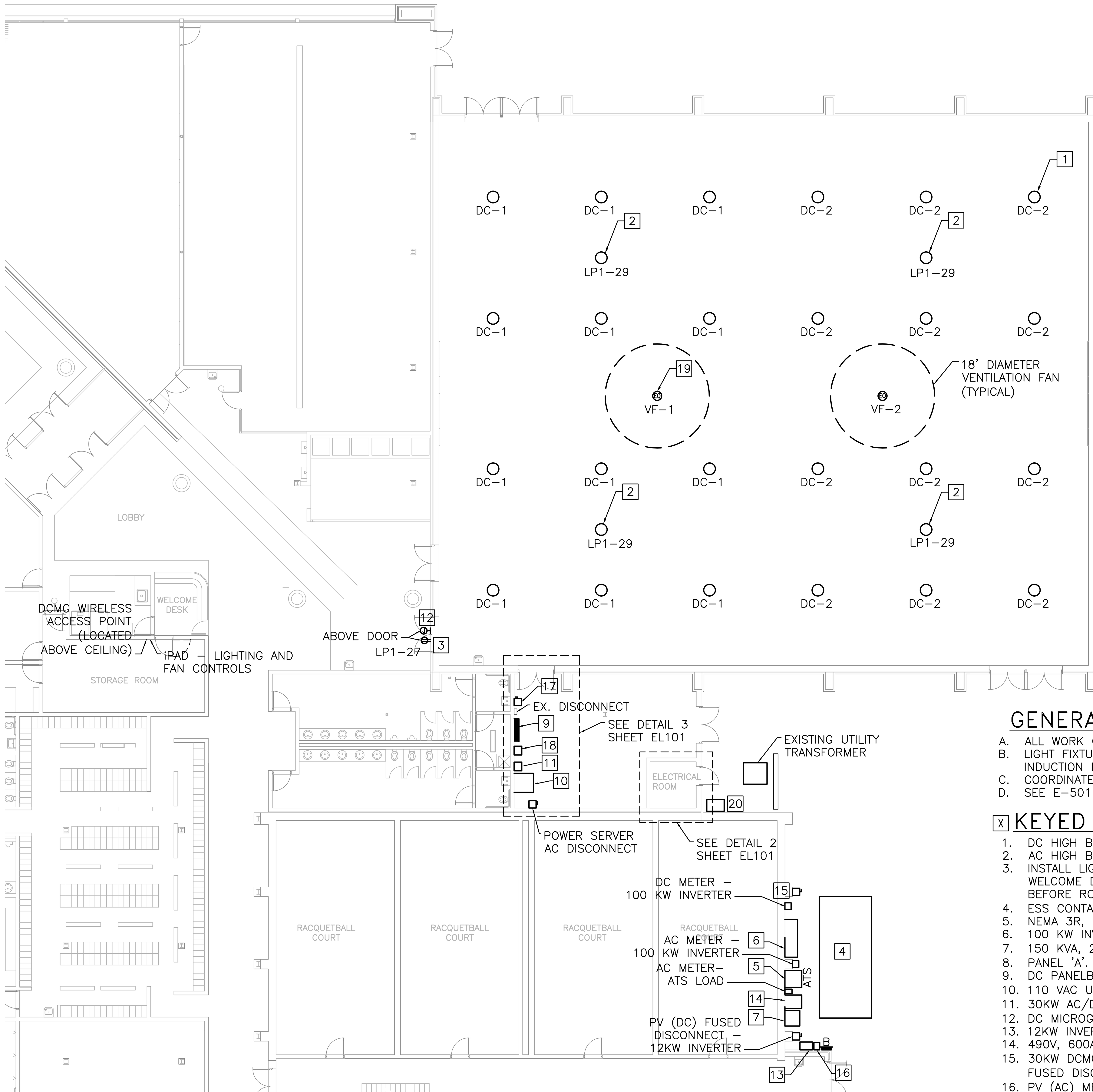

1 ELECTRICAL - GYMNASIUM FLOOR PLAN - LIGHTING

SCALE: 3/32" = 1'-0"

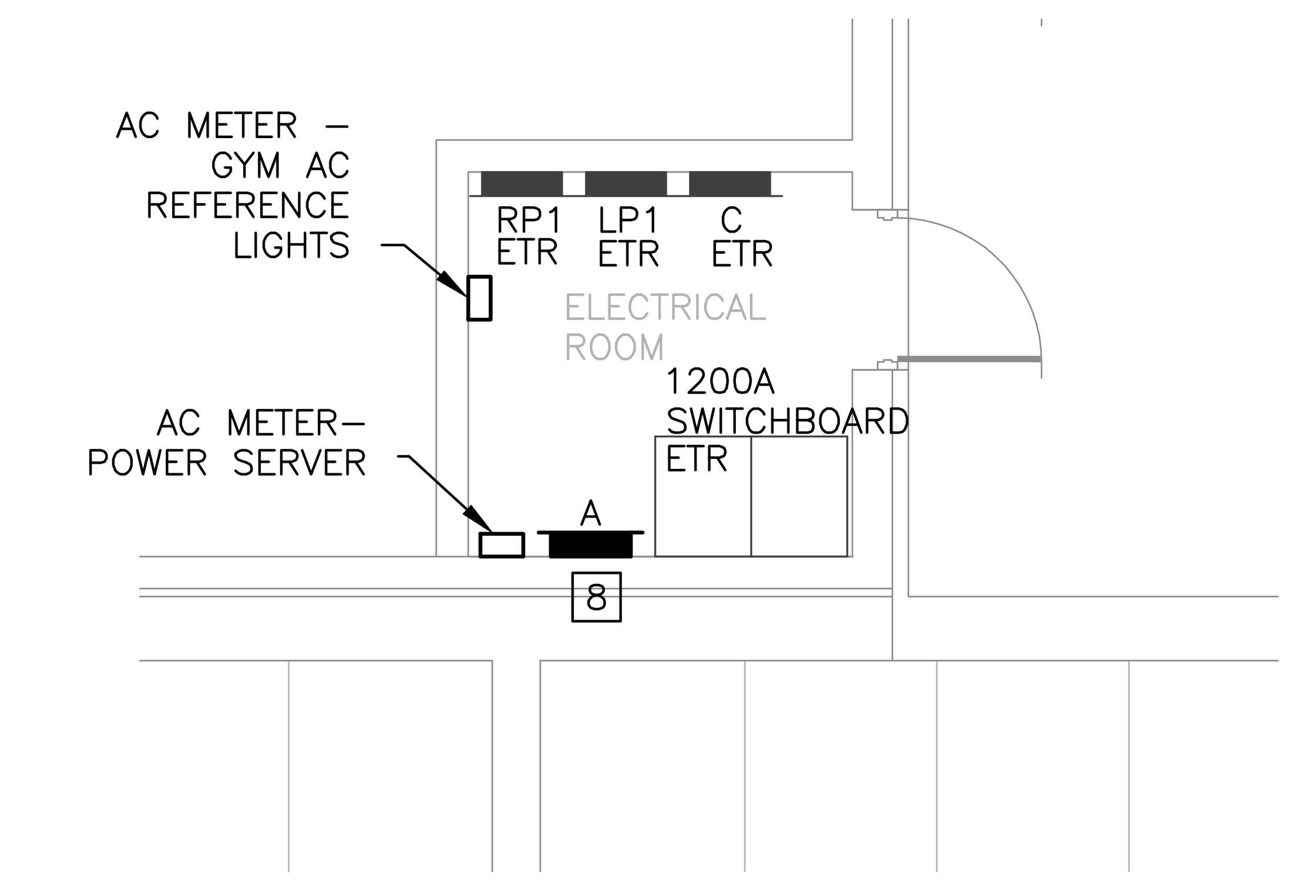

2 ELECTRICAL - EXISTING ENLARGED ELECTRICAL ROOM PLAN

SCALE: 1/4" = 1'-0"

INSTALL ELECTRICAL EQUIPMENT IN AS SMALL A SPACE AS POSSIBLE.

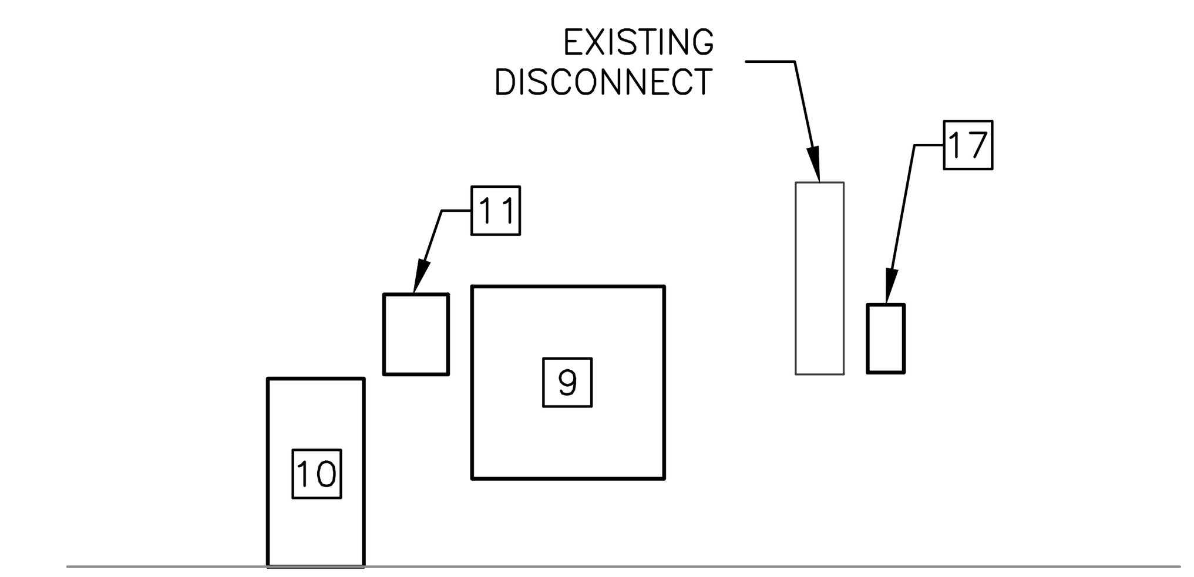

3 ELECTRICAL - ELEVATION OF STORAGE ROOM WALL

SCALE: 1/4" = 1'-0"

GENERAL NOTES:

A. ALL WORK ON THIS SHEET IS PERFORMED DURING PHASE 1.
B. LIGHT FIXTURES ARE MANUFACTURED BY EVERLAST LIGHTING, SERIES EHBUS WITH 250W INDUCTION LAMPS.
C. COORDINATE EXACT LOCATION OF ALL EQUIPMENT WITH THE GOVERNMENT BEFORE ROUGH-IN.
D. SEE E-501 FOR DC CONNECTION TO FANS.

X KEYED NOTES:

1. DC HIGH BAY INDUCTION LIGHT FIXTURE, TYPICAL OF 24.
2. AC HIGH BAY INDUCTION LIGHT FIXTURE IS EQUIVALENT TO THE DC VERSION.
3. INSTALL LIGHTING AND FAN CONTROLS IN THE STORAGE ROOM BEHIND THE WELCOME DESK IN THE LOBBY. COORDINATE EXACT LOCATION WITH GOVERNMENT BEFORE ROUGH-IN.
4. ESS CONTAINER (BY BOSCH).
5. NEMA 3R, 3 POLE, AUTOMATIC TRANSFER SWITCH
6. 100 KW INVERTER.
7. 150 KVA, 208/480 STEP UP TRANSFORMER.
8. PANEL 'A'.
9. DC PANELBOARD AND METERING.
10. 110 VAC UPS (FROM BESS).
11. 30KW AC/DC POWER SERVER.
12. DC MICROGRID DISPLAY (BY BOSCH)
13. 12KW INVERTER. MOUNT ON WALL NEXT TO 100KW INVERTER.
14. 490V, 600A, 3P, NEMA 3R FUSED DISCONNECT. FUSE PER NAMEPLATE.
15. 30KW DCMG PV FUSED DISCONNECT REMOTE/MANUAL (TOP). 30KW PV MANUAL FUSED DISCONNECT (BOTTOM).
16. PV (AC) METER - 12KW INVERTER.
17. 60-AMP, 3-POLE, NEMA-12 FUSED DISCONNECT. FUSED PER NAMEPLATE.
18. ENERGY MANAGEMENT GATEWAY PLC PANEL.
19. DC VENTILATION FAN WITH AC LIGHT (TYPICAL OF 2). FAN AND LIGHT WILL INITIALLY BE SERVED BY AN AC SOURCE. FANS WILL BE CONVERTED TO DC POWER ONCE THE DC MICROGRID IS INSTALLED AND ONLINE. CONDUCTORS SHALL BE REUSED ONCE DC EQUIPMENT IS INSTALLED. NETWORK CABLE IS REQUIRED FOR CONTROLS, COORDINATE INSTALLATION REQUIREMENTS WITH CONTROLS DESIGNER.
20. EXISTING BUILDING ATS.

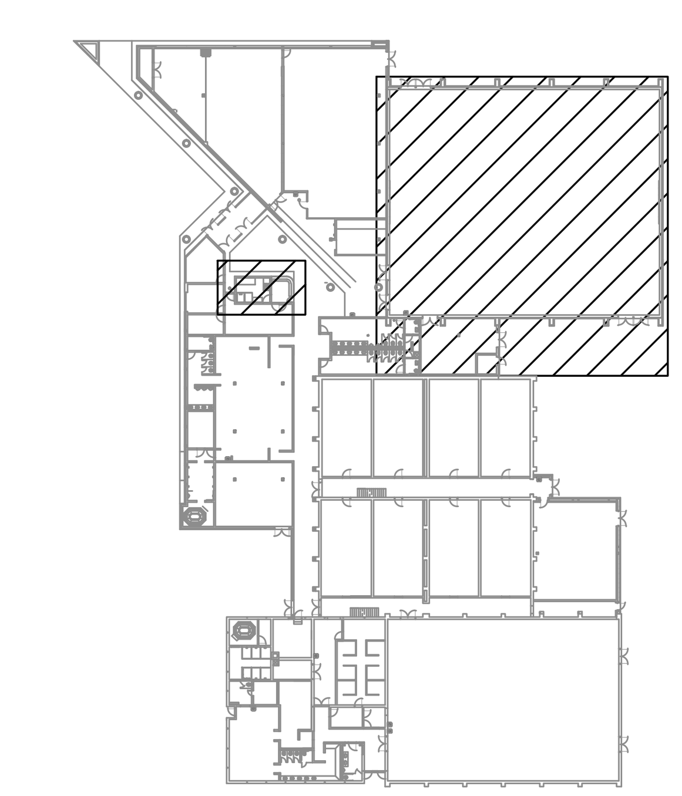

KEYPLAN

NO SCALE:

TRUE NORTH   PLAN NORTH

GRAPHIC SCALE 1/8" = 1'-0"

0 4' 8' 16'

RECORD DRAWING

THIS DRAWING REPRESENTS THE FINAL CONSTRUCTION CONDITIONS, BASED ON FIELD OBSERVATIONS AND/OR OTHER INFORMATION PROVIDED BY THE CONTRACTOR WHICH HAS NOT BEEN VERIFIED BY THE P.E. THE WORK SHOWN ON THIS "RECORD DRAWING" HAS BEEN CONSTRUCTED IN SUBSTANTIAL COMPLIANCE WITH THE PLANS, SPECIFICATIONS, REVISIONS, CHANGE ORDERS AND FIELD CHANGES.

SYMBOL	DESCRIPTION	DATE	BY
1	AS-BUILT DRAWINGS	01/13/2017	

DESIGNED BY: ZAPATA		DATE: 01/19/2017
DWN BY:	CKD BY:	DPW FILE NO.: XXXXXX
SUBMITTED BY: M. CLINE		ESTCP NO. 13 EB-EW1-104
FILE NAME: EL101.DGN		
SIZE: ANSI D	PLOT SCALE: AS SHOWN	PLOT DATE: 01/19/2017

ZAPATA TRUST·INTEGRITY·QUALITY

HERCULES PHYSICAL FITNESS CENTER
DC MICROGRID - BLDG P-402
POPE ARMY AIRFIELD, NORTH CAROLINA

ELECTRICAL - GYMNASIUM FLOOR PLAN - LIGHTING

PLATE REFERENCE NUMBER
EL101
SHEET 9

optima engineering
1927 S[illegible] Tr[illegible] S., S[illegible] 300, C[illegible] NC 28203
333 F[illegible] S., S[illegible] 311, R[illegible] NC 27601
Phone: 704-338-1292 • www.optimaengineering.com

NORTH CAROLINA PROFESSIONAL SEAL 15427 ENGINEER KEITH G. PEHL
1/29/2016

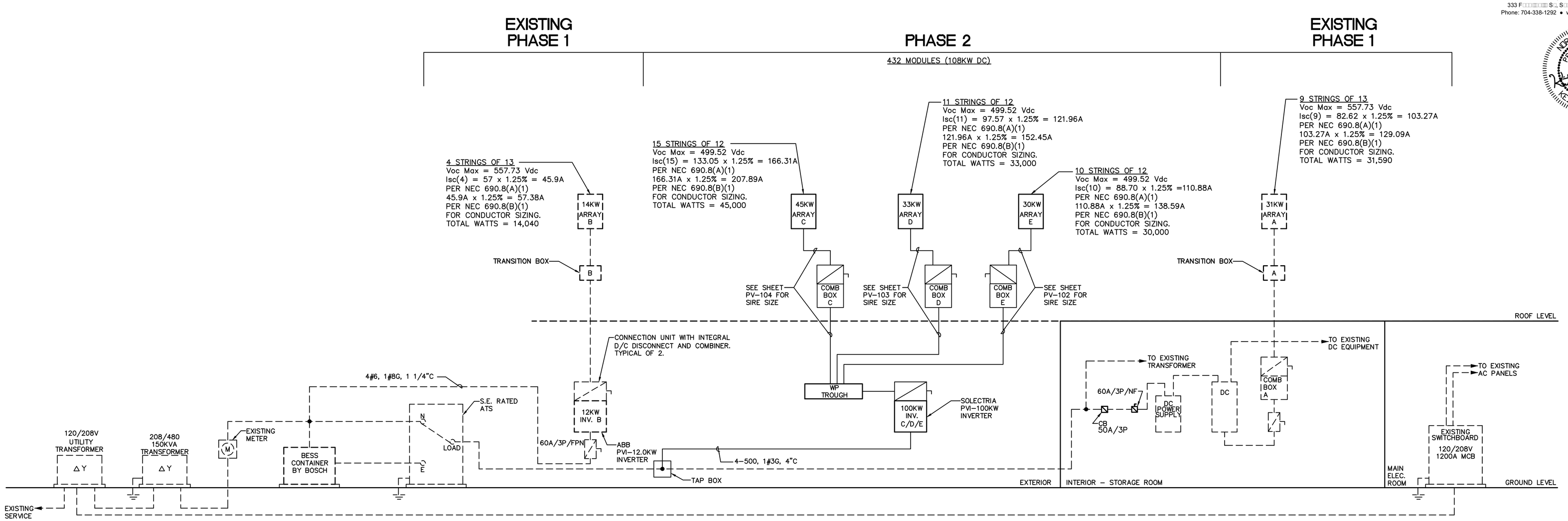

1 POWER RISER DIAGRAM
NO SCALE

NOTES:

1. ARRAYS A & B ARE PHASE 1
2. ARRAYS C, D, & E ARE PHASE 2.
3. ALL DASHED ITEMS ARE EXISTING TO REMAIN.

GENERAL NOTES:

1. ALL SUPPLIED EQUIPMENT SHALL BE UL LISTED.
2. IF DISTANCE FROM SOLAR ARRAY TO EXISTING EARTH GROUND IS GREATER THAN 100 FT. BOND SOLAR MODULE FRAMES TO SUPPLEMENTAL 8FT COPPER GROUND ROD DRIVEN AT CLOSEST POINT TO SOLAR ARRAY.
3. ALL WORK SHALL COMPLY WITH NC BUILDING CODE AND NEC 690. INSTALLER SHALL FOLLOW NEC 2011 ARTICLE 690.
4. ALL DC WIRING SHALL BE COLOR CODED: NEUTRALS SHALL BE WHITE, POSITIVE UNGROUNDED CONDUCTORS SHALL BE RED, AND NEGATIVE UNGROUNDED CONDUCTORS SHALL BE BLACK.
5. AC & DC DISCONNECTS SHALL BE IN COMPLIANCE WITH NEC 690.17.
6. DC DISCONNECT LOCATION SHALL BE IN COMPLIANCE WITH NEC 690.14(C)1. READILY ACCESSIBLE.
7. EACH COMBINER BOX SHALL BE LABELED WITH NAMEPLATE IDENTIFYING THE SUB ARRAY DESIGNATION, NAMEPLATE SHALL BE RED WITH WHITE LETTERS & A MINIMUM 3" IN HEIGHT. EX. SUB-A1.
8. SHORT CIRCUIT STUDY AND PROTECTION DEVICE COORDINATION WILL BE BASED ON FINAL CONDITIONS AND FAULT CONTRIBUTIONS INFORMATION.
9. CONTRACTOR SHALL VERIFY TAP CONNECTION FOR COMPLIANCE WITH NEC AT 100KW INVERTER.

CONDUIT SIZING (PVC TYPE A)				
WIRE SIZE THHN (AWG)	1"	1¼"	1½"	–
10	20	33	44	–
4	5	8	11	–
	# OF CONDUCTORS			

CONDUCTOR SIZING		
WIRE SIZE (AWG)	THHN Cu. @ 90°C	70% 7-9 CURRENT CARRYING CONDUCTORS
12	40A	28A
10	55A	38.5A
8	80A	56A
6	105A	73.5A
4	140A	98A
1	220A	154A
1/0	260A	182A
2/0	300A	210A

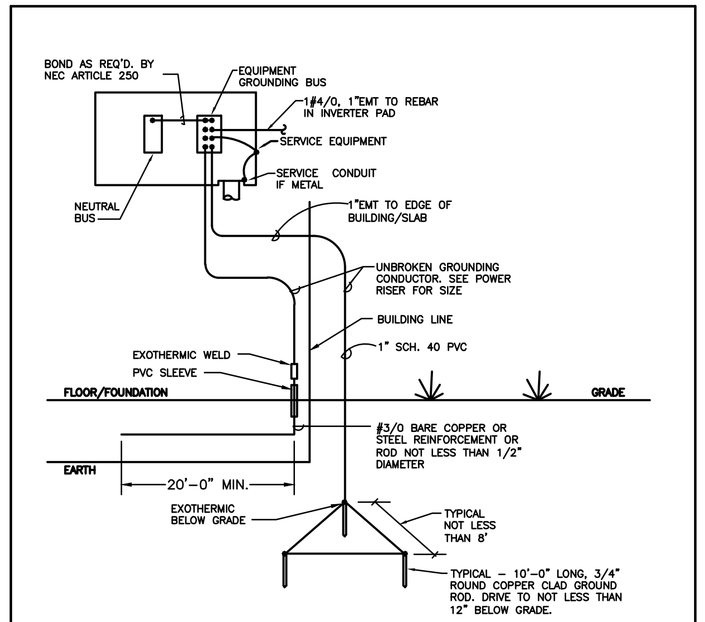

2 SERVICE GROUND DETAIL
NO SCALE

SYMBOL	DESCRIPTION	DATE	BY
4	100 DESIGN SUBMITTAL (FOR CONSTRUCTION)	01/29/2016	A. H
3	100 DESIGN SUBMITTAL (NOT FOR CONSTRUCTION)	10/22/2014	A. H
2	65 DESIGN SUBMITTAL (NOT FOR CONSTRUCTION)	09/11/14	KGP
1	35 DESIGN SUBMITTAL (NOT FOR CONSTRUCTION)	06/11/14	A. H

DESIGNED BY: OPTIMA ENGINEERING
DWN BY: A. H
CKD BY: KGP
SUBMITTED BY: XXX
FILE NAME: XEL-NOTE1.DGN
SIZE: ANSI D
DATE: 01/29/2016
DPW FILE NO.: XXXXXX
ESTCP NO. 13-EB-EW1-104
PLOT SCALE: AS SHOWN
PLOT DATE: 09/11/2014

\\WARENCO log horizontal.jpg

ZAPATA TRUST • INTEGRITY • QUALITY
ZAPATA ENGINEERING, P.A. 4601 CHARLOTTE PARK DRIVE, SUITE 310 CHARLOTTE, NC 28217 PHONE: 704.525.1560 FAX: 704.525.0409 E-MAIL: INFO@ZAPATAENGINEERING.COM

HERCULES PHYSICAL FITNESS CENTER
DC MICROGRID - BLDG P-402
POPE ARMY AIRFIELD, NORTH CAROLINA

POWER RISER DIAGRAM

PLATE REFERENCE NUMBER
PV-101
SHEET 2 OF 7
OPTIMA #: 14-0386

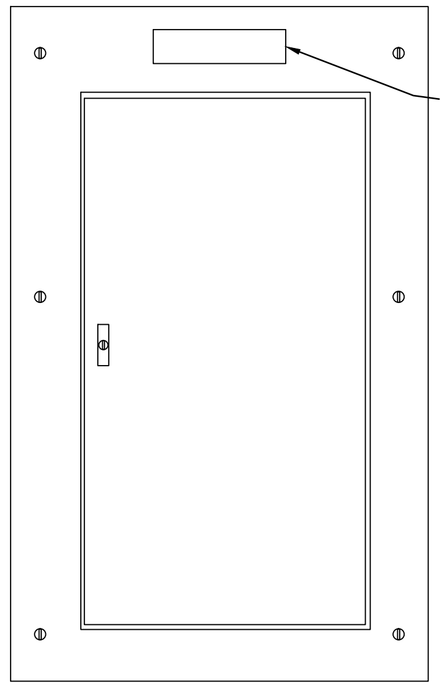

NOTE:
ELECTRICAL CONTRACTOR SHALL IDENTIFY AS SHOWN ABOVE ALL ELECTRICAL PANELS (EXISTING AND NEW) INVOLVED IN THIS PROJECT.

ELECTRICAL PANEL DESIGNATION DETAIL
NO SCALE

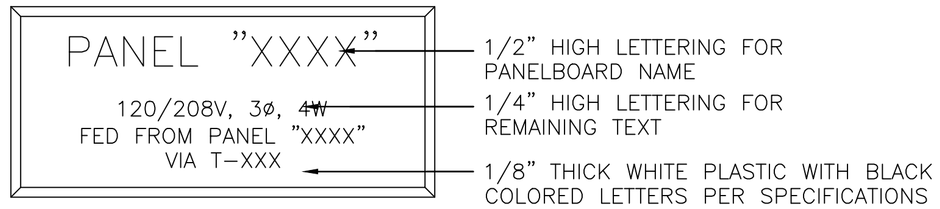

TYPICAL 120/208V PANELBOARD

PANELBOARD NAMEPLATE DETAIL
NO SCALE

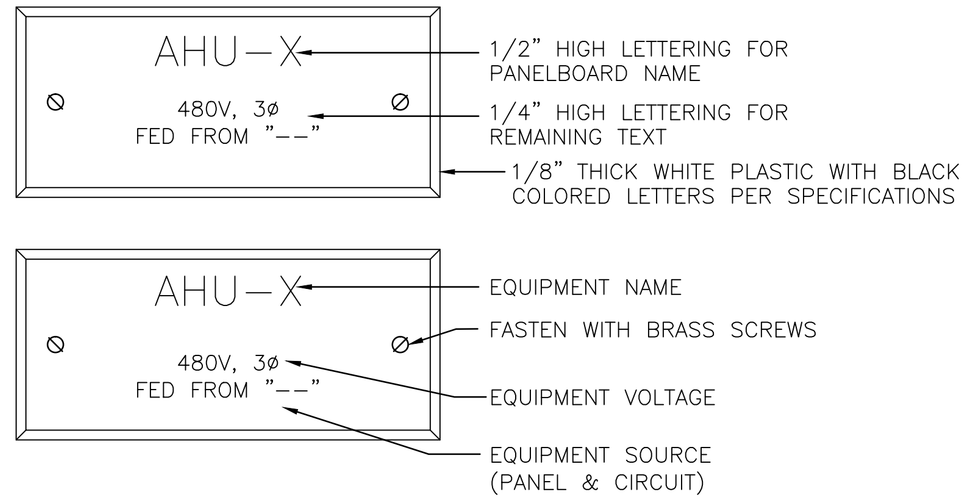

EQUIPMENT NAMEPLATE DETAIL
NO SCALE

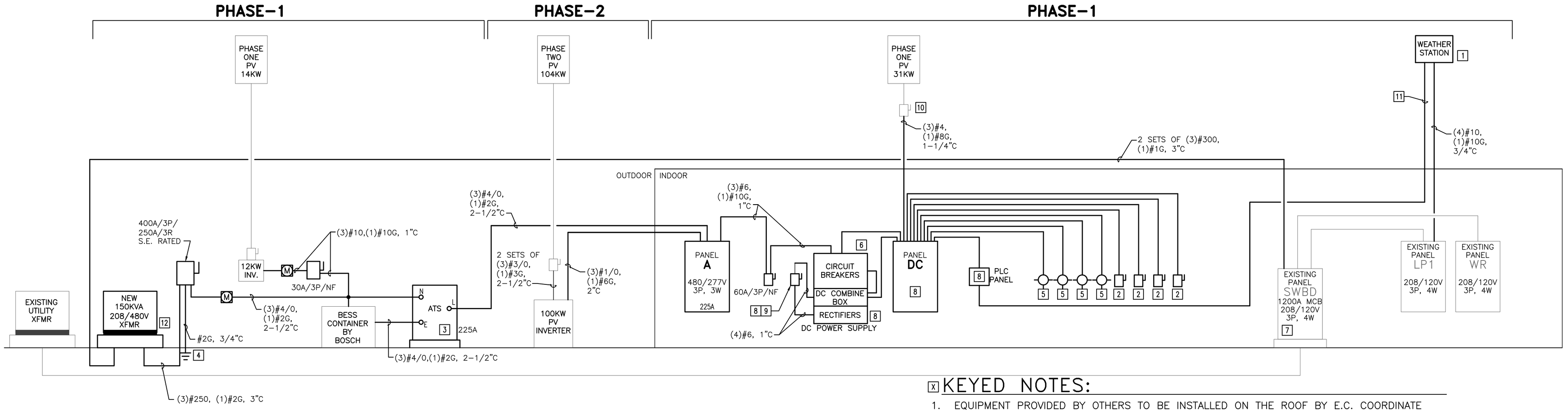

PARTIAL POWER RISER DIAGRAM
NO SCALE

GENERAL NOTES:

A. ALL EQUIPMENT SHOWN DARK SHALL BE PROVIDED AND INSTALLED BY THE E.C., UNLESS OTHERWISE NOTED.
B. ALL DC CONNECTIONS SHALL BE ISOLATED FROM EARTH GROUND.
C. E.C. SHALL PROVIDE CONTROL WIRING FROM THE PV COMBINER BOXES/DISCONNECTS AND CONNECT TO THE DC MICROGRID PLC.
D. ALL COMMUNICATION WIRES SHALL BE TWISTED SHIELDED PAIRS.

[X] KEYED NOTES:

1. EQUIPMENT PROVIDED BY OTHERS TO BE INSTALLED ON THE ROOF BY E.C. COORDINATE EXACT LOCATION WITH PV INSTALLER TO AVOID AFFECTING THEIR SYSTEMS.
2. VENTILATION FAN DISCONNECT. PROVIDE A LABEL THAT STATES "THIS EQUIPMENT IS PART OF THE DC MICROGRID WHICH USES AC AND DC EQUIPMENT. PRIOR TO ANY MAINTENANCE OR REPAIRS, CONTACT DPW OMD ENERGY GROUP AT (910) 396-0321. FEED EACH FAN WITH (3)#10, (1)#10G, 3/4"C.
3. PROVIDE A NEMA 3R, 3 POLE, AUTOMATIC TRANSFER SWITCH.
4. TIE TO EXISTING BUILDING GROUND.
5. DC LIGHTING CIRCUITS. FEED EACH LIGHTING CIRCUIT WITH (4)#10, (1)#10G, 3/4"C.
6. THERE ARE MULTIPLE CONNECTIONS BETWEEN THE DC PANEL AND DC POWER SUPPLY. THE PV POWER IS METERED IN THE DC PANEL, THEN CONNECTED TO THE DC COMBINE BOX IN THE DC POWER SUPPLY. THE OUTPUTS FROM THE CIRCUIT BREAKERS IN THE DC POWER SUPPLY ARE CONNECTED TO THE DC PANEL FOR MONITORING. SEE BOSCH CONTROL SCHEMATICS FOR ADDITIONAL DETAIL.
7. PROVIDE NEW 600A, 3 POLE BREAKER IN AVAILABLE SPACE. MATCH EXISTING PANEL RATINGS.
8. EQUIPMENT PROVIDED BY OTHERS TO BE INSTALLED BY E.C.
9. (4) POLE, 35KW, DC DISCONNECT FOR POWER SUPPLY. PROVIDE 55 AMP DC FUSES FOR EACH POLE.
10. DISCONNECT MOUNTED AT GROUND LEVEL. PV INSTALLER SHALL TERMINATE PV INPUTS AT COMBINER, E.C. SHALL PROVIDE WIRING FROM COMBINER OUTPUT TO DC PANEL.
11. PROVIDE 1"C WITH PULLSTRING FOR INSTALLATION OF COMMUNICATIONS CABLING BY OTHERS.
12. PROVIDE A WYE-DELTA TRANSFORMER.

RECORD DRAWING
THIS DRAWING REPRESENTS THE FINAL CONSTRUCTION CONDITIONS, BASED ON FIELD OBSERVATIONS AND/OR OTHER INFORMATION PROVIDED BY THE CONTRACTOR WHICH HAS NOT BEEN VERIFIED BY THE P.E. THE WORK SHOWN ON THIS "RECORD DRAWING" HAS BEEN CONSTRUCTED IN SUBSTANTIAL COMPLIANCE WITH THE PLANS, SPECIFICATIONS, REVISIONS, CHANGE ORDERS AND FIELD CHANGES.

SYMBOL	DESCRIPTION	DATE	BY
1	AS-BUILT DRAWINGS	01/13/2017	

DESIGNED BY: ZAPATA
DWN BY:
CKD BY:
SUBMITTED BY: M. CLINE
FILE NAME: 12110 E-501.DGN
SIZE: ANSI D
DATE: 01/13/2017
DPW FILE NO.: XXXXXX
ESTCP NO. 13-EB-EW1-104
PLOT SCALE: AS SHOWN
PLOT DATE: 01/19/2017

ZAPATA ENGINEERING
TRUST INTEGRITY QUALITY
ZAPATA ENGINEERING, P.A. 2035
CAMERON STREET, SUITE 21
WILMINGTON, NORTH CAROLINA 28403
PHONE: (910) 256-8340
FAX: (910) 256-8341
E-MAIL: ZAPATA@ZAPATAENG.COM

HERCULES PHYSICAL FITNESS CENTER
DC MICROGRID - BLDG P-402
POPE ARMY AIRFIELD, NORTH CAROLINA

ELECTRICAL - RISER DIAGRAM

PLATE REFERENCE NUMBER
E-501
SHEET 11

Appendix C: Key Component Datasheets

High-quality and high-efficiency
PV yields sensible solar

SUNIVA OPTIMUS® SERIES MONOCRYSTALLINE SOLAR MODULES

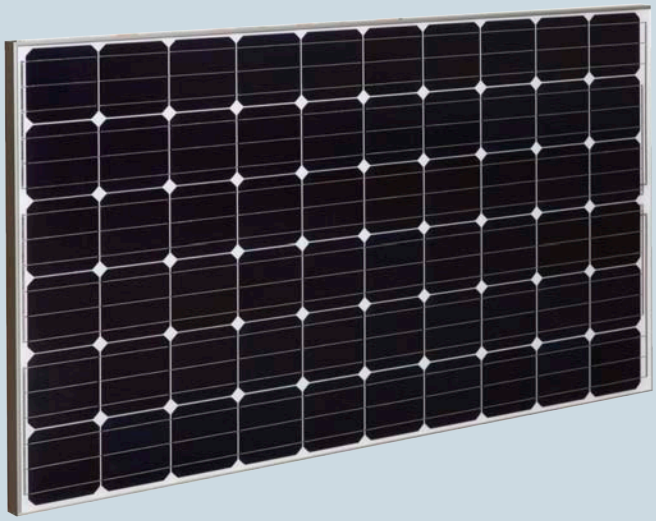

OPTXXX-60-4-100 (60 CELL MODULE)

The Optimus® modules consist of Suniva's latest technology: ARTisun® Select. These superior monocrystalline cells are designed and manufactured in the U.S.A. using our proprietary low-cost processing techniques. Engineered with our pioneering ion implantation technology, high power-density Optimus modules provide excellent value, performance and reliability.

Certifications:

UL 1703
IEC 61215
IEC 61730- 1/2

CEC

AS5033 Compliant
CEC AUSTRALIA

Engineering Excellence

- Built exclusively with Suniva's highest-efficiency ARTisun Select cells, providing one of the highest power outputs per square meter at an affordable manufacturing cost
- Suniva's state-of-the art manufacturing facility features the most advanced equipment and technology
- Suniva is a U.S. –based company spun out from the Georgia Tech University Center of Excellence in Photovoltaics (one of only two such research centers in the U.S.)

Features

- Contains the latest ARTisun Select cell technology - over 19%
- Positive only tolerance
- Marine grade aluminum frame with hard anodized coating
- Industry leading linear warranty (10 year warranty on workmanship and materials; 25 year linear performance warranty delivering 80% power at STC)
- Buy America compliant upon request
- Qualifies for U.S. EXIM financing
- System and design services available

Quality & Reliability

Suniva Optimus modules are manufactured and warranted to our specifications assuring consistent high performance and quality worldwide.

- Rigorous quality management
- Performance longevity with advanced polymer backsheet
- Produced in an ISO 9001: 2008 certified facility
- Passed the most stringent salt spray tests based on IEC 61701
- Passed enhanced stress tests[1] based on IEC 61215 conducted at Fraunhofer ISE[2]
- Certified PID free
- Ask about our validated PAN files

OUR PRODUCTS:

Monocrystalline Modules
OPTIMUS SERIES 60 cell
OPTIMUS SERIES 72 cell

Multicrystalline Modules
MV SERIES 60 cell
MV SERIES 72 cell

Monocrystalline Cells
19%+ efficiency

Balance of Systems Solutions (BOSS)
Racking, Inverters, Batteries, Energy Storage Appliances and EV Chargers

OPTIMUS SERIES: OPT 60 CELL MODULES

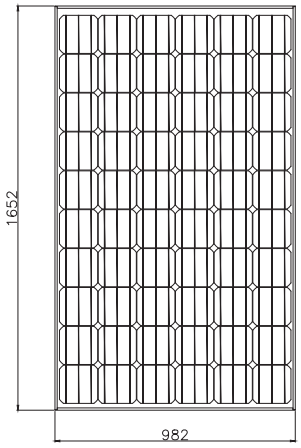

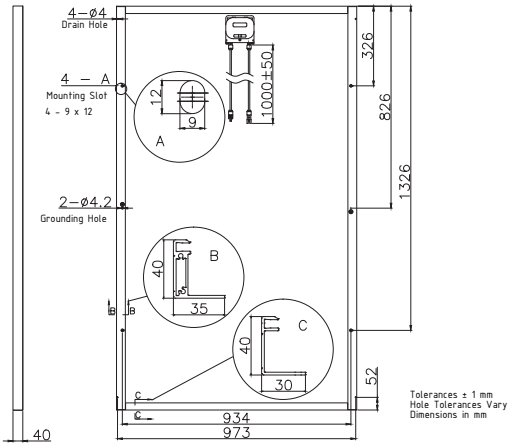

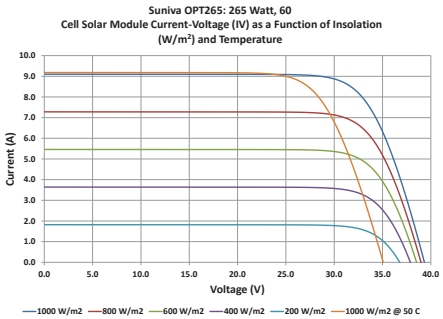

ELECTRICAL DATA (NOMINAL)

The rated power may only vary by -0/+3% and all other electrical parameters by ± 5%

Power Classification	Pmax (W)	255	260	265	270
Module efficiency	%	15.71	16.02	16.33	16.60
Model Number	OPT	255-60-4-100	260-60-4-100	265-60-4-100	270-60-4-100
Voltage at Max. Power Point	Vmp (V)	30.00	30.20	30.70	31.20
Current at Max. Power Point	Imp (A)	8.50	8.60	8.64	8.68
Open Circuit Voltage	Voc (V)	37.90	38.10	38.30	38.50
Short Circuit Current	Isc (A)	9.05	9.08	9.12	9.15

The electrical data apply to standard test conditions (STC): Irradiance of 1000 W/m² with AM 1.5 spectra at 25°C.

DIMENSIONS AND WEIGHT

Cells / Module	60 (6x10)
Module Dimensions	1652 x 982 mm (65.04 x 38.66 in.)
Module Thickness (Depth)	40 mm (1.57 in.)
Approximate Weight	17.9 +/- 0.25kg. (39.5 +/- 0.5 lb.)

CHARACTERISTIC DATA

Type of Solar Cell	High-efficiency ARTisun® Select monocrystalline cells of 156 x 156 mm (6 in.)
Frame	Silver anodized aluminum alloy; black frame available by custom order
Glass	Tempered (low-iron), anti-reflective coating
Junction Box	NEMA IP67 rated; 3 internal bypass diodes
Cable & Connectors	12 AWG (4.0 mm²) cable with MC4 compatible connectors; cable length approx. 1000 mm
Hardware (Available Upon Request)	Grounding screws: (2) #10-32 12.7 mm (#10-32 x 0.5 in.) Stainless steel flat washers: (4) 5 x 10 x 1 mm (0.2 in. ID x 0.394 in. OD x 0.030 in.)

TEMPERATURE COEFFICIENTS

Voltage	ß, Voc (%/°C)	-0.335
Current	α, Isc (%/°C)	+0.047
Power	γ, Pmax (%/°C)	-0.420
NOCT Avg	(+/- 2 °C)	46.0

LIMITS

Max. System Voltage	1000 VDC for IEC, 1000 VDC for UL
Operating Module Temperature	-40°C to +85°C (-40°F to +185°F)
Storm Resistance/Static Load	Tested to IEC 61215 for loads up to 5400 Pa (113 psf); hail and wind resistant

Suniva® reserves the right to change the data at any time. View manual at suniva.com.
[1]UV 90 kWh, TC 400, DH 2000. [2]Tests were conducted on module type OPT 60.
[SAMD_0010]

Headquarters
5765 Peachtree Industrial Blvd.,
Norcross, Georgia 30092 USA
Tel: +1 404 477 2700

www.suniva.com

Please recycle.

Suniva®
The Brilliance of Solar Made Sensible®

03 14 13
(Rev. 16)

CanadianSolar

QUARTECH
CS6P-250 | 255 | 260P

Canadian Solar's new Quartech modules have significantly raised the standard of module efficiency in the solar industry. They introduced innovative four busbar cell technology, which demonstrates higher power output and higher system reliability. Worldwide, our customers have embraced this next generation of modules for their excellent performance, superior reliability and enhanced

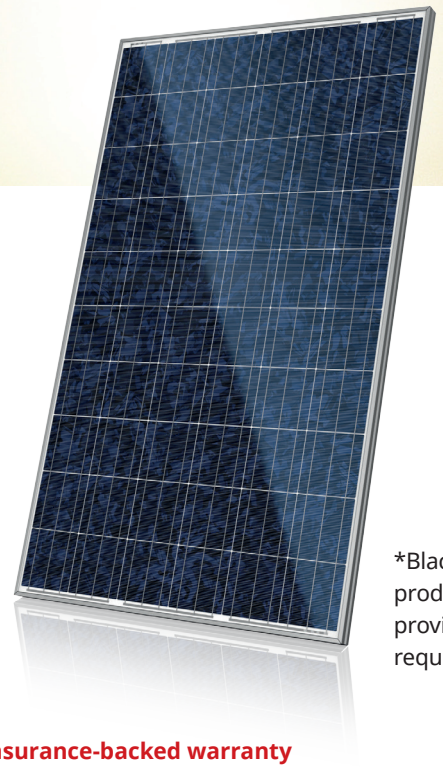

*Black frame product can be provided upon request.

NEW TECHNOLOGY

· Reduces cell series resistance
· Reduces stress between cell interconnectors
· Improves module conversion efficiency
· Improves product reliability

25 years **insurance-backed warranty**
non-cancellable, immediate warranty insurance
linear power output warranty

10 years **product warranty on materials and workmanship**

KEY FEATURES

Higher energy yield
· Outstanding performance at low irradiance
· Maximum energy yield at low NOCT
· Improved energy production through reduced cell series resistance

Increased system reliability
· Long term system reliability with IP67 junction box
· Enhanced system reliability in extreme temperature environment with special cell level stress release technology

Extra value to customers
· Positive power tolerance up to 5 W
· Stronger 40 mm robust frame to hold snow load up to 5400 Pa and wind load up to 2400 Pa
· Anti-glare project evaluation
· Salt mist, ammonia and blowing sand resistance apply to seaside, farm and desert environments

MANAGEMENT SYSTEM CERTIFICATES

ISO 9001: 2008 / Quality management system
ISO/TS 16949:2009 / The automotive industry quality management system
ISO 14001:2004 / Standards for environmental management system
OHSAS 18001:2007 / International standards for occupational health & safety

PRODUCT CERTIFICATES

IEC 61215/IEC 61730: VDE/MCS/CE / JET/SII/CEC AU/INMETRO/CQC
UL 1703 / IEC 61215 performance: CEC listed (US) / FSEC (US Florida)
UL 1703: CSA / IEC 61701 ED2: VDE / IEC 62716: TUV / IEC 60068-2-68: SGS
PV CYCLE (EU) / UNI 9177 Reaction to Fire: Class 1

CANADIAN SOLAR INC. is committed to providing high quality solar products, solar system solutions and services to customers around the world. As a leading manufacturer of solar modules and PV project developer with about 8 GW of premium quality modules deployed around the world since 2011, Canadian Solar Inc. (NASDAQ: CSIQ) is one of the most bankable solar companies

CANADIAN SOLAR INC.
545 Speedvale Avenue West, Guelph, Ontario N1K 1E6, Canada, www.canadiansolar.com, support@canadiansolar.com

MODULE / ENGINEERING DRAWING (mm)

Rear View

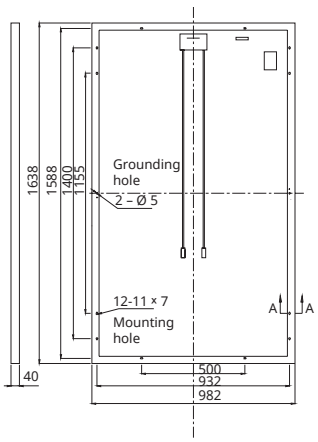

Frame Cross Section A-A

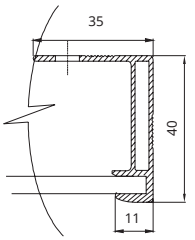

Mounting Hole

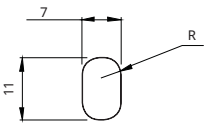

CS6P-255P / I-V CURVES

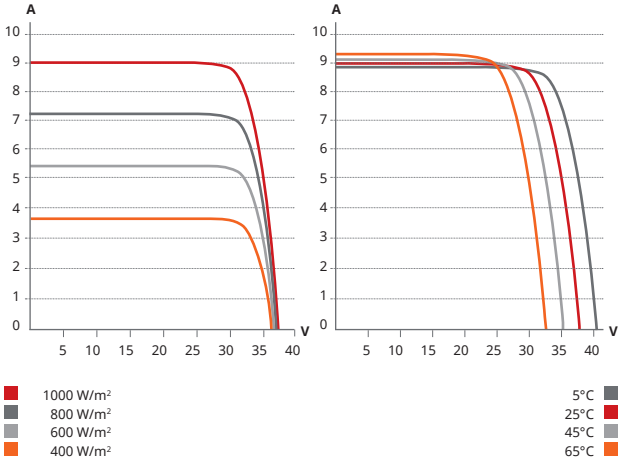

ELECTRICAL DATA / STC*

Electrical Data CS6P	250P	255P	260P
Nominal Max. Power (Pmax)	250 W	255 W	260 W
Opt. Operating Voltage (Vmp)	30.1 V	30.2 V	30.4 V
Opt. Operating Current (Imp)	8.30 A	8.43 A	8.56 A
Open Circuit Voltage (Voc)	37.2 V	37.4 V	37.5 V
Short Circuit Current (Isc)	8.87 A	9.00 A	9.12 A
Module Efficiency	15.54%	15.85%	16.16%
Operating Temperature	-40°C ~ +85°C		
Max. System Voltage	1000 V (IEC) or 1000V (UL) or 600 V (UL)		
Module Fire Performance	TYPE 1 (UL 1703) or CLASS C (IEC61730)		
Max. Series Fuse Rating	15 A		
Application Classification	Class A		
Power Tolerance	0 ~ + 5 W		

* Under Standard Test Conditions (STC) of irradiance of 1000 W/m², spectrum AM 1.5 and cell temperature of 25°C.

ELECTRICAL DATA / NOCT*

Electrical Data CS6P	250P	255P	260P
Nominal Max. Power (Pmax)	181 W	185 W	189 W
Opt. Operating Voltage (Vmp)	27.5 V	27.5 V	27.7 V
Opt. Operating Current (Imp)	6.60 A	6.71 A	6.80 V
Open Circuit Voltage (Voc)	34.2 V	34.4 V	34.5 V
Short Circuit Current (Isc)	7.19 A	7.29 A	7.39 A

* Under Nominal Operating Cell Temperature (NOCT), irradiance of 800 W/m², spectrum AM 1.5, ambient temperature 20°C, wind speed 1 m/s.

PERFORMANCE AT LOW IRRADIANCE

Industry leading performance at low irradiation, +96.5 % module efficiency from an irradiance of 1000 W/m² to 200 W/m² (AM 1.5, 25°C).

As there are different certification requirements in different markets, please contact your sales representative for the specific certificates applicable to your products. The specification and key features described in this Datasheet may deviate slightly and are not guaranteed. Due to on-going innovation, research and product enhancement, Canadian Solar Inc. reserves the right to make any adjustment to the information described herein at any time without notice. Please always obtain the most recent version of the datasheet which shall be duly incorporated into the binding contract made by the parties governing all transactions related to the purchase and sale of the products described herein.

MODULE / MECHANICAL DATA

Specification	Data
Cell Type	Poly-crystalline, 6 inch
Cell Arrangement	60 (6 × 10)
Dimensions	1638×982×40 mm (64.5×38.7×1.57 in)
Weight	18 kg (39.7 lbs)
Front Cover	3.2 mm tempered glass
Frame Material	Anodized aluminium alloy
J-BOX	IP67, 3 diodes
Cable	4 mm² (IEC) or 4 mm² & 12 AWG 1000 V (UL 1000 V) or 12 AWG (UL 600 V), 1000 mm (650 mm is optional)
Connectors	MC4 or MC4 comparable
Stand. Packaging	24 pcs, 480 kg (quantity & weight per pallet)
Module Pieces per Container	672 pcs (40'HQ)

TEMPERATURE CHARACTERISTICS

Specification	Data
Temperature Coefficient (Pmax)	-0.43% / °C
Temperature Coefficient (Voc)	-0.34% / °C
Temperature Coefficient (Isc)	0.065% / °C
Nominal Operating Cell Temperature	45±2°C

PARTNER SECTION

Caution: Please read safety and installation instructions before using the product.

NetSure™ 4015

30 kW 400V DC Power System

System Features

- 30 kW capacity (15 kW N+1)
- Hot pluggable 15 kW rectifiers
- 97% power conversion efficiency
- Input to output isolation
- AC input: 380 VAC, 400 VAC or 480 VAC
- Up to (18) output load breakers
- Battery trays for up to 30 minutes of runtime at 15 kW
- UL 60950-1 Listed (US & Canada), CE Marked

Additional Information

- EmersonNetworkPower.com/400VDC
- Power & Control Sub-Rack Data Sheet
- Load Distribution Sub-Rack Data Sheet
- Battery Tray Data Sheet
- System Application Guide
- NetSure™ 4015 Pre-Quote Form

30 kW System Shown in a 42U Rack

A safe, reliable and efficient AC to DC power system intended for 400V DC critical power applications.

Description

The NetSure™ 4015 is an AC to DC power system designed for applications operating up to 400V DC. The foundation of the system is our patented, next generation 15 kW eSure™ rectifier, featuring high frequency switching technology in a compact package. Equipped with these rectifiers, this 400V DC power system offers high efficiency over a wide operating range in addition to exceptional NetSure™ reliability.

Designed for easy deployment in lab evaluation or field installations, all components of this system fit into standard 19" IT racks. The three major components are:

1. Power and Control Sub-Rack (6U)
2. Load Distribution Sub-Rack (6U)
3. Battery Tray(s) (4U each)

The NetSure™ 4015 is a configurable system that can be integrated into a 24U or 42U tall rack, either with or without batteries.

Safety features include operation with high resistance mid-point ground. With permanent high resistance between both the positive and negative busses and ground [see Figure 1], personal safety is increased. Available current that could accidentally flow through an individual or equipment from line to ground is limited to a level consistent with today's -48V DC systems.

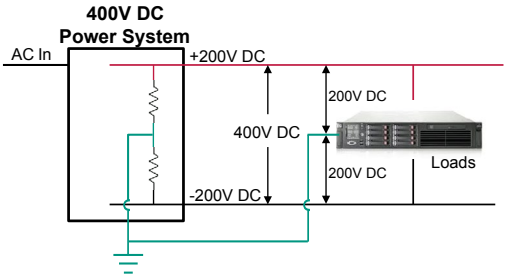

Figure 1: High Resistance Mid-Point Ground Schematic

An independent, online ground fault detection (GFD) system is included to alert users to unintended insulation breakdowns in the system. The NetSure™ 4015 can also be factory configured for other grounding topologies upon request.

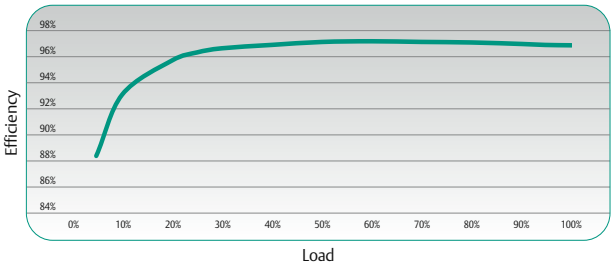

eSure™ R400-15000e Efficiency

EMERSON
Network Power

Technical Specifications

System Input	
Nominal Voltage	380 VAC, 400 VAC, 480 VAC; 3 phase, 4 wire
Input Voltage Range	Operating range: 260 VAC to 530 VAC Full power: 304 VAC to 530 VAC; Derated: 260 VAC to 304 VAC
Input Frequency	45 Hz to 65 Hz
Upstream Breaker (recommended)	63 A @ 400 VAC, 50 A @ 480 VAC; 30 kW full power

System Output	
Voltage Range	290 VDC to 400 VDC adjustable
Output Power	30 kW maximum @ Vout > 336 VDC
Voltage Regulation	0.5% for full operating range
Grounding Configurations	• High resistance mid-point ground with ground fault detection • Negative pole ground
Efficiency	Peak: 97%

Environmental	
Operating Temperature	Full rating: -5 °C to +35 °C; Recommend 20 °C to 25 °C with batteries
Relative Humidity	0% to 95% non condensing
Audible Noise	< 55 dB(A)
EMI	EN 300 386, Class A and FCC Part 15, Class A
RoHS	RoHS compliant (pending)

Optional Battery Tray	
Battery Type	High rate discharge lead acid (VRLA), flame retardant (V0) case
Battery Capacity	35 Watt/cell (15 min. rate), see battery backup table below
Battery Details	28 x 12 V blocks; Enersys DataSafe® NPX-35TFR or equivalent 336 VDC nominal, 378 VDC float
Tray Mechanical	4 RU high, 118 kg (260 lbs) installed

Mechanical Cabinet Specification	
Rectifier Form Factor	Hot pluggable module
Rectifier Weight	10 kg (22 lb.)
Rack Dimensions (H x W x D)	24 RU: 1194 mm x 600 mm x 1000 mm (47" x 24" x 40") 42 RU: 2000 mm x 600 mm x 1000 mm (79" x 24" x 40")
System Weight	See System Application Guide
Cabling Details	Top or bottom cabling; front and rear access required

Safety	
Safety Agencies	UL Listed per UL60950-1 (cUL for Canada) CE Marking per low voltage directive (EN 60950) and the EMC directive
Cabinet	IP 20

Ordering Information

Part Number	Description
584000300	NetSure™ 4015, 30kW 400V DC Power System

Email NetSure4000Series@Emerson.com for more information.

EmersonNetworkPower.com/EnergySystems (North America)
EmersonNetworkPower.eu/EnergySystems (EMEA)

Overview

System Shown in a 24U Rack

1 Load Distribution Sub-Rack (6 RU high)
Up to (9) circuit breakers, output from 6 A-63 A
Optional 125 A main load breaker (req for UL)
Up to (2) sub-racks per system

2 Power and Control Sub-Rack (6 RU high)
2 x 15 kW rectifiers, ACU+ controller
2 x AC input circuit breaker, 3-phase, 4-wire
Local system shutdown
Ground fault detection (HRMG only)

3 Battery Tray (4 RU high)
28 x 35 W/cell – 336 VDC nominal; 378 VDC float
Remote trip c.b.; Up to (5) battery trays/system

Battery Backup Time (min.)

	Number of Strings/Trays				
Load	**1**	**2**	**3**	**4**	**5**
5 kW	15	50	>60	>60	>60
10 kW	9	18	31	44	50
15 kW		10	18	27	32
20 kW		7	12	18	24
25 kW		5	8	13	18
30 kW			6	10	13

Note: Backup times based on 25 ˚C ambient with fully charged batteries.

Solar inverters

ABB string inverters
PVI-12.0-I-OUTD
12kW

Designed for commercial systems, the PVI-12.0-isolated, three-phase inverter is highly unique in its ability to control the performance of the PV panels, especially during periods of variable weather conditions.

The dual Multiple Power Point Tracker (MPPT) maximizes energy production and increases design flexibility.
This dual independent MPPT functionality enables optimal energy harvesting from two sub-arrays oriented at different azimuths, tilts and varying string lengths. The wide input-voltage range makes this inverter suitable for installations with a reduced string size.
The flat efficiency curves offer high-efficiency at all output levels ensuring consistent and stable performance across the entire input voltage and output power range.

This inverter is feature rich, enabling the desired design flexibility to master any design challenge.
The natural convection cooling and electrolytic free design leads to a longer product lifetime and reliability.
This inverter comes with a night wake-up button to access energy harvesting data and information when the inverter is in sleep mode.
The PVI-12.0-I is available with an optional fully-integrated fused DC combiner box equipped either with DC or AC and DC disconnect switches.

Highlights:
- True three-phase bridge topology for DC/AC output conversion.
- Available in 480V and 600V outputs levels.
- This inverter operates with a 97.3 percent efficiency rating.
- High-speed and precise MPPT algorithm which enables real time power tracking and improved energy harvesting.
- The electrolyte-free power converter increases the life expectancy and reliability of the inverter.

Power and productivity
for a better world™

Additional highlights:

- Integrated combiner box equipped with a DC switch in compliance with international standards (-S1,-S2)
- RS-485 communication interface (for connection to laptop or data logger)
- It features a night wake-up button to access energy harvesting data and information when the inverter is sleeping
- The dual independent MPPT allows optimal energy harvesting from two sub-arrays oriented in different azimuths and tilts
- NEMA 4X outdoor enclosure for use under any environmental conditions

Technical data and types

Type code	PVI-12.0-I-OUTD-US	PVI-12.0-I-OUTD-CAN	
Nominal output power	12000W	12000W	
Maximum output power	13200W*	12000W*	
Rated grid AC voltage	480V	480V	600V
Input side (DC)			
Number of independent MPPT channels	2; programmable for 1 MPPT		
Maximum usable power for each MPPT channel	6800W		
Absolute maximum voltage (Vmax)	520V		
Start-up voltage (Vstart)	200V (adj. 120V min.)		
Full power MPPT voltage range	250-470V		
Operating MPPT voltage range	0.7 x Vstart - 520		
Maximum current (Idcmax) for both MPPT in parallel	50A		
Maximum usable current per MPPT channel	25A		
Maximum short circuit current (Isc max.) per MPPT channel	29A		
Maximum short circuit current (Isc max.) for both MPPT in parrallel	58A		
Number of inputs (strings) per MPPT channel	Standard version: 2; -S1 version: 3; -S2 version: 3		
Array wiring termination type	Terminal block, pressure clamp, 20AWG-6AWG		
Output side (DC)			
Grid connection type	3Ø/4W + Ground		
Default voltage range	422-528V	422-528V	528-660V
Nominal grid frequency	60Hz		
Adjustable grid frequency range	57-63Hz		
Maximum current (Iac max/phase)	16.0A$_{RMS}$	16.0A$_{RMS}$	12.8A$_{RMS}$
Power factor	>0.995 (adj. ±0.9)		
Total harmonic distortion (at rated power)	<2%		
Grid wiring termination type	Terminal block, pressure clamp, 12AWG-4AWG		
Fault current	30.6A$_{RMS}$	30.6A$_{RMS}$	18.65A$_{RMS}$
Input protection devices			
Reverse polarity protection	Yes		
Over-voltage protection type	Varistor, 2 for each channel		
PV array ground fault detection	GFDI (GFD fuse) per UL 1741/ NEC 690.5		
Output protection devices			
Anti-islanding protection	Meets UL 1741 / IEEE1547 requirements		
Over-voltage protection type	1 varistor per line (3), 1 gas arrester to PE		
Efficiency			
Maximum efficiency	97.3%		
CEC efficiency	97.0%		
Operating parameters			
Feed-in power threshold	30W$_{RMS}$		
Stand-by consumption	<8W$_{RMS}$		
Communication			
User-interface (display)	16 characters x 2 lines LCD display		
Standard communication interfaces	(1) RS485 connection. Standard Aurora protocol. Optional Modbus		
Optional remote monitoring logger	VSN 700 Data Logger		
Environmental			
Ambient air operating temperature range	-13°F to +140°F (-25°C to +60°C) Derating above +113°F (+45°C)		
Ambient storage temperature range	-40°F to +176°F (-40°C to +80°C)		
Relative humidity	0 -100% condensing		
Acoustic noise emission level	<50 db (A) @1m		
Maximum operating altitude without derating	6560ft (2000m)		

*Capability enabled at nominal AC voltage and with sufficient DC power available

Information in this document is subject to change without notice

Block diagram of PVI-12.0-I-OUTD

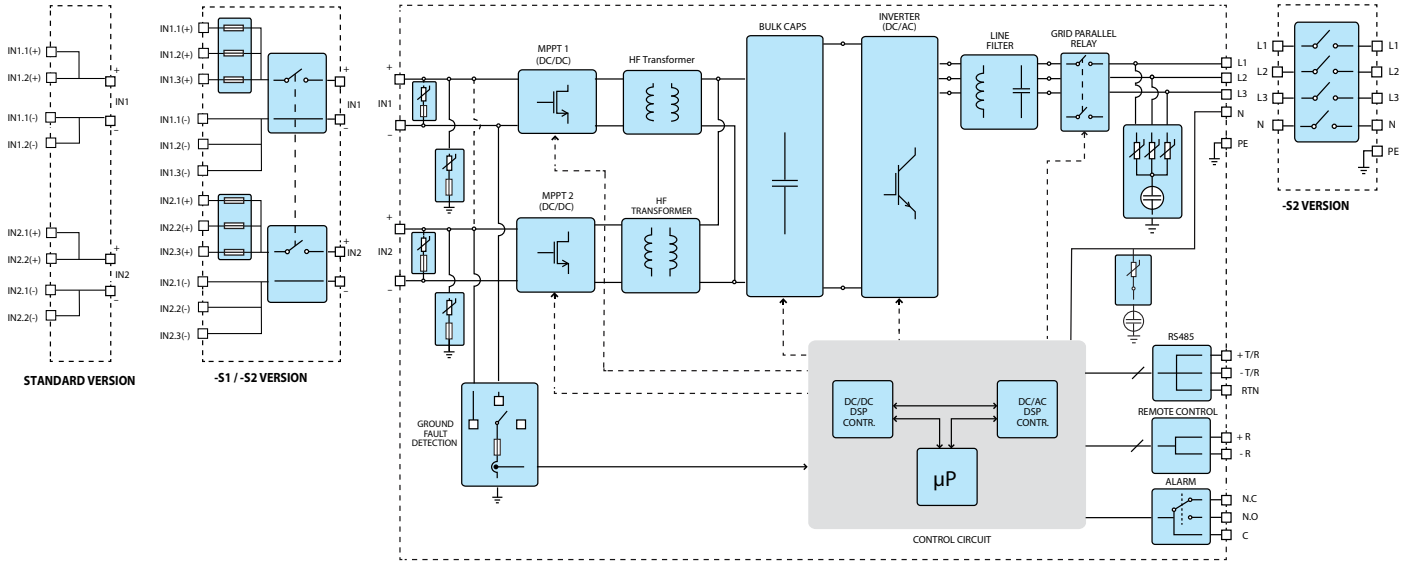

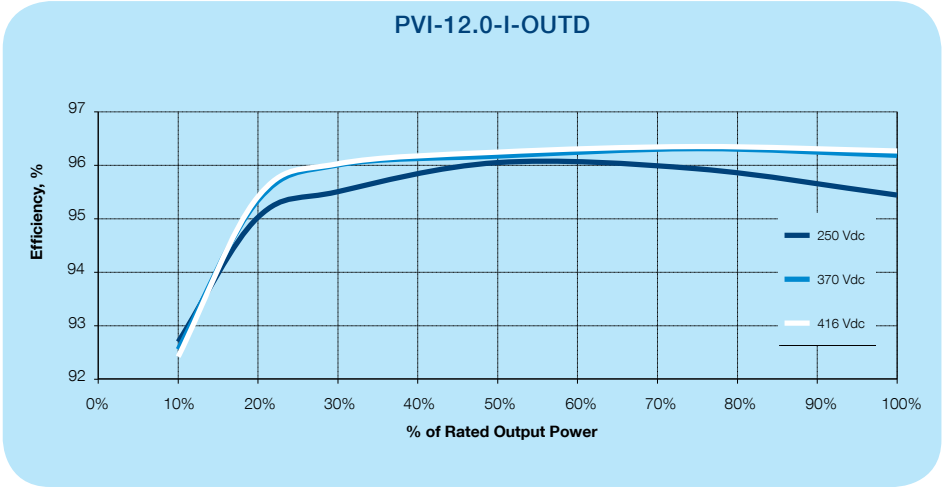

Technical data and types

Type code	PVI-12.0-I-OUTD-US	PVI-12.0-I-OUTD-CAN	
Mechanical specifications			
Enclosure rating	NEMA 4X		
Cooling	Natural convection		
Dimensions H x W x D	Standard: 28.2 x 25.4 x 8.7in / 716 x 645 x 222mm -S1, -S2 version: 37.7 x 25.4 x 8.7in / 958 x 645 x 222mm		
Unit weight	Standard: 101lb (45.8kg); -S1: 107lb (48.5kg); -S2: 114lb (51.7kg)		
Shipping weight	With pallet: 254lb (<115kg); without pallet: 143lb (<65kg)		
Conduit connections	Bottom: (1) 1/2" KO, (2) 1" pluggable opening, (4) 1/2" pluggable openings / Left and Right Side: (1) Concentric KO 3/4", 1"/ Back: (4) Concentric KO 3/4", 1"		
Mounting system	Wall bracket		
Ground fault detector fuse size/type	1A / 600V 10 x 38mm		
Optional string combiner fuse size/type	15A / 600V 10mm x 38mm		
Optional DC switch current rating (per contact)	32A		
Safety			
Isolation level	Isolated - high-frequency transformer		
Safety and EMC standard	UL 1741, IEE1547, IEE1547.1, CSA-C22.2N. #107.1-01		
Safety approval	cCSAus		
Available models			
Standard	PVI-12.0-I-OUTD-US-480-NG	PVI-12.0-I-OUTD-CAN-480-NG	PVI-12.0-I-OUTD-CAN-600-NG
With DC switch and DC fuses	PVI-12.0-I-OUTD-S1-US-480-NG	PVI-12.0-I-OUTD-S1-CAN-480-NG	PVI-12.0-I-OUTD-S1-CAN-600-NG
With AC and DC switches and DC fuses	PVI-12.0-I-OUTD-S2-US-480-NG	PVI-12.0-I-OUTD-S2-CAN-480-NG	PVI-12.0-I-OUTD-S2-CAN-600-NG

Information in this document is subject to change without notice

Support and service

ABB supports its customers with a dedicated, global service organization in more than 60 countries, with strong regional and national technical partner networks providing a complete range of life cycle services.

For more information please contact your local ABB representative or visit:

www.abb.com/solarinverters

www.abb.com

9AKK106103A4854 REV 0.1 EN 03.05.2015 #16634

Power and productivity
for a better world™

KBL Series

LED Low-Bay/High-Bay Luminaire

Rev. Date: V8 08/26/2019

Product Description

KBL LED delivers 20,900(M) or 27,500(H) lumens, allowing for one-for-one replacement or fixture count reduction of 250W, 400W HID or up to six lamp 54W T5HO fixtures. With energy savings of up to 65% over traditional light sources, lightweight construction and multiple mounting options, the KBL is optimized for new construction or retrofit installations.

The KBL delivers even illumination with reflector choices of aluminum, clear acrylic, clear polycarbonate, or white acrylic. Optional lenses offer enhanced uplight and maximum uniformity, making it ideal for a variety of applications including retail, gymnasiums, light manufacturing, and warehouses.

Applications: Retail, gymnasiums (aluminum or polycarbonate reflector), industrial, manufacturing and warehouse spaces.

Shown Fully Assembled with Prismatic Reflector and Universal Mount

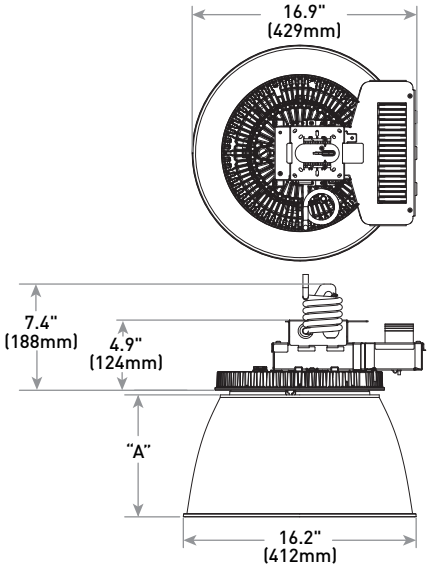

Performance Summary

Initial Delivered Lumens: 20,900 or 27,500 lumens

Operating Temperature Range: M Lumen Package: -40˚C to 50˚C (-40˚F to +122˚F);
H Lumen Package: -40˚C to 40˚C (-40˚F to +104˚F) ; minimum operating temperature of 0˚C (32˚F) for EB, SWC and SWC-NS

Efficacy: Up to 150 LPW

CRI: 70, 80+

CCT: 3000K, 3500K, 4000K, 5000K

Input Voltage: 120-277 VAC or 347-480 VAC (without step-down transformer)

L_{70} Lifetime: > 100,000 hours at maximum operating temperature

Limited Warranty†: 10 years on luminaire/5 years on ML, PML, SWC and SWC-NS options

Limited Warranty Emergency Back Up (EB) Battery: 1 Year Battery Back Up. Test regularly in accordance with local codes

Universal Mounting: Hook & Cord or Pendant Mount

Weight: Maximum 14 lbs. (6.4kg)

Controls: 0-10V dimming to 10%, Multi-Level /Programmable Multi-Level Occupancy, or Synapse Wireless™ Controls

Assembled in the U.S.A. of U.S. and imported parts

† See http://creelighting.com/warranty for warranty terms.

Reflector	"A" Height
ALR16 (Aluminum)	9.0" (229mm)
ACR16 (Clear Prismatic Acrylic)	8.5" (216mm)
AWR16 (White Acrylic)	8.5" (216mm)
PCR16 (Clear Polycarbonate)	8.5" (216mm)

Refer to page 4 for EB20 detail.

Ordering Information

Example: KBL-A-UV-H-40K-7-UL-10V

KBL	A	UV							
Product	**Version**	**Mounting**	**Lumen Package***	**CCT**		**CRI**	**Voltage**	**Controls**	**Options**
KBL	**A**	**UV** Universal Mount: hook and cord with 6ft whip, adaptor plate for pendant	**M** 20,900 Lumens **H** 27,500 Lumens	**30K** 3000K **35K** 3500K	**40K** 4000K **50K** 5000K	**7** 70 CRI **8** 80 CRI	**UL** 120-277V **UH** 347-480V	**10V 0-10V Dimming** **ML Multi-Level** - Refer to ML install instructions - Coverage Lens Mounting Ht: 15-45' (4.6-13.7m) - detects walking to 35' and fork lifts to 45' **PML Programmable Multi-Level** - Refer to PML spec sheets for details - Coverage Lens Mounting Ht: 15-40' (4.6-12.2m) - detects walking to 30' and fork lifts to 40' **Wireless** **SWC Synapse Wireless™ Control** - 120-277V only - Available only with H lumen package! **SWC-NS Synapse Wireless™ Control w/ Network Sensor** - 120-277V only - Available only with H lumen package	**EB20 Integral Emergency** - Not available with UH voltage - Provides 20W and 90 minutes of emergency operation - Not available with SWC or SWC-NS options

* Lumen Package codes identify approximate light output only. Actual lumen output levels vary depending on CCT and reflector/lens selection. Refer to Delivered Lumens & Electrical Data and Reflector Illumination Performance tables for specific lumen values.

US: creelighting.com (800) 236-6800
Canada: creelighting-canada.com (800) 473-1234

Product Specifications

CONSTRUCTION & MATERIALS

- Die cast aluminum heatsink
- IP65 optics with tempered glass lens protect LEDs while keeping the dust out
- Low-profile, lightweight design provides ease of installation
- UV mount is provided with factory installed spring lock hook for mounting, factory installed 6' (1.8m) 16/3 AWG white power cord and an adaptor plate to accept a 3/4 IP pendant (by others)
- Factory calibrated to hang straight
- Designed for downlight applications only
- EB20 comes with factory installed 3' (0.9m) 18/4 AWG white cord w/1.5" (38mm) flying leads
- **Weight:** Maximum 14 lbs. (6.4kg); w/EB20 20 lbs. (9.1kg)

ELECTRICAL SYSTEM

- **Input Voltage:** 120-277V or 347-480V 50/60Hz
- **Power Factor:** > 0.9 at full load
- **Total Harmonic Distortion:** < 20% at full load
- **Operating Temperature Range:** M Lumen Package: -40˚C to 50˚C (-40˚F to +122˚F); H Lumen Package: -40˚C to 40˚C (-40˚F to +104˚F); minimum operating temperature for ML option is -20˚C (-4˚F); minimum operating temperature for SWC, SWC-NS, and EB20 option is 0˚C (32˚F)
- **Transient Protection:** 6kV/3kA tested in accordance to IEEE/ANSI
- When code dictates fusing, a slow blow fuse or type C/D breaker should be used to address inrush current
- EB20 is wired for switched emergency mode (lights can be turned off without going into emergency mode)

0-10V DIMMING

- Continuous dimming to 10% with 0-10V DC control protocol
- 10V Source Current: 0.15mA
- Use only lighting controls with neutral connection or controls intended for use with LED fixtures
- Reference dimming document for additional information

MULTI-LEVEL OPTION (PIR)

- High/low occupancy, dim to min of 30%
- Available with UL and UH voltages
- Refer to KBL install instructions for details on sensor functionality, operation and lumen and power multipliers

PROGRAMMABLE MULTI-LEVEL OPTION (PIR)

- High/low/off photo/motion sensor
- Available with UL and UH voltages
- Refer to PML spec sheet for details on sensor functionality, operation and lumen and power multipliers

SYNAPSE WIRELESS

- Connected lighting via a wireless mesh network
- Utility grade power monitoring (+/-2%)
- Daylight harvesting accessory (see table on page 3)
- Scheduling, zonal control, alerts and notifications

REGULATORY & VOLUNTARY QUALIFICATIONS

- cULus Listed (UL1598; UL8750)
- Designed for indoor use only
- Suitable for damp locations
- Requires minimum 90˚C supply conductors
- LED optics meet IP65 requirements
- UL924 (EB option). Maximum mounting height: 29' (8.8m)
- Meets FCC Part 15, Subpart B, Class A limits for conducted and radiated emissions
- Luminaire with SWC/SWC-NS options meet FCC Part 15, Subpart C limits for conducted and radiated emissions
- Assembled in the U.S.A. of U.S. and imported parts
- RoHS compliant. Consult factory for additional details
- DLC and DLC Premium qualified versions available. Some exceptions apply. Please refer to https://www.designlights.org/search/ for most current information
- ⚠ **CA RESIDENTS WARNING:** Cancer and Reproductive Harm – www.p65warnings.ca.gov

Delivered Lumens & Electrical Data*

Lumen Package	CCT	Delivered Lumens**		System Watts	Efficacy (LPW at 70CRI)	Total Current (A)					
		70 CRI	80 CRI	120-480V		120V	208V	240V	277V	347V	480V
M	3000K	21,300	18,800	142	150	1.20	0.69	0.60	0.51	0.41	0.29
	3500K	22,000	19,700		155						
	4000K	22,100	20,500		156						
	5000K	22,100	20,700		156						
H	3000K	28,000	24,700	189	148	1.60	0.92	0.80	0.68	0.54	0.39
	3500K	28,800	25,900		152						
	4000K	29,100	26,900		154						
	5000K	29,000	27,200		153						

* Data provided at 25˚C (77˚F). Actual wattage may differ by +/- 10% when operating between 120 -277V or 347-480V +/- 10%.
** Initial delivered lumen values based on luminaire without reflector. Refer to reflector Illumination Performance table for lumen multipliers when using reflector accessory.

Delivered Emergency Lumens at 80 CRI*

Lumen Package	3000K	3500K	4000K	5000K
M	2,614	2,741	2,847	2,878
H	2,648	2,775	2,887	2,915

* Emergency lumen values do not include reflector options.

Delivered Emergency Lumens at 80 CRI, ACR16

Lumen Package	3000K	3500K	4000K	5000K
M	2,509	2,631	2,733	2,763
H	2,542	2,664	2,772	2,799

KBL Series Ambient Adjusted Lumen Maintenance[1]

Ambient	Initial LMF	36K hr Reported[2] LMF	50K hr Estimated[3] LMF	75K hr Estimated[3] LMF	100K hr Estimated[3] LMF
25˚C (77˚F)	1.00	0.95	0.94	0.93	0.92
30˚C (86˚F)	0.99	0.94	0.93	0.92	0.91
35˚C (95˚F)	0.98	0.93	0.92	0.91	0.90
40˚C (104˚F)	0.97	0.92	0.91	0.90	0.90
45˚C (113˚F)	0.96	0.91	0.90	0.89	0.89
50˚C (122˚F)	0.95	0.90	0.89	0.89	0.88

[1] Lumen maintenance values at 25˚C (77˚F) are calculated per IES TM-21 based on IES LM-80 report data for the LED package and in-situ luminaire testing. Luminaire ambient temperature factors (LATF) have been applied to all lumen maintenance factors.
[2] In accordance with IES TM-21, Reported values represent interpolated values based on time durations that are up to 6x the tested duration in the IES LM-80 report for the LED.
[3] Estimated values are calculated and represent time durations that exceed the 6x test duration of the LED.

CREE LIGHTING

US: creelighting.com (800) 236-6800
Canada: creelighting-canada.com (800) 473-1234

Accessories

Reflector

ALR16 (Single Pack)
ALR16-MP (Multi-Pack)
- 16" (406mm) Aluminum

ACR16 (Single Pack)
ACR16-MP (Multi-Pack)
- 16" (406mm) Clear Acrylic Prismatic
- Acrylic reflector is not impact resistant nor intended for use unprotected in a gymnasium

AWR16 (Single Pack)
AWR16-MP (Multi-Pack)
- 16" (406mm) White Acrylic
- Acrylic reflector is not impact resistant nor intended for use unprotected in a gymnasium

PCR16 (Single Pack)
PCR16-MP (Multi-Pack)
- 16" (406mm) Clear Polycarbonate
- Suitable for use in gymnasiums; WG-AP wire guard recommended

Notes:
- Single pack SKUs ship as one reflector per box
- Multi-pack SKUs require a minimum order of 10 pieces or more, and ship together in as few boxes as possible
- Acrylic or polycarbonate reflectors and lenses are not intended for use in environments containing airborne corrosive agents such as chemical solvents, cleaners, or cutting fluids

Wire Guards

16" (406mm) Wire Guards
WG-A
- For Aluminum Reflector

WG-AP
- For Acrylic and Polycarbonate Reflectors

Note: Not for use with lens accessories

Full Body Wire Guard
FBGWH
- Suitable for use with reflector and lens accessories
- 8 AWG steel construction w/painted white finish
- Not for use with ML, PML or SWC-NS options

Lenses

16" (406mm) Clear Prismatic Drop Acrylic Lenses
DLA16
- For Aluminum Reflector

DL16
- For Acrylic and Polycarbonate Reflectors

Note: Lenses and WG-A/WG-AP wire guard accessories can't be used together

16" (406mm) Clear Conical Acrylic Lenses
CLA16
- For Aluminum Reflector

CL16
- For Acrylic and Polycarbonate Reflectors

Safety Cables

Galvanized Safety Cables
SC-5
- 5.0' (1.5m) Cable

SC-10
- 10.0' (3.0m) Cable

Field-Installed NEMA® Plugs

AP-515P
- 15 amp 120V Straight Blade Plug

AP-L515P
- 15 amp 120V Twist Lock Plug

Note: Not for use with EB20 option

AP-L615P
- 15 amp 240V Twist Lock Plug

AP-L715P
- 15 amp 277V Twist Lock Plug

AP-L2420P
- 20 amp 347V Twist Lock Plug

AP-L820P
- 20 amp 480V Twist Lock Plug

Field-Installed

Anti-Spin Adaptor
HXB-AS
- Anti-spin accessory for hook and cord mounting configuration

Hand-Held Remote
XA-SENSREM
- For successful implementation of the programmable multi-level option, a minimum of one hand-held remote is required

Synapse Wireless Control Accessories

Synapse Gateway
SS450-002
- 120-277V

Synapse Building Management System (BMS)
BMS-GW
- 120-277V
- Required for BACNET integration

Synapse Daylight Harvesting Kit
KIT-SBOX-DLH
- 120-277V

Optional Reflectors/Lens: shown fully assembled with universal mount

Aluminum Reflector w/Drop Lens

Clear Prismatic Acrylic Reflector

White Acrylic Reflector w/Conical Lens

Drop Lens

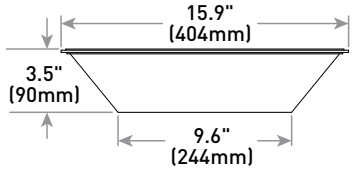

Clear Conical Lens

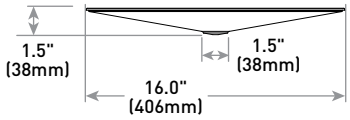

Emergency Battery Pack: EB20

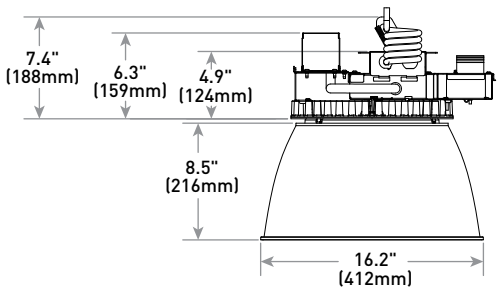

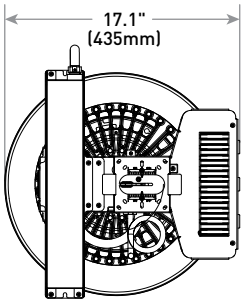

Reflector Uplight Illumination Performance		
Reflector	% of Uplight	Lumen Multiplier
ALR16 (Aluminum)	0%	0.86
ALR16 w/CLA16 (Aluminum w/Clear Conical Lens)	0%	0.76
ALR16 w/DLA16 (Aluminum w/Clear Drop Lens)	2%	0.77
ACR16 (Clear Prismatic Acrylic)	3%	0.96
ACR16 w/CL16 (Clear Prismatic Acrylic w/Clear Conical Lens)	6%	0.93
ACR16 w/DL16 (Clear Prismatic Acrylic w/Clear Drop Lens)	8%	0.93
AWR16 (White Acrylic)	13%	0.93
AWR16 w/CL16 (White Acrylic w/Clear Conical Lens)	16%	0.88
AWR16 w/DL16 (White Acrylic w/Clear Drop Lens)	16%	0.90
PCR16 (Clear Polycarbonate)	2%	0.89
PCR16 w/CL16 (Clear Polycarbonate w/Clear Conical Lens)	5%	0.85
PCR16 w/DL16 (Clear Polycarbonate w/Clear Drop Lens)	7%	0.84

Reference http://creelighting.com/products/indoor/high-bay-low-bay/kbl-series for detailed photometric data. IES files include reflector multipliers.

Cross Reference Reflectors		
Previous Nomenclature	Updated Nomenclature	Description
CXBP16	ACR16	Reflector 16" (406mm) Clear Prismatic Acrylic
CXBP16-MP	ACR16 -MP	Reflector 16" (406mm) Clear Prismatic Acrylic - Multi-Pack
CXBW16	AWR16	Reflector 16" (406mm) White Acrylic
CXBW16-MP	AWR16-MP	Reflector 16" (406mm) White Acrylic - Multi-Pack
CXBC16	PCR16	Reflector 16" (406mm) Clear Polycarbonate
CXBC16-MP	PCR16-MP	Reflector 16" (406mm) Clear Polycarbonate - Multi-Pack
CXBA16N	ALR16	Reflector 16" (406mm) Aluminum
CXBA16N-MP	ALR16-MP	Reflector 16" (406mm) Aluminum- Multi-Pack

US: creelighting.com (800) 236-6800
Canada: creelighting-canada.com (800) 473-1234

CREE LIGHTING

A COMPANY OF *IDEAL INDUSTRIES, INC.*

Bosch BGT 250W, DC Input LED Driver

290Vdc – 600Vdc input.
250W, programmable 0.5A – 1.25A, 100V – 600V output.
0-10V Class 2 dimming.

The Bosch BGT DC LED driver is designed to work directly from a solar panel DC bus up to 600Vdc, increasing the reliability and efficiency of LED lighting in PV-solar powered installations.

Bosch - H6FF250CC-xxxx-yy				
Parameter	Min	Nom	Max	Notes
Input Voltage	100Vdc	380Vdc	600Vdc	DC INPUT ONLY. Input Voltage must be higher than Output LED Voltage.
Output Power		200W	250W	UL Limit.
Output Voltage	100Vdc	200Vdc	600Vdc	LED string voltage. Maximum occurs at highest current and lowest temperature.
Output Current	500mA		1250mA	Programmable from 500mA to 1250mA.
Efficiency	96%			Input Voltage = 290Vdc-600Vdc Output current = 1050mA Output voltage = 190Vdc
Min Tc – Operation	-40C			
Max Tc – Life			50C	
Max Tc – UL			90C	
Max Input Power			260W	
Surge		3kV		Combination wave and IEEE ring wave.
Environmental Protection Rating				UL damp & dry IP54
Dimming (Figure 1)	OFF		100%	Class 2 Turn off at 0.5V
Lifetime				10 year warranty. 100,000 hour operation at Tc = 50C.
Output Current Ripple			+/-200mA	
Output Current Tolerance			+/-7%	
Protection				OTP=85C UVP, OVP, SCP
0-10V dimming excitation		140uA		
Operating Ambient Temp Range	-40C		+55C	This is fixture external ambient temperature. The driver will operate at +55C ambient. The lifetime will be reduced if the Tc temperature exceeds 50C.
Agency Approbations				UL Recognized to UL8750. File #E490930. COAs available from Bosch BGT.
EMC Compliance				FCC Title 47 Part 15 Class A R-EMI
Enclosure (Figure 2)	10.66in x 2.23in x 1.59in 271mm x 57mm x 40.3mm			

WIRING			
INPUT		DATA	
Red	VIN +	Purple	DIM +
Black	VIN -	Gray	DIM -
Green/Yellow	Earth Ground	Orange	24VDC +
OUTPUT		White/Orange	24VDC -
White/Red	LED +	Yellow	AUX +
White/Blue	LED -	White/Yellow	AUX -
		Brown	RS485+
		White/Brown	RS485 -

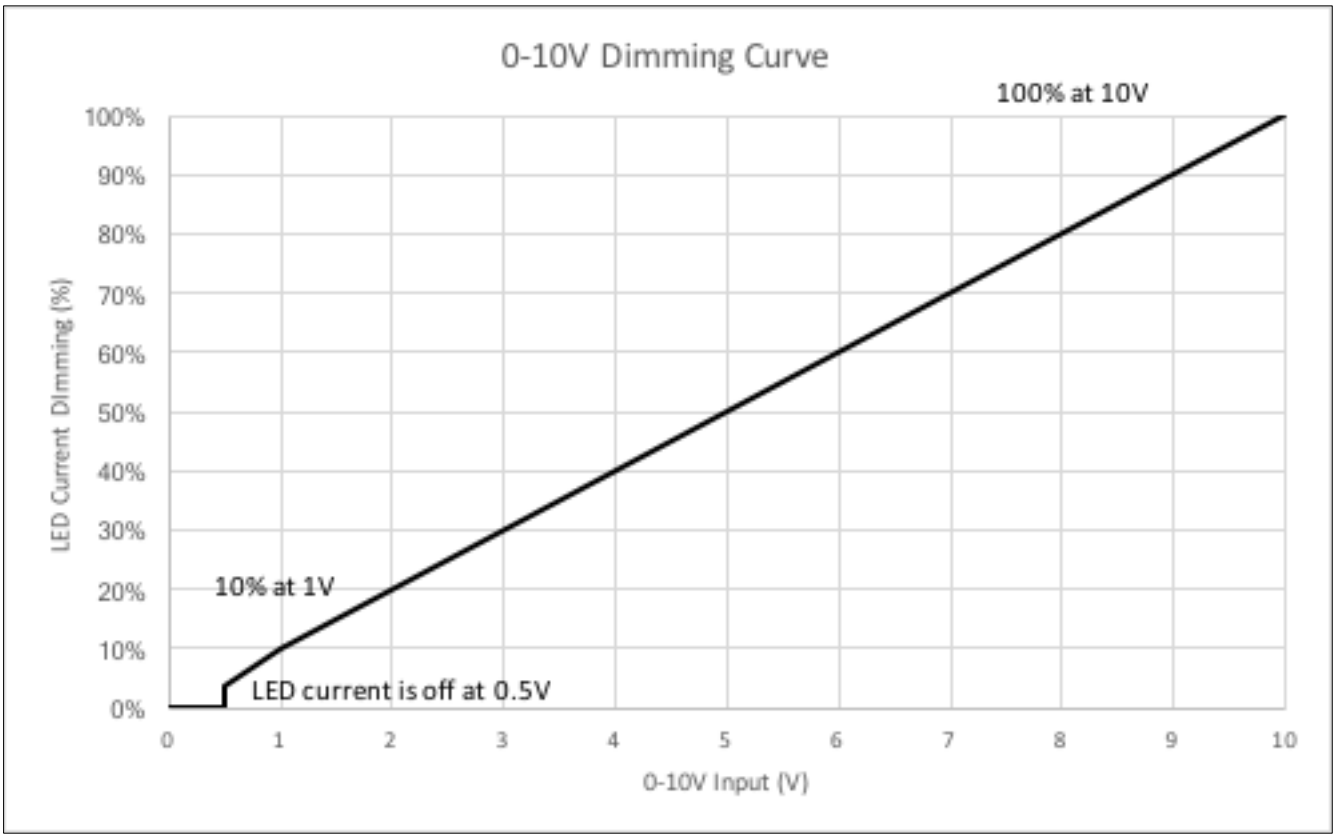

Figure 1. 0-10V Dimming Curve

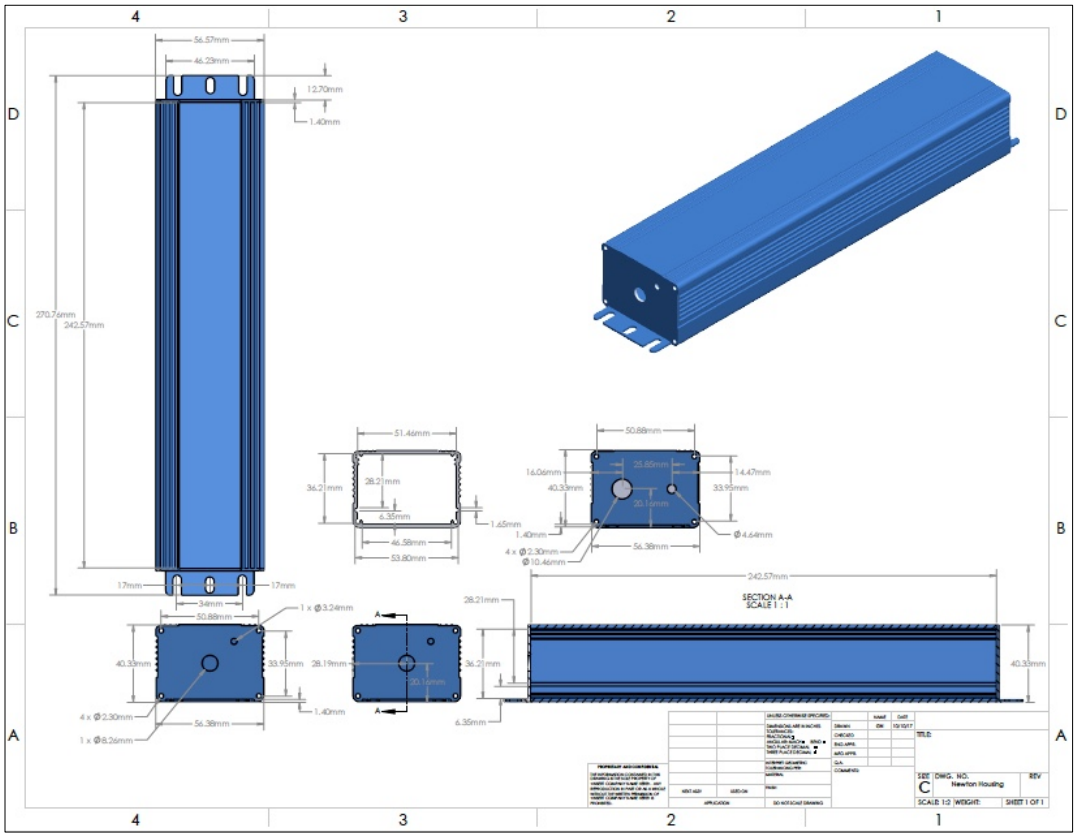

Figure 2. Mechanical Drawing

DC LED DRIVER

Model Series: H6FF200CC-xxxx-x-x

BEFORE YOU BEGIN

Read these instructions completely and carefully.

⚠ WARNING

Risk of electrical shock. Disconnect power before servicing or installing product. Risk of damage. Ensure dimming controller is a maximum of 10V. Voltage greater than 10V can damage power supply.

Prepare Electrical Wiring

Electrical Requirements

- The LED driver must be supplied with 100-600 VDC, and connected to an individual properly grounded branch circuit, protected by a 15 or 20 ampere circuit breaker.

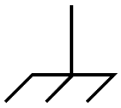

Grounding Instructions

- The grounding and bonding of the overall system shall be done in accordance with National Electric Code (NEC) Article 600 and local codes.

This device complies with Part 15 of the FCC Rules. Operation is subject to the following two conditions: (1) This device may not cause harmful interference, and (2) this device must accept any interference received, including interference that may cause undesired operation.

Note: This equipment has been tested and found to comply with the limits for a Class A digital device, pursuant to part 15 of the FCC Rules. These limits are designed to provide reasonable protection against harmful interference when the equipment is operated in a commercial environment. This equipment generates, uses, and can radiate radio frequency energy and, if not installed and used in accordance with the instruction manual, may cause harmful interference to radio communications. Operation of this equipment in a residential area is likely to cause harmful interference in which case the user will be required to correct the interference at his own expense.

Bosch Building Grid Technologies
256 Raceway Drive Suite 4, Mooresville, NC 28117

Tel: +1-xxx-xxx-xxxx
Email: info@boschbgt.com
http://www.boschbgt.com

Installation Guide

- **Type – DC LED Power Supply**
- **Model number breakdown**

Model#

H6FF200CC1025B3

Series 1 Alpha Character	
H	High-Bay
O	Office
P	Parking Deck

Max Operating Voltage 1 Numeric Character	
6	600Vdc
10	1000Vdc

Feature (Hex Encoded)	
F	Full Feature
F	

Power 3 Numeric Characters	
250	250W
200	200W
150	150W
50	50W

Output Type 2 Alpha Characters	
CC	Constant Current
CV	Constant Voltage

Output Current 4 Numeric Characters	
1025	1025 mA
0700	700mA

Sample Level 1 Alpha Character		
A	A-Sample	Prototype
B	B-Sample	Test Sample
C	C-Sample	Production Intent
D	D-Sample	Production

Sample Revision 1 Numeric Character		
1		
2		
3		
4		

- **Serial number breakdown**

Serial#

LL17062####

Serial Number					
Hex Encode	Hex Encode	YY	MM	DD	Serial
L	L	17	06	02	####

Bosch Building Grid Technologies
256 Raceway Drive Suite 4, Mooresville, NC 28117

Tel: +1-xxx-xxx-xxxx
Email: info@boschbgt.com
http://www.boschbgt.com

Installation Guide

- **LED Driver Features**
  - Compatible with 0-10V Dimming controller
  - Class 1
  - IP54: Dry or damp location rated

TECHNICAL SPECIFICATIONS	MIN	Typical	Max
Input Voltage (VDC)	100	300-500	600
Input Current (A)	-	-	1.025
Output Voltage (VDC)	100	200-500	600
Output Current (ADC)	-	-	1.025
Output Power (W)	-	200	250
Environmental Operating Temperature Range	-20°C	-	+55°C
Environmental Humidity (non-condensing)	10%	-	90%
Environmental Storage Temperature Range	-40°C	-	+125°C
Enclosure Specification	IP54: Dry or damp location rated		
Dimensions	10.66 in. x 2.23 in. x 1.59 in. (270.764 mm x 56.642 mm x 40.386 mm)		

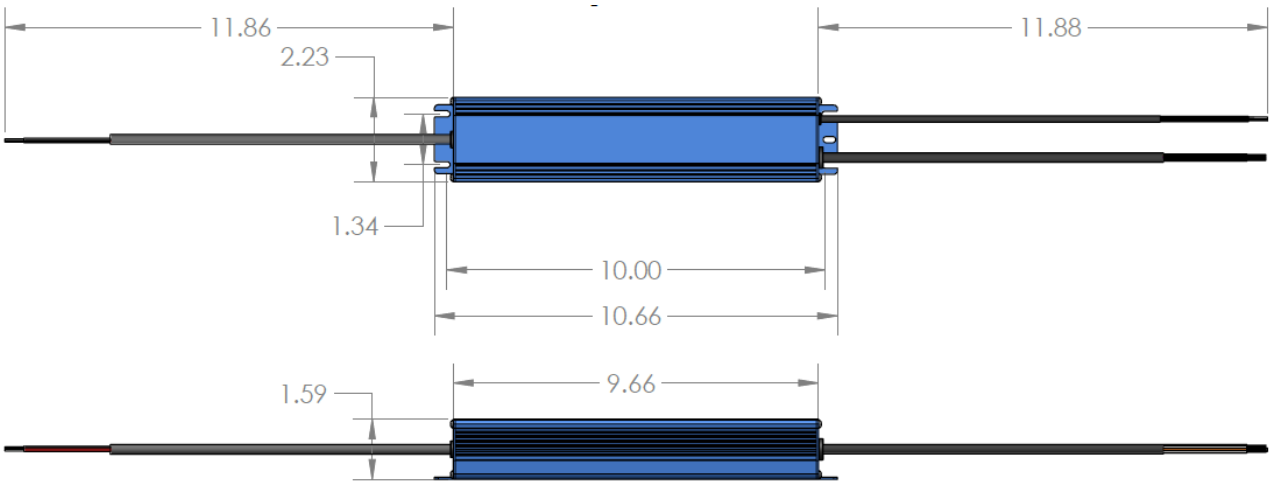

- **Introduction**

This LED power supply is a dedicated LED driving device that delivers a constant current or generates an adjustable current controlled by an external dimmer control. Depending on its types or design concept, some of them can be located in a harsh environment such as dusty, humid places. Bosch's LED power supplies include metal case, and PCB types.

- **Installation**

1) Before beginning any installation or maintenance work, disconnect the power supply from the utility. Ensure that it cannot be re-connected unintentionally!
2) Keep proper ventilation around the unit and do not stack any object on it. Also, a **10-15 cm** clearance must be kept when the adjacent device is a heat source.
3) Mounting orientations other than standard orientation or operate under high ambient temperature may increase the internal component temperature and will require a de-rating in output current.
4) Current rating of an approved primary /secondary cable should be greater than or equal to that of the unit. Refer to its specification.
5) For LED power supplies with waterproof connectors, verify that the linkage between the unit and the lighting fixture is tight so that water cannot intrude into the system.

Installation Guide

6) For dimmable LED power supplies, make sure that your dimming controller is capable of driving these units. For H6FF200CC series, for those with Potentiometer dimming function, require **140 µA** each unit.
7) Wiring: Refer to the diagram below.

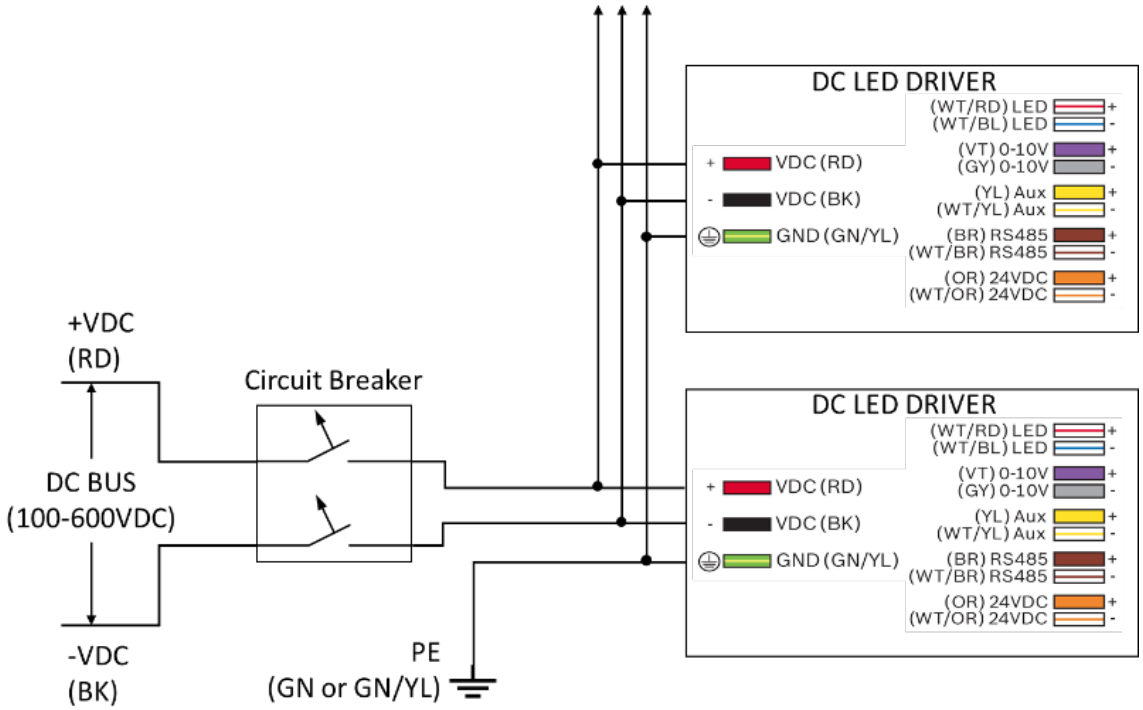

8) The maximum number of the LED PSUs that can be connected to a circuit breaker at 500VDC is shown as below.

Model	20 AMP DC	15 AMP DC
H6FF250CC-1025-x-x	12	9
H6FF200CC-0700-x-x	15	11

9) For other information about the products, refer to www.boschbgt.com for details.

Installation Guide

DIMMING OPERATION

3 in 1 dimming function

- Output constant current level can be adjusted by applying one of the three methodologies between (0-10V+) and (0-10V-)
  1. 0 - 10VDC
  2. 10V PWM signal
  3. Resistance 0-100K Ohm.
- Direct connecting to LEDs is suggested. It is not suitable with additional drivers.
- Dimming source current from power supply: **140 µA** (typ.)

- Applying 0-10VDC

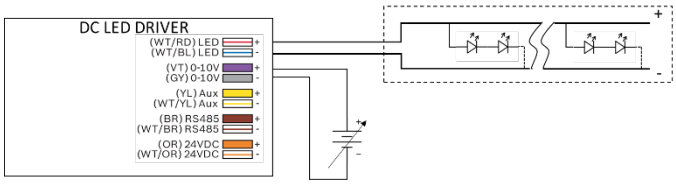

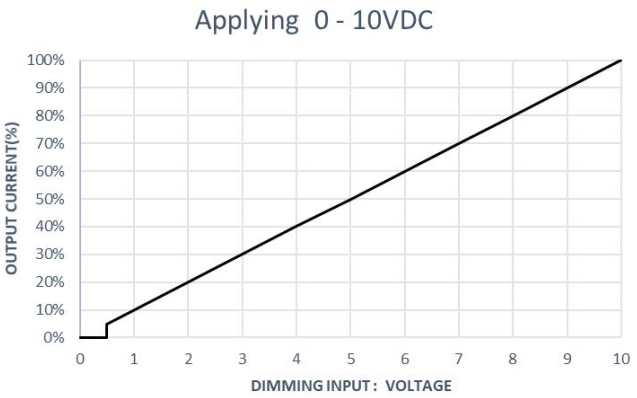

- Applying 10V PWM signal
  (frequency range 100Hz - 3KHz)

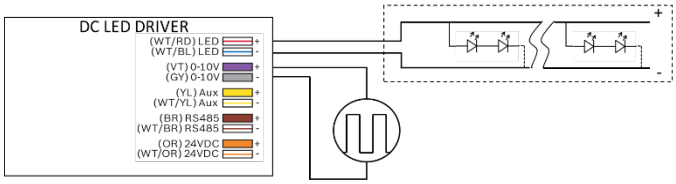

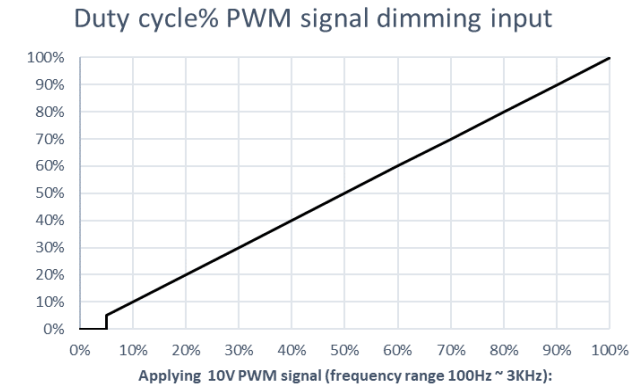

- Applying Resistance
  (0 – 100K Ohm)

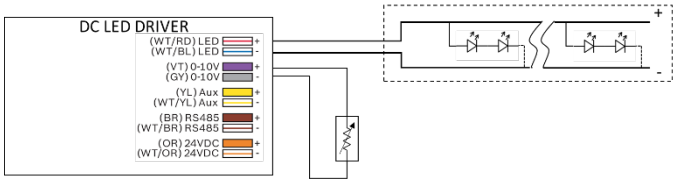

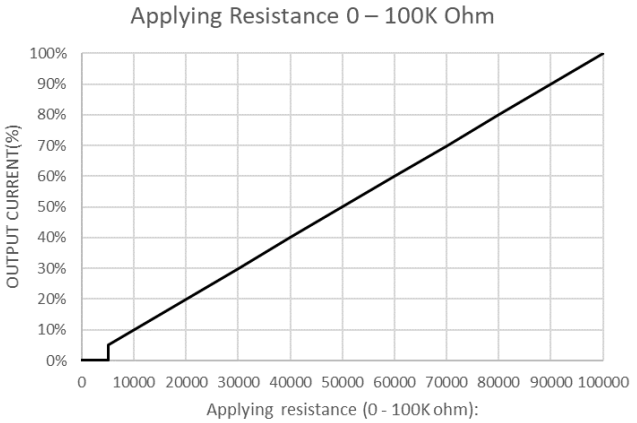

Installation Guide

- **Warning / Caution!!**
  1) Risk of electrical shock and energy hazard. Any failures should be examined by a qualified technician. Do not remove the case of the power supply by yourself!
  2) Risk of irreparable damage. LED power supplies with IP64 to IP66 rating must be located indoors or in a location where these units can be sheltered from the rain if outdoors.
  3) Do not install LED power supplies in places with high ambient temperature or close to fire source. Refer to the specifications about the maximum ambient temperature limitations.
  4) Output current and output wattage must not exceed the rated values on the specifications.
  5) The FG (⏚) must be well connected to PE (protective earth) if the unit equips with it.
  6) All Bosch DC LED drivers are designed in accordance with EMC regulations and the related test reports are available by request. Since they belong to component power supplies and will be installed inside system enclosure, when they are integrated into a system, the EMC characteristics of the end system must be re-verified again.

Manufacturer:

BOSCH - BUILDING GRID TECHNOLOGIES
256 RACEWAY DR.
MOORESVILLE, NC, 28117, USA.
Web: www.boschbgt.com

Menlo Park office:
BOSCH - BUILDING GRID TECHNOLOGIES.
101 Jefferson Drive
Menlo Park, CA 94025

This product is intended to be used as a lamp control gear that is installed after the mains control switch.
Conforms to the following standard:

Features

- Ultra High Efficiency (Up to 93%)
- Constant Current Output
- 0-10V Dimming Control
- Input Surge Protection: 4kV line-line, 6kV line-earth
- All-Around Protection: OVP, SCP, OTP
- Waterproof (IP67) and UL Dry / Damp / Wet Location
  DT models in Wet Locations must be Built-In
- SELV Output
- TYPE HL, for use in a Class I, Division 2 hazardous (Classified) location

Description

The *EUC-200SxxxDT(ST)* series is a 200W, constant-current LED driver that operates from 90-305 Vac input with excellent power factor. It is created for high bay, high mast, arena and roadway lights. The high efficiency of these drivers and compact metal case enables them to run cooler, significantly improving reliability and extending product life. To ensure trouble-free operation, protection is provided against input surge, output over voltage, short circuit, and over temperature.

Models

Output Current	Input Voltage Range(1)	Output Voltage Range	Max. Output Power	Typical Efficiency (2)	Power Factor		Model Number (3)
					120Vac	220Vac	
450 mA	90 ~ 305 Vac	267~445Vdc	200 W	93.0%	0.99	0.96	EUC-200S045ST
450 mA	90 ~ 305 Vac	223~445Vdc	200 W	93.0%	0.99	0.96	EUC-200S045DT
700 mA	90 ~ 305 Vac	171~285Vdc	200 W	93.0%	0.99	0.96	EUC-200S070ST
700 mA	90 ~ 305 Vac	143~285Vdc	200 W	93.0%	0.99	0.96	EUC-200S070DT
1050 mA	90 ~ 305 Vac	114~190Vdc	200 W	92.5%	0.99	0.96	EUC-200S105ST
1050 mA	90 ~ 305 Vac	95~190Vdc	200 W	92.5%	0.99	0.96	EUC-200S105DT
1400 mA	90 ~ 305 Vac	85~142Vdc	200 W	92.0%	0.99	0.96	EUC-200S140ST
1400 mA	90 ~ 305 Vac	71~142Vdc	200 W	92.0%	0.99	0.96	EUC-200S140DT
1750 mA	90 ~ 305 Vac	68~114Vdc	200 W	92.0%	0.99	0.96	EUC-200S175ST
2100 mA	90 ~ 305 Vac	57~95 Vdc	200 W	92.0%	0.99	0.96	EUC-200S210ST(4)
2450 mA	90 ~ 305 Vac	48~81 Vdc	200 W	91.5%	0.99	0.96	EUC-200S245ST(4)
2800 mA	90 ~ 305 Vac	42~71 Vdc	200 W	91.5%	0.99	0.96	EUC-200S280ST(4)
3150 mA	90 ~ 305 Vac	38~63 Vdc	200 W	91.5%	0.99	0.96	EUC-200S315ST(4)
3500 mA	90 ~ 305 Vac	34~57 Vdc	200 W	91.5%	0.99	0.96	EUC-200S350ST(4)
4200 mA	90 ~ 305 Vac	28~47 Vdc	200 W	91.5%	0.99	0.96	EUC-200S420ST(4)
4900 mA	90 ~ 305 Vac	24~40 Vdc	200 W	91.5%	0.99	0.96	EUC-200S490ST(4)
5600 mA	90 ~ 305 Vac	21~35 Vdc	200 W	91.5%	0.99	0.96	EUC-200S560ST(4)

St. Clair Acrylic High Bay

*Protected by U.S. Patents No. 4,839,781, D659,897 and Patent Pending OptiFlec™ System Performance

Description

- Series: EHBUS-CC
- Lamp Life Rating: 100,000 hours
- Lumen Maintenance: 70% over 100,000 hours
- Light Output: 5000K, 82-90 CRI
- IP Rating: IP43
- Applications: Warehouses, factories, retail showrooms, gymnasiums, supermarkets, exhibition halls
- Warranty: 10 Year Limited

Specifications and Patented Feature

- Premium grade acrylic reflector with <2% Haz
- Conical lens lifts main beam and breaks diffuses image
- Stainless steel roll-form clamp band
- US Patented optics improve performance by 20% compared to competing fixture
- Die cast aluminum ballast casing with corrosion-resistant white powder coat finis
- Electronic ballast with high power factor, flicker fre instant re-strike
- Excellent vibration & shock resistance

OptiFlec™ Septum Enhancement combined with EverLast® Reflexors outperforms all other induction systems by 27

Ordering Information

Series
EHBUS-CC — [ ] — [ ] — [ ] — [ ] — [ ] — [ ]

Wattage
100W
120W
150W
200W
250W
300W*

Voltage
120–120-277V
347–347V*
480–480V*

Color Temp
50–5000K
40–4000K*

Cord Options
X–None
3P–120W 3 Prong Plug*
L5–NEMA L5-15 120V*
L6–NEMA L6-15 250V*
L7–NEMA L7-15 277V*

Wire Guard
X– None
WG–Wire Guard*

Dimming
X– None
VD- Variable Dimming*

Bold = Standard
Grey * = Upgrade options available upon request

Example: **EHBUS-CC**-150-120-50-3P-VD

*Legal Notice: Full Spectrum Solutions owns proprietary rights in the EverLast® Series of fixtures in the form of pending patent applications in the US and PC applications for International protection.

Exclusive Features

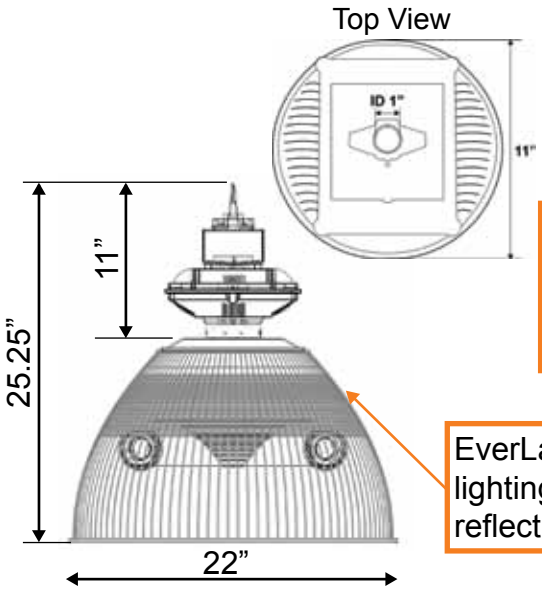

OptiFlec™ Septum Enhancement captures wasted up light directing it towards the Reflexor system as well as increasing down light at work plane

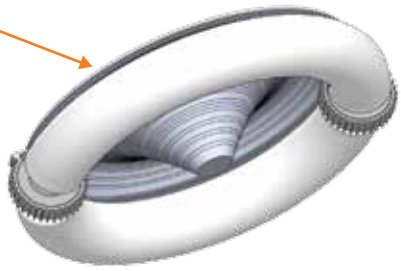

*Patent No. D659,897

EverLast® Reflexors use high optic lighting enhanced resins tuned to high reflective propertie

Photometric Data

250W

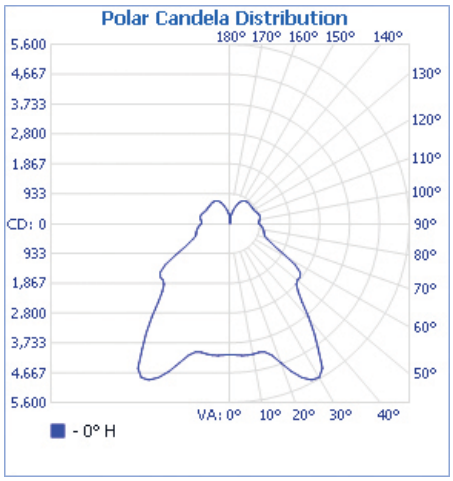

Specification

Lamp Specification

Wattage	Lumens	L/W Ratio	CRI	CCT (KELVIN)	Rated Life
100W	8,400	84	82-85	5000	100,000 hours
120W	10,100	84	82-85	5000	100,000 hours
150W	12,600	84	82-85	5000	100,000 hours
200W	16,800	84	82-85	5000	100,000 hours
250W	21,000	84	82-85	5000	100,000 hours
300W	25,200	84	82-85	5000	100,000 hours

Ballast Specification

System Wattage	Input Voltage	Input Current	Input Freq.	Power Factor	Ambient Temp	THD
111W	120-277V/480V*	0.69-0.30A / 0.17A	50/60Hz	>0.95	-40 to 130 F°	<10%
134W	120-277V/480V*	0.79-0.34A / 0.20A	50/60Hz	>0.95	-40 to 130 F°	<10%
165W	120-277V/480V*	0.98-0.43A / 0.25A	50/60Hz	>0.95	-40 to 130 F°	<10%
215W	120-277V/480V*	1.18-0.51A / 0.30A	50/60Hz	>0.95	-40 to 130 F°	<10%
265W	120-277V/480V*	2.21-1.00A / 0.56A	50/60Hz	>0.95	-40 to 130 F°	<10%
320W	120-277V/480V*	2.65-1.20A / 0.62A	50/60Hz	>0.95	-20 to 130 F°	<10%

Application Image

Southern Felt Co., North Augusta GA

Call Toll Free: 888-383-7578 www.everlastlight.com

POWERFOIL® X 2.0

with Nitro Seal Drive™

18 Ft

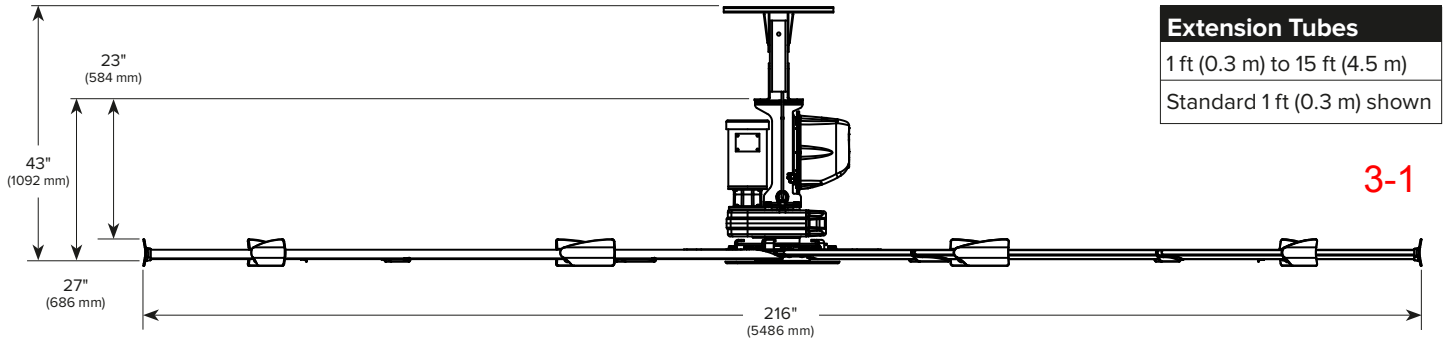

Extension Tubes
1 ft (0.3 m) to 15 ft (4.5 m)
Standard 1 ft (0.3 m) shown

3-1

Technical Specifications

Model number	PFX2.0-18
Number and type of airfoils	10 patented Powerfoil® airfoils 10 patent-pending AirFence™
Airfoil finish	Mill finish aluminum or custom color finish
Winglet (standard color)	10 patented Powerfoil winglets (safety yellow)
Fan weight (as shown)	332 lbs [151 kg]
Motor	1.5 HP [1.1 kw]; c-face motor adaptor
Maximum speed	77 RPM
Maximum amps	5.0 A @ 200—250 V 2.5 A @ 400—480 V
Input power and required breaker	200—250 VAC, 50/60 Hz, 1 Φ, 30 A 200—250 VAC, 50/60 Hz, 3 Φ, 15 A 400—480 VAC, 50/60 Hz, 3 Φ, 10 A
Purpose-built STOBER Drives gearbox	NitroSeal Drive™ with <11 arc minutes backlash, HeliCamber® gear technology, SKF tapered roller bearings, 2-½" [63.5 mm] hollow output shaft, Simrit® double lipped output seals, lifetime synthetic oil, Nitrogen filled and permanently sealed
Redundant safety features	Airfoil retainers, hub clips, safety cables, grade 8 bolts
Onboard controller	ABS/PVC based enclosure, built-in heatsink
Controller	X-series; digital wall keypad Includes 150 ft of factory-assembled CAT5 cable
Fire relay	Included
Mount (standard)	Small I-beam
Mount (options)	Large I-beam, spanned angle iron, small/large L-bracket, Z-purlins
Sound level at maximum speed[1]	< 55 dBA
Minimum airfoil clearances required	2 ft [0.6 m] on sides, 4 ft [1.2 m] below ceiling deck
Certifications (whole fan)	ANSI/UL 507 CAN/CSA C.22.2 No. 113-08

[1]Sound level measured at a blade height of 20 ft [6 m] and 20 ft [6 m] horizontally from center of fan.

X-Series Wall Keypad

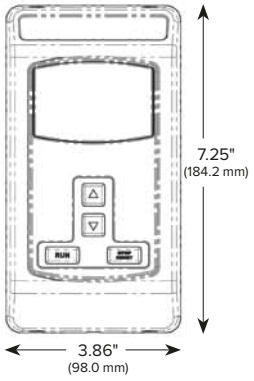

- Provides full control of all fan functions
- Can be located up to 1,000 ft from fan
- Single keypad can operate unlimited number of fans
- Lockout with 4-digit passcode

15 year parts, 1 year labor warranty; certain exclusions apply.
See complete warranty for details.

OPTIONS

- SmartSense365 for year-round automated control
- 24 hr digital timer
- Custom color packages
- 100 W Halide light
- Security camera
- 8 ft — 24 ft diamters

Covered by one or more of the following U.S. Patents: 6,244,821; 6,589,016; 6,817,835; 6,939,108; 7,252,478; 7,284,960; 7,654,798; D587,799; D607,988 and other patents pending.

Big Ass Fan Company | An ISO 9001:2008 certified company

800 Winchester Road, Lexington, KY 40505
877-BIG FANS (877-244-3267)
www.BigAssFans.com

22/1029 Manly Rd, Tingalpa, QLD 4173, Australia
(07) 3292 0100
www.BigAssFans.com.au

BIG ASS FANS®
No Equal.

Appendix D: BESS Documentation

Energy Storage System Operation Manual

Bosch Energy Storage Solutions LLC

BOSCH
Invented for life

100 kW/ 100 KWh Energy Storage System

Operation Manual

Contact Information

Address

Bosch Energy Storage Solutions, LLC

4005 Miranda Avenue,

Palo Alto

CA 94304

Phone: (650) 320 2975

Technical Support:

Phone: 650-320-2975

Email: ryan.balliet@us.bosch.com

Revision Log

Version 1	July 31st 2015	First full version provided to the customer.

WARNING

To reduce the risk of injury or electric shock, do not operate the system without understanding the instructions provided in this document.

No modifications to the Energy Storage System should be performed to the hardware without prior consultation with Bosch Energy Storage Solutions, LLC. Battery operation limits as defined here in should always be followed during normal operation. Working on unit without prior authorization and training will void all warranties.

Components inside the container are electrostatic –discharge sensitive. Proper ESD control and abatement procedures must be followed to avoid ESD damage.

Safety signs for high voltage and risk for electric shock are posted in all the relevant places on the container. Proper precautions must be taken while entering and exiting the container. Only qualified electrical personnel should be allowed to enter the container without supervision.

Abbreviations

AC	Alternating Current
ATS	Automatic Transfer Switch
BESS	Bosch Energy Storage Solutions LLC
BMS	Battery Management System
DC	Direct Current
DCMG	Direct Current Microgrid
DOD	Depth-of-discharge
ESS	Energy Storage System
ESTCP	Environmental Security Technology Certification Program
HVAC	Heating, Ventilation and Air Conditioning
HW	Hardware
LiB	lithium-ion battery
LV	Low voltage
PCC	Point of Common Coupling
PCS	Power Conversion System
PLC	Programmable Logic Controller
SOC	State of Charge
SOH	State of Health
SW	Software
UPS	Uninterruptable Power Supply

Content

1 Introduction

This manual outlines operation and procedures of the 100kW/100 kWh AC energy storage system (ESS) installed at Fort Bragg, NC. The ESS features a bi-directional 100 kVA inverter, with two AC ports for the normal grid operation and off-grid mode, coupled to a 134 kWh_{DC} lithium ion battery (LiB) system. The system is controlled and operated through a central programmable logic controller (PLC). The system is specifically designed to perform grid-tied operations as well as grid-forming operation in the case of grid failure.

The basic features of the system are as follows:

The ESS is designed to deliver full lag and lead power factor up to a maximum of 100 kW continuously[1]. The system functions in three main modes of operation; Automatic mode, Power Command mode and Back-up mode.

In the Automatic mode, the ESS is commanded by the BESS PLC to fully charge the system and be ready for discharge or for emergency back-up applications. The power set point and battery state of charge (SOC) set point are fixed. In the Power Command mode, the user can command different power set points to the system. The user is required to follow the limits provided by BESS for power and SOC during such operation. Back-up is not a user commanded mode but is automatically enabled when there is a grid outage. The ESS switches the inverter to Back-up mode automatically when the grid outage is detected. The batteries then discharge to maintain the AC parameters of 480V, 60 Hz at the automatic transfer switch. When the grid returns, the ESS automatically switches back to its previous mode of operation. The user must follow the limits for battery operation provided by BESS in this mode as well.

In all operation modes, the BESS PLC ensures that safety limits are observed and will shut down the system in case of any abnormal operating conditions. In the case of a fault during operation, the BESS PLC provides the feedback of the type of fault to the customer.

[1] Energy delivered (duration) is contingent on battery parameters such as temperature, SOC being maintained at required limits. De-rating of the battery will be forced at high SOCs (>92%) for charging and low SOCs (<3%) for discharging.

2 System Specifications

AC power rating	100 kW
Nominal AC energy rating	100 kWh (@ 20 kW)
AC voltage (input)	480V, three phase , 60 Hz
DC voltage range	320V – 450 V; 7 battery strings of 16 modules each
Battery SOC	0 – 100 %
Grid forming mode	Enabled ; 480V , 60 Hz
Operating temperature	0-45 °C
Storage temperature	0-45 °C
Safety features	Door sensors, e-stops, fire suppression system with feedback to Fort Bragg
Internal container temperature range	23 ± 5°C (controlled by HVAC)
Humidity	5-95% humidity, non condensing. Installation site has to be dry and to be protected against penetration of water
Expected life	10 years / one cycle per day ≈ 4000 cycles (not guaranteed)
Footprint	20’ ISO shipping container: 20’ x 8’ (6 m x 2.4 m)
Dynamics	Reaction on change of power set point <=2 s

Operation parameters

Power Requirements	480V, 60 Hz, 3 phase, 150 A max
Auxiliary power requirement	480V, 60 Hz, 3 phase, 30 A max
UPS Back-up time for controllers	Up to 9 hours
Average HVAC power requirements	2.0 kW

Safety Standards	
Battery and controllers	UL 1973, UN 38.3, UL 1642
Power Conversion System	UL 1741, IEEE 1547
Fire suppression system	NFPA 72, NFPA 70, NFPA 2001, NC Fire Code (2012)

3 System Description

The ESS fits inside a 20-foot shipping container separated into two distinct compartments. The separation within the ESS separates the DC components (batteries, racks, controllers) from the AC components (inverter, transformer and power lines) and provides isolation between the two sides in case of fire. The outline of the system design is as shown below in Figure 1.

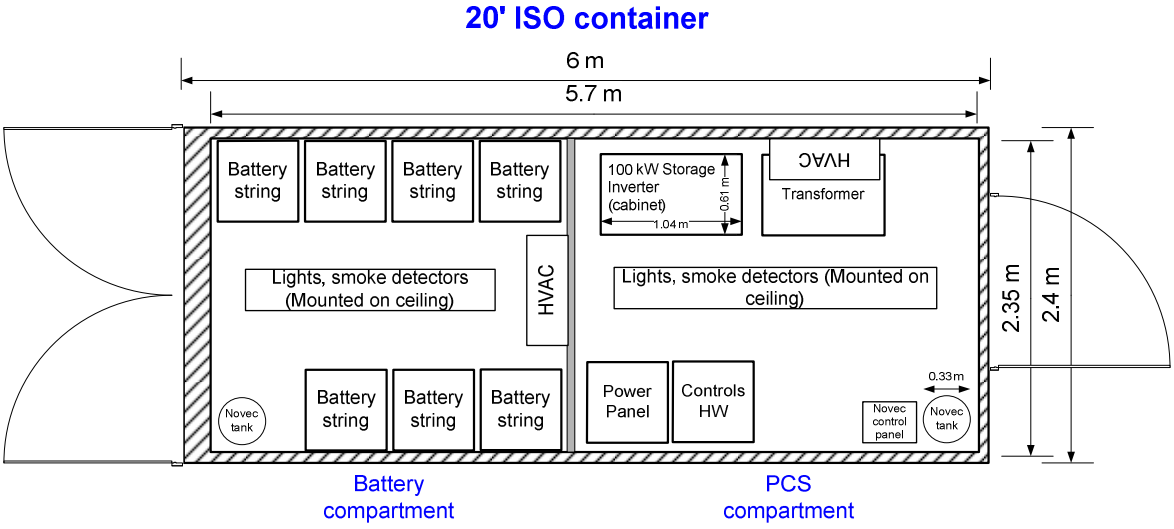

Figure 1: System Layout (top view)

A 90-minute rated firewall is present between the Battery compartment and the PCS compartment. A grounding bar is employed to have a common ground for both the sides of the container. The batteries, controllers, all panels and the inverter are grounded to this common point. The grounding from the external source (building) is bonded to this point to ensure the ESS is bonded to the same ground as the rest of the equipment on-site. A single fire suppression control panel is used with two separate spraying

mechanisms and systems. This is to ensure that the deployment of fire suppression agent occurs only on the side where there is an issue. The main power panel from the fire suppression system is connected to the building's central alarm so as to alert the fire fighters on-base to be at the site in case of an emergency. A detailed description of the safety features and their design is provided in Appendix 4.

The system electrical topology is shown below in Figure 2. The single line diagram is used to provide insights into the main connection points in the system. There are a total of 2 isolation transformers as part of the ESS. The transformer 1 and transformer 2 refer to the isolation transformers at the grid side and the load side respectively. The load side transformer is housed within the ESS container. The Detailed as-built drawing is provided in Appendix 1 of this document. The DC side is negative grounded and the inverter is neutral isolated. This document's scope is for operation of components in the blue box below.

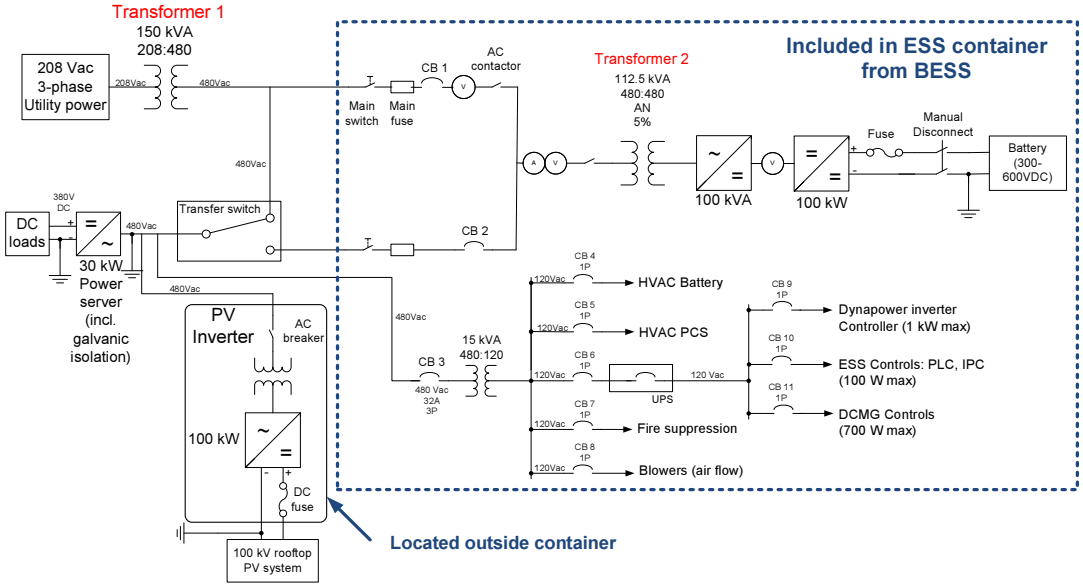

Figure 2: Overall system topology

A brief description of the different components of the system is provided here. For additional details, the user is referred to appendices section.

Battery system

The detailed specification of the battery modules and the connection and disconnection procedure are provided in Appendix 2.

Chemistry

The Li-ion battery provided by Sony Corporation employs a lithium iron phosphate chemistry, was chosen for this system due to its superior safety, ability to cycle through the full range of battery state of charge without any adverse degradation effects, robust thermal characteristics, long cycle life, and efficiency.

Manufacturer

BESS has carefully evaluated all major Li-ion battery manufacturers to select the best supplier based on battery performance, durability, and safety, as well as supplier experience, quality, and financial strength. The battery components have been in series production since 2010 and have been deployed in multiple small and large projects at various customer sites worldwide. More than 470 storage projects are in operation today.

Lifetime discharge cycles

The batteries chosen for this system are distinguished by excellent cycle life. The battery cells have demonstrated over 6000 charge-discharge cycles at 100 % DOD. For this test, the cells were charged from 0 % to 100 % SOC at a 1C rate and then discharged completely at a 1C rate repeatedly. After 6000 cycles at an ambient temperature of 23 ºC, the cells retain 80% of their beginning of life capacity.

Self-discharge characteristics

The batteries exhibit a self discharge rate of <0.002% per day when the system is off. When the BMU is powered on by the battery, the BMU shuts off the batteries and controllers once the SOC is less than 0.5 %. If the BMU is on, as it is when the system is in an idle state, the ESS will have a self discharge rate of less than 3% per day.

SOC operating range

Unlike other lithium ion battery chemistries (transition metal oxide based), the lithium iron phosphate chemistry is stable throughout the entire SOC range (0 to 100 %). Therefore, there are no requirements of average SOC per day or storage SOC range. It is ideal to store the batteries at about 50% SOC for long-term storage when the system

is off, as this offers the flexibility of full power charge/discharge when the system comes online and minimizes the risk of over-discharge due to self-discharge of the battery.

Battery balancing

During normal operation of the battery system, the presence of temperature variations, along with the variations in actual current/voltage experienced by the individual modules, the battery strings can gradually become imbalanced. The explained state of imbalance exists when there is disparity in the states of charge for modules within a string and/or from string to string. An imbalanced system can slightly reduce the amount of energy available. However, any imbalance can be corrected though a special balancing procedure. Therefore, balancing of the battery strings is performed once every month. In this operation, the battery strings are equilibrated to the same temperature and are charged slowly such that all the battery strings and modules reach the same SOC value of 100%. During this procedure, the battery controller internally manages the charge and discharge of individual modules and strings to reduce the in-homogeneity. During this operation, the system will be unavailable for the remote controller's Power Commands. However, if the ESS is needed for back-up operation, the balancing operation will be interrupted. On return of the grid power, the balancing process will resume until completion.

For the ESS, the balancing operation has been scheduled for the 1st Sunday of every month at 9 PM. Typical duration of the balancing operation can range between 4-8 hours depending on the level of in-homogeneity in the system.

Round-trip efficiency

The round-trip efficiency of the ESS is determined by the combined efficiency of the battery system and the PCS. The DC round trip efficiency of the proposed battery system is very high (>93.5 % within the operating range used for the ESS) compared to other storage technologies (60 to 85 %). Figure 3 below shows typical values for DC roundtrip efficiency of the battery modules for full depth-of-discharge cycles at different discharge times when the charge current is identical to the discharge current and the ambient temperature is 23 °C.

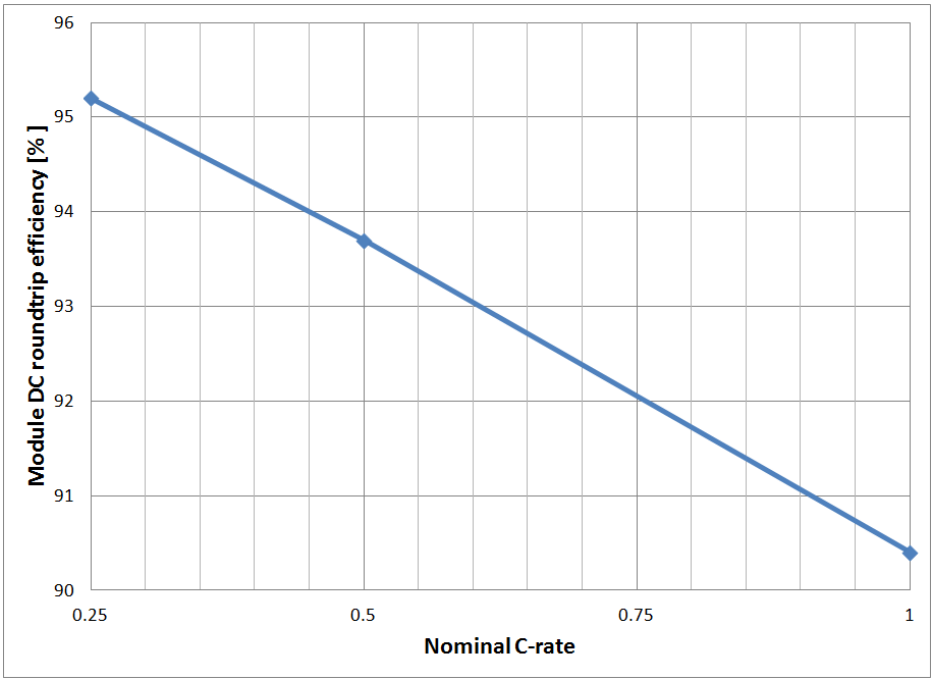

Figure 3: DC roundtrip efficiency of the battery module.

Discharge capability

A distinguishing feature of the battery chosen is excellent high-rate performance. The battery is capable of completing a full discharge in less than two hours while still retaining more than 95 % of its maximum energy, as shown in Figure 4. Also, unlike other Li-ion chemistries, which show dramatic degradation at lower states of charge, the lithium ion phosphate chemistry has been shown to be robust and can be discharged to near zero state of charge without any significant impact on life. This reduces the over-sizing required for system design.

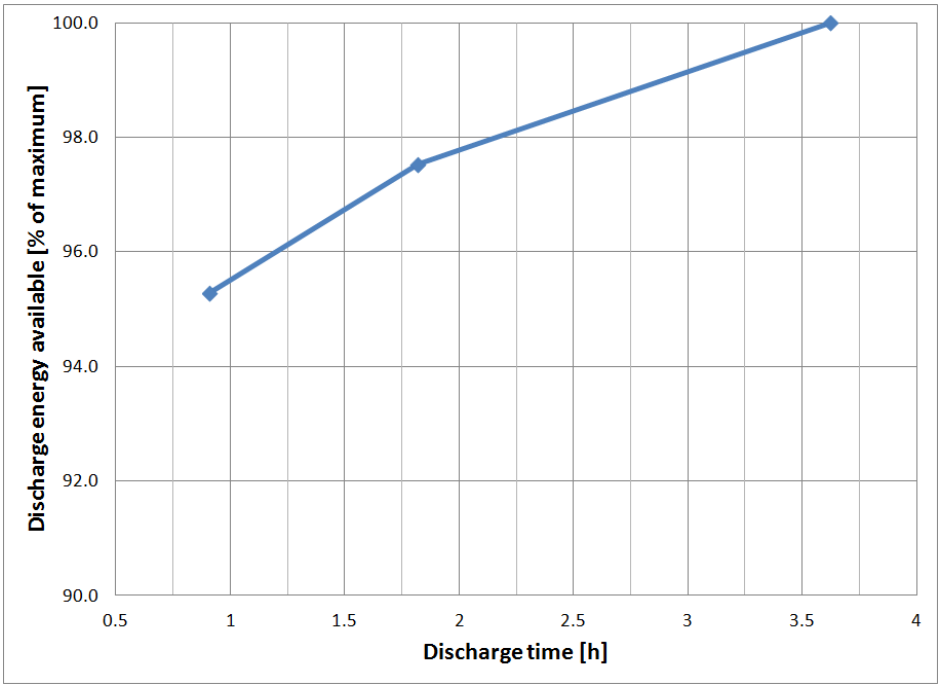

Figure 4: Battery module discharge performance.

Charge acceptance

In addition to excellent discharge performance, the battery subsystem also has superior charge characteristics. It can be charged to over 91 % of its full capacity well within the nominal discharge time of the system. For example, if the ESS has an AC discharge energy to power ratio of one hour, the battery system will be able to charge to 91 % capacity or higher within one hour. De-rating of charging power is necessary at higher SOCs to enable a full charge. The high-power charge capability of the battery also enables equal capacity for both up and down regulation across a broad range of states of charge. Figure 5 below shows the SOC as a function of time at the module level while charging at an ambient temperature of 23 °C

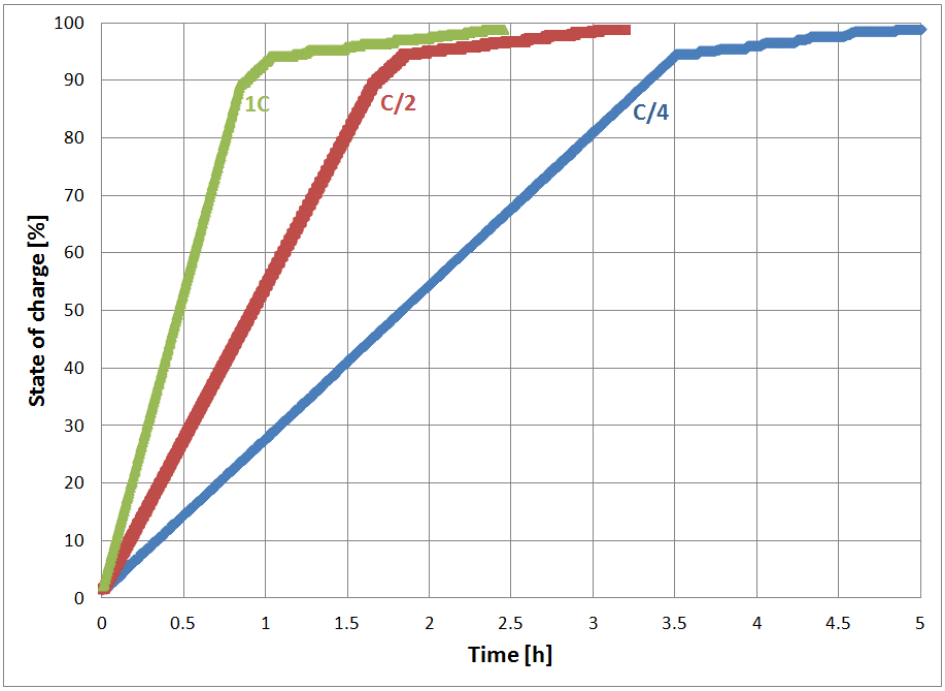

Figure 5: Battery module charge performance.

Energy density

The energy density for the cells is 270 kWh/m^3, and at the module level it is 82 kWh/m^3. For the standard building block used in the ESS, which is a rack containing a string of modules, the energy density is 40 kWh/m^3.

Over-charge/discharge protection, state-of-charge reporting, active cell balancing

The battery management system is equipped with safety hardware and software controls to prevent abnormal or unsafe operation. Over-discharge/charge protection is built into the hardware through circuit breakers and fuses. A software control system comprising strategies for alert, warning, and disconnect is also built in to enable safe disconnection of the system. There is also an added layer of software controls enabled on the PLC to perform these actions, providing the system with the redundancy required to prevent unsafe operation.

State of charge is reported by the supplier's battery management system. Typical accuracy range is ±2 %. There are also periodic automatic calibration steps performed during normal operation to maintain the accuracy over time.

Power Conversion System

The PCS includes bi-directional inverters, all necessary switchgear on DC and AC sides, over-current protection devices, transformers, and switchgear equipment. The PCS is built to comply with all applicable standards including anti-islanding protection per UL 1741 and IEEE 1547 standards. The system also includes manual disconnects for diagnostics and maintenance purposes.

The inverter of the system is specifically designed for use with storage systems and has a high efficiency of 97% at rated power. The unit offers transition from Grid-Tied to Stand-alone mode or from Stand-Alone to Grid-Tied through a dynamic transfer. In the Stand-Alone mode, the control is through voltage (U) and the frequency command (F). U and F commands have been preset for the ESS at 480V and 60 Hz respectively. After a grid fault and upon the grid restoration the PCS synchronizes the inverter output to match the grid voltage and frequency prior to transfer back to Grid-Tied mode. The PCS wait time, the time the PCS must wait before allowing connection back to the grid, for this process has been set to 90 s for the ESS. The Automatic transfer Switch(ATS), used on-site, must have a wait time equal to or less than this value.

The output voltage of the inverter is 480 VAC. Its control system implements high and low voltage ride-through functions per IEEE 1547. If the grid voltage deviates away from the nominal value, the inverter will automatically disconnect from the grid within the required clearing time per IEEE 1547 standard. The AC voltage protection range parameters have been fixed for the ESS based on the voltages observed on-site at Fort Bragg. The three phase output voltages and currents are sinusoidal and with total harmonic distortion to meet or exceed IEE1547 requirements.

The control system also implements high and low frequency ride-through functions per IEEE 1547 limits. If the grid frequency deviates away from the nominal value, the inverter will automatically disconnect from the grid within the required clearing time per IEEE 1547 standard. The AC frequency protection range parameters have also been fixed for the ESS based on the voltages observed on-site at Fort Bragg.

For a complete description of the control method and operation of the inverter, please refer to Appendix 3.

The efficiency of the inverter to perform AC to DC conversion was measured for the ESS at various power levels. The results are shown in Figure 6. The system is found to be better than 97% at power levels closer to full power and is better than 95% even at ¼ of the rated power of operation.

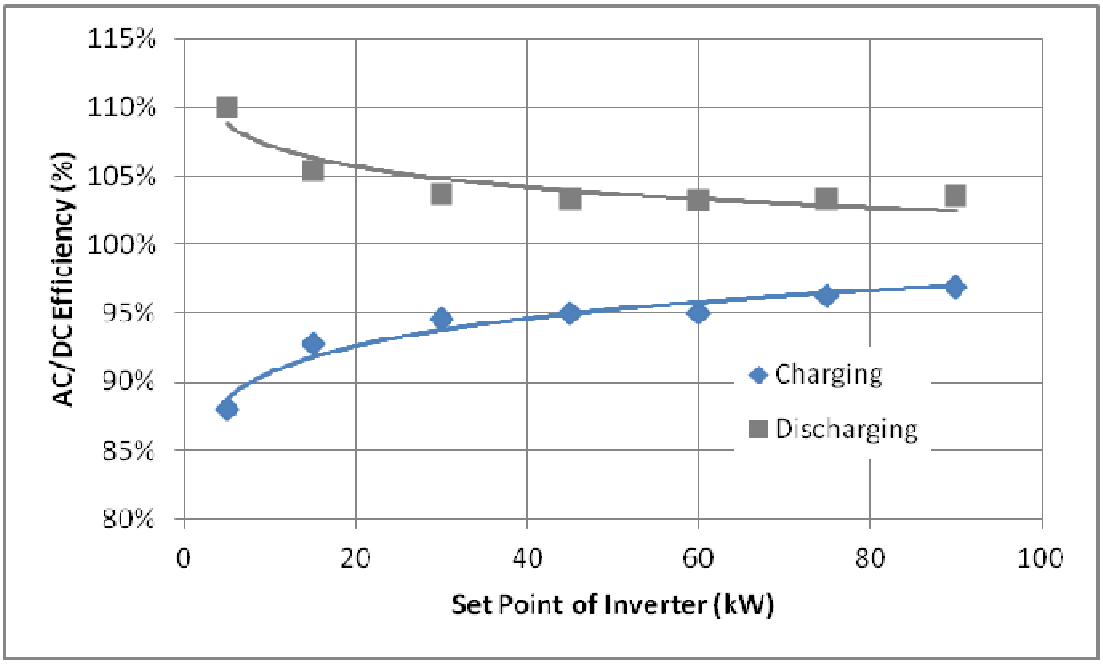

Figure 6: Efficiency for AC/DC conversion for the Inverter; Overall efficiencies of >95% is observed at powers >E/4

Thermal management

Two split heating, ventilation and cooling (HVAC) units are provided with the ESS. The location of the indoor component of these units is shown in Figure 1. The heat loads and the desired operating range for the components are listed in the table below. The design of the HVAC system was done in order to meet these requirements.

HVAC for Battery compartment	
Maximum heat generated from all batteries (@ full rated power)	4.5 kW
Operating temperature range	23 ± 5°C (measured at any location)
Air flow required	>300 CFM
Controls of HVAC	HVAC cooling and heating are controlled through the BESS PLC. Based on the internal cell temperatures of the batteries the operation of the HVAC units are conducted

Coefficient of performance (COP)	>2.5 ($kWh_{thermal}/kWh_{electric}$)

HVAC for PCS compartment	
Max heat generated from Storage inverter, transformer and other equipment in PCS compartment	5.5 kW
Operating temperature range	0 ~40°C (Even though higher temperatures is allowed, as a safety limit, the ambient temperature in the PCS cabinet is regulated to below 30°C.)
Air flow required	>500 CFM
Controls of HVAC	HVAC units are again controlled through the BESS PLC program
Coefficient of performance	>2.5 ($kWh_{thermal}/kWh_{electric}$)

HVAC operation is only permitted if the ESS is not in a faulted state. In case of a fault, the system needs to be reset (by sending the fault acknowledge signal described in the following sections) and the HVAC operations resumed. In case of ambient temperatures higher than 45°C, which arises from allowing the system to stay in faulted state for a long time, it is recommended to restart the system to allow the HVAC units to cool the system before returning to normal operation.

In addition to the HVAC units, there are also cross ventilation fans that are installed in the system. The purpose of these cross ventilation fans is to enable mixing of hot and cold air within the aisle of the battery strings and thereby ensure uniform temperature for the modules within each string. The Fan operation is also shut down in case of a fault and is only triggered when the internal cell temperatures for the battery cells exceed 25°C.

4 Remote Interface Control

The following summarizes the status and data interchange between the ESS's PLC and the customer PLC. The data communication uses Modbus TCP over Ethernet. Table 1 shows all the variables (data) passed from the BESS PLC to the user and table 2 lists

all the values variables sent from user's remote controller to the BESS PLC. The variable update rate for the BESS PLC is 1 Hz.

TCP MOBUS SETTINGS:

IP Address: 192.168.101.25

Port: 504

Table 1: BESS PLC to the Remote Controller

Reg. Add	Description	Data Type	Word Size	Unit	Notes
0	Present time	int16	1	Year	Time value as registered by the BESS PLC. This can also be used as heartbeat to ensure connection is live.
1	Present time	int16	1	month	
2	Present time	int16	1	Day	
3	Present time	int16	1	H	
4	Present time	int16	1	Min	
5	Present time	int16	1	S	
6	Ready	Bool	1	None	Ready Boolean is used to determine if the ESS is able to be commanded by the Remote Controller. 0: Battery NOT ready to receive commands 1: Battery ready to receive commands
7	Warning Code	int16	1	None	0: No warning 1: System SOC operation limit warning (>95.5% or < 4%) 2: Ambient Temperature is higher than normal (>37°C) 3: Invalid power command from user
8	Fault code	int16	1	none	0: No error 1: Fault in the Battery 2: Fault in the Inverter 3: E-stop or Door sensors have tripped 4: Ambient temperature has exceeded limits (>45°C) 5: Minimax system has triggered an alarm 6: Shut-down command failure
9	Command Number	int16	1	none	5 : ESS is in OFF state 8: ESS is in normal mode (power mode)

					4: ESS is in Back-up mode 9: ESS is in Faulted mode
10	Energy to charge battery fully from present state	int16	1	kWh/10	Estimated kWh charge that can be accepted by the ESS
11	Energy to discharge battery fully from present state	int16	1	kWh/10	Estimated kWh of discharge that can be extracted from the ESS
12	SOC	int16	1	%	The current State of Charge of the ESS
13	AC power	int16	1	kW/10	The AC power being delivered or commanded by the inverter
14	AC current	int16	1	A/10	The AC current flowing through the inverter
15	Maximum charge power limit	int16	1	kW/10	The maximum charge power that can be accepted by the ESS
16	Maximum discharge power limit	int16	1	kW/10	The maximum discharge power that can be commanded from the ESS
17	Maximum charge current limit	int16	1	A/10	The maximum charge current that can be accepted by the batteries in the ESS. This limit does not account for the AC-DC efficiency losses in the system.
18	Maximum discharge current limit	int16	1	A/10	The maximum discharge current that can be delivered by the batteries in the ESS. This limit does not account for the AC-DC efficiency losses in the system.
19	ESS Average Ambient Temperature	int16	1	°C/10	Average ambient temperature of the ESS container
20	Length auto balancing	int16	1	min	Time required for finishing the battery balancing procedure. During this time, the ESS will not be available for remote controller's command mode
21	Time until balancing	int16	1	h	Number of hours before the next balancing operation
22	DC voltage	int16	1	V/10	DC Voltage of the Battery strings
23	Energy Discharged by the ESS	int16	1	kWh/10	Total cumulative energy discharged from the battery over the lifetime
24	Energy Charged by the ESS	int16	1	kWh/10	Total cumulative energy charged by the battery from the grid over the lifetime
25	State of Health	uint16	1	%	This represents the state of health of the batteries in the ESS. The batteries should not be operated once this value reaches <80%. At beginning of life, this value is

					=100%;
PV inverter variables currently not used. These registers can be modified if additional information from the ESS is needed. PV control will be done through DCMG server to eliminate redundancy in controlling PV inverter.					
26	Voltage L2-L3	int16	1	V/10	
27	Voltage L3-L1	int16	1	V/10	
28	Phase sequence	uint16	1	Hz/10	
29	Energy	uint16	1	kWh/10	
30	On grid hours	uint16	1	Hour	
31	On fan hours	uint16	1	Hour	
32	AC contactor cycles	uint16	1	Count	
33	Critical Alarm	uint16	1	None	
34	Info Alarms	uint16	1	None	
35	Inverter status	uint16	1	None	
36	DC current Z1	int16	1	A/10	
37	DC current Z2	int16	1	A/10	
38	DC current Z3	int16	1	A/10	
39	DC current Z4	int16	1	A/10	
40	DC current Z5	int16	1	A/10	
41	DC current Z6	int16	1	A/10	
42	DC current Z7	int16	1	A/10	
43	DC current Z8	int16	1	A/10	
44	Total DC current all zones	int16	1	A/10	
45	Inverter Manufactured year and month	uint16	1	None	
46	Inverter manufactured day and serial number	uint16	1	None	
47	Modbus level supported	uint16	1	None	
48	AC Reconnect over voltage setting	int16	1	V/10	
49	AC over freq setting	int16	1	Hz/10	
50	AC under freq setting	int16	1	Hz/10	

51	Internal temperature 1	int16	1	DegC/10	
52	Internal temperature 2	int16	1	DegC/10	
53	Internal temperature 3	int16	1	DegC/10	
54	Inverter output current average	uint16	1	A/10	

Table 2: Remote Controller to the ESS data

Reg. Add	Description	Data Type	Word Size	Unit	Notes
75	System time	int16	1	year	Time value sent by the remote controller used as a check to ensure live connection between the remote controller and the BESS PLC
76	System time	int16	1	month	
77	System time	int16	1	day	
78	System time	int16	1	h	
79	System time	int16	1	min	
80	System time	int16	1	s	
81	Fault Acknowledge	Bool	1	none	Default value sent to the ESS should be 0. In case of a fault, recommendation is to consult with BESS technical support. After discussion, a value of 1 is sent to acknowledge the fault.
82	AC Meter	int16	1	kW/10	The meter reading of the loads operating in the DC micro grid at any given time.
83	DC load	int16	1	kW/10	The meter reading of the DC loads at any given time.
84	WeatherHawk Solar	int16	1		Weather Hawk variables sent from DCMG to BESS. Currently, these are not being used but can be used in the future if any optimization process is required.
85	WeatherHawk AirTemp	int16	1	°C/10	
86	WeatherHawk RH	int16	1	%	
87	WeatherHawk Barometer	int16	1	kPA/10	
88	WeatherHawk Windspeed	int16	1	ms/10	
89	WeatherHawk	int16	1	deg	

	WindDirect				
90	WeatherHawk WindGust	int16	1	ms/10	
91	WeatherHawk WindGust	int16	1	mm/10	
92	WeatherHawk Snow_acc_yearly	int16	1	?	
93	Control of system by DCMG	Bool	1	None	This is always true when DCMG is controlling the system
94	Modes of operation	int16	1	None	This variable determines the mode of operation of the ESS. In case of a start-up (either after shut-down or after fault), the remote controller needs to send a mode command of 0, to start-up the system. For shutting down the system, mode command value of 5 is sent to the BESS PLC. 0 : Start-up of system 1 : Automatic mode 3 : Power Command mode 5 : Shutdown the ESS
95	ATS Status	Bool	1	None	ATS feedback is used by the ESS to return to operation in case of shut-down during back-up mode operation. The system will not automatically re-start until the ATS status feedback goes to TRUE. 0 : Grid available 1 : Backup
96	AC power command	int16	1	kW/10	Power set point for the ESS
97	Network ID	int16	1	None	
98	AC over Voltage setting	int16	1	V/10	
99	AC critical over voltage	int16	1	V/10	
100	AC under voltage setting	int16	1	V/10	
101	AC critical under voltage	int16	1	V/10	
102	AC under frequency setting	int16	1	Hz/10	
103	Over voltage	uint16	1	s/10	

	clearing time				
104	Under voltage clearing time	uint16	1	s/10	
105	Under frequency clearing time	uint16	1	s/10	
106	UL Fault reconnect wait time	uint16	1	s/10	
107	PV Inverter power set point	uint16	1	kW/10	This is the power set point of the PV inverter that will be connected to the ATS. This value should never be greater than the load value sent in register 83
108	Remote disable	uint16	1	-	
109	Protection fault recovery time	uint16	1	s/10	

5 General operation

This section will describe the operating procedures and the sequences of events during the ESS operation. The ESS can be controlled either remotely from the BESS PLC (administrative purposes only) or through the remote controller via the commands explained in section 4. Administrative access and control of the ESS will only be used by the BESS team for performing software updates, as well as troubleshooting and maintenance operations.

There are three main modes of operation for the ESS. They are:

1. Automatic mode
2. Power Command mode
3. Back-up mode

Each of these modes and the limits to be observed in these modes are described in detail in this section. Before start-up of operation of the ESS, the following checklist must be verified as true:

- The main breaker for the AC grid power feeding into the container is turned ON
- The automatic transfer switch is in Normal state
- The two 3 pole breakers inside the container (SF1, SF2 in as-built drawing 100631-E-001) are closed

- The UPS powering the BESS PLC, inverter PLC and the Minimax control system is powered ON
- The auxiliary panel breaker (CBS in as-built drawing 100631-E-001) is in ON state
- The E-stop button of the inverter is not engaged
- Container doors are closed and locked
- The E-stop buttons on the outside walls of the container are not engaged

After verification of the above, the ESS is ready to be operated by performing a start-up of the system.

System Start-up

System start-up is commanded by the user while sending an operation mode of 0 (Reg 94). On receipt of this command, the ESS performs internal checks to ensure all temperature and voltage limits are valid before powering up the PCS. After the normal start of the PCS equipment, the battery strings are powered on by the BESS PLC. The start-up sequence of the battery strings involves the following steps:

1. DC contactor between the AC and DC side of the ESS is closed.

2. The voltage of the DC bus of the inverter is set to 400 V. This wakes up the battery controllers which then report the status of the individual battery strings

3. The BESS PLC then connects the string with the lowest SOC (lowest voltage) followed by charging this string at a power of 25 kW

4. Charging is continued until the current string reaches an SOC level in range of other strings. Once the strings within connection range are identified, the PLC commands the connection of these strings. Charging is resumed once all the strings in the range are connected. This process is continued until all strings (7 total strings) are connected.

5. After all the strings are connected the BESS PLC sends a Ready Boolean (Reg. 6) value of TRUE which signifies that the ESS I now ready to be controlled through the remote controller.

Automatic Mode of operation

This is the normal mode of operation of the ESS. The mode is commanded by the user. This mode is mainly designed to get the ESS charged and be readily available for off-grid mode or back-up operations.

In this mode of operation, the BESS PLC performs task of maintaining the battery limits, and charges the ESS to ensure that the battery SOC is >=95%. It will also maintain the

SOC at this value by periodically charging to compensate for the self-discharge of the battery. The battery charging rate is set at 50 kW for this mode. This set point can be adjusted by BESS (administrative operation) if it is desired by the user. The ESS will suspend automatic mode of operation if the balancing process is triggered. Once the balancing of the battery strings is complete, the system resumes operation in automatic mode.

A flow-chart of operation of the system in automatic mode is shown here:

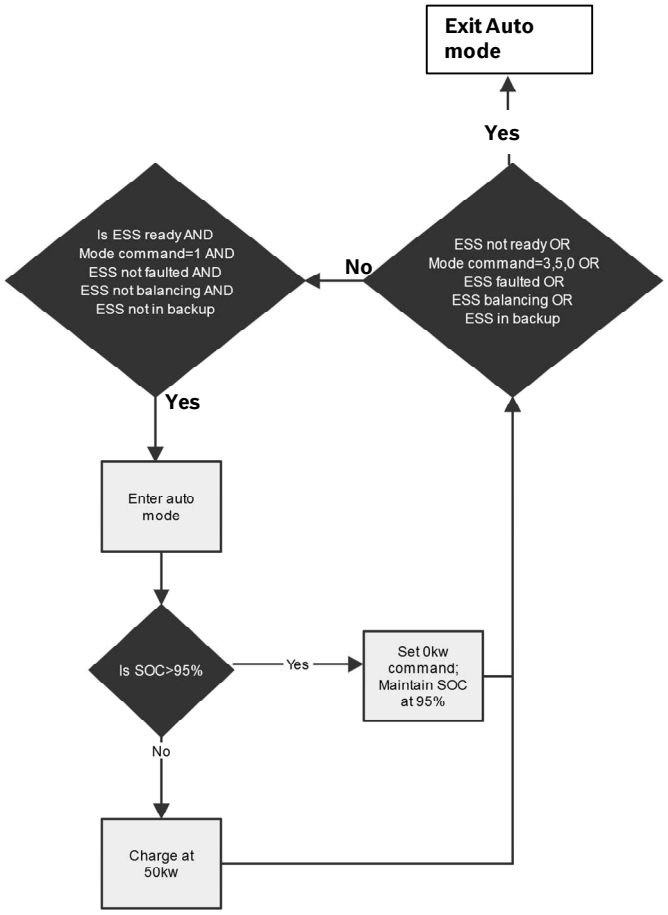

Figure 7: Flow chart for automatic mode of operation; SOC is maintained by periodically charging the ESS to compensate for the self-discharge. Currently, this occurs for every 1% drop in SOC

A typical operation profile of the ESS during the automatic mode of operation is shown in Figure 8 . The ESS starts charging at 50 kW (AC power=+50 kW), when the operation mode (commanded by the user) goes to 1. At this point, the ESS continues to charge at 50 kW until the SOC reaches value >=95%. The system power is set to 0 kW.

The SOC of the ESS will decrease during this period due to self-discharge of the battery. When the SOC drops below 1% of this original SOC set-point, a charging pulse of +15 kW is applied to top off the battery so as to maintain the SOC at the desired value of >=95%. Once the Operation mode is changed back to 3 (Power Command mode), the ESS immediately starts following the power set point as sent by the user; in this case, the value is -10 kW (battery is discharging at 10 kW).

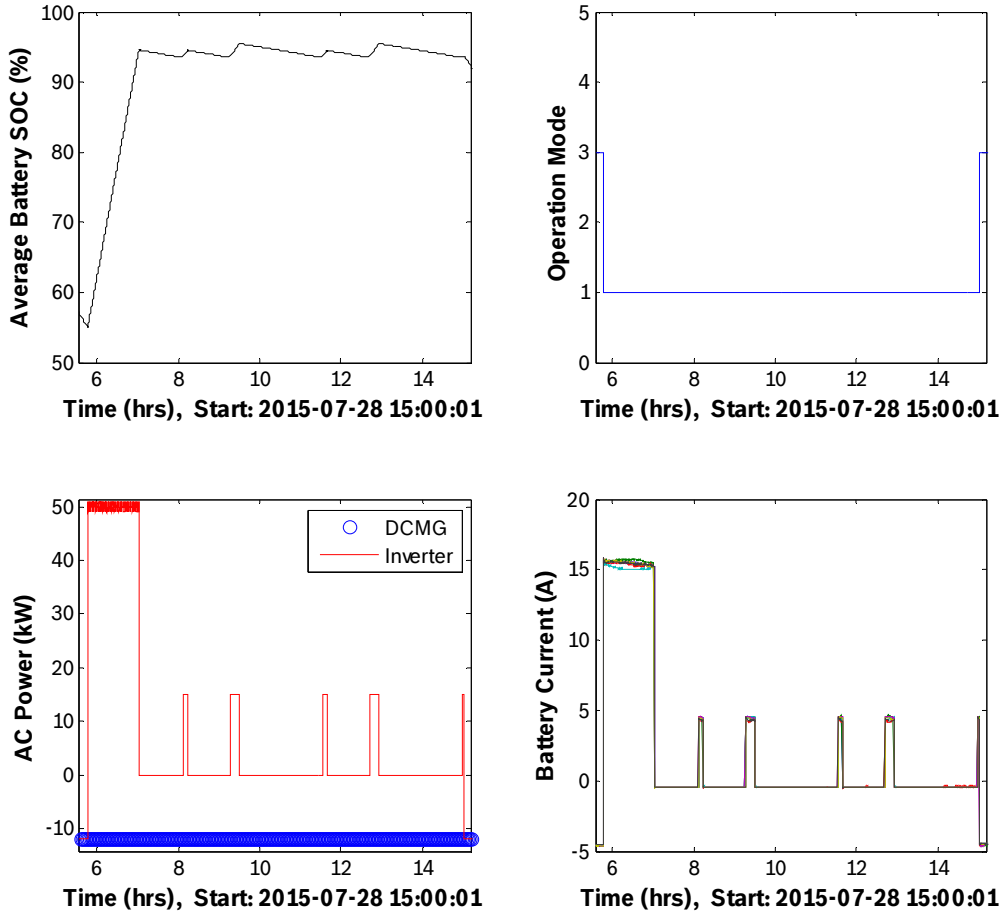

Figure 8: System in Automatic Mode of operation

The following table outlines the criteria for entry and exit of the ESS from the Automatic mode of operation.

Table 3: Entry and Exit state flow in Automatic mode

Status in Automatic mode	Criteria	System Status requirements	Operations allowed for ESS
Enter into automatic mode; (remain in automatic mode)	• Mode Command from Remote Controller (Reg.94) = 1	• No faults in system • Ready Boolean(Reg 6 in Table 1) is TRUE • Grid status is OK	• Only charging is performed by the ESS. • No external power set points maybe allowed
Exit from automatic mode;	• Mode Command from Remote Controller (Reg.94) = 0, 3, 5 • Balancing operation has been triggered • Grid outage occured shifting the system to Back-up mode • System ready boolean is FALSE • System has faulted	• System in automatic mode	• On normal exit, the ESS will follow the system commands from the user • On fault, the system will exit into fault state

Power Command Mode of operation

In this mode, the ESS operates at the power set points sent by the user. Charge and discharge operations are both allowed and the power set points are determined by the user. There are battery limits that must be obeyed by the user. Safeguards have been implemented in the BESS software in case of violation of limits. Warning will be sent to the user if any of the limits are violated during normal operation.

Limits:

Variable	Limits	On violation
ESS Power requested	Setpoint : -100≤P0≤100	Warning code 3 (Reg 7)
Battery SOC	Range: 4≤SOC≤95.5	Warning code 1 (Reg 7)

Internal checks are implemented to ensure no abnormal operation occurs for the system during normal operation. The actual power implemented by the ESS will depend on the state of the system. The maximum allowed power for the ESS at any given time is provided as a feedback from the BESS PLC through registers 15 & 16. This can be

used as a feedback by the user to determine the power commands to be issued to the ESS. If however the set point sent to the ESS is not in agreement with these limits, then the ESS will automatically regulate the operation to the nearest possible value to the set point. For example, if the ESS is commanded to charge at 100 kW, however if the battery current limits are capped at 56 A (internal regulation by the battery controller), then the ESS will only perform ~25 kW in response to the 100 kW. This regulation is built-in to protect again operation outside the normal operating limits.

The ESS will suspend operation in Power Command mode of operation if the balancing process is triggered. Once the balancing of the battery strings is complete, the system resumes operation in Power Command mode. During the balancing period, the system will provide a Ready Boolean value (Reg 6) of FALSE.

A flow-chart of operation of the system in power mode is shown here:

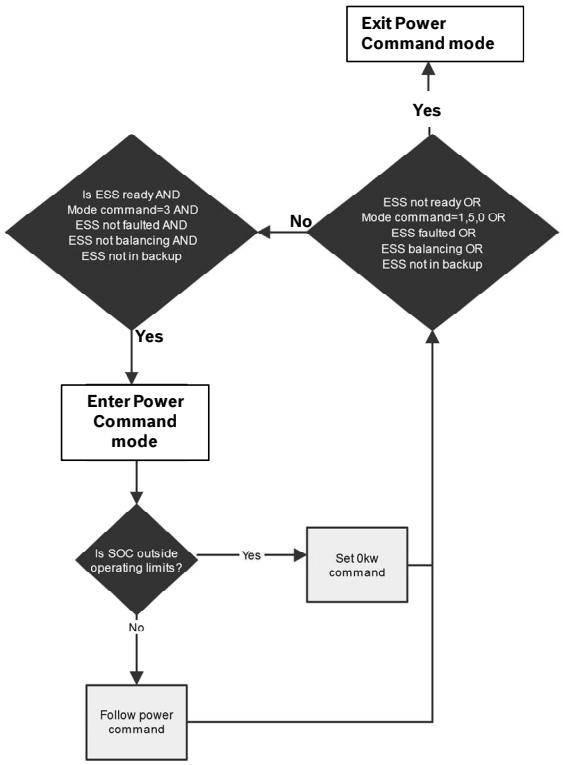

Figure 9: Flow chart for Power Command mode of operation

A typical operation profile of the ESS during the Power Command mode is shown in Figure 10. The operation mode (commanded by the user) is 3. The power commanded by the DCMG PLC is changing with time depending on the availability of the PV. This

profile represents the peak shaving/ load-shifting operation being performed by the ESS under the commands from DCMG. The ESS responds to the various set points sent by the DCMG server and follows it until the SOC reaches a lower limit. If the incoming set point calls for discharge and the SOC of the ESS is <4%, the ESS over-rides the incoming set point with +2.5 kW. Similarly, if the incoming set point calls for charge and the ESS SOC is >95.5 %, the ESS over-rides the incoming set point with 0 kW. The limits of 4 and 95.5 % are set that maximum power (±100 kW) operations are possible for the ESS.

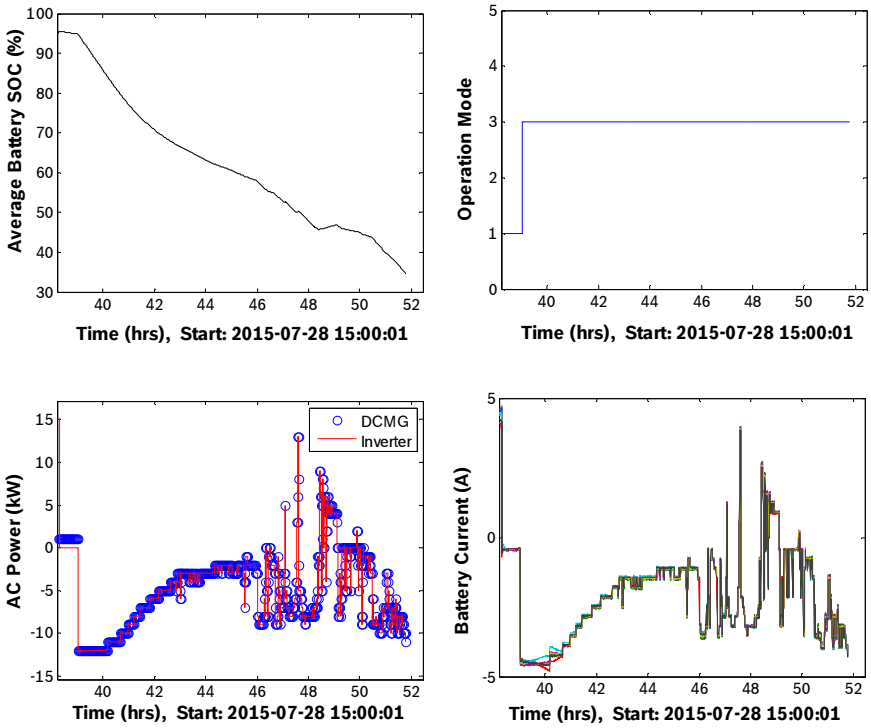

Figure 10: System in Power Command mode of operation

The following table outlines the criteria for entry and exit of the ESS from the Automatic mode of operation.

Table 4: Entry and Exit state flow in Power Command mode

Status in Automatic mode	Criteria	System Status requirements	Operations allowed for ESS
Enter into Power	• Mode Command from Remote	• No faults in system	• Charging and discharging are

Command mode or remain in Power Command mode	Controller (Reg.94) = 3	• Ready Boolean(Reg 6 in Table 1) is TRUE • Grid status is OK	allowed upto maximum power limits • Warning will be provided if any of the limits are violated during operation
Exit from Power Command mode	• Mode Command from Remote Controller (Reg.94) = 0,1, 5 • Balancing trigger has been enabled • Grid outage occured shifting the system to Back-up mode • System ready boolean is FALSE • System has faulted	• System in Power Command mode; operation mode =3	• On normal exit, the ESS will follow the commands based on it current operation mode • On fault, the system will exit into fault state

Back-up mode or emergency operation

This is an automated mode of operation. This mode cannot be commanded by the user and is not controlled by the user but is controlled by the inverter in the ESS. The inverter used for this ESS is capable of operating in Grid-Tied mode and Stand-alone mode. In Grid-Tied mode, all the other modes of operation mentioned above are available. In the case of grid outage, the inverter automatically transfers to Stand-alone mode. In this mode, the inverter regulates an AC output voltage of 480V and a frequency of 60 Hz by discharging the battery as needed. No power can be commanded from the system. The system will regulate the power delivered by the ESS based on the load it sees in order to maintain the 480V and 60 Hz. In the absence of any external load, the ESS consumes ~2 kW to power up the auxiliary components such as the HVAC, and UPS for the controllers as well as the Minimax control panel. In the presence of an external load, the battery discharges to maintain the load as long as none of the battery limits are violated. On return of the grid, the inverter switches back to the normal mode within 90 seconds of return of the grid and will resume the previous operation mode. For example, if the system was performing charging before the failure of the grid at 50 kW, it will return to this set point on return of the grid.

However, if during operating in this mode, any battery limits are violated, e.g. battery is completely discharged or is unable to meet the power requirements, the system will be forced to shut-down. After a shut-down, the system will re-start on its own upon the return of the grid only when the ATS status feedback (Reg 95) = 0. After the system reaches Ready state, it will resume the operation it was performing before the grid outage occurred. All the limits of the Power Command mode or Automatic mode will be applied at this stage to the prevent battery from over-discharging.

A flow-chart of operation of the system in power mode is shown here:

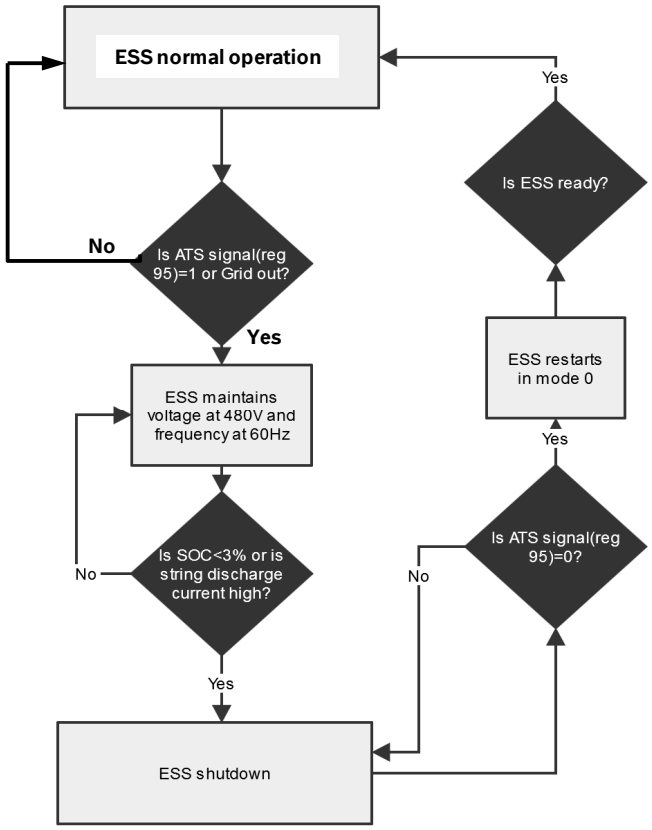

Figure 11: Flow chart for Back-up mode of operation

The following table outlines the criteria for entry and exit of the ESS from the Automatic mode of operation.

Table 5: Entry and Exit state flow in Back-up mode

Status in Automatic mode	Criteria	System Status requirements	Operations allowed for ESS
Enter into Back-up mode	• Grid outage occurs	• No faults in system • Ready Boolean(Reg 6 in Table 1) is TRUE	• Only discharging is possible and is regulated by the inverter to meet the requirement of forming the grid at 480V and 60 Hz. Discharge power is equal to the load required to meet this criterion
Exit from Back-up mode	• Grid returns • System faults • System shut-down due to in-sufficient battery capacity	• System is maintaining 480V and 60 Hz for the load	• On normal exit, the ESS will follow the commands based on it current operation mode • On fault, the system will exit into fault state • On shut-down exist, the system requires ATS (Reg 95) feedback to become FALSE; after re-start, system will resume operation @ previous state

Shut-down mode of operation

System shut-down can be commanded by the user while sending an operation mode of 5 (Reg 94). On receipt of this command, the ESS performs the following actions to shut-down the ESS.

1. The power setpoint of the inverter is ramped down to zero.

2. The DC contactors between the AC and DC side of the ESS is opened.

3. Shut-down command is sent to the inverter controller.

4. Shut-down command is sent to the battery controller.

5. Feedback from the controllers is received to confirm shut-down. If shut-down operation failed, it is repeated 3 times. If after 3 attempts, the shut-down of the ESS is

not possible, the ESS will send a fault code 6 (Reg 8). In case of such a fault, BESS should be contacted to determine the course of action.

6 Value streams

There are two main value streams currently envisioned for the ESS. The first and primary application is to provide emergency back-up operation for the DCMG loads in case of grid outage. The second value stream is designed to perform PV self-consumption to reduce the overall grid purchase required to run the DCMG loads.

PV self-consumption

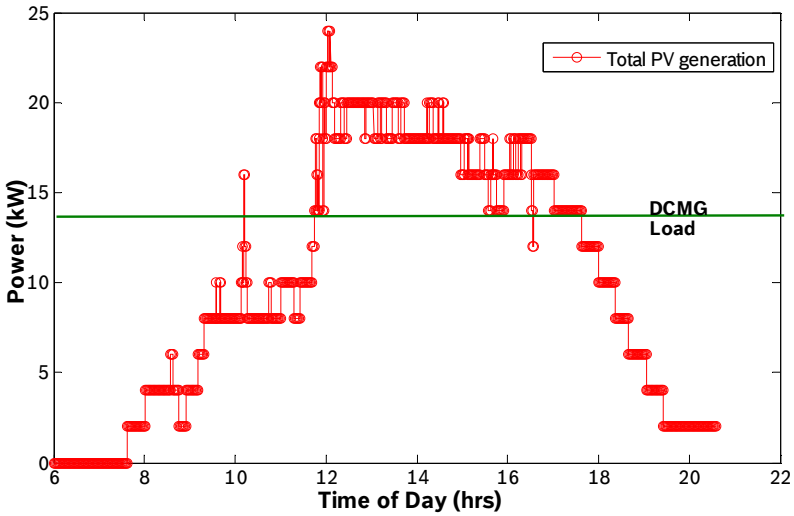

Figure 12: Typical PV and load profiles during a summer day; (assumptions: Total PV is assumed to be sum of both the reference PV (31 kW) and the 15kW PV connected to the AC panel)

Figure 12 is used to illustrate the logic behind load-shifting application. A typical PV profile is shown above for a summer day. For the profile shown here, the PV generation increases during the day starting at 6 AM and reaches its peak at midday. The PV generation then decreases during the late afternoon heading into the evening. The load in this example, as shown by the green line remains steady for almost the entire day. As a result, in the normal operation, the difference between the PV generation and load is purchased from the grid. On the other hand, during the period when there is excess PV, the excess energy is exported to the grid. In this operation mode (without the use of the ESS), the DCMG loads are purchasing energy from the grid whenever there is PV shortage.

If the ESS were used to discharge during the period where there isn't sufficient PV to support the DCMG loads, and charge itself with the excess PV when there is excess, we can reduce the overall purchase from the grid. For a day where there is no excess PV available (shown in example above), the ESS discharges ~ 112 kWh, supporting the DCMG loads by making up the deficit between the PV available and the load. In the current scenario, there isn't always sufficient PV to completely charge the ESS during the day. As a result, the ESS will need to "purchase" energy to charge itself from the grid during the night. The ESS needs to be fully charged in the night in order to provide support for the DCMG loads in case of an emergency such as grid outage.

However, after the installation of phase II PV, there should be sufficient excess PV during the day to charge the ESS, so as to reduce the consumption from the grid to as little as possible. Given that the ESS is capable of charging at up to 100 kW power, the ESS can effectively use all of the excess PV to charge itself. Such an operation can in essence make the DCMG system almost entirely grid independent for most of the days (when there is sufficient PV), while still being able to provide back-up operation and emergency grid forming support during grid outage.

A flow chart describing the logical flow for such a value stream is shown in Figure 13. The PV value referred to in the flow chart should correspond to sum of all the PV available on-site related to the DCMG project. The conditions for the SOC limits are provided to ensure that the battery is not over-discharged or charged to very high SOCs (better for battery life).

The ESS is fully capable of performing the PV self-consumption function. However, it is the user's responsibility to command the ESS to perform the function as defined in Figure 13.

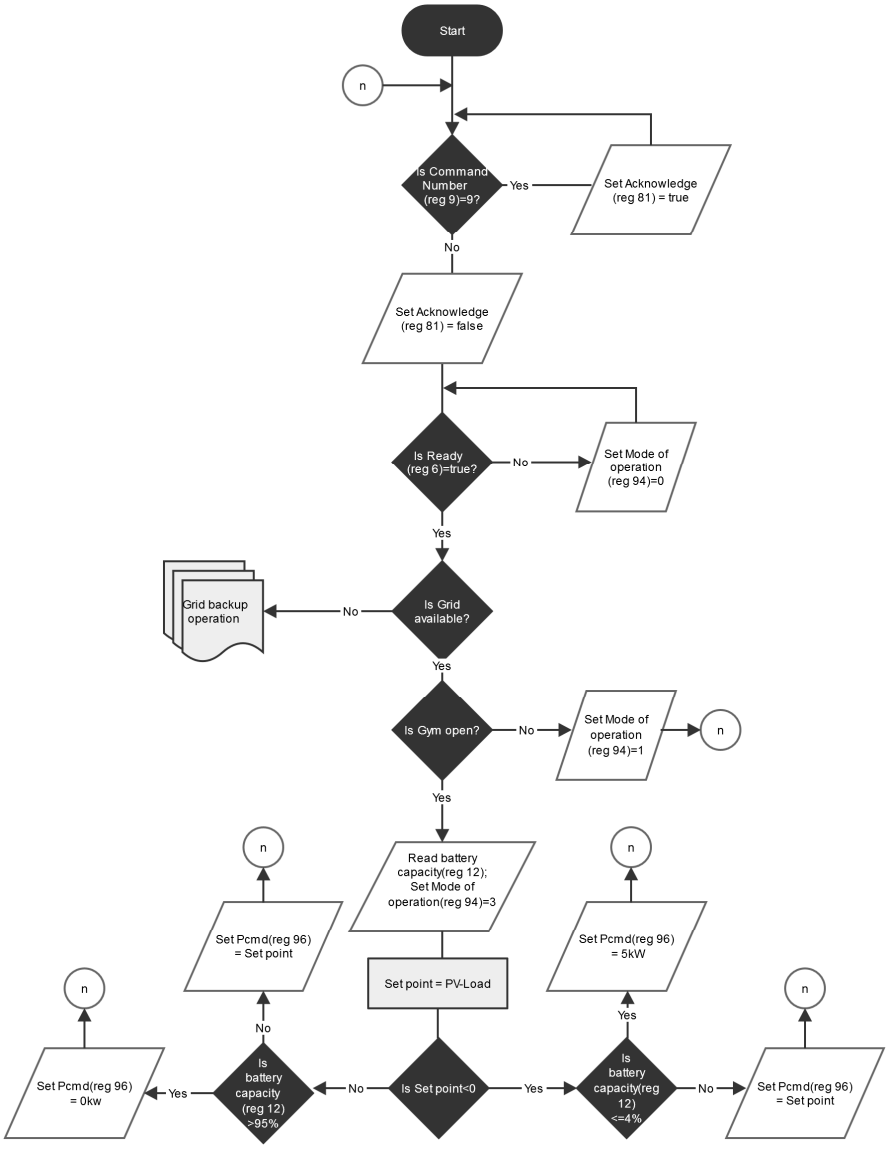

Figure 13: PV self consumption value stream for the ESS

Emergency Back-up operation

One of the primary purposes of the ESS is to provide emergency power in the case of a grid outage. In order to meet this requirement, the ESS stays fully charged in the evening/night time when there is no PV (DC connected) to power the DCMG loads on their own. When the grid outage occurs, the ESS goes into the back-up mode of operation (described in section 5). In this mode, the ESS regulates the transfer switch (in emergency mode) to maintain 480V and 60 Hz. This will then power up the DCMG

system to maintain the DCMG loads until the grid returns to normal operation. In the current phase of operation, where there is no excess PV installed on the ATS side, the ESS primarily acts as the energy source to support the loads as needed. After Phase II, when the additional PV is installed on the ATS side, in addition to supporting the loads, the ESS will also form the grid required to keep generating energy through this PV inverter. This inverter will use the grid formed by the ESS as its primary grid. **Caution: Excess PV (more than required by the load) cannot be fed back to the ESS in this mode of operation.** The ESS's inverter cannot regulate the charging power (current limits required for the safe battery operation) in the back-up mode. As a result, if excess power is sent to the ESS, it can force the inverter or the batteries to fault and shut down. The PV generation must be regulated such that the PV generation is never greater than the load required. A tolerance of up to ±2 kW is acceptable for the ESS. Care must be taken to ensure the set points are set accordingly in this scenario. For normal operation, where there is no PV, the ESS will automatically follow the load that is being addressed while still maintaining 480V and 60 Hz on the emergency side of the ATS. Once the grid returns, the ESS goes back to grid tied operation mode and resumes the operation it was performing before entering the Emergency Back-up operation.

7 List of possible Faults for the ESS

Fault codes are provided to the user to notify them of a fault in the system. Table 6 gives an overview of possible causes for each fault type and the action to be taken in each case.

Table 6: List of possible faults in the ESS

Fault Code	Possible causes	Action to be taken
Battery fault (code =1)	• Over-charge of a battery module • Over-discharge of a battery module • Over temperature • Under temperature • Communication loss • Module SOH too low (<80%) • Cell voltages out of range (too high or too low)	• Shut system down. Contact BESS technical support team.
Inverter fault (code =2)	• Inverter ground loop fault (ground current leakage) • Inverter DC section fault (unable to maintain charge or discharge setpoints with battery modules; occurs when the battery controller disables charge/discharge)	• Shut system down. Contact BESS technical support team.

	• Inverter Overvoltage fault (current limit is too low to regulate power without violating voltage limits) • Inverter overtemperature fault (cooling failure) • Door fault (inverter door wasn't closed properly) • Watch dog timer fault (communication loss between inverter and BESS PLC)	
User intervention fault (code =3)	• E-stop button was pressed • The container doors were opened • The BESS PLC was powered off or is not responding	• Confirm that this fault occured due to user intervention and that the the reason for the intervention has been addressed. • Acknowledge the fault and continue operation. •

Ambient temperature fault (code =4)	• HVAC system failure
	• System was previously in fault state for very long time during which time the system heats up to exceed the 45°C limit within the container
		• For HVAC failure:
		  ○ Acknowledge the fault.
		  ○ Shut down system.
		  ○ Fix HVAC system. Do not operate without a fully operational HVAC system.
		• If the fault is due to an internal temperature rise that occured because the HVAC was not on due to another fault:
		  ○ Acknowledge the fault.
		  ○ Shut down the system.
		  ○ Allow the system to cool to below 45 C

Minimax fault (code =5)	• Fire suppression system has been activated	• Shut down system. • Contact BESS technical support team. • Only authorized personnel (fire fighters) should be allowed to enter the container if the Minimax alarm has tripped.
Shut-down failure (code=6)	• This can occur if the battery controller stops responding to the commands sent from the PLC. This can be the result of a bad controller , IGBT failure within the controller or failure of communication	• BESS personnel need to be on-site to investigate the failure • No electrical work should be performed without disabling the fuses in the battery side of the container

8 Warranty

BESS provides a standard warranty of 1 year against defects. BESS warrants for a period of 1 year, that the ESS is free from defects in material and workmanship for the

following components: battery modules, battery management unit (BMU), Energy Management Unit (EMU), connection cables, power conversion system (PCS), the heating / ventilation and air conditioning unit (HVAC), the transformer and the cabinets used for the installation. In case of a warranty claim, BESS decides in its sole discretion whether the defective products or components are repaired, or appropriate replacement products are supplied or the products are reimbursed to the customer. The customer bears the costs of dismantling and reassembly, as well as for return shipment of the products. All other costs, including installation costs, other losses, or resulting damages caused by the defect are not covered by this warranty.

9 Emergency procedure

In case of emergency or if there is any electrical work that needs to be performed on-site, the following procedure should be used to de-energize the ESS from operation.

The ESS is designed to provide grid support in the absence of the main grid. Therefore, shutting off the breaker connected to the ESS is not sufficient to completely de-energize the system. Turning the grid breaker, will engage the back-up mode of the inverter and the ESS will continue to feed 480V, 60 Hz through the automatic transfer switch.

1. E-stop buttons have been provided on both sides of the container. In case of emergency, the E-stop buttons should be pressed. This will initiate a shut-down of the ESS.

2. After this is done, then the main panel powering the ESS should be turned off to prevent any accidental re-start of the system while work is being done.

3. After all the electrical work is finished on-site, the E-stop button needs to be released. The AC breaker on the panel can then be powered back on. The system is then ready to be started again.

In case of E-stop being used, the personnel at the user site need to be alerted regarding the activity being performed.

Figure 14: Emergency stop procedure

10 Fire emergencies

The ESS is equipped with a Minimax system with the control panel wired to provide an alarm to the fire fighting personnel on the base. In addition, there are strobe lights and alarms that will also sound in case of a fire emergency. The following actions are also taken within the ESS.

1. The electrical circuit will be shut-down in case of this fault

2. The HVAC units and fans will also be shut-down so as to hold the dispersed agent within the container.

Before entering the container:

1. Ensure the main circuit breakers connecting to the container are shut-off

2. Ensure the personnel entering the container are wearing personal protective equipment, including self-contained breathing apparatus (SCBA)

3. Leave the container doors open and do not re-engage the system until after thorough review is complete. Contact BESS immediately using the contact information provided to the local personnel. The agent will dissipate into atmosphere once the doors open. The agent of choice for this system is environmentally approved and is known to not be harmful to human beings in the surrounding area.

The user is obligated to provide the Minimax manual to the local personnel on base to get them familiarized with the fire suppression system. The maintenance of the fire suppression system is also the responsibility of the user.

11 Appendix I: As-built drawings for the ESS

12 Appendix II: Battery module specification and operation documentation

13 Appendix III: Operation manual for both Dynapower and the Solectria PV inverters

14 Appendix IV: Safety system design and Minimax certification documentation

15 Appendix V: Maintenance and operation procedures

16 Appendix VI: Testing and commissioning report

Bosch Energy Storage Solutions

From	Our Reference	Telephone	Palo Alto, CA
BESS/ENG G1/PJ-NBA7	Ram Subbaraman	+1(650)320-1533	July 30th 2015

To John Saussele (RBNA/PJ-DCMG), Dusan Brhlik (RBNA/PJ-DCMG)

cc Jasim Ahmed (G6/PJ-ESS); Thielitz Cordelia (G6/PJ-ESS G6/PJ-ESS1 BESS/GM); Balliet Ryan (BESS/ENG); Srikanth Pallavi (BESS/EPT); Karalic Adi (BESS/EPT);

Subject **: BESS energy storage system testing and commissioning before delivery to DCMG: 07/16/2015- 07/30/2015**

Revision Log

Version 1	July 30th 2015	First full version.

Introduction

This document provides a summary of the testing activities carried out at by the BESS team, during the weeks of 07/16/2015 – 07/30/2015. The purpose of the document is to summarize the key results obtained through the testing of the system and is evaluation of the system meeting the customer requirements. The testing procedures were developed internally, as there is no customer specification at this moment.

Abbreviations

AC	Alternating Current
ATS	Automatic Transfer Switch
BESS	Bosch Energy Storage Solutions LLC
BMS	Battery Management System
DC	Direct Current
DCMG	Direct Current Microgrid
DOD	Depth-of-discharge
E-rate	1E = power at which system will deliver energy for 1 hr of continuous operation
ESS	Energy Storage System
ESTCP	Environmental Security Technology Certification Program
HVAC	Heating, Ventilation and Air Conditioning
HW	Hardware
LiB	lithium-ion battery
LV	Low voltage
PCC	Point of Common Coupling
PCS	Power Conversion System
PLC	Programmable Logic Controller
SOC	State of Charge
SOH	State of Health
SW	Software
UPS	Uninterruptable Power Supply

Table of Contents

1 System Description

The system configuration is as follows:

The system is connected to the grid through a 208/480 V isolation transformer. In addition, an isolation transformer is installed between the inverter and the battery side (line and load side of the inverter). The load side of the inverter is connected to the Automatic transfer switch to enable switching to emergency mode when the grid fails. The line side is connected to the AC panel through a 150A breaker.

The system discharges and charges from the grid during normal operation. The main breaker is switched off to test the automatic mode of operation.

All on-site operations were performed through the dispatch manager with BESS controlling the system. The two weeks of testing under customer mode is tested where DCMG sends the operation commands to the energy storage system (ESS). DCMG is provided with the battery relevant information from the BESS PLC as part of the customer interface. The customer interface document is also attached with this documentation set.

Battery HVAC and Fan operations were controlled through the following logic:

1. Battery HVAC/fans ON if Max Cell Temperature of any string >25^{o}C
2. Battery HVAC/fans OFF if Max Cell Temperature < 22^{o} C

Data recorded during the testing has been stored on the Bosch cloud and is used by the BESS team for online monitoring and diagnostics of the system.

2 Start-up and Shut down operations

1) The ESS is started up from OFF state to READY state by following the sequence below. The total time required for the transition between these two states is recorded. Three consecutive start-up procedures yielded near identical times, without any communication faults. The initial SOCs of all strings were ensured to be within 1%.

    a. Power on Inverter; Enter Voltage mode

    b. Set voltage to 400 V and close the DC contactor switch

    c. Allow for the BMUs to wake up and report the values for the strings

    d. Power on the EMU and after a 15s delay and establish communication with all BMUs

    e. Choose a power setpoint, +15 kW and command the EMU to close the IGBT switches for the strings based on the connection procedure

    f. Continue connection operation until all strings are connected.

    g. Perform charging/discharging operation once all strings are functional.

    The total time for this operation was found to be ~4.2 minutes.

2) The ESS is then moved from READY state to OFF state. The time required for this state transition is estimated. Three successful consecutive shut-down sequences were measured and the average time was estimated.

    a. Reduce power set point to 0 kW

    b. Move the inverter to OFF state, along with opening the DC contactor to disconnect the Inverter and batteries.

    c. Open all BMU IGBTs, followed by sending module power OFF command

    d. Wait for 2 minutes to allow for shut-down of all batteries. Check if all BMU voltages report 0 (corresponds to BMUs being OFF). If this is true, move to shutdown of the EMU. If not, recycle power of the EMU, and re-send the shut-down commands again until the V from BMU is 0.

    The total time for this operation was found to be ~4.1 minutes.

This procedure was repeated over 15 times to ensure that the start-up and shut-down sequences work robustly. Also, shut-down sequence as part of the fault testing was performed to ensure proper shut-down of the system in case of any abnormal operation.

3 Balancing

Battery strings when operating at varying thermal and electrical loads, undergo deviations from each other. It is therefore necessary to perform balancing of the strings periodically (once every month) to ensure uniformity in the battery strings and thereby ensuring optimal performance and life characteristics.

Balancing has been set up to automatically occur on the 1st Sunday of every month at 9:00 PM. The typical time for balancing ranges from 4-8 hours depending on the extremes in operation experienced by the battery. If during balancing, there is a grid outage, the system will automatically return to back-up mode to provide emergency back up. After the grid power returns, the balancing will automatically complete before resuming normal operations.

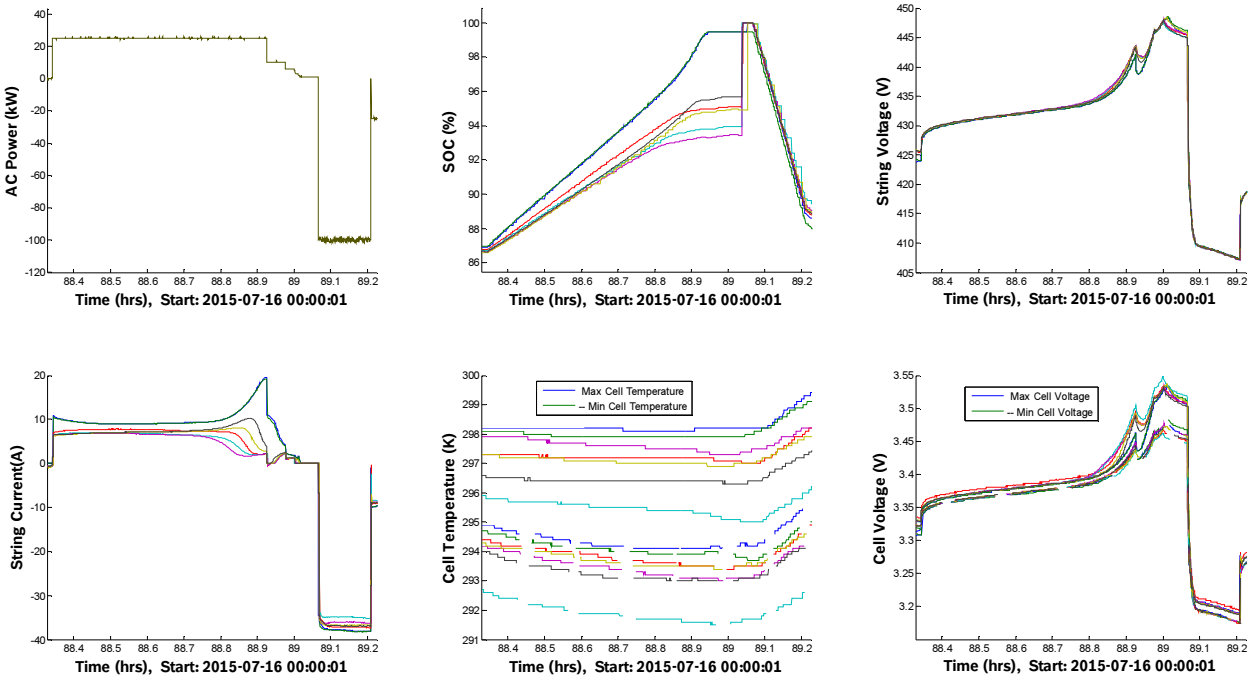

Figure 1: Balancing operation of 7 strings

Balancing completion is determined by internal criteria identified by the BESS team. At the end of balancing (all strings at same SOC >99.5%), the strings discharge to 95% and resume normal operation.

4 Efficiency map for inverter

In order to determine the efficiency of the inverter during both charge and discharge, the ESS's SOC was adjusted to either 27% or 80% for charging or discharging respectively.

Steps of 15 kW were applied for 5 minutes while monitoring all battery relevant variables. The DC power as estimated by the product of current and voltage reported by the battery controller was compared with the AC power setpoint as reported by the inverter. The efficiency for AC to DC conversion (charging) was found to be >95% for all powers greater than 25 kW with an efficiency of 88% at powers <=5 kW. The SOC at the end of charging ramp was 67.5%. Cumulative energy input to the system during the charging ramp = 52.37 kWh @ an average power of 45 kW. Charging efficiency, defined as the kWh input to the ESS vs. actual SOE change for the system, is estimated to be ~94%

Similarly, 15 kW steps were applied in the discharge direction for the ESS starting at an initial SOC =80%. The efficiency of DC to AC conversion was again found to be >95% for all powers >25 kW and the lowest efficiency of 87% at powers <=5kW. The discharge efficiency, defined as the kWh output by the ESS vs. actual SOE change for the system, is estimated to be ~95%

Charging:

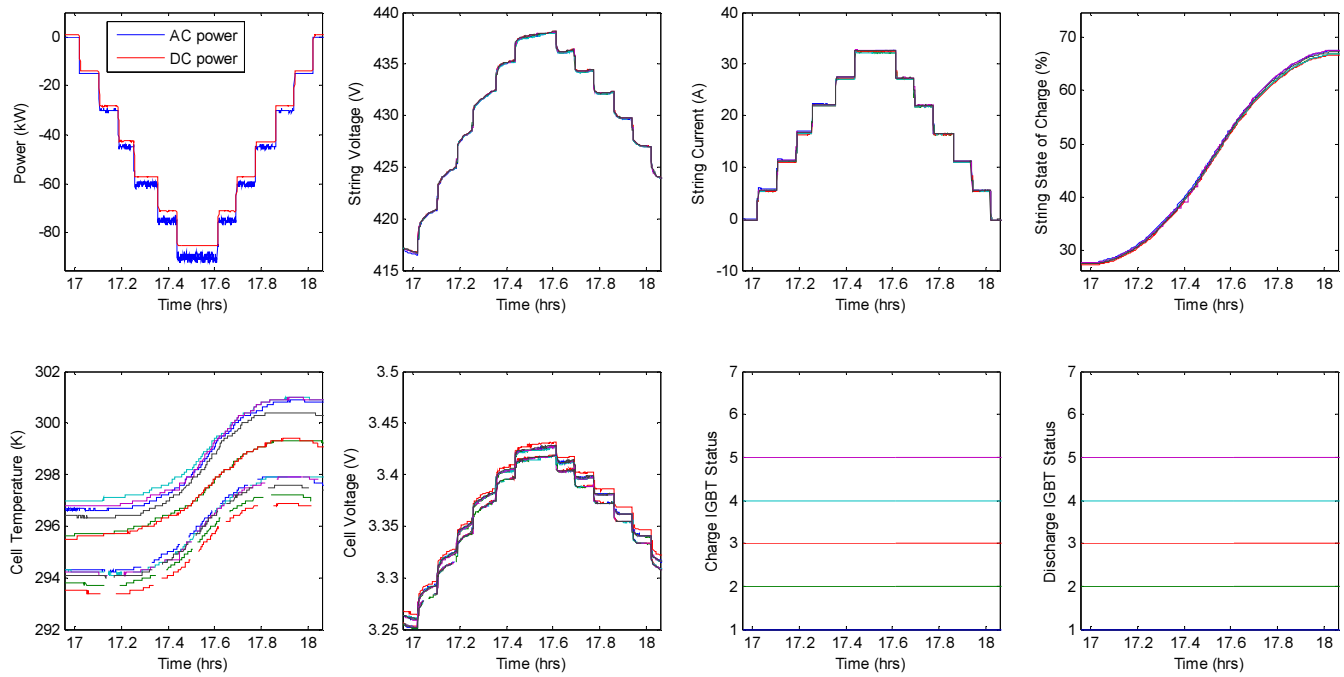

Figure 2: Efficiency map, charging ramp

Discharging:

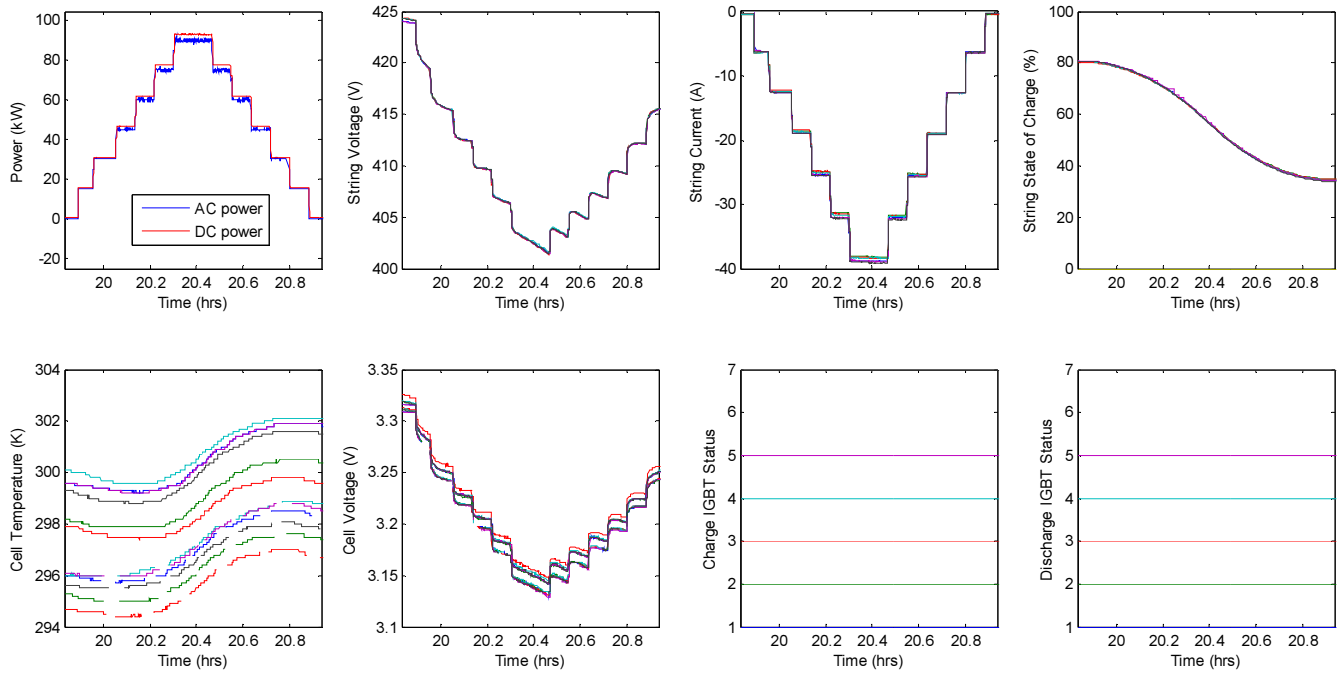

Figure 3: Efficiency mapping, Discharge ramp

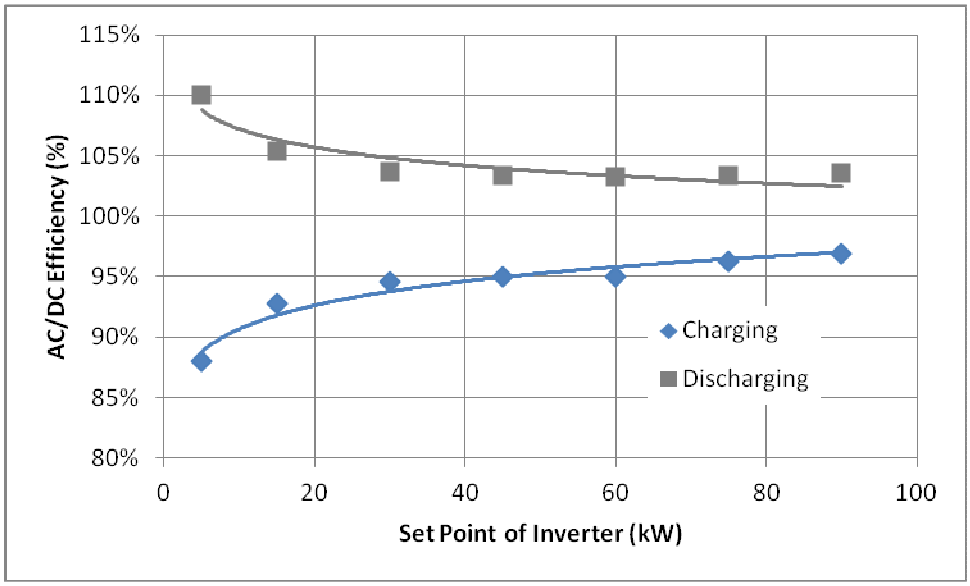

Figure 4: Efficiency for AC/DC conversion for the Inverter; Overall efficiencies of >95% is observed at powers >E/4

5 Capacity calibration @ E/4 , E/2 and 1E

Capacity of the ESS was measured at 3 different E-rates. The ESS was charged fully (100% SOC) and a discharge at the chosen power was performed. Three powers were chosen, low (E/4), medium (E/2) and high (1E) to measure the AC capacity of the ESS. The following assumptions are relevant for these measurements.

a. SOC of all strings charged up to 100%
b. Batteries' cell temperatures are at close to room temperature (298 K) during the start of discharge
c. Load bank set to fixed power set point
d. Discharge ended when average SOC of connected strings <= 10%
e. Measured capacity of the system = Capacity at SOC(10%)/0.93. The EMU de-rates the discharge below SOC of 3%, so this capacity is considered un-available at the required power of operation.

E/4 Discharge (25 kW):

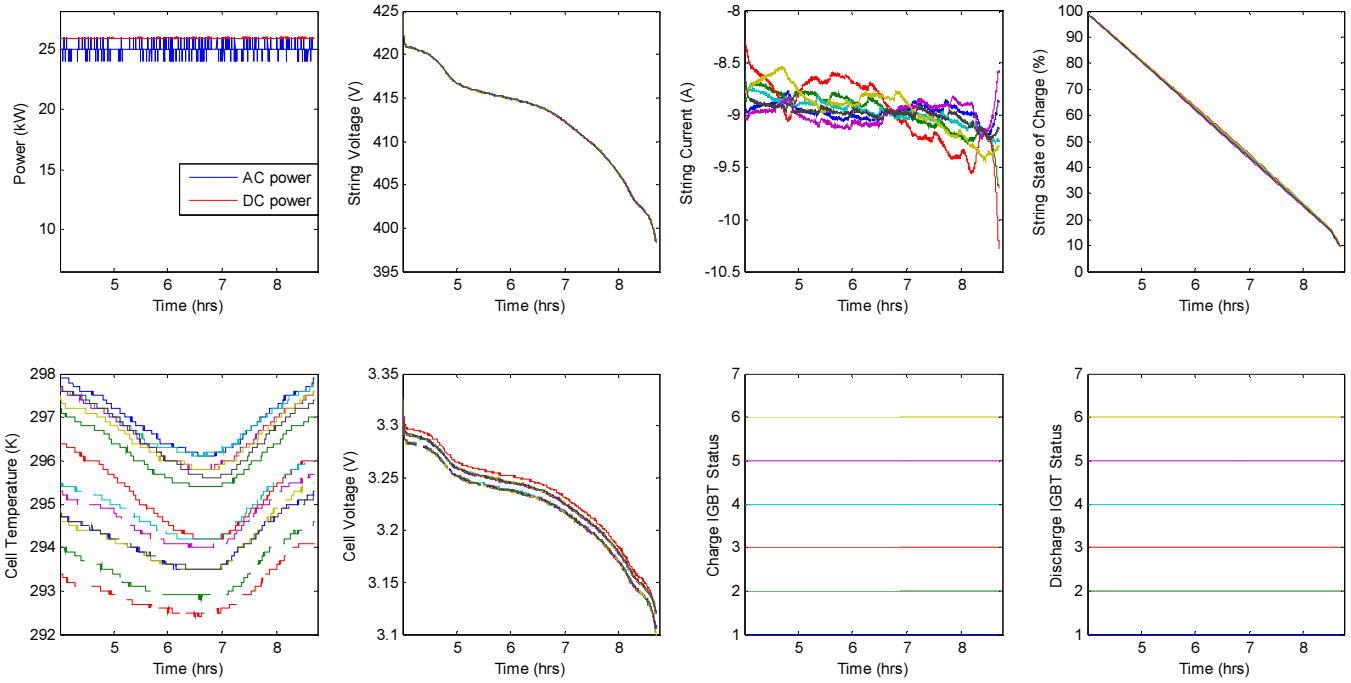

Figure 5: 25 kW constant power discharge

E/2 Discharge (50 kW):

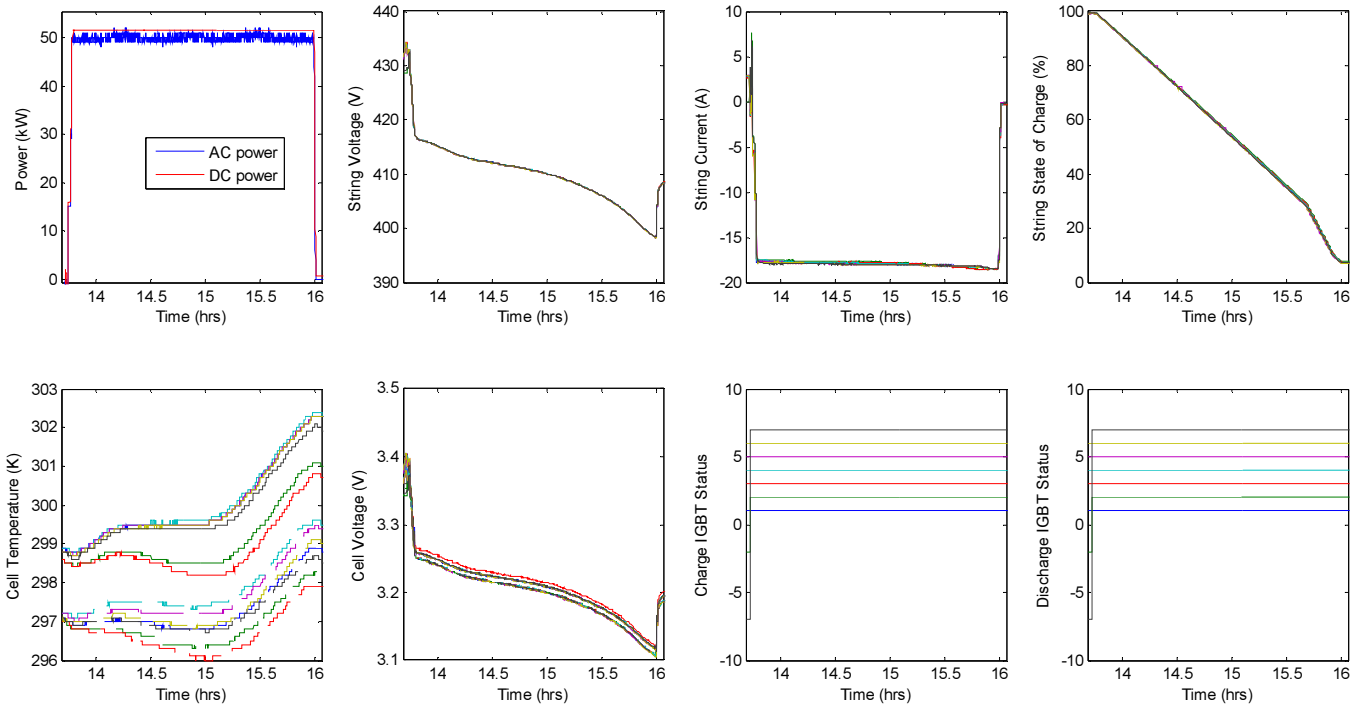

Figure 6: 50 kW constant power discharge

1E Discharge (100 kW):

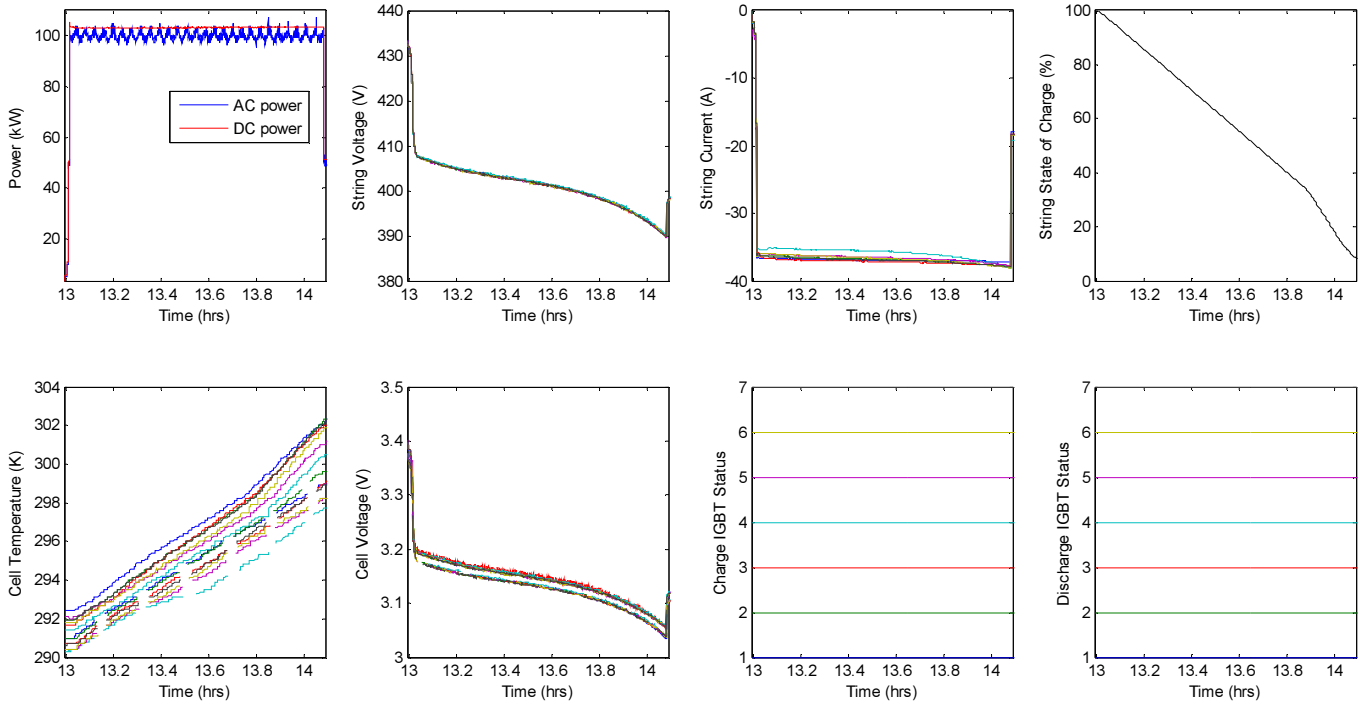

Figure 7: 100 kW constant power discharge

Capacities estimated from the three E-rates can then be used to estimate the Peukert type relationship between power and energy. The rated energy for the system is defined as the energy available from the system (AC) at a E-rate of E/4. The power energy relationship is shown in figure 10.

E-rate	AC (kWh)*
E/4 (25 kW)	125
E/2 (50 kW)	120
1E (100 kW)	115

* Capacity as measured from 100%-10% SOC;

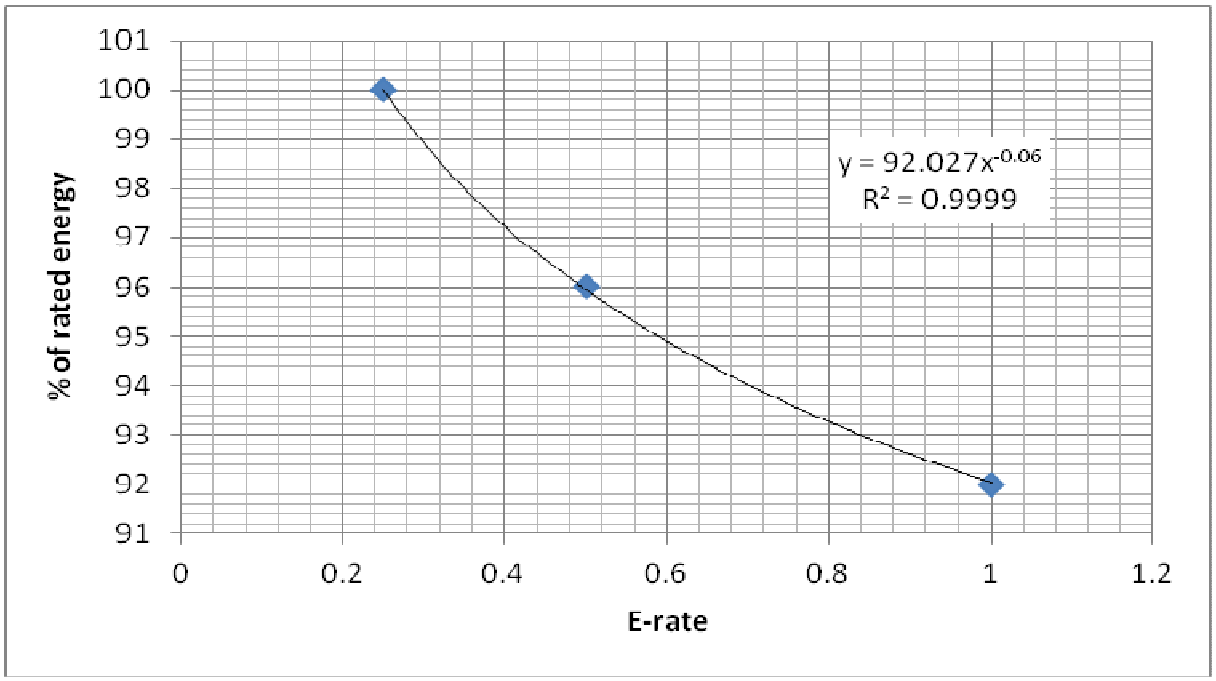

Figure 8: Power - Energy relationship for ESTCP system

Single and multiple continuous cycles were performed for the system under two different conditions: (i) E/2 rate power and (ii) 1E power.

Cycle tests were performed to demonstrate that the system operation is within expected specifications for the energy storage system. Given that there is no real load profile specified for the energy storage system at this moment, we used the standard cycling between 5%-89% at different powers. This provides us a good measure of the system's capabilities.

6 Cycling at 50 kW

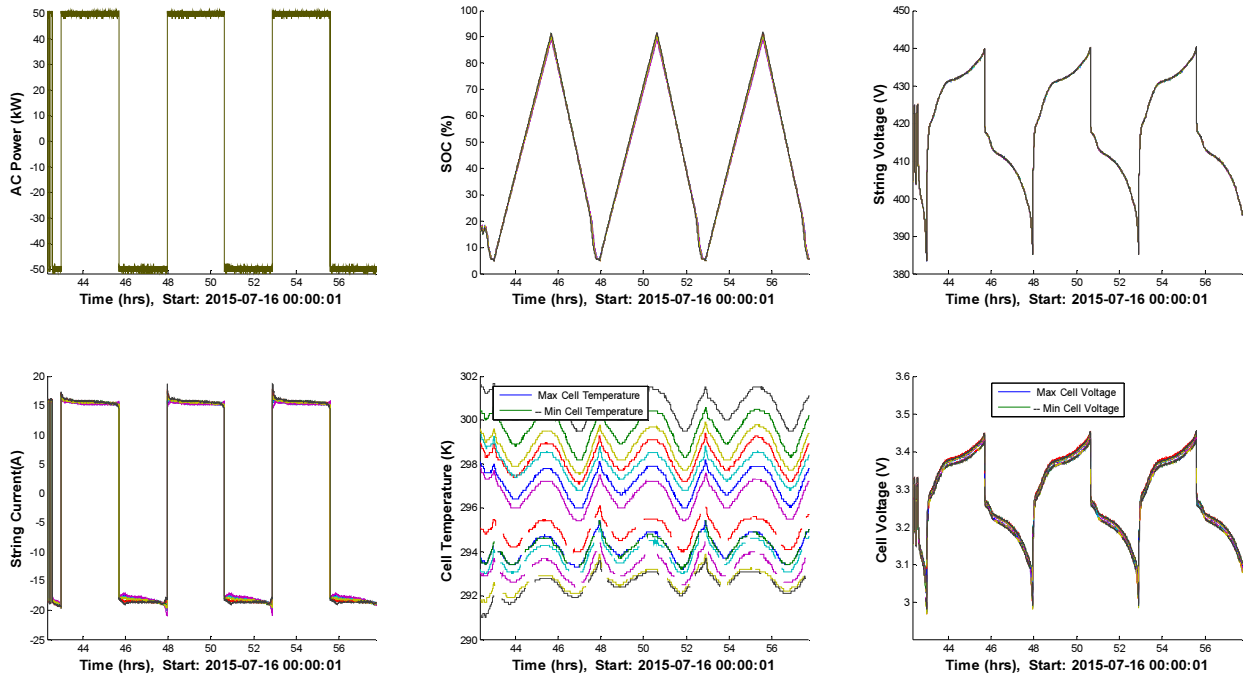

Figure 9: Cycling of the ESS at 50 kW

The ESS was subjected to ~3.5 continuous cycles at 50 kW. The SOC of the battery was cycled between 5% and 89%. The battery was found to operate without any de-rating in this range. The internal temperature of the battery is well within the desired value of 45°C (318 K). The overall efficiency for the cycles is well within those listed in the previous sections.

7 Cycling at 100 kW

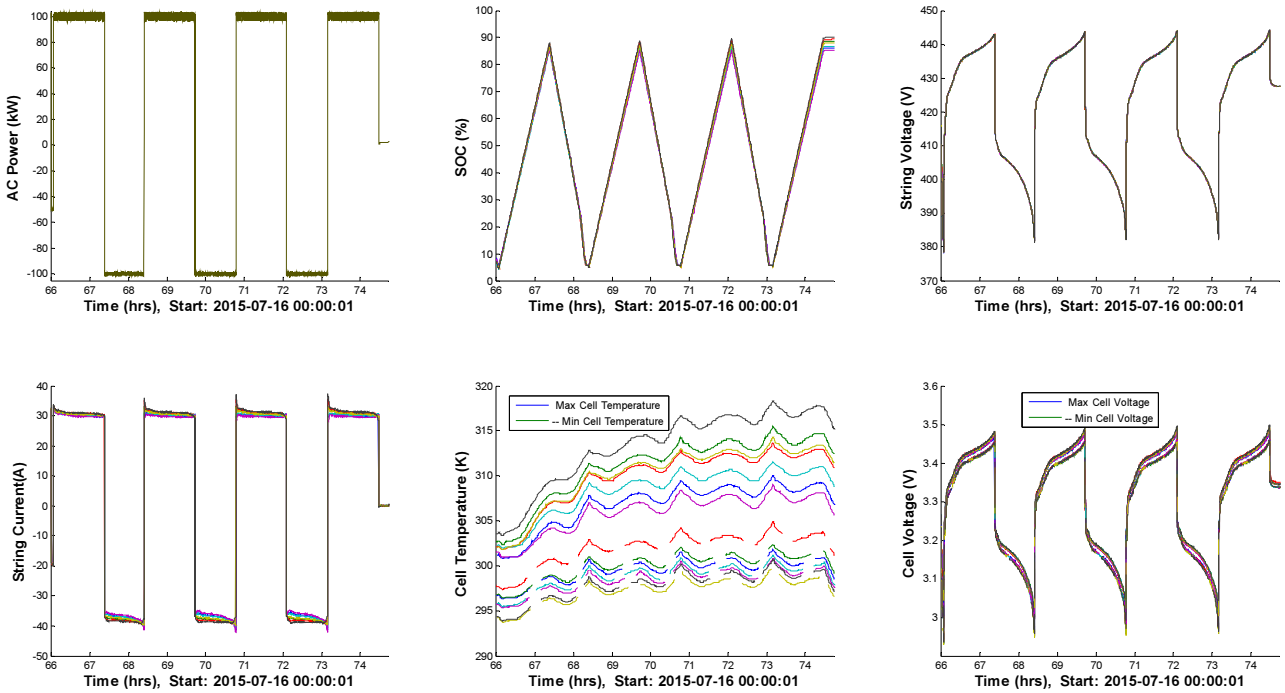

Figure 10: Single continuous cycle at 100 kW

Continuous cycling at 100 kW was also performed on-site to study the impact of such harsh cycling on the ESS. None of the safety or thermal limits set within the system was violated. The system performed as expected during the 3.5 cycles. The string internal temperatures were within the upper bounds for operation limits and well under the safety limits of >55°C (328 K).

The cycling tests were merely performed as a worst case representation of any customer value stream operation possible for the ESS. Based on the various ESS deployed by BESS, the typical cycle profile expected is well within 1-1.5 cycles per day with maximum % of the time spent at high power <20%. Based on these characterization tests, the ESS is deemed to be qualified for operation at Fort Bragg. The ESS was then operated under the customer command mode for extended period of time. Stability of receiving commands from the DCMG PLC as well as the stability of the overall system was verified during this experiment.

8 Customer PV self consumption operation

The original requirement for BESS, during the phase I of the project, is to have the ESS perform the operation of back-up storage system. Under this mode of operation, the ESS will essentially always be maintaining high SOC without performing any other operation.

In order to maximize the utilization of the ESS during day-to-day operation, BESS recommended the following operation profile for DCMG:

1. During the time period between 10:00PM and 6:00 AM, the ESS is maintained in the back-up ready mode; the SOC of the battery is maintained at >95%. The ESS is connected and performing 0 kW operation during this time. In case of a grid failure, the ESS will then perform the role of maintaining the grid for the PV inverter as well as supplying the power needed to keep the DCMG loads online. This operation mode is denoted by #1 in the graph below. The descriptions of the different modes and their limits are provided in the documentation for the s/w provided.

2. During the day between 6:00 AM and 10:00 PM, the ESS helps in off-setting the difference between the available PV and required load. The set point is calculated as the difference between the PV available and load. Thus, if there is excess PV available, the ESS can be charged and if there is insufficient PV to support the DCMG load, then the ESS supplements the needed energy. If the ESS is always charged through the PV, then the DCMG loads are essentially operating without any purchase from the grid, demonstrating energy independence. This operation mode is denoted by #3 (power mode).

The above profile was provided to the DCMG team with the limits for battery operation between 5% and 95%. The system was operated under the control of commands from the DCMG PLC for over 2 weeks. Below, the behavior over a few consecutive days is shown. During the beginning of the day (and the end of the evening), the battery is predominantly discharging to off-set the insufficient PV to meet the load requirements. At night time, the battery is charged up to full SOC (95% in this case) to maintain ready state for the emergency back-up mode.

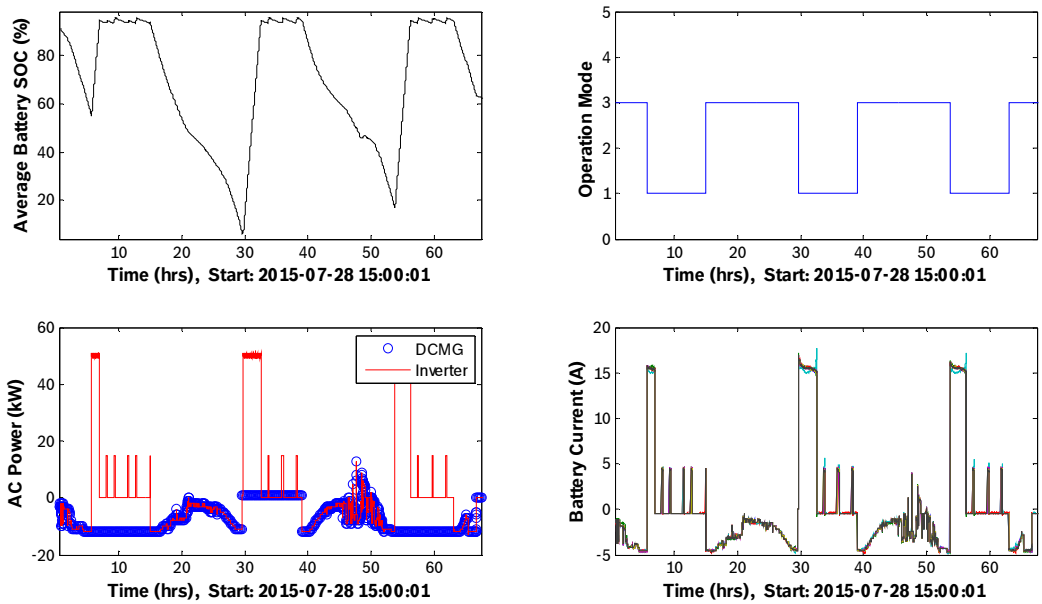

Figure 11: Customer load profile operation

9 Back-up mode operation

The ESS has been designed to provide back-up power during grid outage. It is expected to serve two main applications. During the grid outage:

1. The ESS is expected to regulate a local grid, 480V, 60 Hz connection to enable the continued operation of the PV inverters connected to the load side of the automatic transfer switch. This PV is then expected to provide the required power to operate the loads in the building.

2. When the PV available is insufficient (night time, clouds etc...), the ESS then acts as the energy source to maintain the DCMG building loads without any interruption.

Since the PV inverter will not be installed until Phase II, the second mode of operation was tested. The ESS run status is a variable used to understand the mode of operation of the ESS. During normal operation, this variable is at a value of 8. This corresponds to power mode of operation. During the off-grid mode, the ESS run status moves to 4. On return of the grid power, the run status returns to 8. This feedback is included in the system variables exchanged between DCMG and BESS.

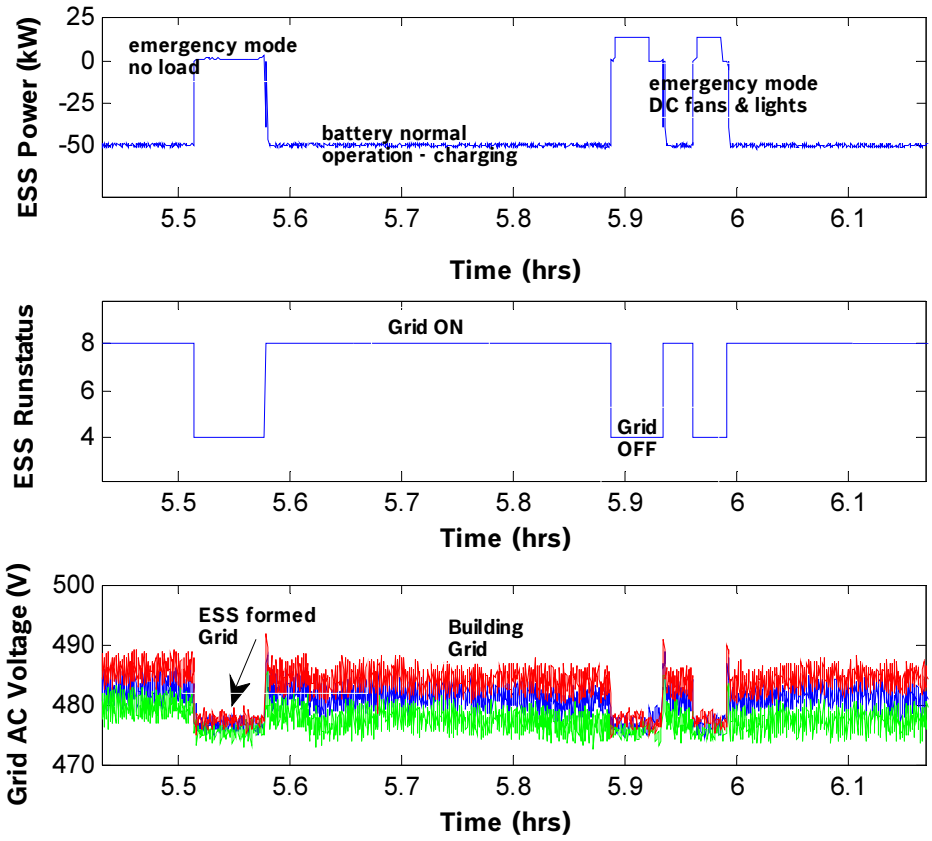

Figure 12: Back-up mode operation

In the case shown above, the emergency mode operation of the ESS is triggered by turning the main breaker from the transformer OFF. In the first case, no load was on-line, as a result the ESS sees a 0 kW load and the self-discharge is the amount of power required to maintain 480V, 60 Hz across the transfer switch. After the grid is turned back on, the battery resumes the operation being performed previously. When the load is online, (shown in the cases at t>5.9 hrs), the ESS moves to state =4, and the load of 15 kW is supported by the ESS. The lime lag between when the ESS moves to state 4 and when the actual load is realized is due to the lag in the transfer switch.

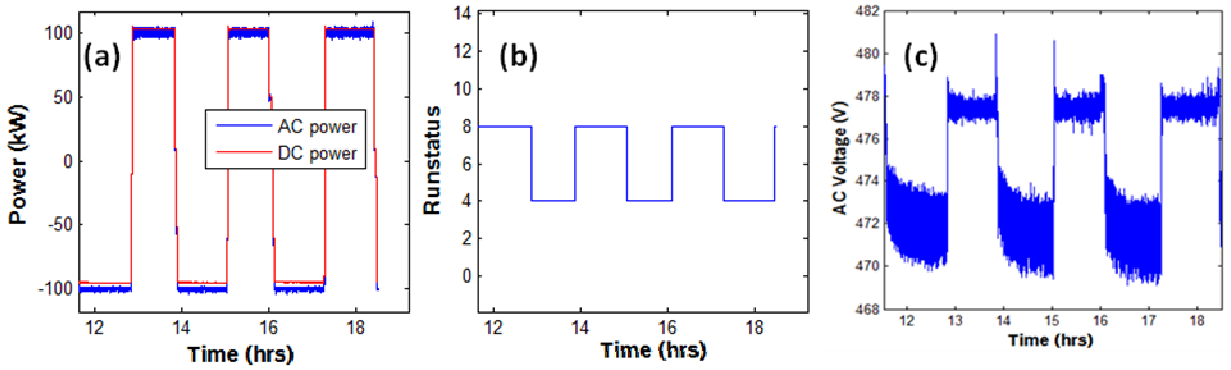

Figure 13: Full power back -up mode operation for the ESS

Even though the load at the Fort Bragg site is not >15 kW, we wanted to test the ability of the ESS to support loads up to 100 kW. For this purpose, during our testing in California, the system was tripped into the back-up mode by removing the grid source (diesel generator). When this happens, the ESS seamlessly switches to back-up mode and powers the 100 kW load bank connected to the load side. There was no delay observed during this transition further confirming that the behavior observed above is due to the ATS delay or possibly some load side controls.

Appendix E: BESS Monthly Test Reports

MONTHLY SYSTEM PERFORMANCE REPORT

Bosch Energy Storage Solutions

PJ Fort Bragg

Prepared by:	Ryan Balliet (BESS/ENG)
Date prepared:	9/11/2015
Version:	1
Report Start:	8/1/2015
Report End:	8/31/2015
Installation site:	Fort Bragg, NC
System AC rating:	100 kW, 100 kWh
Commissioning complete:	7/31/2015
Days since commissioning:	31

	Month	To Date
Cycles complete:	19	19
AC energy discharged [MWh]:	2.1	2.1
AC energy charged [MWh]:	3.3	3.3
Grid backup events:	0	0
Availability [%]:	94	94
Downtime [d]:	1.9	1.9

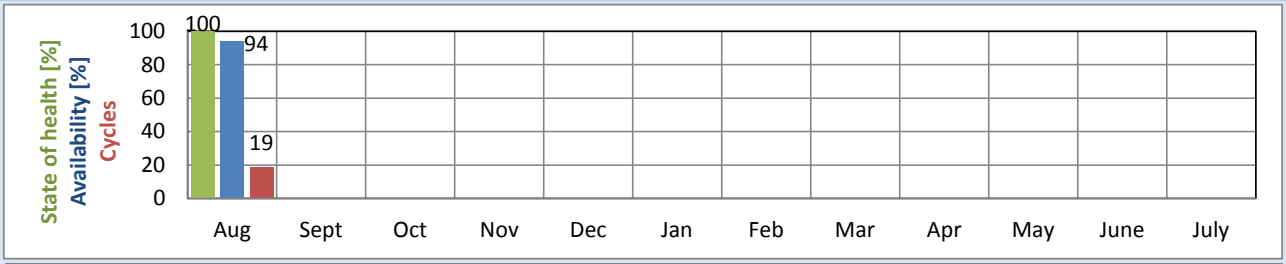

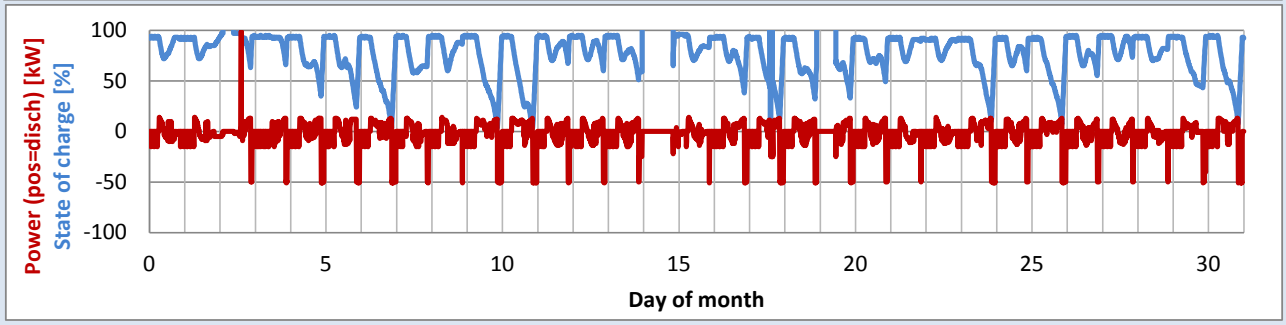

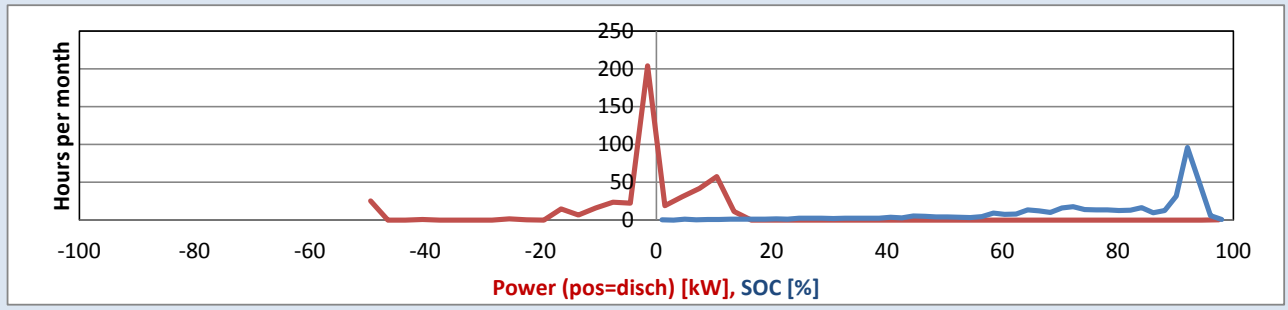

Downtime events:

Number	Site date, time	Reason	Action taken
1	8/3/15 1:55 AM	All strings disconnected during balancing, causing inverter to fault as it tried to set a power command on an empty bus.	Discharge implemented during balancing to prevent simultaneous disconnection.
2	8/14/15 8:51 PM	String connection procedure led to inadvertent balancing.	String connection procedure modified. Top of charge SOC limit reduced to eliminate inadvertent balancing.
3	8/19/15 9:31 PM	Inverter fault -- "Overcurrent Slow". Cause being investigated--no high currents detected in data.	Data sent to DynaPower for analysis. Follow-up scheduled.

MONTHLY SYSTEM PERFORMANCE REPORT

Bosch Energy Storage Solutions

PJ Fort Bragg

Prepared by:	Ryan Balliet (BESS/ENG)
Date prepared:	10/9/2015
Version:	1
Report Start:	9/1/2015
Report End:	9/30/2015
Installation site:	Fort Bragg, NC
System AC rating:	100 kW, 100 kWh
Commissioning complete:	7/31/2015
Days since commissioning:	61

	Month	To Date
Cycles complete:	19	39
AC energy discharged [MWh]:	2.1	4.1
AC energy charged [MWh]:	3.3	6.5
Grid backup events:	0	0
Availability [%]:	93	93
Downtime [d]:	2.1	4.0

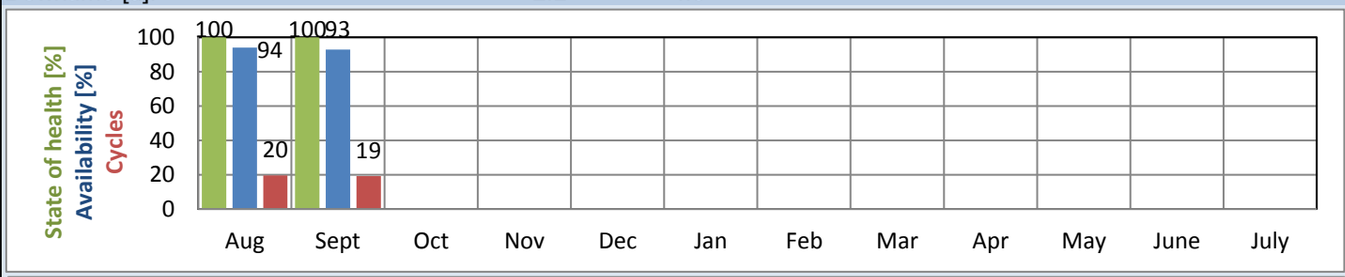

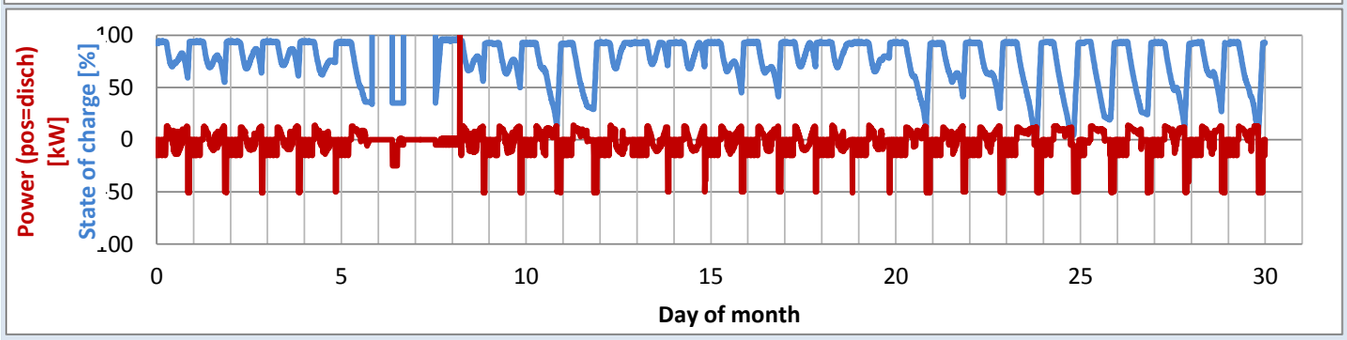

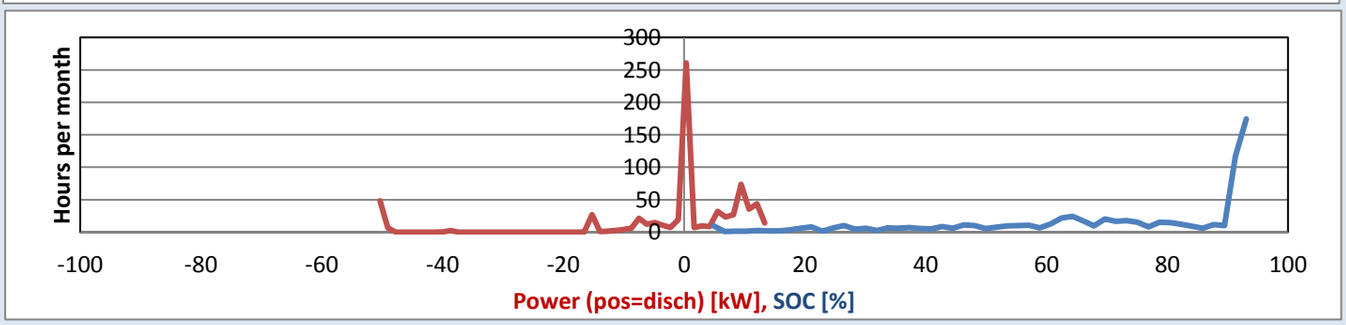

Downtime events:

Number	Site date, time	Reason	Action taken
1	9/6/15 1:55 AM	Inverter fault -- "Intermediate bus overvoltage fault". Cause being investigated--no high voltage detected in logged data.	Data sent to DynaPower for analysis. DynaPower preparing firmware with high-speed data logging capability.
2	9/7/15 4:26 PM	All strings disconnected during balancing, causing inverter to fault as it tried to set a power command on an empty bus.	Balancing postponed until revised procedure can be defined and tested.

MONTHLY SYSTEM PERFORMANCE REPORT

Bosch Energy Storage Solutions

PJ Fort Bragg

Prepared by:	Ryan Balliet (BESS/ENG)
Date prepared:	11/10/2015
Version:	1
Report Start:	10/1/2015
Report End:	10/31/2015
Installation site:	Fort Bragg, NC
System AC rating:	100 kW, 100 kWh
Commissioning complete:	7/31/2015
Days since commissioning:	92

	Month	To Date
Cycles complete:	19	58
AC energy discharged [MWh]:	2.0	6.2
AC energy charged [MWh]:	3.3	9.8
Grid backup events:	0	0
Availability [%]:	96	94
Downtime [d]:	1.2	5.2

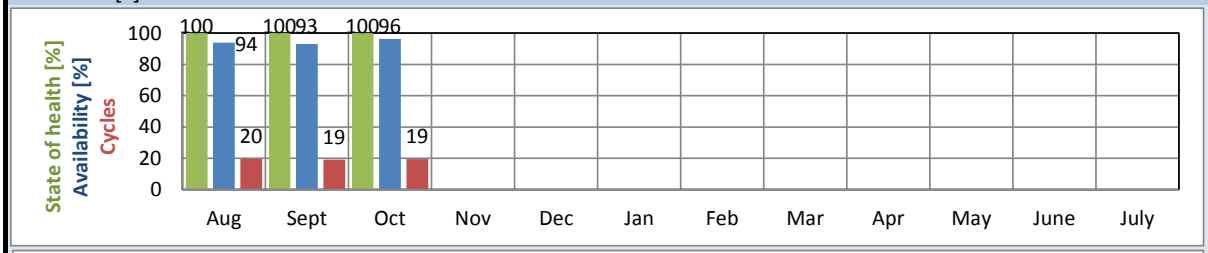

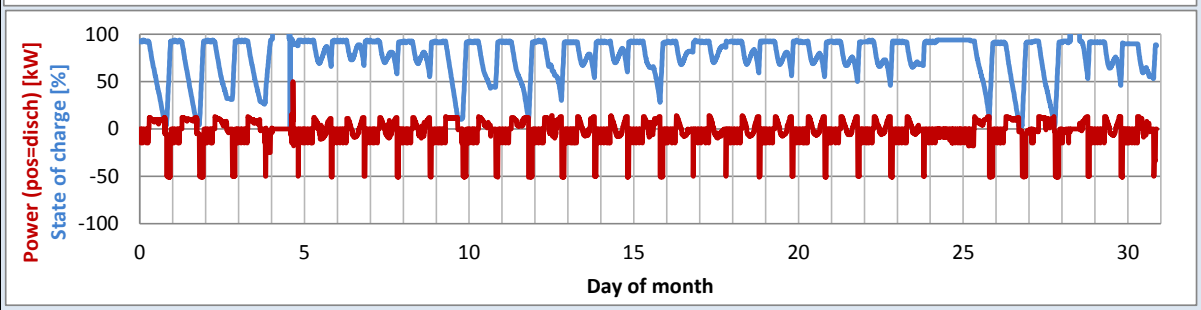

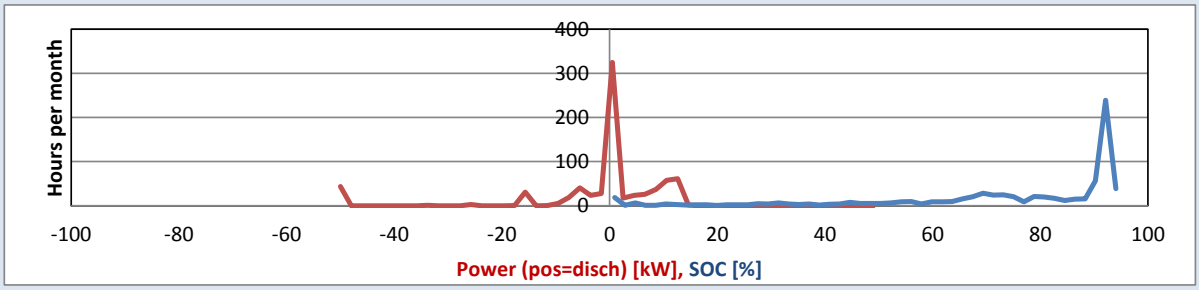

Downtime events:

Number	Site date, time	Reason	Action taken
1	10/5/15 12:41 AM	All strings disconnected during balancing, causing inverter to fault as it tried to set a power command on an empty bus.	Balancing postponed until revised procedure can be defined and tested.
2	10/29/15 6:11 AM	During string connection procedure near top of charge, the single connected string was automatically disconnected from the DC bus by the battery controller. This in turn caused the inverter to fault because it was trying to set a power when the DC bus was empty.	String connection procedure changed so that the highest SOC string is connected first and the others are picked up on discharge rather than the lowest being connected first and the rest being picked up on charge.

MONTHLY SYSTEM PERFORMANCE REPORT

Bosch Energy Storage Solutions

PJ Fort Bragg

BOSCH Invented for life

Prepared by:	Ryan Balliet (BESS/ENG)
Date prepared:	12/10/2015
Version:	1
Report Start:	11/1/2015
Report End:	11/30/2015
Installation site:	Fort Bragg, NC
System AC rating:	100 kW, 100 kWh
Commissioning complete:	7/31/2015
Days since commissioning:	122

	Month	To Date
Cycles complete:	20	78
AC energy discharged [MWh]:	2.1	8.3
AC energy charged [MWh]:	3.3	13.2
Grid backup events:	0	0
Availability [%]:	95.2	94.6
Downtime [d]:	1.4	6.6

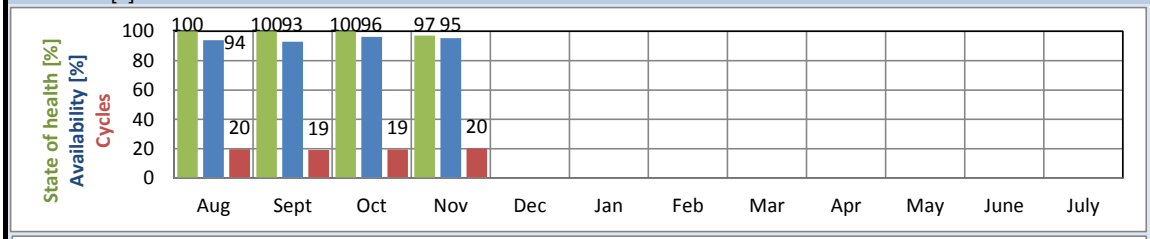

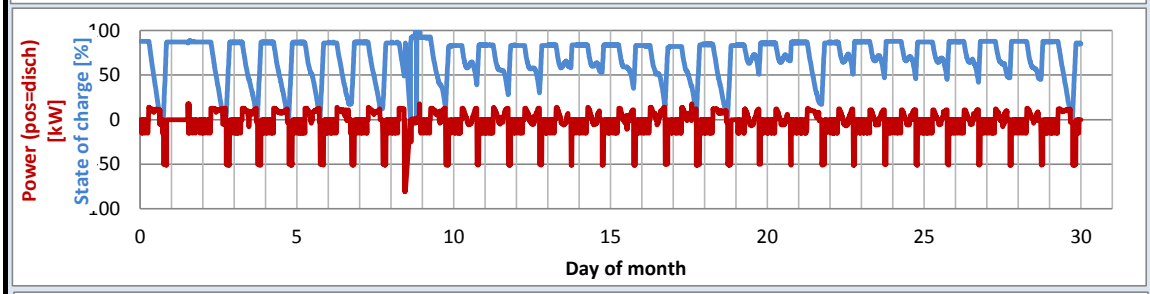

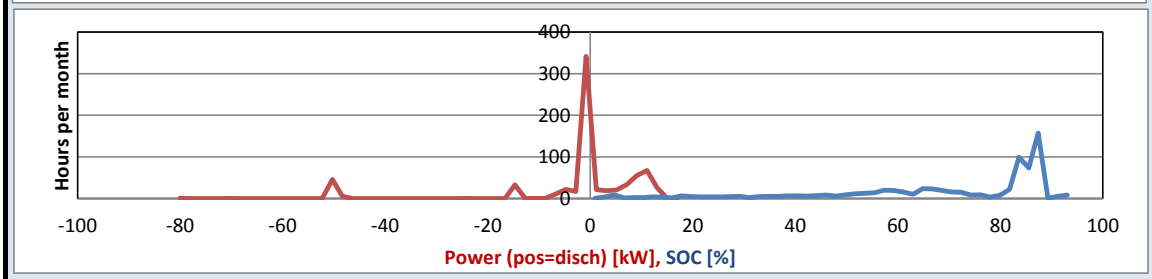

Downtime events:

Number	Site date, time	Reason	Action taken
1	11/1/15 8:23 PM	All strings disconnected due to EMU attempting to balance strings at high state of charge, causing inverter to fault as it tried to set a power command on an empty bus.	Changed top of charge condition to be based on maximum, rather than average, SOC.
2	11/9/15 10:00 AM	System intentionally taken offline for 12 h(with advance permission from PJ-BGT team) to test software change intended to eliminate faults during balancing. Rather than changing the power setpoint to zero based on the EMU current limits, tried to set power to zero based on the DC bus voltage. However, testing showed that this strategy was not effective at eliminating faults.	Balanced system with manual intervention in case of faults. Subsuently discussed issue further with inverter supplier, who suggested tests to investigate why built-in inverter voltage limit is not effective. This will be performed in December (at a time coordinated with PJ-BGT).

MONTHLY SYSTEM PERFORMANCE REPORT

Bosch Energy Storage Solutions

PJ Fort Bragg

Prepared by:	Ryan Balliet (BESS/ENG)
Date prepared:	1/5/2016
Version:	2
Report Start:	12/1/2015
Report End:	12/31/2015
Installation site:	Fort Bragg, NC
System AC rating:	100 kW, 100 kWh
Commissioning complete:	7/31/2015
Days since commissioning:	153

	Month	To Date
Cycles complete:	22	100
AC energy discharged [MWh]:	2.3	10.5
AC energy charged [MWh]:	3.6	16.8
Grid backup events:	0	0
Availability [%]:	96.8	95.0
Downtime [d]:	1.0	7.6

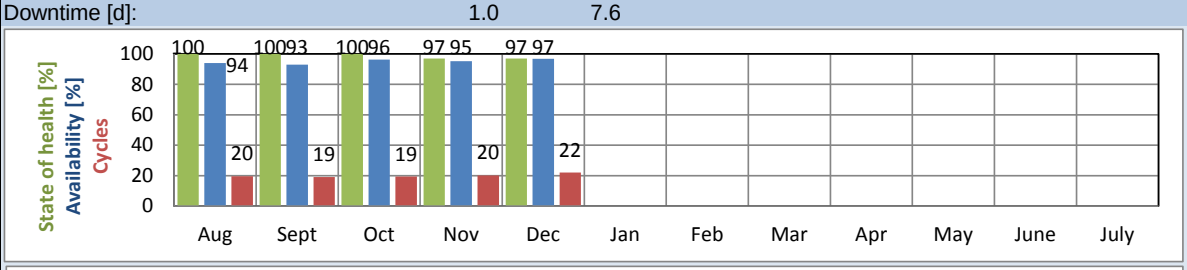

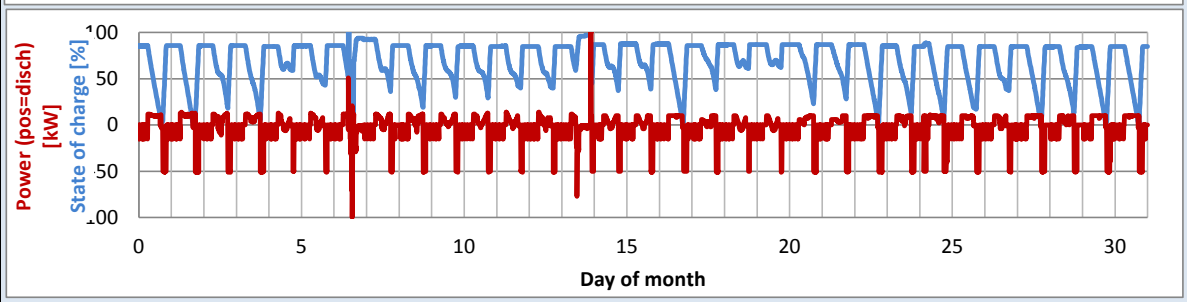

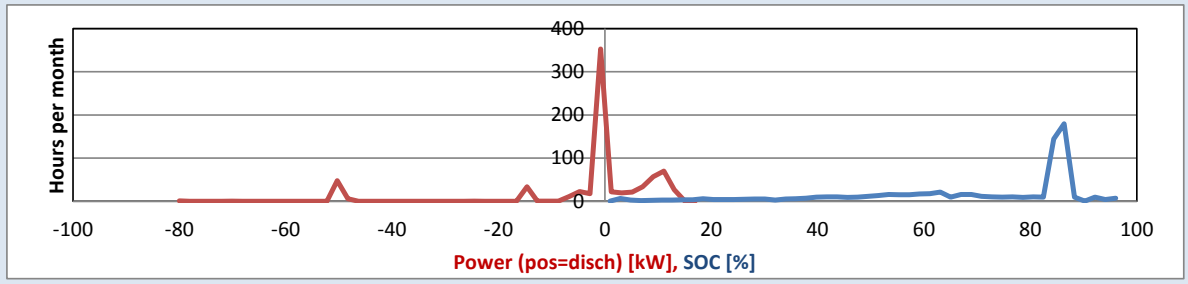

Downtime events:

Number	Site date, time	Reason	Action taken
1	12/7/15 10:00 AM	System intentionally taken offline for 12 h (with advance permission from PJ-BGT team) to test software change intended to eliminate faults during balancing. Testing was successful, but time was insufficient to test all possible failure modes.	Additional time scheduled for 12/14 to complete testing.
2	12/14/15 10:00 AM	System intentionally taken offline for 12 h (with advance permission from PJ-BGT team) to complete testing of software change intended to eliminate faults during balancing. All tests completed and balancing performed without fault.	Monthly balancing on the first Sunday of each month, which had been suspended due to faults, reactivated.

MONTHLY SYSTEM PERFORMANCE REPORT

Bosch Energy Storage Solutions

PJ Fort Bragg

Prepared by:	Ryan Balliet (BESS/ENG)
Date prepared:	2/1/2016
Version:	1
Report Start:	1/1/2016
Report End:	1/31/2016
Installation site:	Fort Bragg, NC
System AC rating:	100 kW, 100 kWh
Commissioning complete:	7/31/2015
Days since commissioning:	184

	Month	To Date
Cycles complete:	21	121
AC energy discharged [MWh]:	2.1	12.6
AC energy charged [MWh]:	3.4	20.2
Grid backup events:	0	0
Availability [%]:	100.0	95.9
Downtime [d]:	0.0	7.6

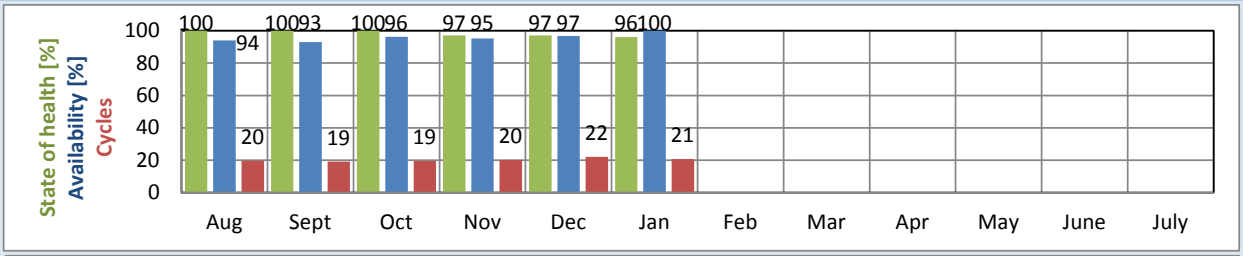

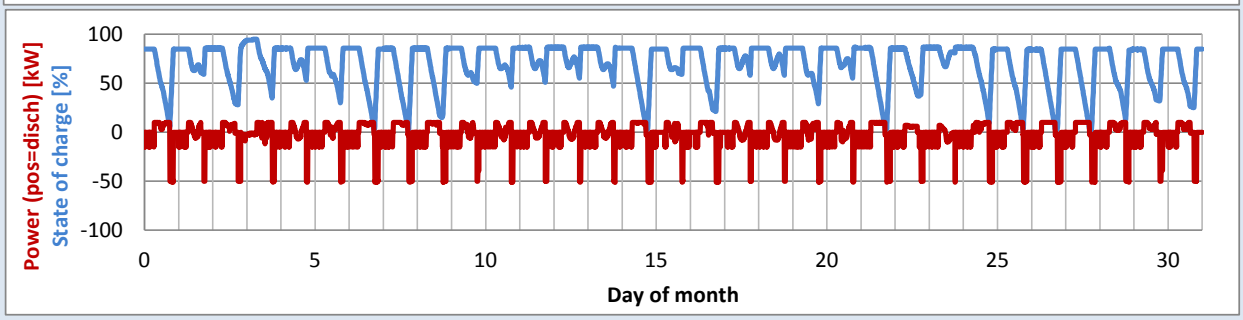

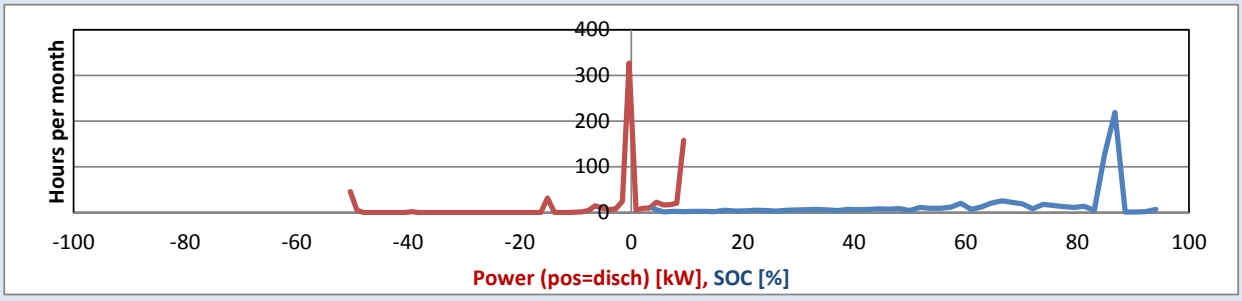

Downtime events:

Number	Site date, time	Reason	Action taken

N/A. No downtime events this month.

MONTHLY SYSTEM PERFORMANCE REPORT

Bosch Energy Storage Solutions

PJ Fort Bragg

Prepared by:	Ryan Balliet (BESS/ENG)
Date prepared:	3/2/2016
Version:	1
Report Start:	2/1/2016
Report End:	2/29/2016
Installation site:	Fort Bragg, NC
System AC rating:	100 kW, 100 kWh
Commissioning complete:	7/31/2015
Days since commissioning:	213

	Month	To Date
Cycles complete:	23	144
AC energy discharged [MWh]:	2.4	15.1
AC energy charged [MWh]:	3.7	23.9
Grid backup events:	0	0
Availability [%]:	100.0	96.4
Downtime [d]:	0.0	7.6

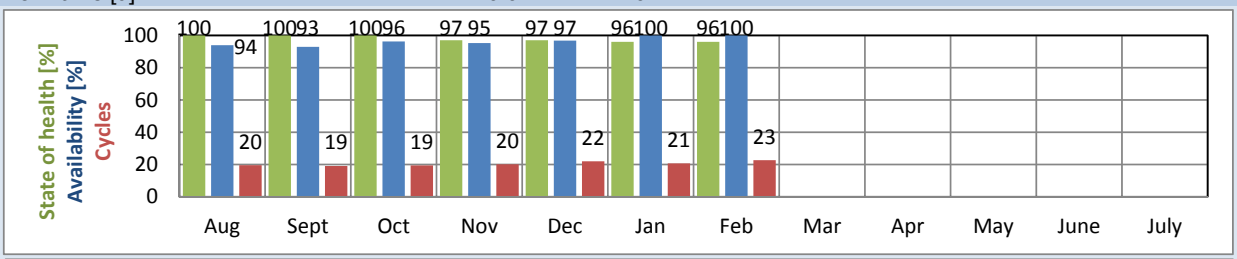

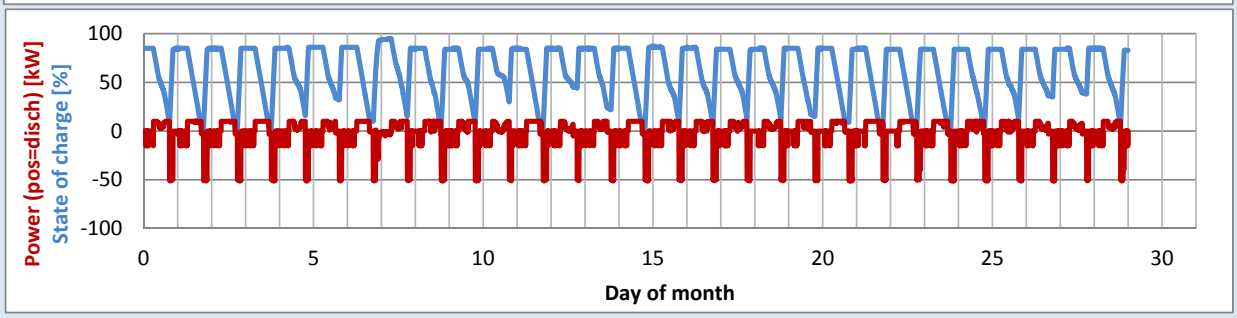

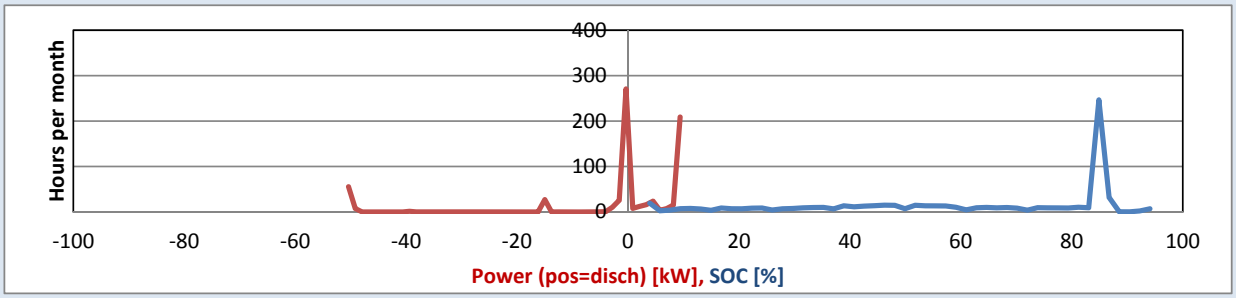

Downtime events:

Number	Site date, time	Reason	Action taken

N/A. No downtime events this month.

MONTHLY SYSTEM PERFORMANCE REPORT

Bosch Energy Storage Solutions

PJ Fort Bragg

BOSCH Invented for life

Prepared by:	Chris Pais (BESS/ENG)
Date prepared:	4/11/2016
Version:	1
Report Start:	3/1/2016
Report End:	3/31/2016
Installation site:	Fort Bragg, NC
System AC rating:	100 kW, 100 kWh
Commissioning complete:	7/31/2015
Days since commissioning:	244

	Month	To Date
Cycles complete:	21	165
AC energy discharged [MWh]:	2.3	17.4
AC energy charged [MWh]:	3.5	27.5
Grid backup events:	0	0
Availability [%]:	94.0	96.1
Downtime [d]:	1.9	9.5

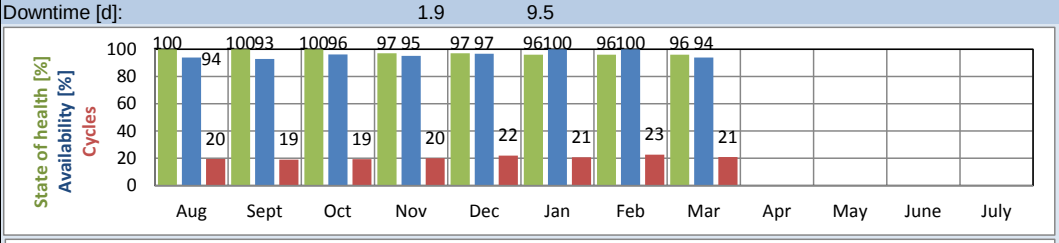

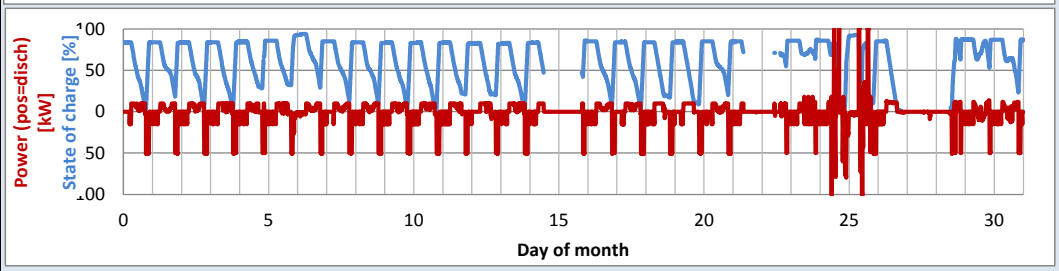

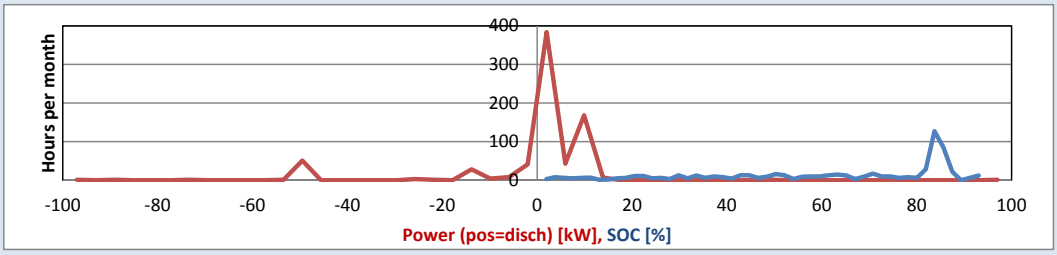

Downtime events:

Number	Site date, time	Reason	Action taken
1	3/15/16 11:27 AM	System shut down by Skan Electric in order to perform electrical upgrade for Phase II. Once BESS received permission from Skan to restart, system was restarted and returned to PJ-BGT control. During the integration process, Skan observed that the ESS did not transition to off-grid mode as expected. Downtime not included in availability calculation since it was part of Phase II upgrade.	BESS added to its action item list for its upcoming site visit verifying off-grid capability of the ESS. See next row for further information.
2	3/22/16 8:34 AM	System shut down by BESS to complete its integration work for Phase II. This included demonstrating control of the 100 kW PV inverter in on-grid and off-grid mode. Two BESS engineers (project and controls) were onsite at Ft. Bragg, with additional remote support from Palo Alto. Downtime not included in availability calculation since it was part of Phase II upgrade.	In addition to integrating the Solectria inverter, BESS found the software issue that prevented the system from entering off-grid mode on 3/15. This was fixed and the fix was verified.
3	3/27/16 7:58 PM	System automatically shut down due to string with low-SOC. This condition occurred due to a software issue.	Software issue identified, fixed, and the fix verified. Skan electric visited site to check health of battery controller and modules in low-SOC string under BESS direction. All components normal. Procedure for reconnecting string being developed with input from SONY. System operating with low-SOC string disconnected.

MONTHLY SYSTEM PERFORMANCE REPORT

Bosch Energy Storage Solutions

PJ Fort Bragg

BOSCH Invented for life

Prepared by:	Chris Pais (BESS/ENG)
Date prepared:	5/2/2016
Version:	1
Report Start:	4/1/2016
Report End:	4/30/2016
Installation site:	Fort Bragg, NC
System AC rating:	100 kW, 100 kWh
Commissioning complete:	7/31/2015
Days since commissioning:	274

	Month	To Date
Cycles complete:	22	187
AC energy discharged [MWh]:	2.3	19.7
AC energy charged [MWh]:	3.6	31.1
Grid backup events:	1	1
Availability [%]:	99.3	96.5
Downtime [d]:	0.2	9.7

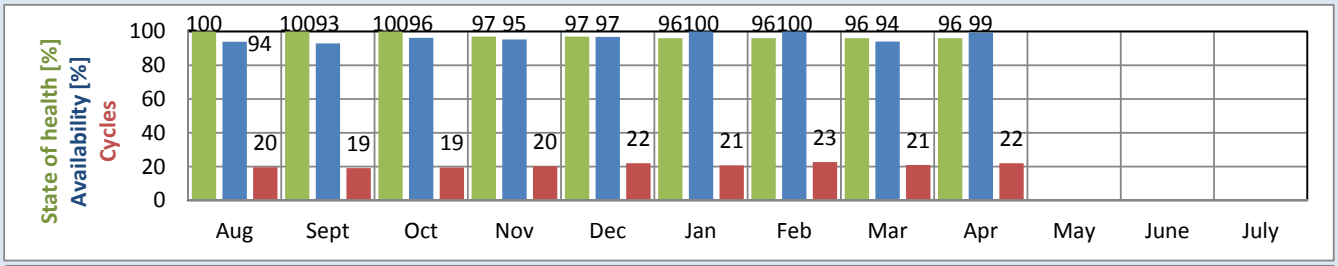

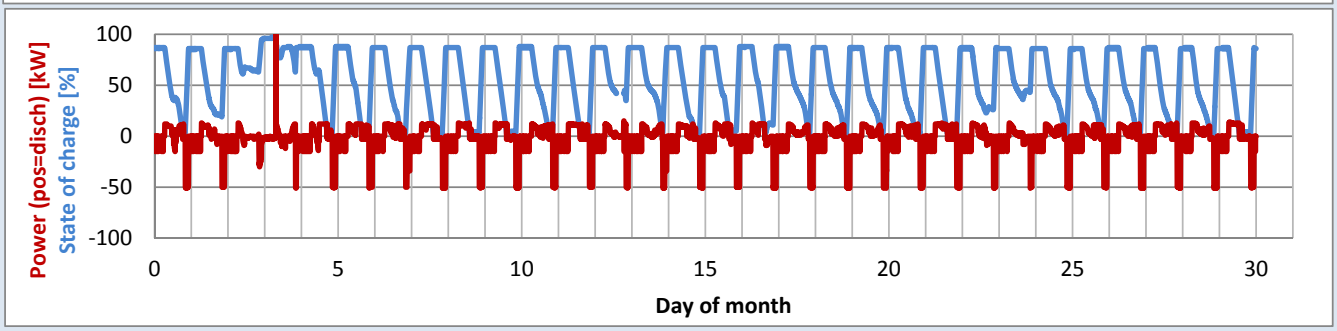

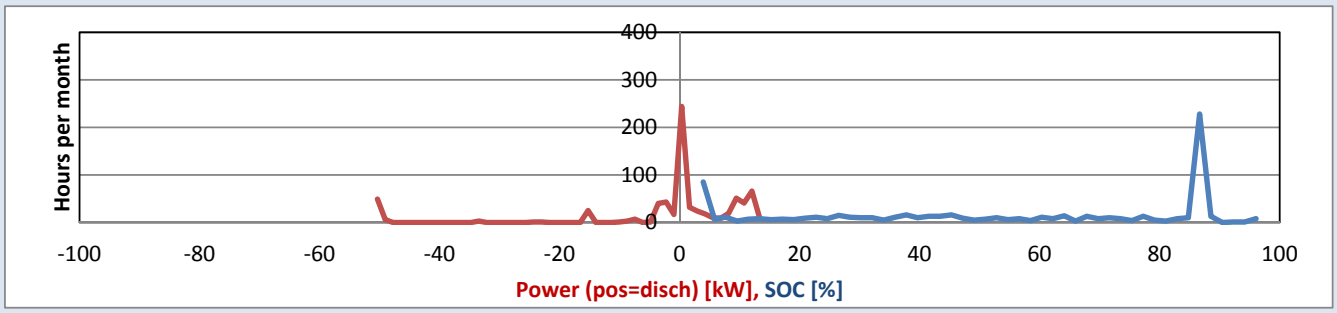

Downtime events:

Number	Site date, time	Reason	Action taken
1	4/13/2016 13:57:00 AM	Software update pushed during operation resulted in shutdown due to incompatibility of some fields.	Software fixed to remove incompatibility.

MONTHLY SYSTEM PERFORMANCE REPORT

Bosch Energy Storage Solutions

PJ Fort Bragg

Prepared by:	Chris Pais (BESS/ENG)
Date prepared:	6/2/2016
Version:	1
Report Start:	5/1/2016
Report End:	5/31/2016
Installation site:	Fort Bragg, NC
System AC rating:	100 kW, 100 kWh
Commissioning complete:	7/31/2015
Days since commissioning:	305

	Month	To Date
Cycles complete:	22	209
AC energy discharged [MWh]:	2.6	22.3
AC energy charged [MWh]:	3.9	35.0
Grid backup events:	0	1
Availability [%]:	97.1	96.5
Downtime [d]:	0.9	10.6

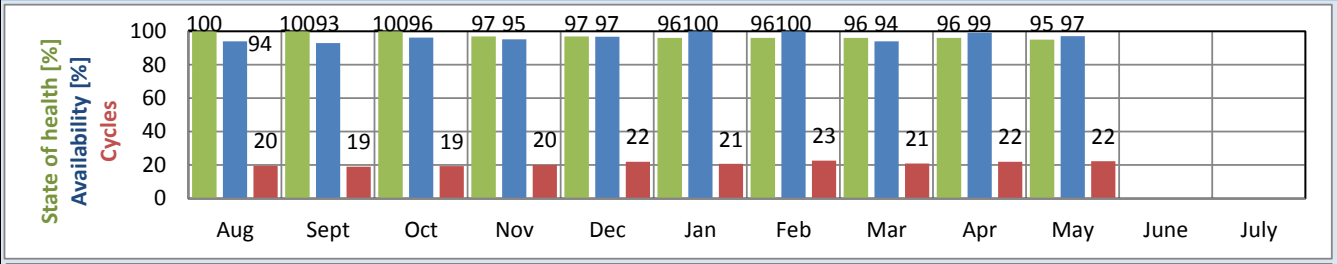

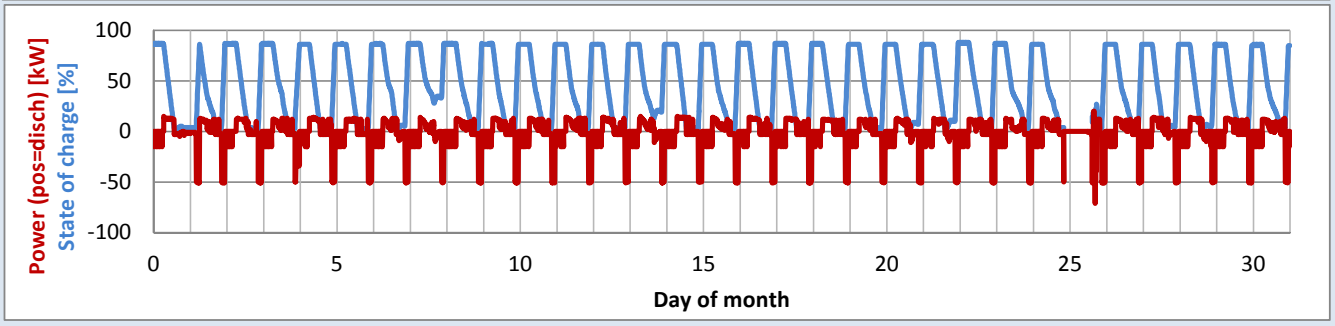

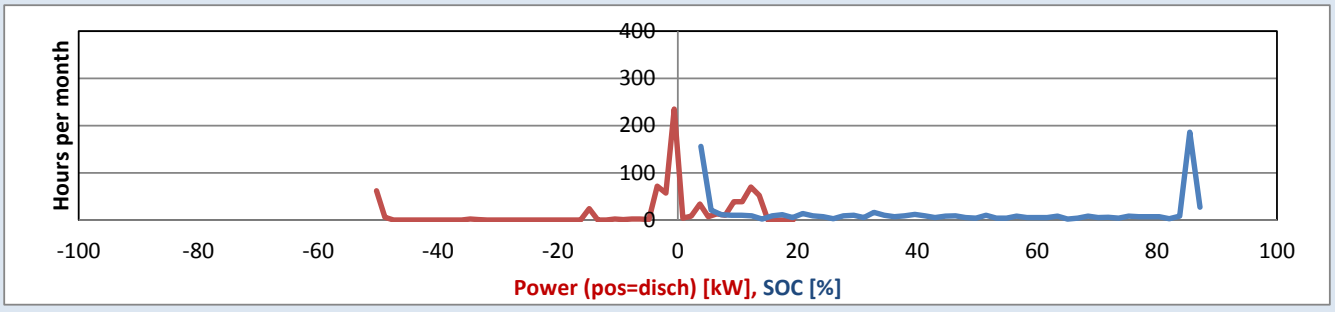

Downtime events:

Number	Site date, time	Reason	Action taken
1	5/25/16 19:44:08	This was planned downtime. PJ-BGT was notified in advance. During downtime diagnostic testing and manual charging of two modules in string 4 was completed.	Data sent to SONY for review. Development of a procedure to connect string 4 underway.

MONTHLY SYSTEM PERFORMANCE REPORT

Bosch Energy Storage Solutions

PJ Fort Bragg

Prepared by:	Chris Pais (BESS/ENG)
Date prepared:	7/5/2016
Version:	1
Report Start:	6/1/2016
Report End:	6/30/2016
Installation site:	Fort Bragg, NC
System AC rating:	100 kW, 100 kWh
Commissioning complete:	7/31/2015
Days since commissioning:	335

	Month	To Date
Cycles complete:	17	227
AC energy discharged [MWh]:	1.9	24.2
AC energy charged [MWh]:	3.0	37.9
Grid backup events:	0	1
Availability [%]:	76.1	94.7
Downtime [d]:	7.2	17.7

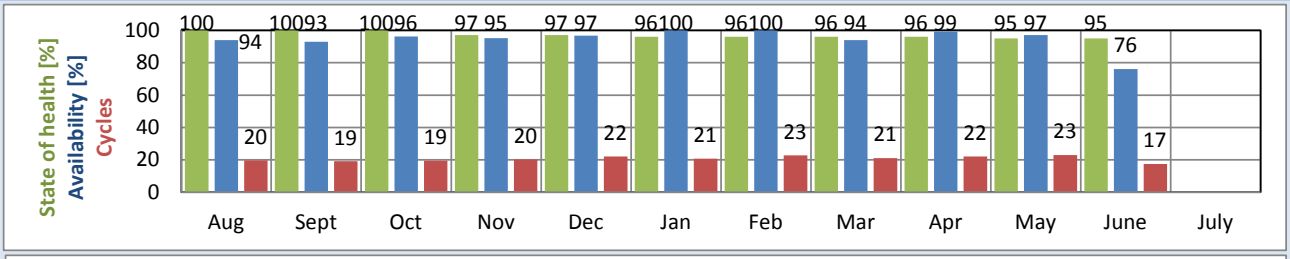

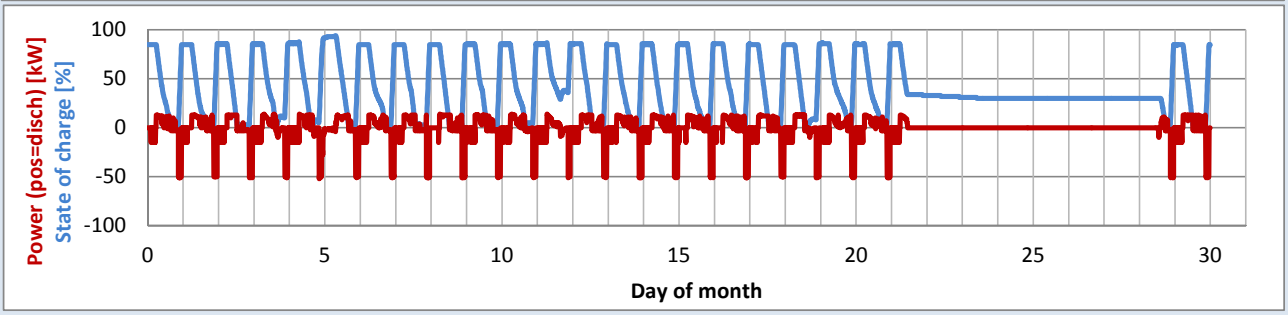

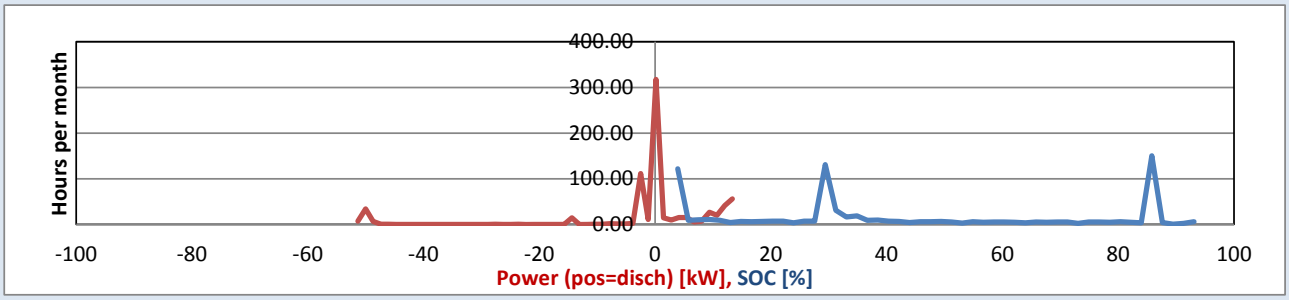

Downtime events:

Number	Site date, time	Reason	Action taken
1	6/22/16 10:42:12	Inverter control board failed. Root cause currently being investigated. For this report, the downtime associated with the failure has been included in the availability calculation. However, if the root cause investigation shows that the system failed due to an external disturbance outside the intended operating range of the ESS, a revised report will be issued.	Unscuccessfully attempted to establish communication with inverter. Consulted inverter manufacturer (DynaPower). Their diagnonsis was control board failure. DynaPower shipped replacement part to Skan Electric and sent a technician to the site who (with the help of Skan electric) replaced the board. The system then functioned normally. DynaPower currently diagnosing control board and will report back regarding probable cause of failure.

MONTHLY SYSTEM PERFORMANCE REPORT

Bosch Energy Storage Solutions

PJ Fort Bragg

Prepared by:	Chris Pais (BESS/ENG)
Date prepared:	8/9/2016
Version:	1
Report Start:	7/1/2016
Report End:	7/31/2016
Installation site:	Fort Bragg, NC
System AC rating:	100 kW, 100 kWh
Commissioning complete:	7/31/2015
Days since commissioning:	366

	Month	To Date
Cycles complete:	17	227
AC energy discharged [MWh]:	1.9	24.2
AC energy charged [MWh]:	3.0	37.9
Grid backup events:	0	1
Availability [%]:	76.1	94.7
Downtime [d]:	7.2	17.7

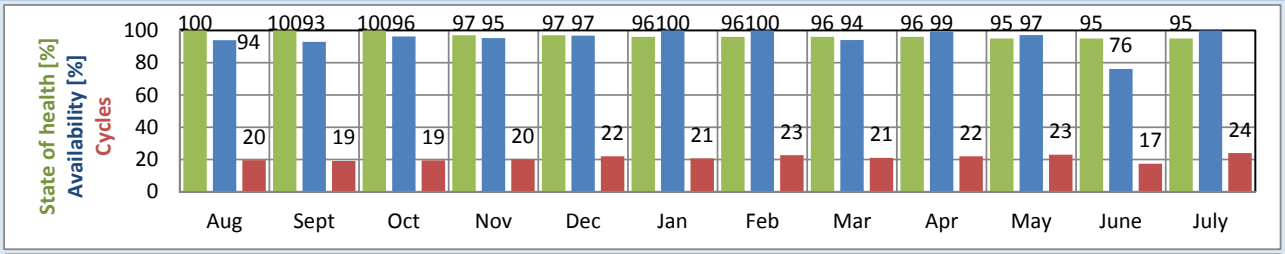

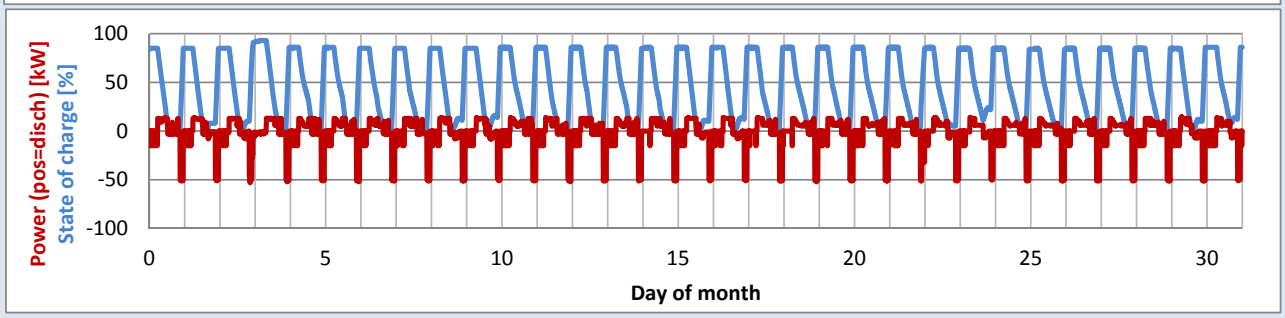

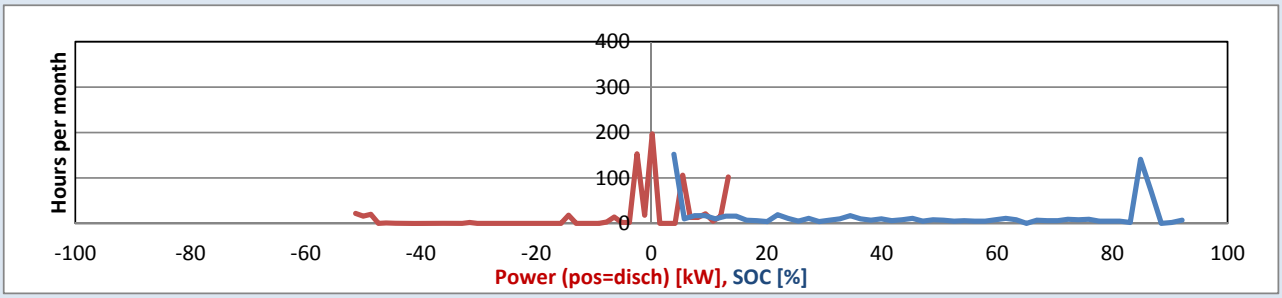

Downtime events:

Number	Site date, time	Reason	Action taken
1	7/15/16 15:38:24	Review of site data showed that the grid voltage went from 480 V to 0 V four times in a period of 12 minutes, each time recovering after 8 to 10 seconds. After the final voltage fluctuation, the system reconnected automatically and resumed normal operation.	Email was sent to Dusan Bhrlik to verify if any site work was being done to cause such a fluctuation. Dusan confirmed that no site work was being done. No other mitigating action was envisaged, and none was taken.

MONTHLY SYSTEM PERFORMANCE REPORT

Bosch Energy Storage Solutions

PJ Fort Bragg

Prepared by:	Chris Pais (BESS/ENG)
Date prepared:	9/6/2016
Version:	1
Report Start:	8/1/2016
Report End:	8/31/2016
Installation site:	Fort Bragg, NC
System AC rating:	100 kW, 100 kWh
Commissioning complete:	7/31/2015
Days since commissioning:	397

	Month	To Date
Cycles complete:	17	227
AC energy discharged [MWh]:	1.9	24.2
AC energy charged [MWh]:	3.0	37.9
Grid backup events:	0	1
Availability [%]:	76.1	94.7
Downtime [d]:	7.2	17.7

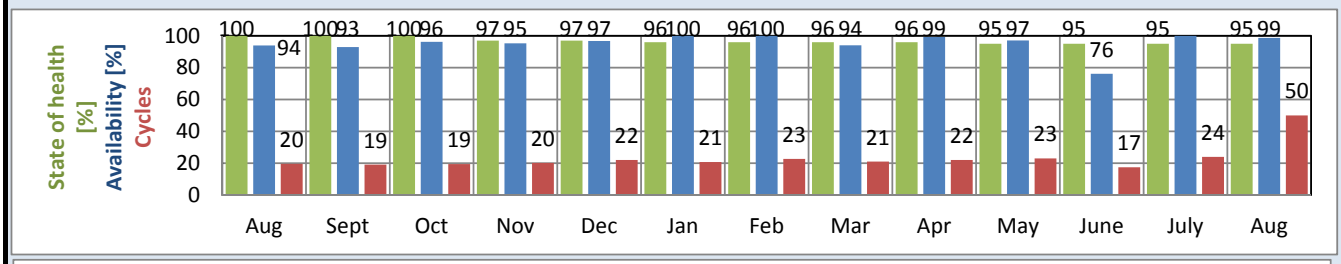

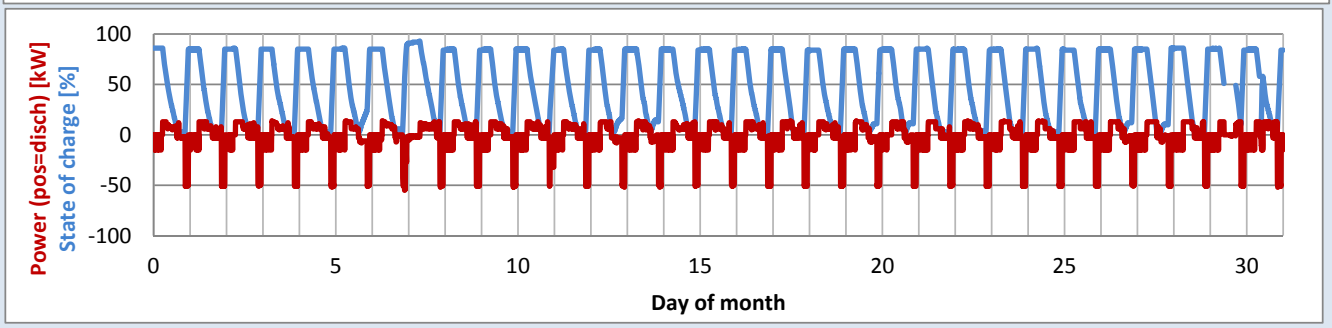

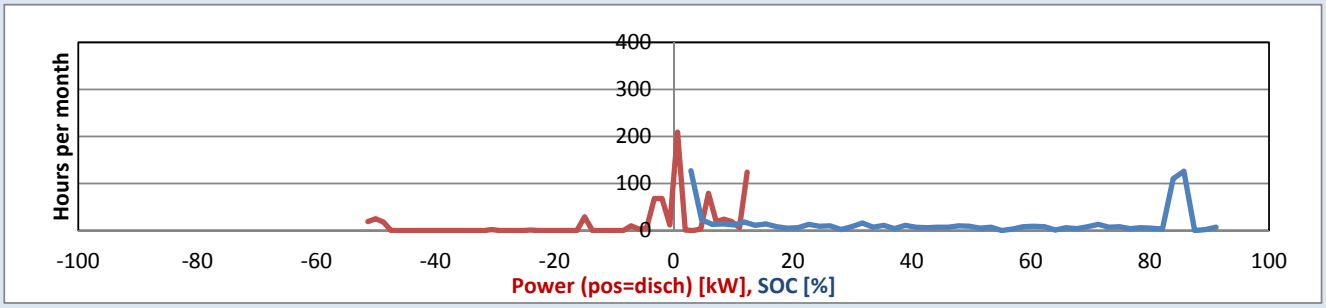

Downtime events:

Number	Site date, time	Reason	Action taken
1	8/30/16 9:06:00	System was shut down to connect String 4	Attempted to connect String 4, and collected data for review with battery manufacturer.
2	8/31/16 8:35:00	System was shut down to connect String 4	String 4 successfully connected.

MONTHLY SYSTEM PERFORMANCE REPORT

Bosch Energy Storage Solutions

PJ Fort Bragg

Prepared by:	Chris Pais (BESS/ENG)
Date prepared:	10/4/2016
Version:	1
Report Start:	9/1/2016
Report End:	9/30/2016
Installation site:	Fort Bragg, NC
System AC rating:	100 kW, 100 kWh
Commissioning complete:	7/31/2015
Days since commissioning:	427

	Month	To Date
Cycles complete:	26	300
AC energy discharged [MWh]:	3.0	32.5
AC energy charged [MWh]:	4.4	50.3
Grid backup events:	0	1
Availability [%]:	100.0	95.8
Downtime [d]:	0.0	18.1

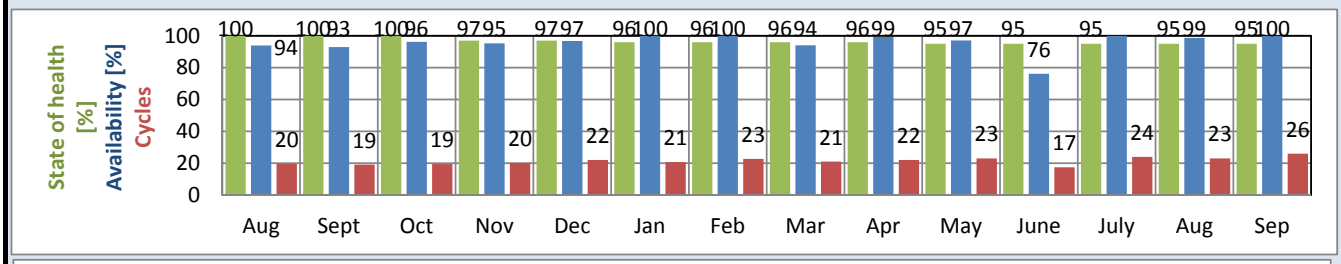

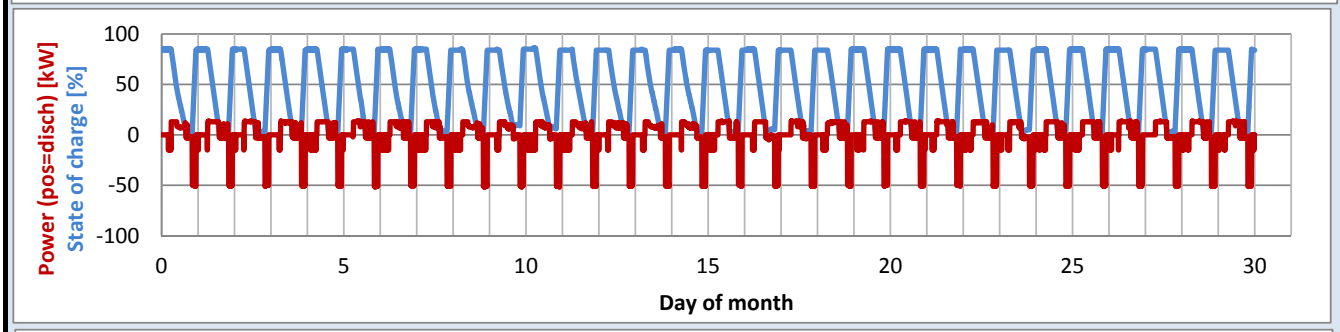

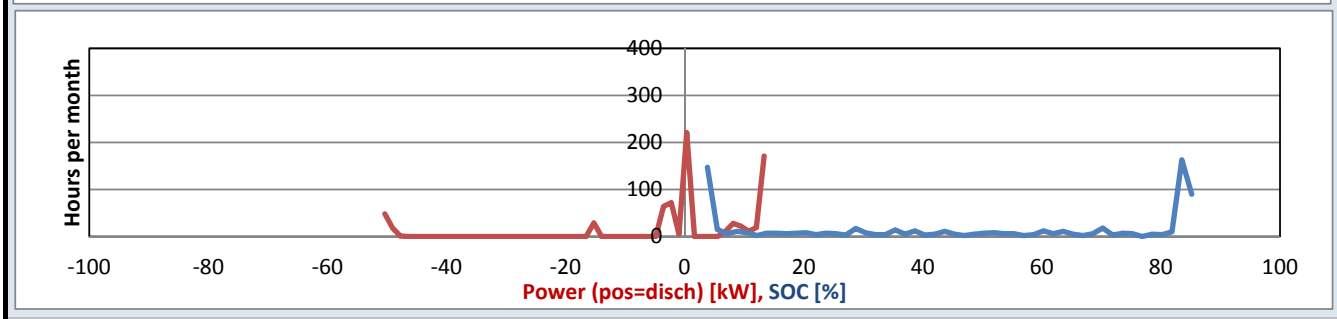

Downtime events:

Number	Site date, time	Reason	Action taken
1	None		
2			

MONTHLY SYSTEM PERFORMANCE REPORT

Bosch Energy Storage Solutions

PJ Fort Bragg

Prepared by:	Chris Pais (BESS/ENG)
Date prepared:	11/22/2016
Version:	1
Report Start:	10/1/2016
Report End:	10/31/2016
Installation site:	Fort Bragg, NC
System AC rating:	100 kW, 100 kWh
Commissioning complete:	7/31/2015
Days since commissioning:	458

	Month	To Date
Cycles complete:	8	308
AC energy discharged [MWh]:	0.9	33.4
AC energy charged [MWh]:	1.3	51.6
Grid backup events:	0	1
Availability [%]:	41.7	92.1
Downtime [d]:	18.1	36.2

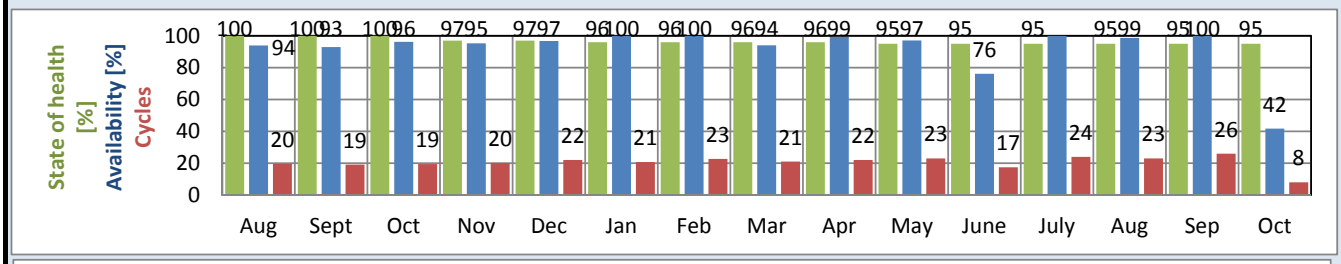

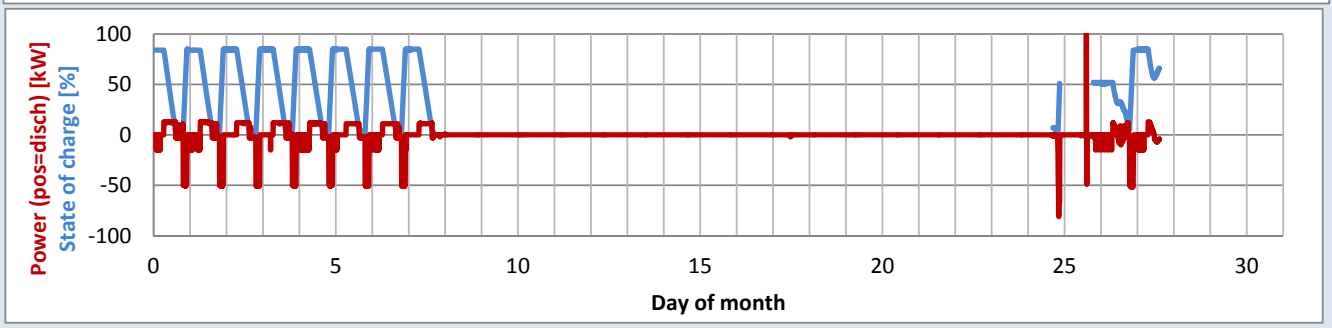

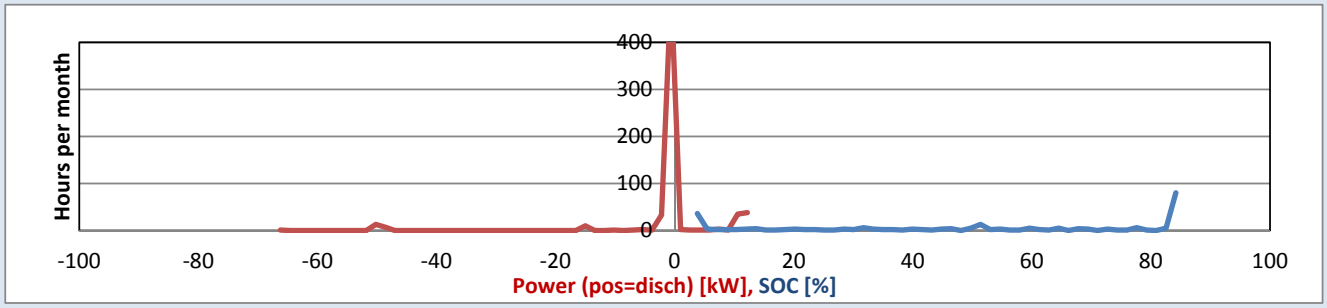

Downtime events:

Number	Site date, time	Reason	Action taken
1	10/8/16 16:16:00	Email notification system annunciated "Inverter Faulted" followed by "No Error". The system tripped due to a grid disturbance experienced during Hurricane Matthew and was unable to get back online.	No hardware deficiencies were found with the inverter. Reliable inverter restart was achieved after the tuning parameters of the inverter were modified by Dynapower.
2	10/27/16 15:23:00	Forced shutdown to allow SKAN electric to enter PCS room to install DCMG equipment.	None. System restarted after the PCS door was shut.

Data shown until 28Oct2016 only due to database availability

MONTHLY SYSTEM PERFORMANCE REPORT

Bosch Energy Storage Solutions

PJ Fort Bragg

Prepared by:	Chris Pais (BESS/ENG)
Date prepared:	12/1/2016
Version:	1
Report Start:	11/1/2016
Report End:	11/30/2016
Installation site:	Fort Bragg, NC
System AC rating:	100 kW, 100 kWh
Commissioning complete:	7/31/2015
Days since commissioning:	488

	Month	To Date
Cycles complete:	22	332
AC energy discharged [MWh]:	2.4	35.8
AC energy charged [MWh]:	3.7	55.3
Grid backup events:	4	5
Availability [%]:	100.0	92.6
Downtime [d]:	0.0	36.2

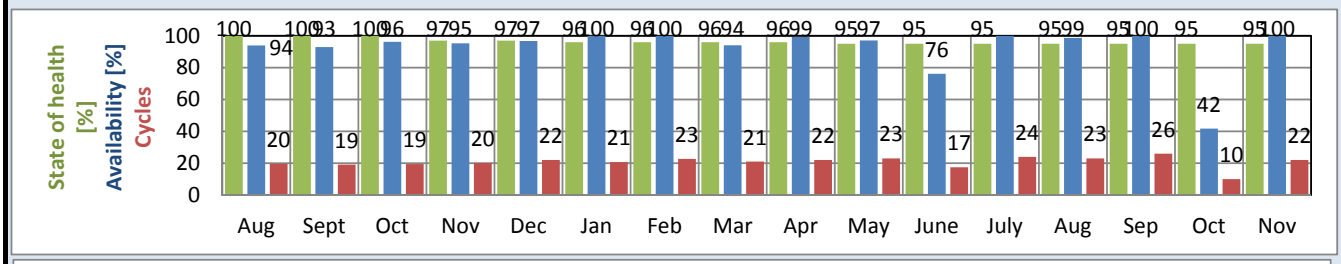

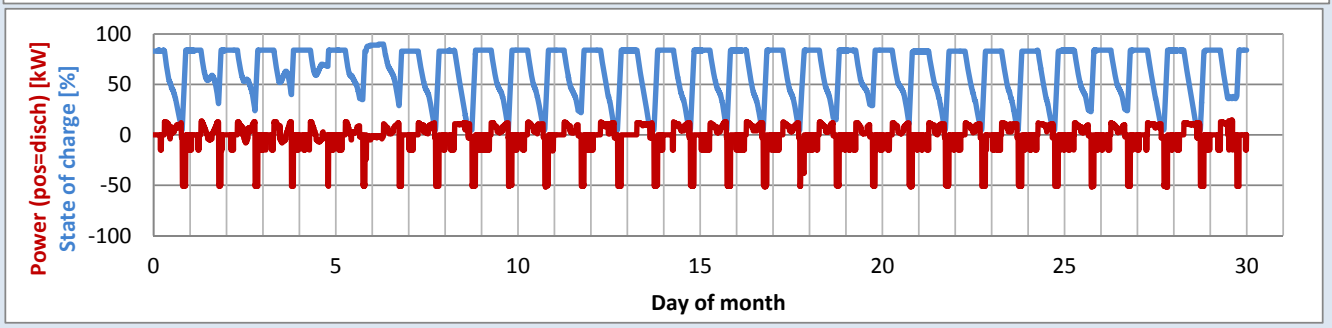

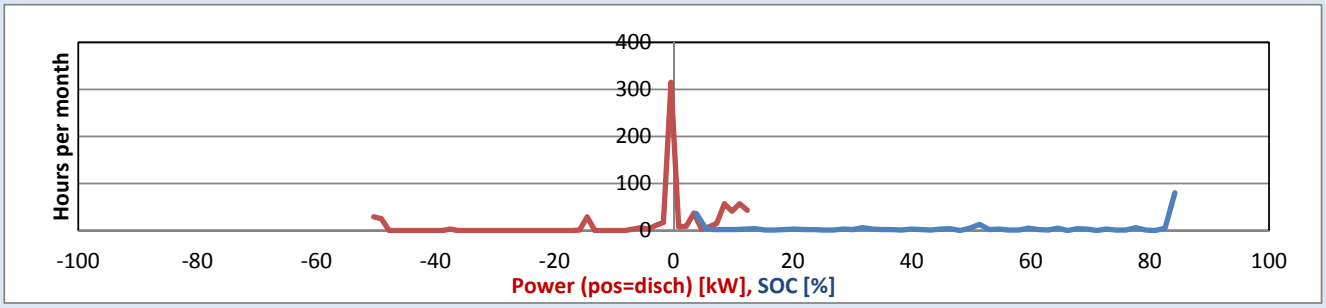

Downtime events:

Number	Site date, time	Reason	Action taken
1	11/4/16 10:40:00	Ron Fisher of SKAN had to enter PCS room to install a timer for DCMG's data collection system	System restarted by itself. Not accounted for in downtime since outage was requested by customer.
2	11/30/16 11:22:00	Dusan Bhrlik of DCMG was on site for island testing of the BESS and PV system.	System was put back online after completion of testing. Not accounted for in downtime since outage was requested by customer.

MONTHLY SYSTEM PERFORMANCE REPORT

Bosch Energy Storage Solutions

PJ Fort Bragg

BOSCH Invented for life

Prepared by:	Fang Chen (RTC2)
Date prepared:	1/3/2016
Version:	1
Report Start:	12/1/2016
Report End:	12/31/2016
Installation site:	Fort Bragg, NC
System AC rating:	100 kW, 100 kWh
Commissioning complete:	7/31/2015
Days since commissioning:	519

	Month	To Date
Cycles complete:	26	358
AC energy discharged [MWh]:	2.8	38.6
AC energy charged [MWh]:	4.1	59.4
Grid backup events:	4	5
Availability [%]:	100.0	93.0
Downtime [d]:	0.0	36.2

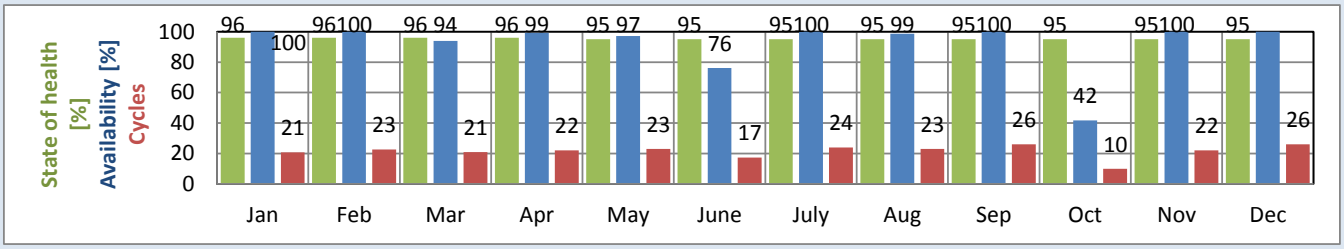

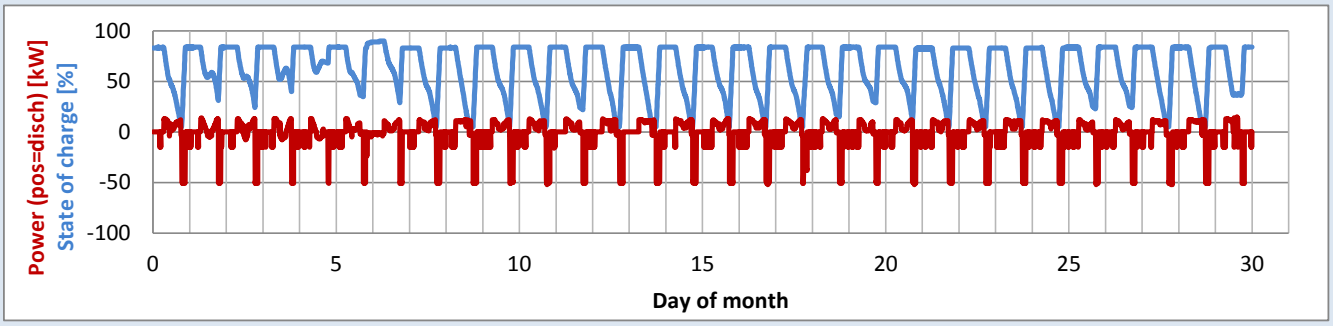

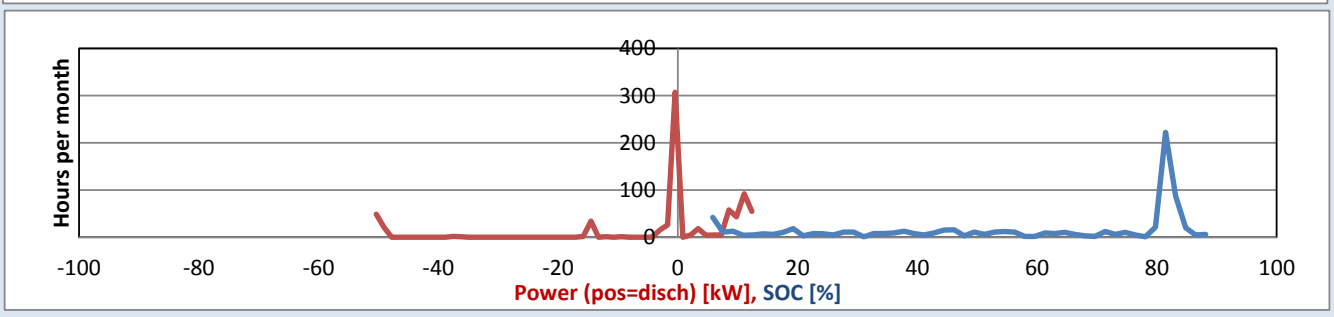

Downtime events:

Number	Site date, time	Reason	Action taken

N/A. No downtime events this month.

MONTHLY SYSTEM PERFORMANCE REPORT

Bosch Energy Storage Solutions

PJ Fort Bragg

BOSCH
Invented for life

Prepared by:	Fang Chen (RTC2)
Date prepared:	2/15/2017
Version:	1
Report Start:	1/1/2017
Report End:	2/1/2017
Installation site:	Fort Bragg, NC
System AC rating:	100 kW, 100 kWh
Commissioning complete:	7/31/2015
Days since commissioning:	551

	Month	To Date
Cycles complete:	24	382
AC energy discharged [MWh]:	2.6	41.2
AC energy charged [MWh]:	4.0	63.4
Grid backup events:	0	5
Availability [%]:	100.0	93.4
Downtime [d]:	0.0	36.2

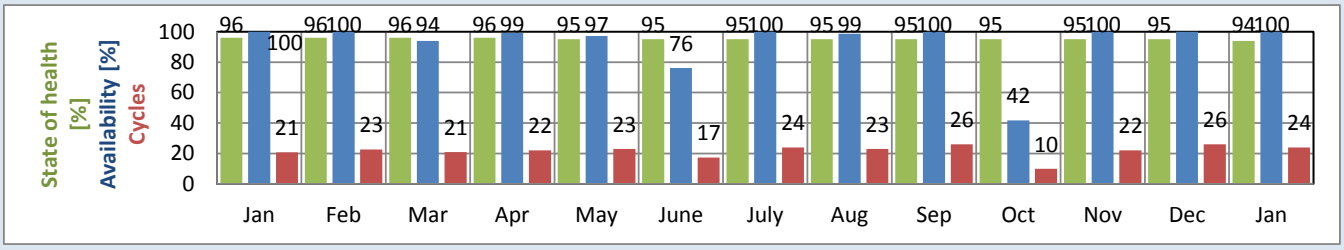

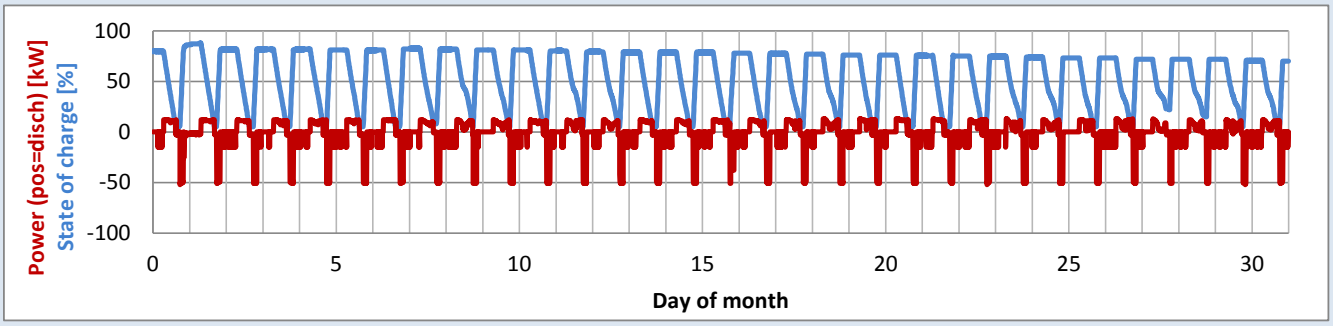

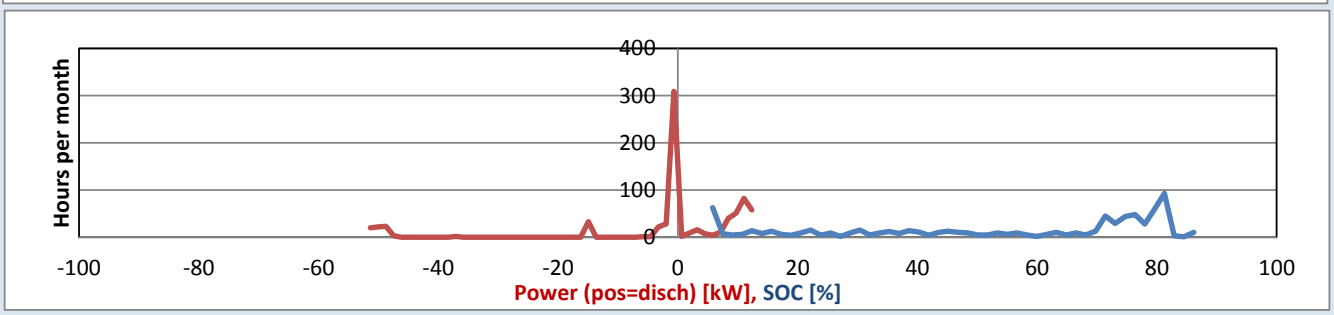

Downtime events:

Number	Site date, time	Reason	Action taken

N/A. No downtime events this month.

Appendix F: Fort Bragg Case Study

Bosch Building Grid Technologies - DC Microgrid
Hercules Fitness Center - Ft Bragg, NC

Hercules Fitness Center's Innovative DC Microgrid System Revolutionizes Energy Utilization While Increasing Resiliency

Direct Current Architecture Powers Building Loads Directly from Onsite Solar

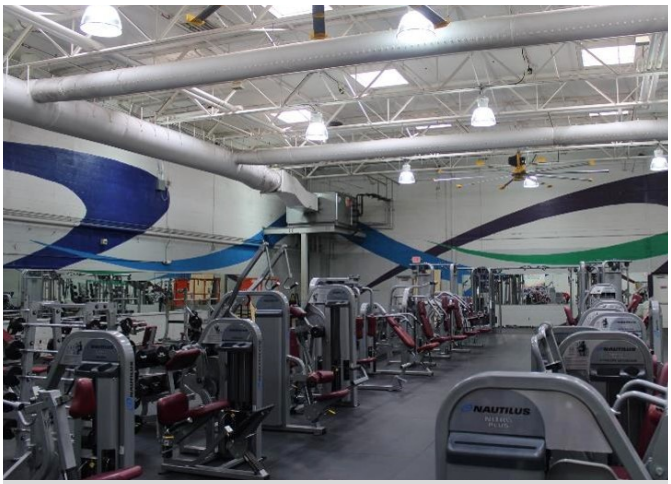

Hercules Fitness Center

The Facility

The Hercules Fitness Center at Fort Bragg, North Carolina serves two primary functions for the over 50,000 active duty residents and 14,000 civilians who work on the post. In non-crisis times the facility serves as one of the 14 fitness and recreation centers for the MWR (Moral Wellness & Recreation) division located on base. Site amenities include cardio & weight lifting facilities, a gymnasium, racquetball courts, a track, a sauna, and a juice bar. In addition the facility offers group fitness classes, & massage therapy.

In addition to keeping families healthy, the center also serves as an emergency shelter during emergencies or extreme weather events like Hurricane Matthew which hit the area with 15 inches of rain and strong winds in October of 2016.

PV Array

Overview

Bosch Building Grid Technologies (Menlo Park, California) and U.S. Army (Ft Bragg, North Carolina) have provided a novel approach to increase efficiency and resiliency for commercial & industrial building applications. The Direct Current (DC) microgrid system installed at Ft Bragg maximizes the use of solar energy by eliminating power conversion devices and providing DC power directly to both lighting and ventilation loads. This novel approach increases the reliability and safety of building power distribution architecture through the use of DC power. Additional efficiency gains are obtained by eliminating AC-DC power conversion at the input stage on both the luminaires and industrial fans. During grid outages at the fitness center, the solar PV arrays stay safely operational as there is no inverter connection to the utility grid that would usually disconnect the PV power. As the PV system is connected directly to the DC loads, this enables a very cost effective "islanding" strategy without requiring transfer switches or grid-forming inverters.

Lithium Ion Battery

As part of the second-phase of the demonstration, a 100 kWh Lithium-Ion energy storage system was added to the building to provide back-up power during evening and/or night time grid outages or to supplement the PV power. As a result, the reliance on other backup power sources such as diesel generators is eliminated or significantly reduced.

System Performance

Energy

Baseline Annual Energy Usage:	115,632 kWh
New Annual Energy Usage:	60,088 kWh
Annual Energy Savings:	-55,544 kWh

Efficiencies

Baseline AC System:	16.0% Loss
DC Microgrid:	3.1% Loss
Improvement:	12.9%

Energy Savings ($)

Annual Savings:	$ 4,807 USD
25 Year Energy savings:	**$127,750 USD**

www.BoschBGT.com

Bosch Building Grid Technologies - DC Microgrid
Hercules Fitness Center - Ft Bragg, NC

Hercules Fitness Center's Innovative DC Microgrid System Revolutionizes Energy Utilization While Increasing Resiliency
Direct Current Architecture Powers Building Loads Directly from Onsite Solar

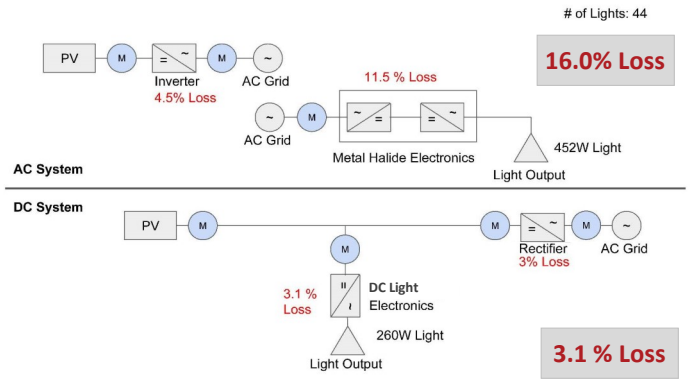

Utilization of Solar Energy Comparison

Equipment Installed

- Replacement of (44) 452W AC metal halide lights with 260W DC lights
- (4) 18' Diameter DC Ceiling Fans
- 150 kW rooftop solar array (15kW used for DC lighting & ventilation)
- DC Power-Server
- DC Distribution Panel
- Bosch Energy Management Gateway (EMG)
- Existing AC wiring infrastructure was utilized and converted it to DC.

The Technology

The Bosch DC microgrid system synchronizes onsite distributed generation (solar PV and energy storage) directly to energy-efficient building loads (DC lighting, ventilation, and motors) via a 380 V nominal DC network. This system eliminates the use of AC/DC rectifiers at the loads and reduces the need for DC/AC inverters that are currently required to interconnect solar PV to the electric utility.

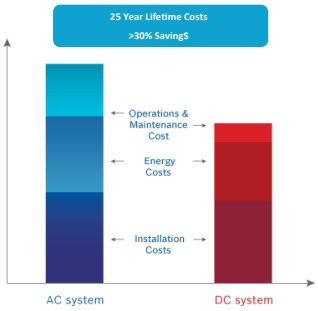

The reduction in power conversion equipment eliminates the most common points of failure in the system, making the overall system more efficient (7-10% increase in solar energy utilization as compared to a new state-of-the-art solar and lighting system) and reliable, therefore reducing maintenance costs that add up to greater than 30% savings over the 25 year life of the system.

Resiliency is provided by connecting critical DC loads during grid outages directly with the generation sources on the DC network, without requiring expensive transfer switch equipment.

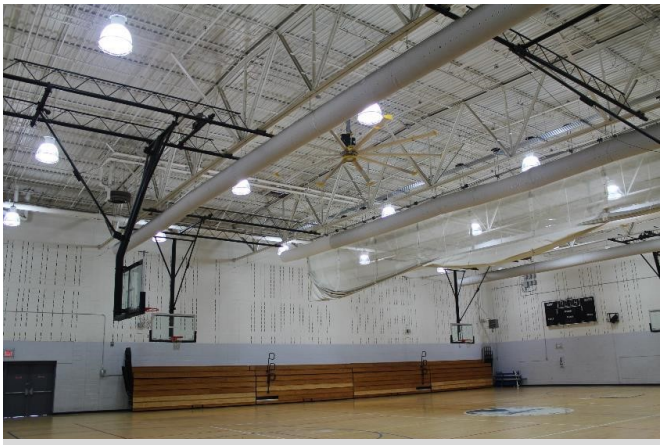

DC Lighting & Ventilation Fans

Conclusion

The Bosch DC microgrid system will save Fort Bragg over $125,000 in electricity costs over a 25 year life cycle. In addition, the long-life performance of DC components will also dramatically reduce the maintenance cost, during those years.

Upon completion of the project, the Army has engaged Bosch in an additional phase for the Hercules Fitness Center which will include the installation of DC HVAC units to be installed into the same DC Microgrid. The combined efficiency of both lighting and HVAC along with the resiliency of the DC Microgrid with battery storage will provide the most cost effective and reliable system for Fort Bragg for years to come

Bosch Building Grid Technologies
101 Jefferson Drive
Menlo Park, CA 94025
1-877-BOSCHDC (267-2432)

CS-001|6-2017

www.BoschBGT.com

Appendix G: NREL Analysis

Energy Savings Analysis for a Novel DC Microgrid Platform for High Bay Lighting Systems: Interim Report

Stephen Frank, Eric Bonnema, Jennifer Scheib, Eric Wilson

Produced under direction of Robert Bosch LLC by the National Renewable Energy Laboratory (NREL) under TSA 14-666 and Task No WTKB.1000.

NREL is a national laboratory of the U.S. Department of Energy
Office of Energy Efficiency & Renewable Energy
Operated by the Alliance for Sustainable Energy, LLC

This report is available at no cost from the National Renewable Energy Laboratory (NREL) at www.nrel.gov/publications.

Strategic Partnership Project Report
NREL/TP-5500-64014
June 2015

Contract No. DE-AC36-08GO28308

NREL
NATIONAL RENEWABLE ENERGY LABORATORY

Energy Savings Analysis for a Novel DC Microgrid Platform for High Bay Lighting Systems: Interim Report

Stephen Frank, Eric Bonnema, Jennifer Scheib, Eric Wilson

Prepared under Task No. WTKB.1000

NREL is a national laboratory of the U.S. Department of Energy
Office of Energy Efficiency & Renewable Energy
Operated by the Alliance for Sustainable Energy, LLC

This report is available at no cost from the National Renewable Energy Laboratory (NREL) at www.nrel.gov/publications.

National Renewable Energy Laboratory
15013 Denver West Parkway
Golden, CO 80401
303-275-3000 • www.nrel.gov

Strategic Partnership Project Report
NREL/TP-5500-64014
June 2015

Contract No. DE-AC36-08GO28308

NOTICE

Cover Photos by Dennis Schroeder: (left to right) NREL 26173, NREL 18302, NREL 19758, NREL 29642, NREL 19795.

NREL prints on paper that contains recycled content.

Acknowledgments

NREL developed this report under NREL Technical Services Agreement TSA-14-666 with funding from Robert Bosch LLC. NREL gratefully acknowledges the following individuals for their contributions to this report: Sharmila Ravula (Bosch) and Danny Fregosi (Bosch) for supplying performance data, reviewing the methodology, and providing valuable technical insight; Marjorie Schott (NREL) for creating the illustrations; Mike Heaney (NREL) for assistance with the uncertainty analysis; Shanti Pless (NREL) for assistance with model development and quality assessment; Kim Trenbath (NREL) for coordinating peer review and copy editing; Jay Burch (Mountain Energy Partnership) and Paul Holliday (Holliday Electrical Mechanical Engineering, pllc) for technical review; and Maureen McIntyre (McIntyre Communications, Inc.) for copy editing. Despite our reliance on the data and technical expertise provided by these individuals, the ultimate responsibility for the analysis findings rests with the authors of this report.

List of Acronyms

AC	alternating current
AC/DC	alternating current to direct current
ASHRAE	American Society of Heating, Refrigerating and Air-Conditioning Engineers
DC	direct current
DC/AC	direct current to alternating current
DCMG	direct current microgrid
DOE	U.S. Department of Energy
HVAC	heating, ventilation, and air conditioning
LED	light emitting diode
LPD	lighting power density
MATLAB	Matrix Laboratory
MPPT	maximum power point tracking
NREL	National Renewable Energy Laboratory
PV	photovoltaic
SAM	System Advisor Model
TMY3	Typical Meteorological Year version 3

Executive Summary

In today's high-efficiency commercial facilities, a large and growing portion of the building load uses direct current (DC) electricity internally rather than alternating current (AC). In a traditional AC power system, connecting local photovoltaic (PV) generation to local DC loads requires two energy conversion steps: inversion (DC/AC) at the PV array and rectification (AC/DC) at the DC load. Approximately 10% of PV energy is lost in these conversion stages.

In contrast, Robert Bosch LLC (Bosch) has developed an innovative DC microgrid (DCMG) platform for high bay lighting systems that drives light emitting diode (LED) fixtures directly from a local PV source without the need for a dedicated PV inverter (Figure ES-1).

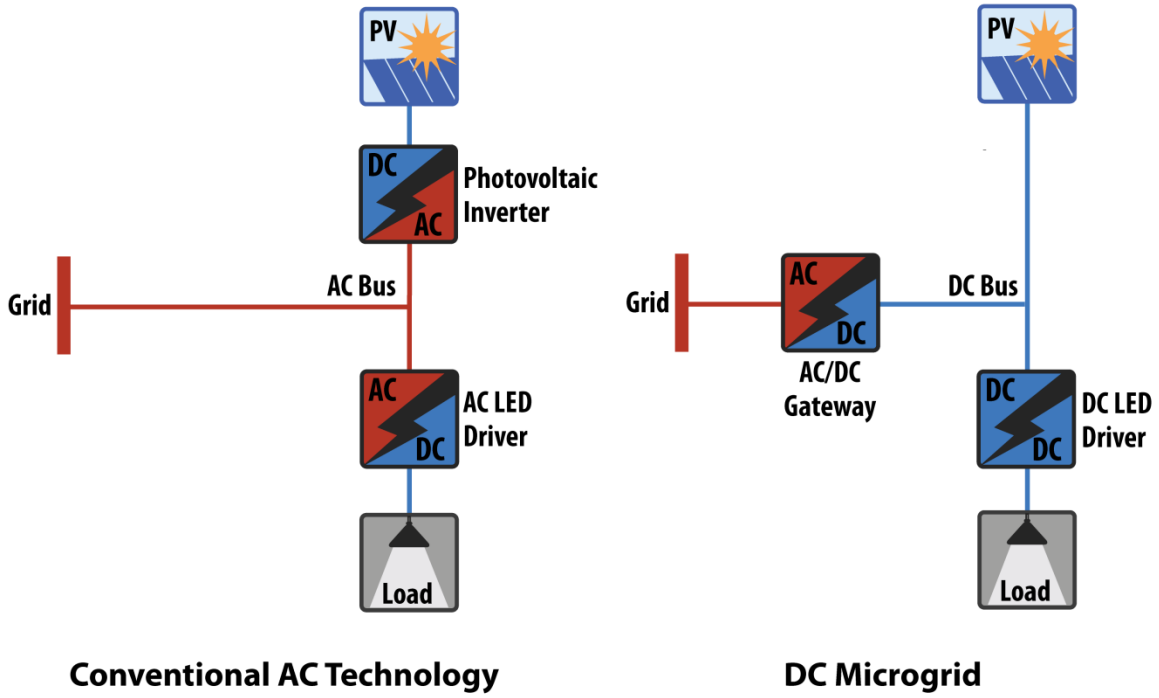

Figure ES-1. Comparison of traditional AC and Bosch DCMG system types
Illustration by Marjorie Schott, NREL

In the Bosch DCMG, a single, high efficiency DC/DC conversion significantly reduces the loss associated with PV-to-load energy transfer, and a separate AC/DC gateway converter supplies the balance of power required to operate the LED lighting load when local generation is insufficient, such as at night. There are two possible versions of the Bosch DCMG: a unidirectional version that uses connected PV to power local DC loads only and a bidirectional version that also enables export of surplus PV generation to the electric grid.

The National Renewable Energy Laboratory (NREL) performed a simulation study to analyze the energy performance of both the unidirectional and bidirectional versions of the Bosch DCMG in high bay LED lighting applications for several typical scenarios in various locations throughout the United States. In the analysis, NREL assumed a simple lighting system containing only a PV array, an LED lighting load, a DC LED driver, and an AC/DC gateway, as

illustrated in Figure ES-1. NREL simulated the performance this basic system in a variety of scenarios resulting from the combination of:

- *Four building types:* box retail, supermarket, refrigerated warehouse, and non-refrigerated warehouse
- *Five operating schedules:* 6 a.m.–10 p.m 5 days/week, 6 a.m.–10 p.m. 7 days/week, 8 a.m.–8 p.m. 7 days/week, 24 hours/day 5 days/week, and 24 hours/day 7 days/week
- *Two DCMG types:* unidirectional and bidirectional
- *Five PV array sizes:* 100%, 125%, 150%, 200%, and 250% of installed high bay lighting load capacity
- *554 geographic locations:* 544 in the contiguous United States and 10 in Hawaii.

The set of analysis cases (scenarios) examined was not an exhaustive combination of all these categories but rather a selective subset representing likely design cases. For each analysis case, NREL developed a baseline system model that represents conventional AC technology and an equivalent DC microgrid system model with identically sized PV generation and lighting load. NREL simulated the AC baseline and DC microgrid models for each geographic location and compared the systems' performance.

At present, no single simulation environment is well equipped to model both building energy performance and DC microgrids. Therefore, NREL developed a multistep simulation approach that combines three energy modeling tools: EnergyPlus for whole building energy simulation, System Advisor Model (SAM) for PV array simulation, and tailored MATLAB functions for electric power distribution system efficiency analysis. Simulation and energy analysis proceeded in four steps:

1. *Development of seed models:* NREL created building and PV array seed models for each combination of building type, operating schedule, and PV array size.
2. *Baseline simulation:* NREL applied site-specific adjustments and simulated each seed model at each of the 554 geographical locations.
3. *Performance comparison of distribution systems:* Using the results from the baseline simulations, NREL developed site-specific models for the AC baseline and DC microgrid distribution systems, then simulated both system types for each analysis case.
4. *Evaluation of whole building impact:* Using the results of the distribution system energy analysis, NREL evaluated the whole building energy impact of the high bay lighting system for both system types.

NREL computed eight key performance metrics for each simulated case:

1. *High bay lighting system grid energy intensity:* the net annual electricity consumption of the high bay lighting system normalized by the floor area
2. *High bay lighting system energy efficiency:* the ratio of total output (load) energy to total input (source) energy, including energy from both the electric grid and the PV array

3. *High bay lighting system PV utilization fraction:* the fraction of PV energy that is either delivered to the load or exported to the electric grid
4. *High bay lighting system grid utilization fraction:* the fraction of grid energy that is delivered to the load
5. *Site change in electricity intensity:* change in net annual site electricity consumption for the Bosch DCMG compared to the AC baseline, normalized by floor area
6. *Site change in natural gas intensity:* change in annual site natural gas consumption for the Bosch DCMG compared to the AC baseline, normalized by floor area
7. *Site change in total energy intensity:* change in total net annual site energy consumption for the Bosch DCMG compared to the AC baseline, normalized by floor area.
8. *Site change in monthly peak demand:* change in monthly peak electricity demand for the Bosch DCMG compared to the AC baseline, normalized by floor area.

Figures ES-2 through ES-4 summarize the analysis results for each metric. The results show that for buildings with continuous daily operation (seven days per week) the Bosch DCMG significantly improves the energy performance of the Bosch high bay LED lighting system compared to an AC baseline with equivalent LED light fixtures. The Bosch DCMG improved the fraction of PV energy that performs useful work from approximately 0.90 for the AC baseline to approximately 0.97 for the Bosch DCMG and improved lighting system annual energy efficiency from approximately 92% for the AC baseline to approximately 95% for the Bosch DCMG, with small variations in response to design parameters and operating conditions.

In addition, the Bosch DCMG indirectly benefits buildings by reducing cooling load and, if applicable, refrigeration load compared to the AC baseline. The Bosch DCMG reduces cooling load in two ways: it reduces overall waste energy from the lighting system and it shifts a portion of the waste energy from conditioned to unconditioned space. The reductions were most significant in hot, humid climates. Conversely, the loss of waste heat in the winter increased site natural gas consumption compared to the AC baseline, with the greatest increases in cold climates. In nearly all locations, the net indirect impact of the Bosch DCMG on site HVAC energy was a reduction of site energy compared to the AC baseline, with the strongest reductions in hot, humid, and sunny climates. The Bosch DCMG also reduced building monthly peak electricity demand in nearly all cases. The magnitude of this reduction varied significantly by building type, operating schedule, time of year, and geographic location.

The Bosch bidirectional DCMG, which allows export of surplus PV energy, performed well for all array sizes, building types, and building operating schedules. In contrast, the Bosch unidirectional DCMG performed well only for system designs and building operating schedules that did not result in significant curtailment of PV production; the Bosch unidirectional DCMG did not perform well for buildings with five days per week operation or buildings with significantly oversized PV systems relative to the connected lighting load.

More broadly, this analysis supports the larger body of evidence that DC distribution systems in commercial buildings can produce significant energy savings. In principle, building-scale DC microgrids are not limited to lighting products. The energy savings are worth investigating for

other DC load types, including telecommunication equipment, variable frequency motor drives, and consumer electronic loads.

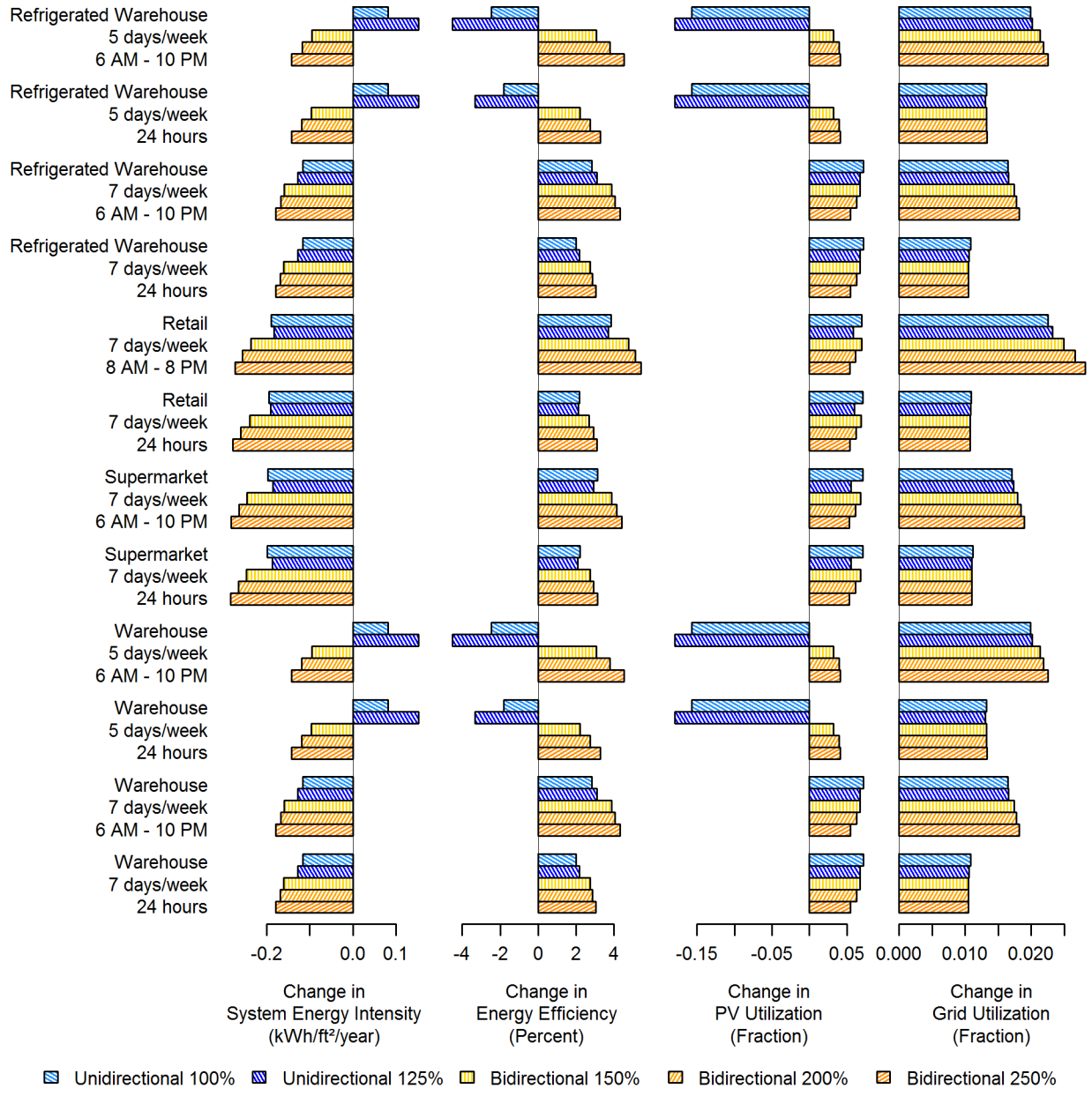

Figure ES-2. Average change in lighting system metrics Bosch DCMG compared to AC Baseline

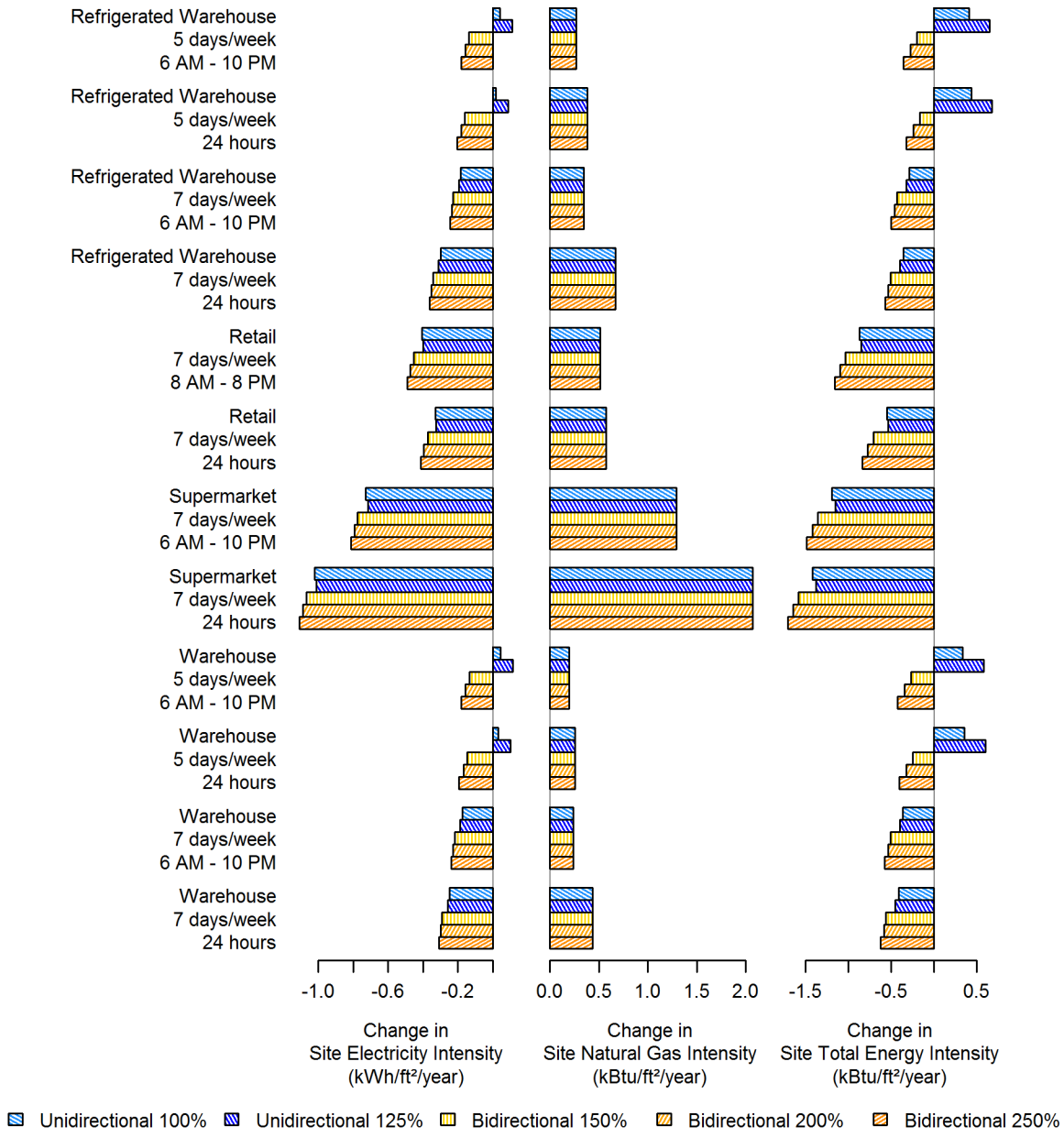

Figure ES-3. Average change in site energy metrics
Bosch DCMG compared to AC Baseline

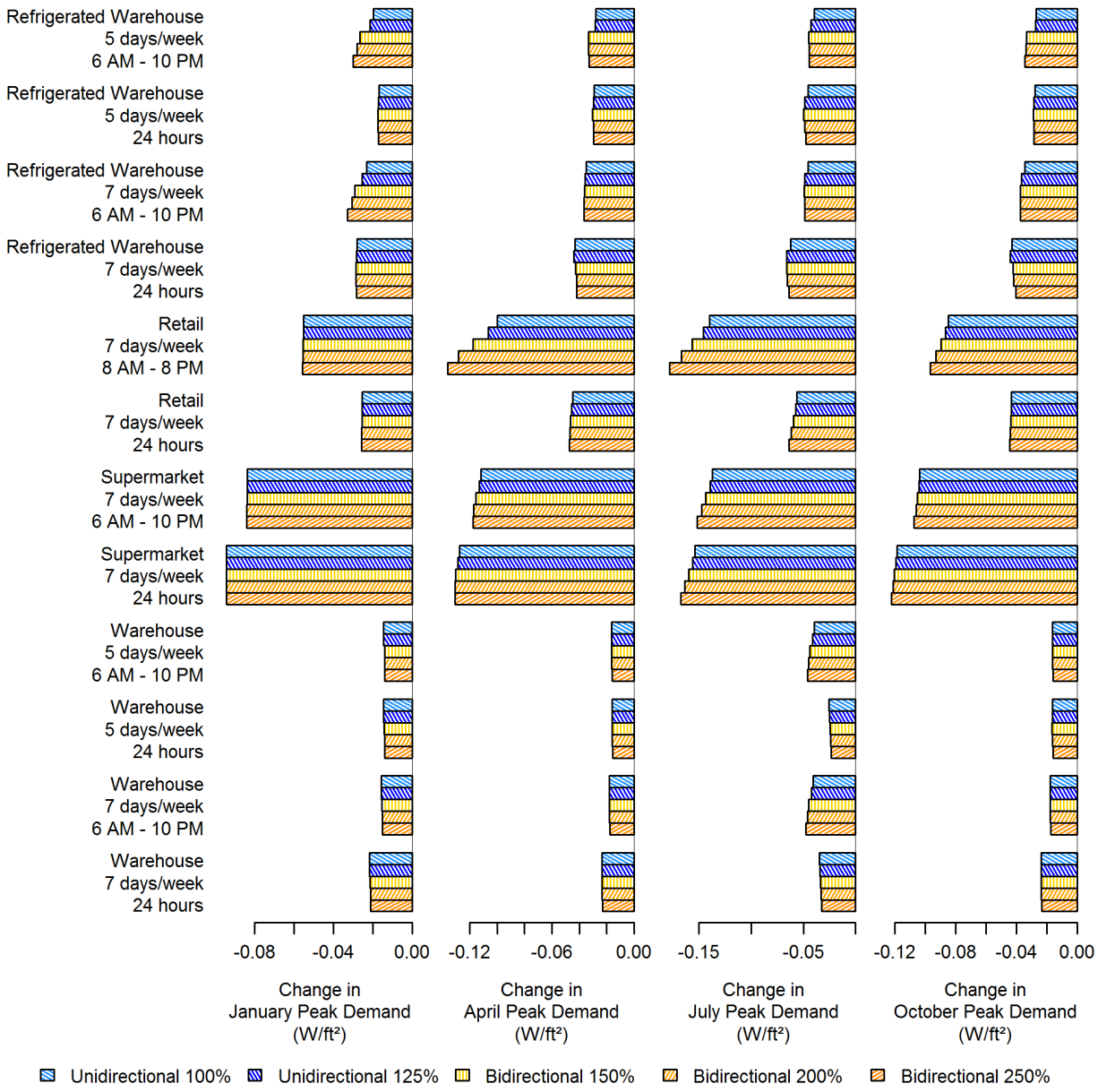

Figure ES-4. Average change in site monthly peak electricity demand
Bosch DCMG compared to AC Baseline

Table of Contents

List of Figures

List of Tables

1 Introduction

In today's high-efficiency commercial facilities, a large and growing portion of the building load uses direct current (DC) electricity internally rather than alternating current (AC). Examples of DC-internal loads include high-efficiency fluorescent and light emitting diode (LED) lighting, variable frequency drives for motors, consumer electronics, and computing equipment. Connecting these DC loads to the conventional AC electric grid requires AC/DC power conversion, also known as rectification. Typically, rectification occurs at the point of use: AC is distributed to each individual load and each load contains its own rectifier.

Building-level DC distribution systems, also termed DC microgrids (DCMG), have been proposed as a high-efficiency alternative to AC distribution (Savage, Nordhaus, and Jamieson 2010; AlLee and Tschudi 2012), in particular when integrating DC-native distributed energy sources, such as photovoltaic (PV) arrays. Integrating DC sources with DC loads via a DCMG replaces two inefficient power conversion stages, inversion (DC/AC) at the DC source and rectification (AC/DC) at the load, with one or more high-efficiency DC/DC conversions that match voltages between sources and loads.[1] When load exceeds local generation, a central high-efficiency rectifier procures the balance of power from the electric grid.

Recently, several companies have commercialized DCMG systems that conform to the voluntary DC distribution standards developed by the EMerge Alliance (EMerge Alliance 2012) . In particular, Robert Bosch LLC (Bosch) has developed an innovative DCMG platform for high bay lighting systems that drives LED fixtures and other DC loads directly from a local PV source without the need for a dedicated PV converter. Bosch intends to market two versions of this system: a unidirectional version that uses connected PV to power local DC loads only and a bidirectional version that also enables export of surplus PV generation to the electric grid.

Bosch commissioned the National Renewable Energy Laboratory (NREL) to perform a simulation study to analyze the energy performance of both versions of the Bosch DCMG for several typical scenarios in various locations throughout the United States. This report presents the study results. The remainder of this section provides the project motivation, the technology description, and the scope of the analysis. Section 2 discusses the modeling methodology and Section 3 summarizes the analysis results. Section 4 gives the conclusions and discusses future work. The report appendices include details of the model inputs and geographical maps of the Bosch DCMG performance for various analysis cases.

1.1 Technology Description

The Bosch DCMG platform consists of a DC bus with a directly-connected PV array, a set of loads connected via DC/DC converters, and a central AC/DC gateway that provides the balance of power from the electric grid (Figure 1). This arrangement, which is patented by Bosch, accommodates energy transfer from PV to load with only a single conversion step. The DC bus operates at a nominal voltage of 380 VDC, but may float to accommodate maximum power point tracking (MPPT) for the PV array. The gateway converter, which is not in the path of energy

[1] All else being equal, DC/DC conversion is inherently more efficient that AC/DC conversion (either rectification or inversion) because DC/DC conversion requires fewer power processing stages and operates at a small average current for the same power output.

transfer from PV to load, nevertheless achieves MPPT via DC bus voltage control by minimizing the balance of power required from the electric grid.

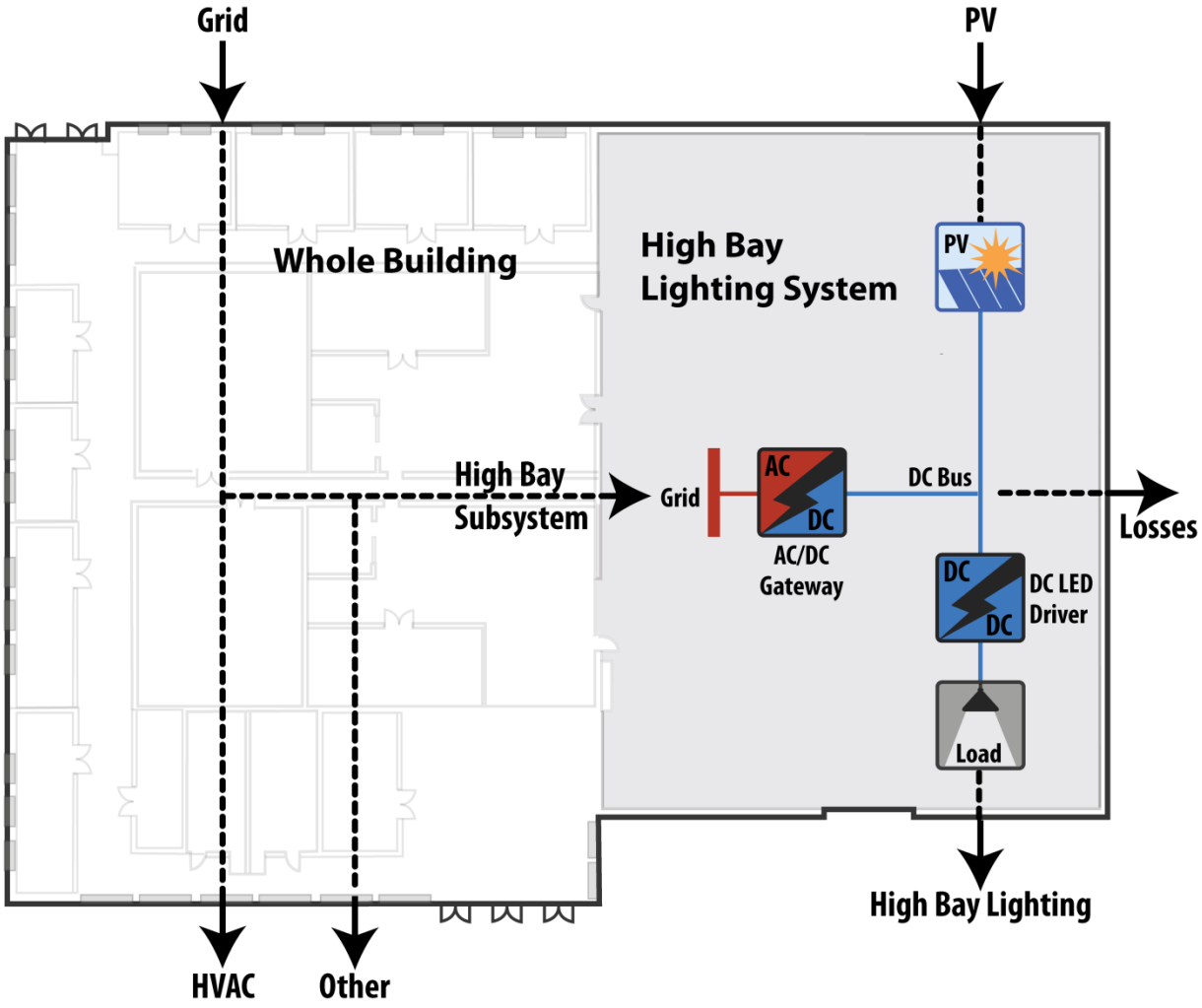

Figure 1. Bosch DC microgrid solution for high bay lighting systems
Illustration by Marjorie Schott, NREL

Bosch is developing both unidirectional and bidirectional versions of the Bosch DCMG platform. In the unidirectional version, the gateway converter supplements the PV generation with energy from the grid in order to meet the load but cannot export energy to the grid. In the bidirectional version, the gateway converter can accommodate two-way energy transfer, enabling the export of surplus PV energy. The bidirectional version mitigates the risk of PV curtailment in the event of low load.

In principle, the Bosch DCMG platform is applicable to any building system with significant DC load that is coincident with PV generation. However, Bosch's product offerings (LED lighting fixtures and DC fans) presently focus on high bay applications. Therefore, the Bosch DCMG platform is most applicable to building types with large high bay spaces and near-continuous daytime lighting loads, including "box" retail stores, supermarkets, and both refrigerated and non-refrigerated warehouses.

1.2 Motivation

In a traditional AC power system, connecting PV generation to DC loads requires two conversion steps: inversion (DC/AC) at the PV array and rectification (AC/DC) at the DC load. Replacing these two power conversion steps with a single, high efficiency DC/DC conversion significantly reduces the loss associated with PV-to-load energy transfer (Figure 2).

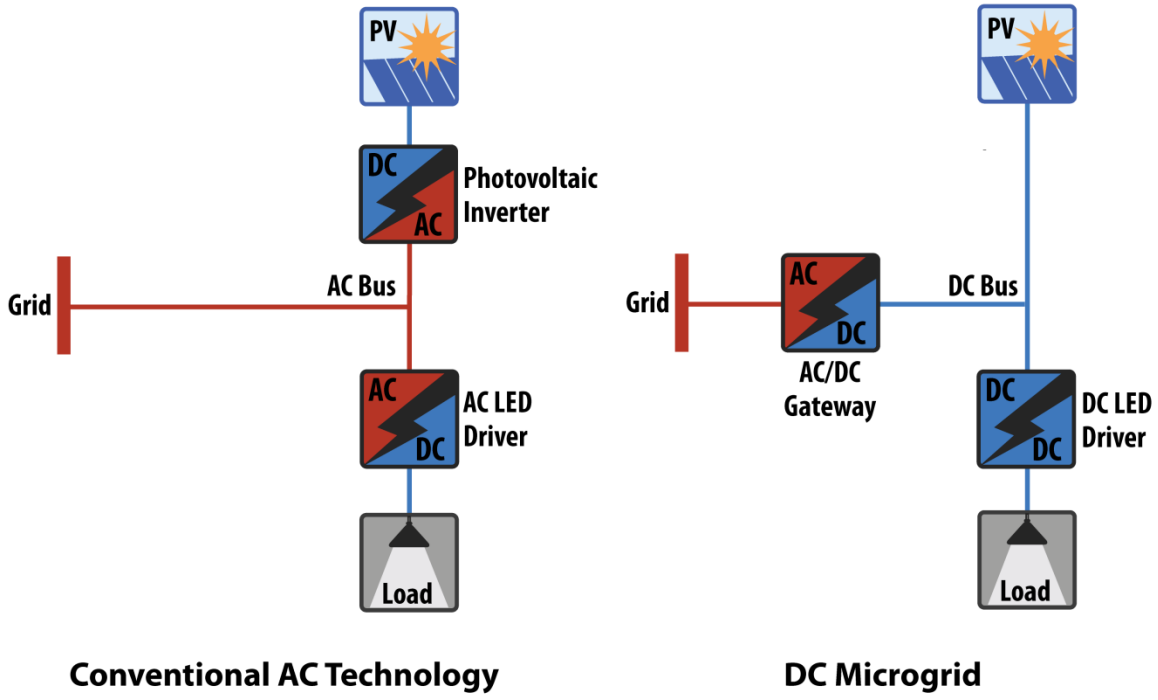

Figure 2. Comparison of traditional AC and Bosch DCMG system types
Illustration by Marjorie Schott, NREL

Consider a simple, fixed efficiency model for a traditional AC system with PV inverter efficiency η_{PV} and AC LED driver efficiency $\eta_{\text{LED,AC}}$. At full load, the driver used in Bosch AC LED high bay lighting fixtures has an efficiency $\eta_{\text{LED-AC}} \approx 93.7\%$, while a typical high-efficiency PV inverter has an efficiency $\eta_{\text{PV}} \approx 97\%$. Thus, the composite efficiency for PV-to-load energy transfer in the system is:

$$\text{AC Baseline PV-to-load Efficiency} \approx \eta_{\text{PV}}\eta_{\text{LED-AC}} \approx 91\%$$

In contrast, in the Bosch DCMG under development, the DC LED driver has a projected full load efficiency $\eta_{\text{LED-DC}} \approx 97.7\%$—a 6.7% improvement in PV-to-load energy transfer efficiency. This estimate aligns well with observed PV-to-load performance gains at first-generation Bosch DCMG demonstrations supplying induction lighting fixtures in Plymouth, Michigan, and Charlotte, North Carolina, where instantaneous measurements have shown 7% to 10% more efficient use of PV energy compared to a similarly sized, co-located AC baseline system.

PV-to-load energy transfer is not the only energy transfer in the system, however. The connection to the AC electric grid supplies the balance of power required to operate the LED lighting load when PV generation is insufficient, such as at night. At first glance, the two converters used in the Bosch DCMG for grid-to-load energy transfer appear less efficient than the single converter in the traditional AC system. In practice, however, the Bosch DCMG allows separation of the rectification stage from the DC/DC conversion that occurs in the DC LED driver, such that both conversion stages exhibit high efficiency.

For example, in the Bosch DCMG under development, the gateway rectifier has a projected full load efficiency of $\eta_{\text{Gateway}} \approx 97.0\%$, resulting in a composite grid-to-load efficiency of:

$$\text{Bosch DCMG Grid-to-load Efficiency} \approx \eta_{\text{Gateway}}\eta_{\text{LED-DC}} \approx 94.8\%$$

Thus, the projected Bosch DCMG composite grid-to-load efficiency still exceeds the 93.7% efficiency of the Bosch AC LED driver.

Given annual DC PV energy production E_{PV} and annual DC lighting load energy E_{Load}, which are identical for the two system types, this simple model allows estimation of the energy savings associated with Bosch DCMG operation. In the AC case, the net annual grid energy is:

$$E_{\text{Grid-AC}} \approx \frac{E_{\text{Load}}}{\eta_{\text{LED-AC}}} - \eta_{\text{PV}}E_{\text{PV}}$$

In the Bosch DCMG, the net annual grid energy is:

$$E_{\text{Grid-DC}} \approx \frac{\left(\frac{E_{\text{Load}}}{\eta_{\text{LED-DC}}} - E_{\text{PV}}\right)}{\eta_{\text{Gateway}}}$$

Consider a hypothetical 100,000 ft^2 retail store with an average high bay lighting DC power density of 1.0 W/ft^2 located in Detroit, MI (near the site of Robert Bosch LLC's DCMG test facility in Plymouth, MI). This hypothetical facility has a connected DC lighting load of 100 kW. If the PV array is sized to match the lighting load, then, given the average irradiance in Detroit, the approximate annual PV energy production is:

$$E_{\text{PV}} \approx (100\text{ kW})(4.0\text{ sun-hours/day})(365\text{ days/year}) = 146\text{ MWh/year}$$

If the store operates 12 hours per day every day, the approximate annual lighting load energy is:

$$E_{\text{Load}} \approx (100\text{ kW})(12\text{ hours/day})(365\text{ days/year}) = 438\text{ MWh/year}$$

Under the simple, fixed-efficiency model,

$$E_{\text{Grid-AC}} \approx \frac{438\text{ MWh/year}}{0.937} - 0.970 \cdot 146\text{ MWh/year} = 325.8\text{ MWh/year}$$

$$E_{\text{Grid-DC}} \approx \frac{\left(\frac{438\ \text{MWh/year}}{0.977} - 146\ \text{MWh/year}\right)}{0.970} = 311.7\ \text{MWh/year}$$

$$E_{\text{Savings}} \approx E_{\text{Grid-AC}} - E_{\text{Grid-DC}} = 14.1\ \text{MWh/year}$$

For this hypothetical store, the anticipated savings from using a Bosch DCMG for the high bay lighting system are 14.1 MWh/year, or 0.14 kWh/ft^2/year.

Although these figures are promising, the simple model considered above does not address many phenomena which affect real systems, such as:

- Reduced converter efficiencies at partial loading
- Curtailment of PV energy due to over-generation or low load conditions
- Use of bidirectional gateway converters to export surplus PV energy
- The effect of DC voltage on converter efficiency
- Performance degradation associated with non-ideal converter sizing
- The impact of LED driver efficiency on facility cooling and heating load.

The motivation for this study is to predict and analyze the performance of the Bosch DCMG using a detailed model that incorporates these phenomena, such that the benefits of the Bosch DCMG may be quantified in detail for various scenarios, including for other building applications, in locations throughout the United States, and for various DCMG configurations (type of gateway converter and total PV array size).

1.3 Analysis Scope

In this study, NREL analyzed the performance of the Bosch DCMG in high bay lighting applications in a variety of scenarios resulting from the combination of:

- *Four building types:* box retail, supermarket, refrigerated warehouse, and non-refrigerated warehouse
- *Five operating schedules:* 6 a.m.–10 p.m 5 days/week, 6 a.m.–10 p.m. 7 days/week, 8 a.m.–8 p.m. 7 days/week, 24 hours/day 5 days/week, and 24 hours/day 7 days/week
- *Two DCMG types:* unidirectional and bidirectional
- *Five PV array sizes:* 100%, 125%, 150%, 200%, and 250% of installed high bay lighting load capacity
- *554 geographic locations:* 544 in the contiguous United States and 10 in Hawaii.

The set of analysis cases (scenarios) is not an exhaustive combination of all these categories but rather a subset. Table 1 displays the combinations of building type and operating schedule selected for simulation and Table 2 displays the combinations of DCMG type and PV array size. NREL simulated each identified combination of building type + operating schedule and DCMG type + PV array size at each of the 554 geographic locations.

Table 1. Combinations of Building Type and Operating Schedule Selected for Simulation

Building / Schedule	Retail	Supermarket	Refrigerated Warehouse	Non-Refrigerated Warehouse
6 a.m.–10 p.m. 5 days/week			✓	✓
6 a.m.–10 p.m. 7 days/week		✓	✓	✓
8 p.m.–8 p.m. 7 days/week	✓			
24 hours/day 5 days/week			✓	✓
24 hours/day 7 days/week	✓	✓	✓	✓

Table 2. Combinations of DCMG Type and PV Array Size Selected for Simulation

Array Size[a] / DCMG Type	100%	125%	150%	200%	250%
Unidirectional DCMG	✓	✓			
Bidirectional DCMG			✓	✓	✓

[a] Nominal array size relative to total installed high bay lighting load

For each analysis case, NREL developed a baseline system model using conventional AC LED technology and an equivalent Bosch DCMG system model with identically sized PV generation and lighting load. NREL simulated the AC baseline and Bosch DCMG models for each geographic location and computed eight key performance metrics from the results:

1. High bay lighting system grid energy intensity
2. High bay lighting system energy efficiency
3. High bay lighting system PV utilization fraction
4. High bay lighting system grid utilization fraction
5. Site change in electricity intensity
6. Site change in natural gas intensity
7. Site change in total energy intensity
8. Site change in monthly peak demand.

(Section 2.3 provides the mathematical definitions for these metrics.) NREL developed geographic performance maps for both the AC baseline and Bosch DCMG system types for the first four metrics, as well as geographic performance comparison maps for all eight metrics.

2 Methodology

At present, no single simulation environment is well equipped to model both building energy performance and DC microgrids. Therefore, NREL developed a multistep simulation approach that combines three energy modeling tools:

EnergyPlus for whole building energy simulation

System Advisor Model (SAM) for PV array simulation

Tailored *matrix laboratory* (*MATLAB)* functions for electric power distribution system efficiency analysis

Prior to developing the analysis workflow, NREL defined a standard evaluation framework for comparative analysis of AC and DC electric power distribution systems (Section 2.1). Simulation and energy analysis then proceeded in four major steps:

1. *Development of seed models:* NREL developed seed models for each combination of building type, operating schedule, and PV array size using a variety of input data. Sections 2.2.1 and 2.2.2 describe the resulting EnergyPlus building models and SAM PV models, respectively.
2. *Baseline simulation:* For each seed model, NREL performed site-specific design adjustments and simulated the model at each of the 554 geographical locations. The outcome of this process was a full set of input data for use in the distribution system efficiency analysis. Again, Sections 2.2.1 and 2.2.2 describe this process for the building models and PV models, respectively.
3. *Performance comparison of distribution systems:* Using the results from the baseline simulations, NREL developed site-specific models for the AC baseline and Bosch DCMG distribution systems types (Section 2.2.3). To ensure a fair comparison, the DC PV generation and DC load in each analysis case are identical for the AC baseline and Bosch DCMG. NREL then simulated the energy performance of both system types for each analysis case and computed energy metrics for the high bay lighting system (Section 2.3).
4. *Evaluation of whole building impact:* Using the results of the distribution system energy analysis, NREL evaluated the whole building energy impact of the high bay lighting system for both the AC baseline and Bosch DCMG distribution system types. In the AC baseline case, the baseline building simulation data was suitable for reuse without modification. For the Bosch DCMG, NREL modified the building models to reflect the Bosch DCMG system performance and re-simulated each building model as described in Section 2.2.1. The final results are summarized in site energy intensity metrics (Section 2.3.5) and site electricity demand metrics as described in (Section 2.3.6).

Figure 3 illustrates the analysis workflow.

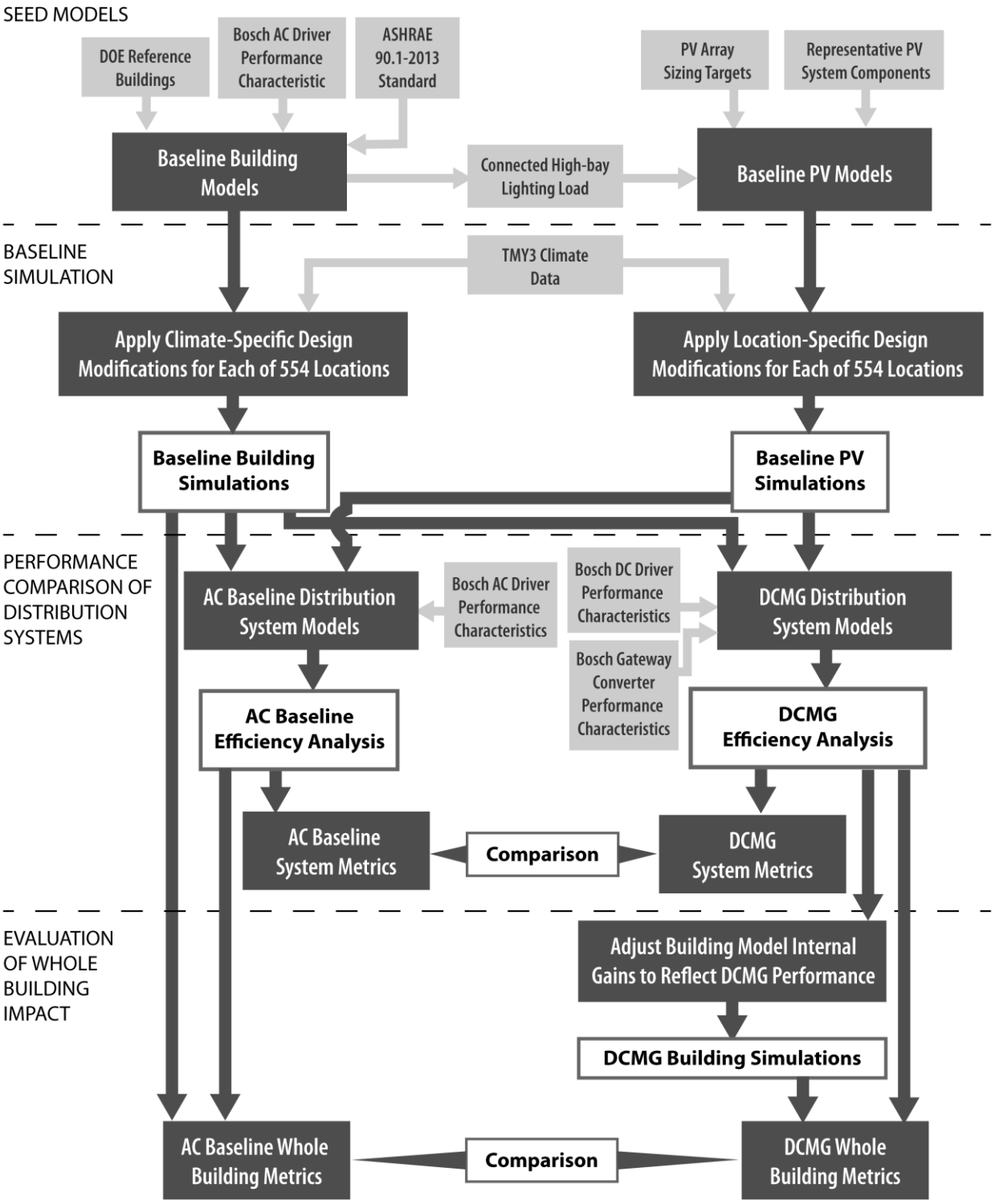

Figure 3. Simulation workflow for Bosch DCMG analysis
Illustration by Marjorie Schott, NREL

NREL selected the geographic locations for the analysis to illustrate the impact of climate on system performance throughout the contiguous United States and the state of Hawaii. The National Solar Radiation Data Base maintains a set of Typical Meteorological Year version 3 (TMY3) weather data files for 1,020 climate sites throughout the United States (Wilcox and Marion 2008). From this master set, NREL used a reduced set of 544 sites within the 48 contiguous states with high data quality and reduced geographic redundancy (Lopez 2015) as well as 10 TMY3 sites in Hawaii, for a total of 554 sites (Figure 4).

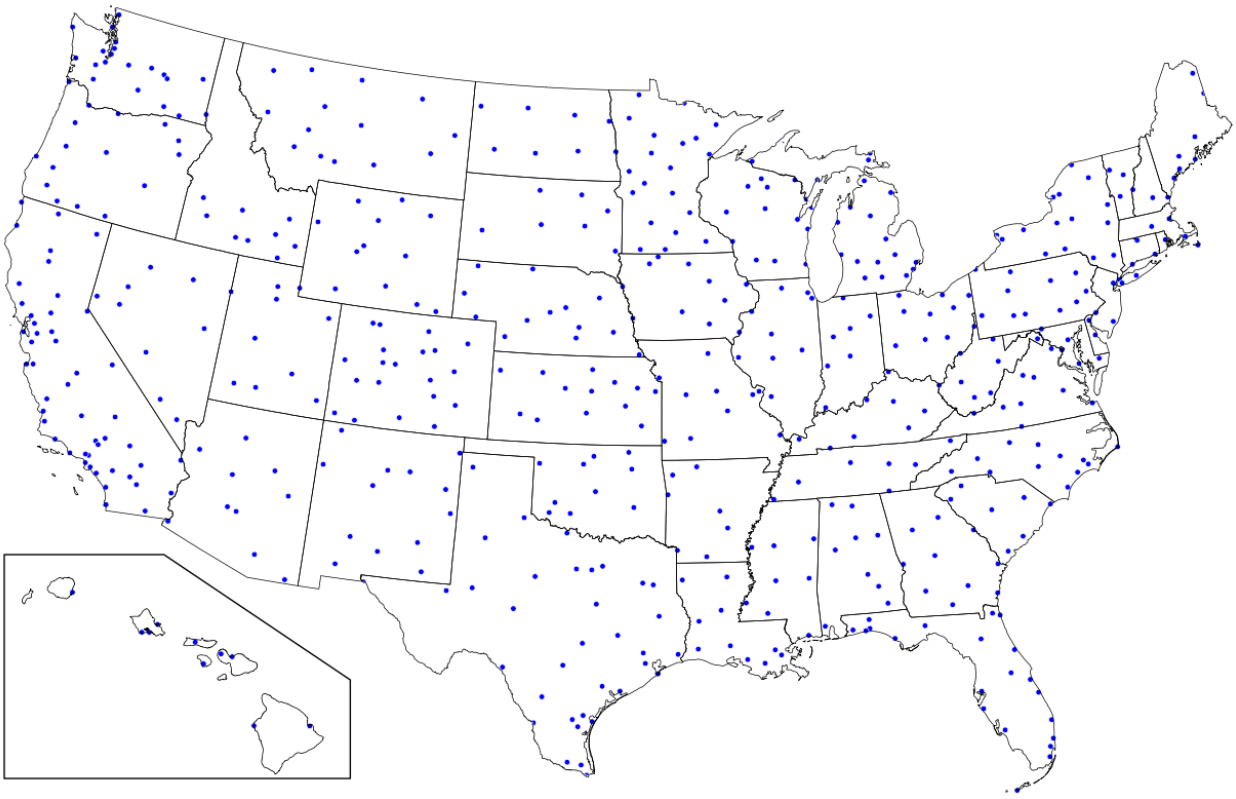

Figure 4. TMY3 climate sites selected for geospatial mapping
Illustration by Eric Wilson, NREL

This report summarizes the analysis results at these weather sites using color-coded geographic maps of system performance. Section 2.4 describes the development of these maps.

2.1 Evaluation Framework

An unbiased comparison of energy performance between conventional AC technology and an equivalent DCMG system requires that the definitions of energy inputs and outputs are consistent between the two system types. For this purpose, NREL researchers adopted a generic conceptual representation of a building electric power distribution network that contains a PV source, a DC load, and a connection to the electric grid (Figure 5).

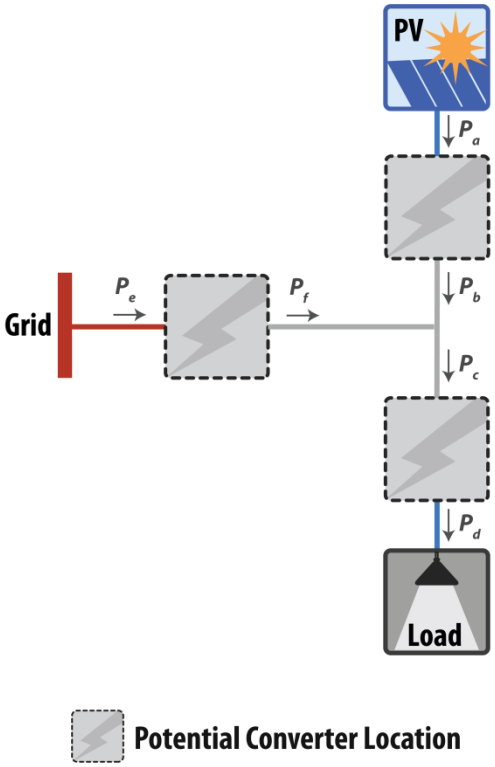

Figure 5. Conceptual representation of a building electric power distribution network with local PV generation, DC load, and grid interconnection
Illustration by Marjorie Schott, NREL

There are three possible converter locations identified in the figure: at the PV source, at the load, and at the grid interconnection.[2] The wiring between these converters may be either AC or DC depending on the system configuration. In addition, the figure identifies six power measurement points P_a–P_f, one on each side of each of the three converters. The PV source and grid measurements use the source convention (positive for power supplied), while the load measurements use the load convention (positive for power consumed).

As defined, the system boundaries include any losses that may vary with the choice of distribution system but excludes losses that occur outside the local scope of the distribution system, such as device-internal electrical or mechanical losses. This approach is best practice for comparing AC and DC distribution systems (Frank and Rebennack 2015). Power P_a is the gross PV generation after subtracting array losses (soiling, shading, mismatch, etc.) but before power conversion losses associated with a PV inverter or DC/DC converter. Similarly, P_e measures the AC input power to the local network and excludes distribution system losses upstream of the point of interconnection.

Depending on the selection and configuration of converters, the generic network of Figure 5 may represent either a conventional AC system or the Bosch DCMG (Figure 6).

[2] In a physical implementation of any particular network design, there may be zero, one, or multiple converters at each identified converter location, but conceptually they are lumped together and analyzed as a single converter.

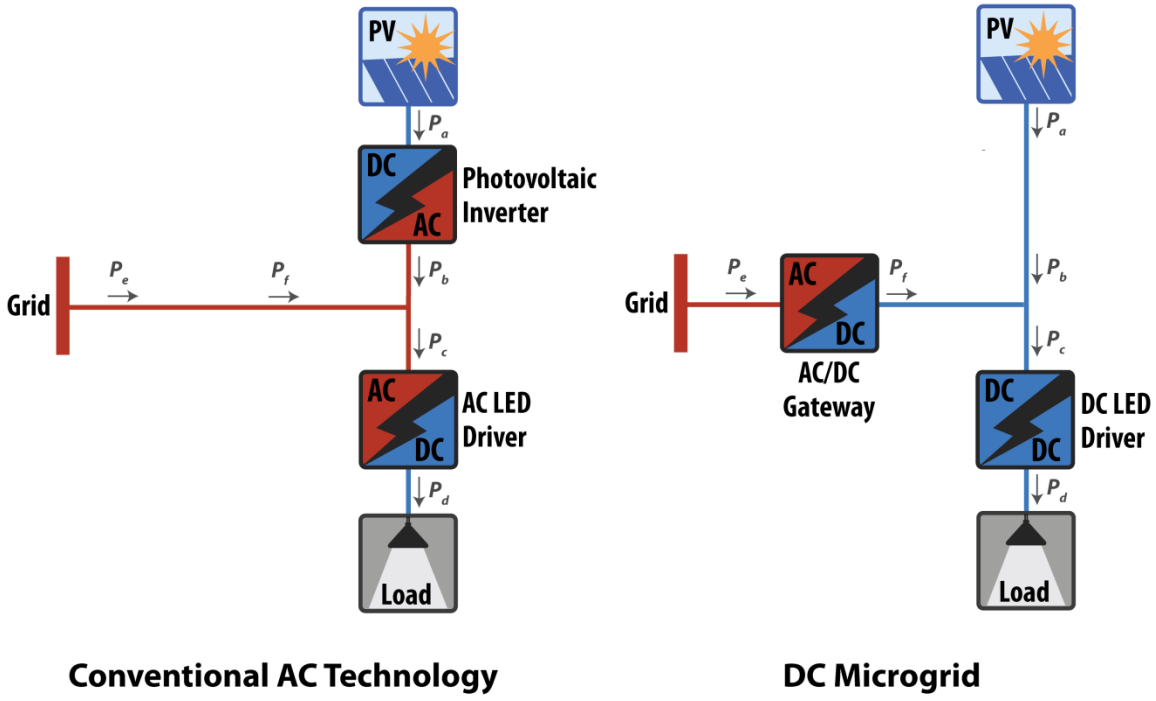

Figure 6. Power flow definitions for AC baseline and Bosch DCMG system types
Illustration by Marjorie Schott, NREL

In the AC case, there is no central AC/DC converter and $P_e = P_f$. The PV system uses a conventional PV inverter and the load uses an AC driver. In the Bosch DCMG case, there is instead no converter at the PV source and therefore $P_a = P_b$ (except in cases of curtailment; see below). A DC driver matches voltage between the PV source and the lighting load, and a central, or gateway, AC/DC converter provides the balance of power.

Curtailment represents a special case for the Bosch DCMG in which $P_b < P_a$. Curtailment occurs if the available generation exceeds the combined load demand and export capacity of the gateway inverter. In such cases, the model represents the curtailed energy conceptually as a system loss between points a and b.

2.2 Models

Calculating the system power flows requires three inputs:

1. High bay lighting load pre- or post-converter (P_c or P_d) at each simulation time step
2. PV array power generation pre- or post-converter (P_a or P_b) at each simulation time step
3. An electric power distribution system model including converter models for the LED driver, PV inverter, and/or gateway converter, as appropriate.

EnergyPlus models for each building type / operating schedule combination provide the high bay lighting load (Section 2.2.1), and SAM models for each building type / PV array size combination provide the PV array generation data (Section 2.2.2). To compute the energy

performance of the high bay lighting system for each analysis case, NREL combined these data using customized electric power distribution models developed in MATLAB (Section 2.2.3).

2.2.1 Building Models

NREL selected EnergyPlus (EnergyPlus 2013) as the simulation tool for the building energy models. EnergyPlus is a thermal load simulation and energy analysis program that models the physical interactions of building energy systems, including heat transfer; internal heat gains from occupants and equipment; and heating, ventilation, and air conditioning system performance. Each EnergyPlus release is heavily tested and formally validated using BESTEST validation methods (Judkoff and Neymark 1995).

NREL selected a subset of the U.S. Department of Energy (DOE) Commercial Reference Building Models (Deru et al. 2011) to provide prototypes for the four building types identified in Section 1.3. The DOE Commercial Reference Building Models are standard or reference energy models for the most common commercial building types and serve as starting points for energy efficiency research. The complete set includes fifteen commercial building types and one multifamily residential building and represents approximately two-thirds of the national commercial building stock. Each model is provided as an EnergyPlus input description file.

The Commercial Reference Building Models were developed by consensus between DOE, NREL, Pacific Northwest National Laboratory, and Lawrence Berkeley National Laboratory. The input parameters came from several sources. Some were obtained from ANSI/ASHRAE/IES Standards 90.1-2004, 62.1-2004, and 62.1-1999; others were determined from studies of data and standard practices. Although the models represent reasonably realistic building characteristics and construction practices, they are not intended to represent the energy use of any particular building nor are they intended to act as targets against which to rate the energy performance of single existing or proposed buildings. Rather, they are hypothetical models with ideal operations that illustrate typical performance characteristics for general building categories. The models may be used to assess new technologies; optimize designs; analyze advanced controls; develop energy codes and standards; and conduct lighting, daylighting, ventilation, and indoor air quality studies. The models also provide consistency in modeling approaches and implementation across commercial building types.

In consultation with Bosch, NREL selected three building types from the Commercial Reference Building set: stand-alone retail, supermarket, and warehouse. These building types are the most likely to employ high bay lighting and are therefore most applicable for the analysis. To represent recently constructed buildings, NREL selected the “New 2004” (ASHRAE 90.1-2004) model vintage for each building type. In addition, NREL made several modifications to the reference models:

- Added walk-in refrigeration to the standard warehouse model to derive a refrigerated warehouse model
- Scaled stand-alone retail building from 24,692 ft² to 98,769 ft² to better represent large, or “big box,” retail stores
- Simplified schedules and adjusted operating hours to correspond with the combinations identified in Table 1

- Modified holiday schedules to be more typical of each selected operating schedule, with only three holidays for buildings with seven days per week operation.

Appendix A provides additional detail about these modifications.

The Commercial Reference Building Model set includes separate energy models for representative cities within each of the 15 climate zones and subzones in the United States. Each model is tailored to its respective climate zone based on applicable building codes. For instance, buildings in colder climates require higher levels of insulation. For each selected building type, NREL used the 15 seed models to create location-specific models at each of the 554 geographic locations identified for simulation. These modifications included setting the model's geographic coordinates and elevation, altering the assumed design conditions to match the location, and modifying equipment sizes to match the location's design conditions; details are in Appendix A.

Finally, NREL updated space-by-space lighting power densities (LPDs) from ASHRAE standard 90.1-2004 to ASHRAE standard 90.1-2013, then further modified the LPDs in the high bay spaces to represent the performance of an AC LED high bay lighting solution over a typical standard-compliant solution. The AC baseline and Bosch DCMG system models use identical LED fixtures; the system lighting load differs only in the type of LED driver employed (AC or DC). This approach therefore isolates the energy impact of the Bosch DCMG itself from the broader impact of replacing typical light fixtures with energy efficient LED fixtures.

Table 3 documents the typical, standard-compliant LPD assumed for each space type used in the retail, supermarket, and warehouse models and the fractional multipliers that define the Bosch AC baseline LED LPD in relation to the typical value.[3] The refrigerated and non-refrigerated warehouse models use the same values. Details regarding the development of the LPDs are provided in Appendix A.

[3] NREL used a mid-bay LED fixture (as opposed to a true high-bay fixture) as the reference for LED fixture efficacy. The mid-bay selection was made because it is the more appropriate design choice for both the supermarket and stand-alone retail models. The mid-bay fixture has a lower efficacy than a high-bay fixture, which results in a more conservative energy savings estimate for the LED retrofit. However, the adjective "high-bay" is used throughout the report because it is a more common term and because it is descriptive of the intended application of the Bosch DCMG platform.

Table 3. Typical LPDs and LPD Multipliers for Bosch AC LED Replacement Fixtures

		Typical Fixture (ASHRAE 90.1-2013)			*Replacement Fixture (Bosch LED)*		
Building Type	**Zone**	**Type**	**LPD**	**Efficacy**	**Type**	**Efficacy**	**LPD Multiplier**
Retail	Back space	Fluorescent industrial strip	0.63 W/ft²	81 lm/W	LED recessed troffer	88 lm/W	0.92
	Core retail	Fluorescent recessed troffer	1.44 W/ft²	64 lm/W	LED recessed troffer	88 lm/W	0.73
	Front entry	Compact fluorescent downlight	1.11 W/ft²	41 lm/W	LED downlight	52 lm/W	0.79
	Front retail	Fluorescent recessed troffer	1.44 W/ft²	64 lm/W	LED recessed troffer	88 lm/W	0.73
	Point of sale	Fluorescent recessed troffer	1.44 W/ft²	64 lm/W	LED recessed troffer	88 lm/W	0.73
Supermarket	Bakery	Fluorescent recessed troffer	1.44 W/ft²	64 lm/W	LED recessed troffer	88 lm/W	0.73
	Deli	Fluorescent recessed troffer	1.44 W/ft²	64 lm/W	LED recessed troffer	88 lm/W	0.73
	Dry storage	Fluorescent industrial strip	0.63 W/ft²	81 lm/W	LED recessed troffer	88 lm/W	0.92
	Produce	Fluorescent recessed troffer	1.44 W/ft²	64 lm/W	LED recessed troffer	88 lm/W	0.73
	Sales	Fluorescent recessed troffer	1.44 W/ft²	64 lm/W	LED recessed troffer	88 lm/W	0.73
Warehouse	Bulk storage	Fluorescent industrial strip	0.58 W/ft²	81 lm/W	LED recessed troffer	88 lm/W	0.92
	Fine storage	Fluorescent industrial strip	0.95 W/ft²	81 lm/W	LED recessed troffer	88 lm/W	0.92

Performing the full set of modifications yielded a total of 6,648 baseline models (12 building type/operating schedule combinations at 554 locations) that represent the typical operation of the Bosch AC LED baseline high bay lighting system. For each model, NREL assumed that:

1. All energy consumption associated with the high bay lighting system in each zone, including both driver losses and power output, produces internal heat gains to the conditioned space.
2. The PV array and inverters are located outside of conditioned space and do not contribute any internal gains to the building.

Under these assumptions, the same AC baseline building model is applicable for all PV array sizes, and the baseline simulations may be performed independent of the PV system simulations (see Figure 3). The simulations yielded pre-converter load power P_c at each time step for the AC baseline of each analysis case.

Modeling the Bosch DCMG analysis case corresponding to each AC baseline requires knowledge of the difference in internal gains between the AC baseline and the Bosch DCMG at each simulation time step. Consistent with the assumptions for the AC baseline, NREL assumed that the LED driver losses and light output contributed internal gains to the conditioned space but that the gateway converter does not. Nevertheless, the internal gains for the Bosch DCMG case may differ slightly for each PV array size because bus voltage influences the DCMG system performance (see Section 2.2.3).

To capture the effect of the change in building internal gains in the Bosch DCMG cases, NREL performed a second set of 33,240 simulations (12 building type/operating schedule combinations, 5 PV array size/DCMG type combinations, and 554 locations) following the electric power distribution system efficiency simulations for the Bosch DCMG (see Figure 3). This second set of simulations allowed the computation of whole building metrics for Bosch DCMG performance compared to the AC baseline; see Sections 2.3.5 and 2.3.6.

2.2.2 Photovoltaic System Models

NREL selected SAM (System Advisor Model 2014) as the modeling platform for the photovoltaic arrays. SAM provides detailed performance models for several types of renewable energy systems, including flat-plate PV arrays. SAM uses best-in-class simulation techniques developed at NREL, Sandia National Laboratories, the University of Wisconsin, and elsewhere. SAM's accuracy for modeling flat-plate PV system generation on both an annual and hourly basis has been well validated (Freeman et al. 2013).

In consultation with Bosch, NREL selected the following system components for all PV systems:

- SolarWorld SW 270 monocrystalline PV module (270 W)
- ABB/Power-One PVI-10.0-I PV inverter (480 V, 10 kW).

These components are representative of the highest-efficiency devices presently available in the grid-tied PV market segment. Using these components, NREL developed PV array models in SAM for each combination of building type and PV array scaling factor—a total of 20 template models. (Because the PV array is sized with respect to total connected load rather than average

load, the array size is identical for all operating schedules for a particular building type.) For each array model, NREL sized the PV array such that the derated array wattage approximately equals the total installed high bay lighting load multiplied by the array scaling factor from Table 3. NREL simulated each of the 20 template models at each of the 554 geographic locations, yielding a total of 11,080 simulation runs. System sizing details and modeling assumptions are provided in Appendix B.

In each analysis case, the PV array size and configuration is identical for the baseline AC and Bosch DCMG systems; the systems differ only in the presence or absence of the PV inverter. Therefore, a single SAM model is sufficient to simulate DC production data for both systems. For the baseline system, the SAM model output provides both the DC and AC array power (P_a and P_b in Figure 6, respectively) at each time step. For the Bosch DCMG system, only the DC array power P_a is used as input to the electricity distribution efficiency model. SAM's MPPT algorithm also provides the optimal PV array operating voltage at each time step; this voltage is then assigned to the DC bus in the Bosch DCMG system model.

2.2.3 Electricity Distribution Efficiency Model

Dedicated tools for energy efficiency analysis of mixed AC-DC electric power distribution systems are not readily available. Therefore, NREL developed custom electric power distribution system models using MATLAB (MATLAB 2014) for the AC baseline and Bosch DCMG systems illustrated in Figure 6.

In compact building electric power distribution systems without transformers, wiring resistive losses are generally negligible compared to power electronics conversion losses. Therefore, the modeling approach neglects wiring losses in the analysis such that in all cases $P_c = P_b + P_f$. Since wiring losses in DC distribution systems are typically slightly lower than in AC distribution systems of similar voltage (Sannino, Postiglione, and Bollen 2003), this is a conservative analysis approach that slightly biases the results in favor of the AC baseline.

To model the converters, NREL adapted the Sandia PV inverter model (King et al. 2007) to represent generic power electronics converters. NREL's output-referenced power electronic converter performance model has the form:

$$P_{\text{in}} = P_{\text{out}} + \alpha_1 + \alpha_2 P_{\text{out}} + \alpha_3 P_{\text{out}}^2 + \alpha_4 (V - V_0) + \alpha_5 P_{\text{out}} (V - V_0) + \alpha_6 P_{\text{out}}^2 (V - V_0)$$

in which

P_{in} = The converter input power

P_{out} = The converter output power

V = Converter terminal voltage at variable voltage terminal

V_0 = Nominal voltage at converter variable voltage terminal

P_{out} = The converter output power

α_1–α_6 = Empirically derived converter loss coefficients

The model assumes that the voltage at only one terminal (either input or output) varies significantly. Voltage effects are fit with respect to the variable voltage terminal.

This model is mathematically equivalent to the Sandia PV inverter model but uses a different expression of the loss coefficients. The accuracy of the Sandia model has been well established for PV inverters (King et al. 2007), for which test data is widely available. Little public test data is available for other types of power electronics converters (for instance, DC/DC converters). For the converter performance data supplied by Bosch, the model is reasonably accurate given the spread in the data (see Appendix C).

The output-referenced model is appropriate when converter output power is known and input power is unknown. For the reverse case, NREL developed an input-referenced model with the form:

$$P_{\text{out}} = P_{\text{in}} - \beta_1 - \beta_2 P_{\text{in}} - \beta_3 P_{\text{in}}^2 - \beta_4 (V - V_0) - \beta_5 P_{\text{in}} (V - V_0) - \beta_6 P_{\text{in}}^2 (V - V_0)$$

The coefficients in the input-referenced and output-referenced cases differ slightly, but typically the two forms of the model produce nearly equivalent converter performance curves.

In the case of the Sandia model, the coefficients are estimated sequentially from specific inverter performance characteristics. For the Bosch DCMG analysis, however, NREL fitted the loss coefficients for both input-referenced and output-referenced converter models from public data and Bosch-supplied measurements using linear least squares. Given measured performance data and simulation data supplied by Bosch and from public sources, NREL generated best-fit empirical models for each of the system converters (Table 4).

Table 4. System Converter Models and Full Load Efficiencies at Nominal Voltage

System Type	Converter	Full Load Efficiency	Standard Error (Efficiency)
AC baseline	PV inverter	96.9%	0.14%
AC baseline	AC LED driver	93.7%	1.06%
Bosch DCMG	Gateway rectifier (AC/DC)	97.0%	1.46%
Bosch DCMG	Gateway inverter (DC/AC)	96.9%	0.14%
Bosch DCMG	DC LED driver	97.7%	0.25%

For the Bosch bidirectional DCMG, NREL modeled each power flow direction in the gateway converter separately; this is consistent with how Bosch intends to design and operate the system. Source data, modeling details, and model diagnostics for each of the converters in Table 4 are provided in Appendix C.

Rather than size the converters in the AC baseline and Bosch DCMG systems to exactly match the PV generation and load, NREL opted to use discrete sizes which reflect Bosch's anticipated product offerings in order to investigate the impact of available converter sizes on overall system performance. For a more general comparison of AC and DC distribution systems, artificially sizing the converters to optimal values would provide a better estimate of the technical potential

savings associated with DC distribution. In real design scenarios, however, converter sizing is non-trivial, in particular with respect to PV curtailment in the Bosch unidirectional DCMG (see Section 3). Therefore, modeling discrete converter sizes which match Bosch's product offerings lends an important element of realism to the analysis, despite the somewhat artificial sizing mismatch that results from the models' underlying assumptions about building floor area.

Rather than model multiple parallel converters, NREL scaled the full load capacity such that a single converter model represented, in aggregate, all converters of each specific type. NREL selected the total converter capacity to reflect a typical system design for each analysis case. For the AC baseline system, the converter sizes are pre-determined by the simulation inputs:

- The connected high bay lighting load defines the total AC LED driver capacity
- The baseline PV model defines the total PV inverter capacity.

For the Bosch DCMG, NREL followed Bosch's design philosophy in sizing the system. Bosch anticipates that the Bosch DCMG gateway will contain a converter bank containing up to four 15-kW rectifiers that can be individually staged to match load requirements. For the Bosch bidirectional DCMG, each gateway will also include one or more 10-kW inverters, with the total inverter capacity sized to equal the difference between connected PV generation capacity and connected DC load. NREL therefore sized the Bosch DCMG for each analysis case as follows:

1. To estimate the total DC connected load, NREL multiplied the AC connected load by 0.97 (a conservative ratio based on the AC and DC driver full load efficiencies, using worst-case DC driver efficiency under unfavorable voltage conditions).
2. NREL computed an optimal rectifier capacity per gateway (15-, 30-, 45-, or 60-kW) and number of gateways that best matched the connected load. For modeling simplicity, all gateways are assumed to be identically sized. This yielded the total system gateway rectifier capacity.
3. For the Bosch bidirectional DCMG, NREL computed the number of inverters per gateway based on the difference between the connected PV capacity and connected DC load. Together with the previously computed number of gateways, this yielded the total system gateway inverter capacity.

Appendix C documents the converter sizing for each combination of building type and PV array size.

Given the scaled converter models for each analysis case, NREL computed the energy performance for the AC baseline and Bosch DCMG system types using the simulation data from the baseline building and PV models as inputs. For the Bosch DCMG, NREL scaled the gateway efficiency model to properly represent the number of active rectifiers during each time step. This analysis yielded powers P_a–P_f for every hour of the year.

2.3 Performance Metrics

Using the conceptual network diagram of Figure 5, it is possible to develop standard performance metrics for the lighting system in terms of the six labeled power measurements. To define the energy metrics on an annual basis, we discretize the analysis into a set of uniform time

periods $\boldsymbol{T}$ that span an entire year, each with duration Δt. Within each time period $t \in \boldsymbol{T}$ the system is assumed to operate at steady state (powers P_{at}–P_{ft} are constant) such that $E_{at} = P_{at}\Delta t$, $E_{bt} = P_{bt}\Delta t$, and so forth.[4]

This report examines four energy performance metrics for each analysis case:

1. Grid energy intensity
2. Energy efficiency
3. PV utilization fraction
4. Grid utilization fraction.

Consistent with the network boundaries defined in Section 2.1, we report each of these metrics with respect to the high bay lighting subsystem only, rather than the building as a whole. However, the lighting subsystem efficiency does impact whole building performance. For example, a reduction in lighting energy decreases cooling load in summer but increases heating load in winter. Three additional energy comparison metrics capture these effects:

1. Site change in electricity intensity
2. Site change in natural gas intensity
3. Site change in total energy intensity.

Finally, the performance of the lighting subsystem also impacts the building peak electricity demand, which is a driving factor in electricity costs for commercial consumers. A final metric, computed separately for each month of the year, captures this effect:

Site change in monthly electricity peak demand.

2.3.1 Grid Energy Intensity

The grid energy intensity is the total annual grid electricity consumption of the high bay lighting subsystem normalized by the floor area of the building (A_{Floor}):

$$\text{Grid Energy Intensity} = \frac{\sum_{t \in \boldsymbol{T}} E_{et}}{A_{\text{Floor}}}$$

This metric varies significantly with PV system size and is therefore most useful for comparing analysis scenarios with identically sized PV arrays. From a cost perspective, this metric provides the fairest point of comparison between distribution system design alternatives.

2.3.2 Energy Efficiency

The system energy efficiency is the ratio of total output (load) energy to total input (source) energy:

$$\text{Energy Efficiency} = \eta_E = \frac{\sum_{t \in \boldsymbol{T}} E_{dt}}{\sum_{t \in \boldsymbol{T}} (E_{et} + E_{at})}$$

[4] The notation $t \in \boldsymbol{T}$ indicates an operation that occurs over all time periods in set $\boldsymbol{T}$.

Energy efficiency differs from instantaneous (power) efficiency, which depends on the power flows at a particular instant in time and may vary significantly. Energy efficiency is equivalent to weighted average instantaneous efficiency with weights proportional to system load at each time step.

Because it properly balances changes in efficiency for energy delivered from both PV and the grid with respect to the total energy delivered from each source, system energy efficiency is the fairest metric for evaluating the energy performance of the entire engineered system. However, a better system energy efficiency does not necessarily equate to a lower energy cost because the metric does not differentiate in cost between PV-sourced energy (zero cost following PV installation) and grid-sourced energy (nonzero cost).

2.3.3 PV Utilization Fraction

The PV utilization fraction is a PV-specific efficiency metric defined as the fraction of PV energy that serves a useful purpose, that is, the fraction either delivered to the load or exported to the electric grid. Equivalently, the PV utilization fraction may be defined as one minus the PV loss fraction, in which the PV loss fraction is the portion of total PV energy lost in AC/DC or DC/DC conversion.

The key challenge in defining this metric is properly attributing system losses to one of three possible energy flow paths:

1. PV to load (point a to point d)
2. PV to grid (point a to point e)
3. Grid to load (point e to point d).

Losses associated with the PV-to-load and PV-to-grid paths are attributable to the PV source and reduce the PV utilization fraction. Losses associated with the grid-to-load path are not attributable to the PV source and therefore do not reduce the PV utilization fraction.

The exact formula for the metric depends on whether the system is exporting energy to or importing energy from the grid.

Case 1: Grid Export

In the grid export case ($E_f \leq 0$), the PV subsystem supplies the entirety of the system load and exports surplus to the grid. There is no grid-to-load energy delivery, so all system losses are attributable to the PV source. Therefore, the useful energy is the energy delivered to the load, E_d, and the energy delivered to the grid, $-E_e$. Therefore, the PV utilization fraction is:

$$\text{PV Utilization Fraction (Export)} = \frac{E_d - E_e}{E_a}$$

Case 2: Grid Import

In the grid import case ($E_f > 0$), both PV and the grid are supplying energy to the load, and system losses must be apportioned between the two sources.

Losses in the PV converter ($E_a - E_b$) are wholly attributable to the PV source.

Losses in the grid converter ($E_e - E_f$) are wholly attributable to the grid source.

Losses in the load converter ($E_c - E_d$) are split between the PV-to-load and grid-to-load paths proportional to the power supplied by each at point c.

Following this convention, the useful PV energy is the fraction of E_d supplied by the PV source:

$$\text{Useful PV Energy} = E_d \left(\frac{E_b}{E_b + E_f} \right)$$

An alternative but mathematically equivalent[5] expression of this same quantity expressed this energy in terms of the load converter efficiency:

$$\text{Useful PV Energy} = \left(\frac{E_d}{E_c} \right) E_b$$

Therefore, the PV utilization fraction is:

$$\text{PV Utilization Fraction (Import)} = \frac{\left(\frac{E_d}{E_c} \right) E_b}{E_a}$$

Metric Definition

Combining the definitions for the grid import and grid export cases and summing over all time steps, the final metric is:

$$\text{PV Utilization Fraction} = \frac{\sum_{t \in \boldsymbol{T} | E_{ft} \leq 0} (E_{dt} - E_{et}) + \sum_{t \in \boldsymbol{T} | E_{ft} > 0} \left(\frac{E_{dt}}{E_{ct}} \right) E_{bt}}{\sum_{t \in \boldsymbol{T}} E_{at}}$$

2.3.4 Grid Utilization Fraction

The grid utilization fraction is the counterpart to the PV utilization fraction—it provides a measure of the efficiency of grid-to-load energy transfer. The metric only applies during grid import operation, and, following the same conventions for attributing losses, may be defined similarly to the PV utilization fraction for the import case.

During import, the useful grid energy is the fraction of E_d supplied by the grid:

$$\text{Useful Grid Energy} = E_d \left(\frac{E_f}{E_b + E_f} \right)$$

Or equivalently:

[5] By energy balance, $E_c = E_b + E_f$. Performing this substitution and rearranging yields the second expression.

$$\text{Useful Grid Energy} = \left(\frac{E_d}{E_c}\right) E_f$$

The grid utilization fraction is therefore:

$$\text{Grid Utilization Fraction} = \frac{\sum_{t \in \boldsymbol{T} | E_{ft} > 0} \left(\frac{E_{dt}}{E_{ct}}\right) E_{ft}}{\sum_{t \in \boldsymbol{T} | E_{ft} > 0} E_{et}}$$

2.3.5 Site Energy Impacts

To assess the whole building (site) impact of the choice of high bay lighting system, NREL simulated the performance of the entire building in EnergyPlus using the internal heat gains associated with each system type: the AC baseline and the Bosch DCMG. This process yielded separate annual site electricity, natural gas, and total energy consumption for the two cases:

$$E_{\text{SiteElectric}} = \text{Net annual electric energy consumption of the entire builiding}$$
$$E_{\text{SiteNaturalGas}} = \text{Net annual natural gas energy consumption of the entire building}$$
$$E_{\text{SiteEnergy}} = \text{Net annual total energy consumption of the entire building}^{6}$$

The following comparison metrics summarize the site impacts normalized to floor area:

$$\text{Site Change in Electricity Intensity} = \frac{E_{\text{SiteElectric,DC}} - E_{\text{SiteElectric,AC}}}{A_{\text{Floor}}}$$

$$\text{Site Change in Natural Gas Intensity} = \frac{E_{\text{SiteNaturalGas,DC}} - E_{\text{SiteNaturalGas,AC}}}{A_{\text{Floor}}}$$

$$\text{Site Change in Total Energy Intensity} = \frac{E_{\text{SiteEnergy,DC}} - E_{\text{SiteEnergy,AC}}}{A_{\text{Floor}}}$$

The site change in electricity intensity includes the change in grid energy intensity of the high bay lighting subsystem rather than being in addition to it. The site change in total energy intensity combines the direct and indirect effects of the Bosch DCMG on electricity and gas consumption into a single metric.

2.3.6 Site Peak Demand Impacts

The same time series data required to compute the site energy impacts may also be used to compute the monthly peak demand impact of using the Bosch DCMG. Over a given time period, the change in peak demand is the difference between the maximum site demand using the Bosch DCMG and the maximum site demand using the AC baseline system. The change in peak demand is then normalized by floor area to provide direct comparison between buildings of differing size:

$$\text{Site Change in Peak Electricity Demand} = \frac{\max\left(P_{\text{SiteElectric,DC}}\right) - \max\left(P_{\text{SiteElectric,AC}}\right)}{A_{\text{Floor}}}$$

[6] $E_{\text{SiteEnergy}} = E_{\text{SiteElectric}} + E_{\text{SiteNaturalGas}}$

For utility billing, demand is typically averaged over a 15 minute period. However, because the simulations used an hourly time step, NREL computed hourly demand averages for use with the peak demand calculation. This metric is computed separately for each month of the year.

2.4 Geographical Performance Maps

Using the 554 sites identified in Figure 4, NREL developed scripts that visualize the model results as geographical performance maps. NREL implemented the scripts in the Python scripting language primarily using the Matplotlib Basemap Toolkit (Whitaker 2015). The scripts employ an inverse distance weighting method for multivariate interpolation (using 0.5 for the power parameter, which determines the local influence of each point) to produce continuous color maps from the 544 data points within the contiguous United States.

NREL elected to display the results for the 10 TMY3 locations in Hawaii as single points because the numerous microclimates in Hawaii preclude the use of interpolation to produce a meaningful map. However, the 10 locations in Hawaii correspond to the areas with largest population density.

3 Results

For buildings that operate seven days per week, the Bosch unidirectional DCMG delivered an improvement in annual PV energy utilization of approximately 6%–8% and a high bay lighting grid electricity reduction of approximately 0.1–0.3 kWh/ft^2/year. To put this number in perspective, for the retail store modeled in this analysis, using the Bosch DCMG technology saves 10–30 MWh per year—approximately 2%–6% and 1%–4% of the total lighting energy consumption for stores with daily and 24-hour operation , respectively.

For buildings that operate five days per week, however, PV curtailment during low load conditions (weekends) significantly reduced Bosch DCMG performance, particularly in sunny climates. For such buildings, the Bosch unidirectional DCMG decreases PV energy utilization consumption by up to 20% compared to the AC case. The Bosch bidirectional DCMG still performs better than the AC baseline due to the ability to export, but the PV energy utilization improvement over baseline is reduced to 2%–5% due to the increase in gateway inverter losses.

Due to the interaction of the lighting load with heating, ventilation, and air conditioning (HVAC) systems, whole building energy impacts varied widely by climate zone and building type. For all building types, the Bosch DCMG used grid electricity slightly more efficiently than the baseline AC case. As a result, the Bosch DCMG reduced internal heat gains to the conditioned space, in turn reducing cooling load (primarily electricity) but increasing heating load (primarily natural gas). In slightly under half of all simulations, the reduction in site cooling energy exceeded the increase in site heating energy, resulting in greater site energy savings than achieved by the Bosch DCMG alone.

In the vast majority of cases, the Bosch DCMG produced site peak demand savings in all months compared to the AC baseline case. Typical peak demand savings were approximately 0.02–0.08 W/ft^2, or 0.5%–5% of the whole building peak demand, depending on building type and location. Demand savings were greater during the summer months.

Other key findings include:

1. Except for buildings operating five days per week, the Bosch DCMG performed well in all climates compared to the AC baseline. The improvement in PV utilization was slightly higher in cloudy climates because the Bosch DCMG reduces or, in the unidirectional case, eliminates inverter operation at inefficient part-load ratios.
2. On average, the Bosch unidirectional DCMG with the 100% nominal array scaling factor performed the best when compared to the corresponding AC baseline. In contrast, comparing solely among the various Bosch DCMG options, the Bosch bidirectional DCMG with 150% nominal array scaling factor slightly outperformed the unidirectional system. Nevertheless, PV utilization fraction for the unidirectional and bidirectional DCMG was similar across all climate zones and building types. Regional differences produced more variation in the metrics than the selection of DCMG type.
3. Use of discrete PV array and converter sizing resulted in significant sizing mismatch for buildings with lower levels of connected DC load, in particular for the warehouse and refrigerated warehouse building types. For the 100% nominal array scaling factor the PV array and gateway rectifier size mismatches for the warehouse and refrigerated

warehouse building types were 18% and 45%, respectively. This sizing mismatch directly affected the system grid energy intensity (which scales linearly with PV array size), but did not significantly affect system energy efficiency, PV utilization fraction, or grid utilization fraction when compared to the retail and supermarket building types.

4. Except for buildings operating five days per week, PV curtailment was not significant when the PV array is sized less than or equal to the connected DC load.[7] For the 100% nominal array scaling factor, annual PV production lost to curtailment averaged approximately 0.5% across all analysis cases and never exceeded 1.1%.
5. For the Bosch unidirectional DCMG, PV array oversizing significantly increases PV curtailment due to overproduction. For the retail store and supermarket building types (seven days per week operation), the 125% nominal array scaling factor produced an average curtailment of approximately 2% of annual PV energy production. Conversely, undersizing (due to converter size mismatch) reduces PV curtailment to negligible levels; this phenomenon occurred in particular with the 100% nominal (82% actual) array scaling factor for the warehouse and refrigerated warehouse building types.
6. Given the assumed operating schedules, building operating hours had a minimal impact on Bosch DCMG PV utilization. For buildings with other than 24-hour operation, PV curtailment during early morning and late evening hours occurred occasionally but had a negligible impact on an annualized basis.

3.1 Summary of Metrics

Figures 7–14 summarize the performance of the Bosch DCMG relative to the AC baseline for the eight performance metrics presented in Section 2.3; Tables D-1 through D-11 in Appendix D provide the same results in tabular form.[8] The Bosch DCMG improved the lighting system performance of all building types and operating schedules with the notable exception of Bosch unidirectional DCMG systems installed in buildings with five days per week operation.

[7] When there is a mismatch, PV array size is always rounded down to the nearest discrete match to minimize the potential for curtailment; see Appendix B.

[8] To conserve space, monthly demand results are displayed only for four months of the year representing the four seasons: January, April, July, and October.

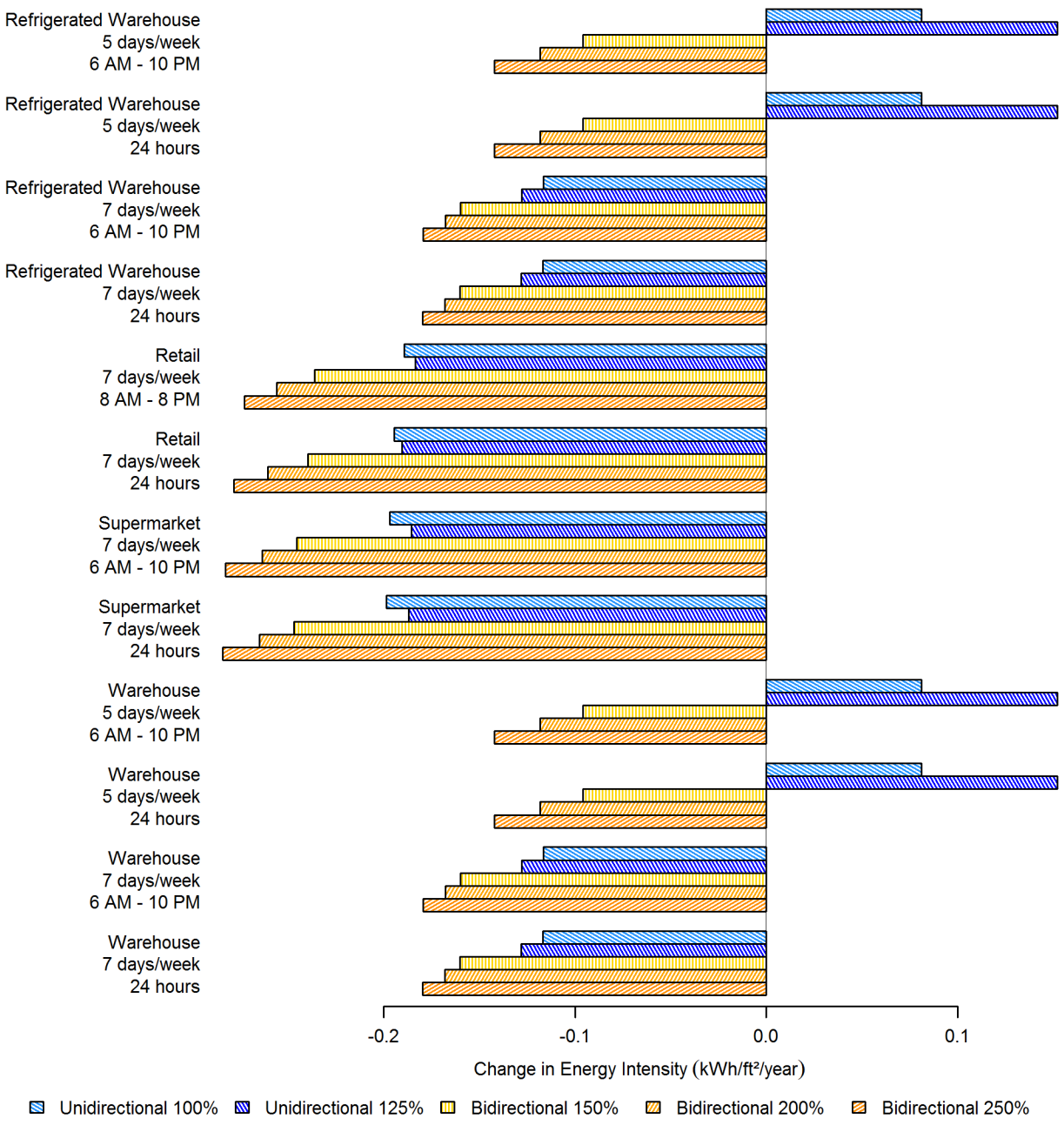

Figure 7. Analysis results—Average change in system grid energy intensity
Bosch DCMG compared to AC Baseline (kWh/ft^2/year)

For buildings operating seven days per week, Bosch DCMG grid energy savings compared to the AC baseline are approximately proportional to the average LPD for each building type. Thus retail stores (LPD ≈ 0.97) and supermarkets (LPD ≈ 0.98) exhibit roughly 1.5 times the energy savings of warehouses (LPD ≈ 0.64 for both types). Converter sizing mismatch has only a minor effect on the overall energy savings.

For buildings with a Bosch unidirectional DCMG operating five days per week, PV curtailment resulted in lost energy compared to the AC baseline.

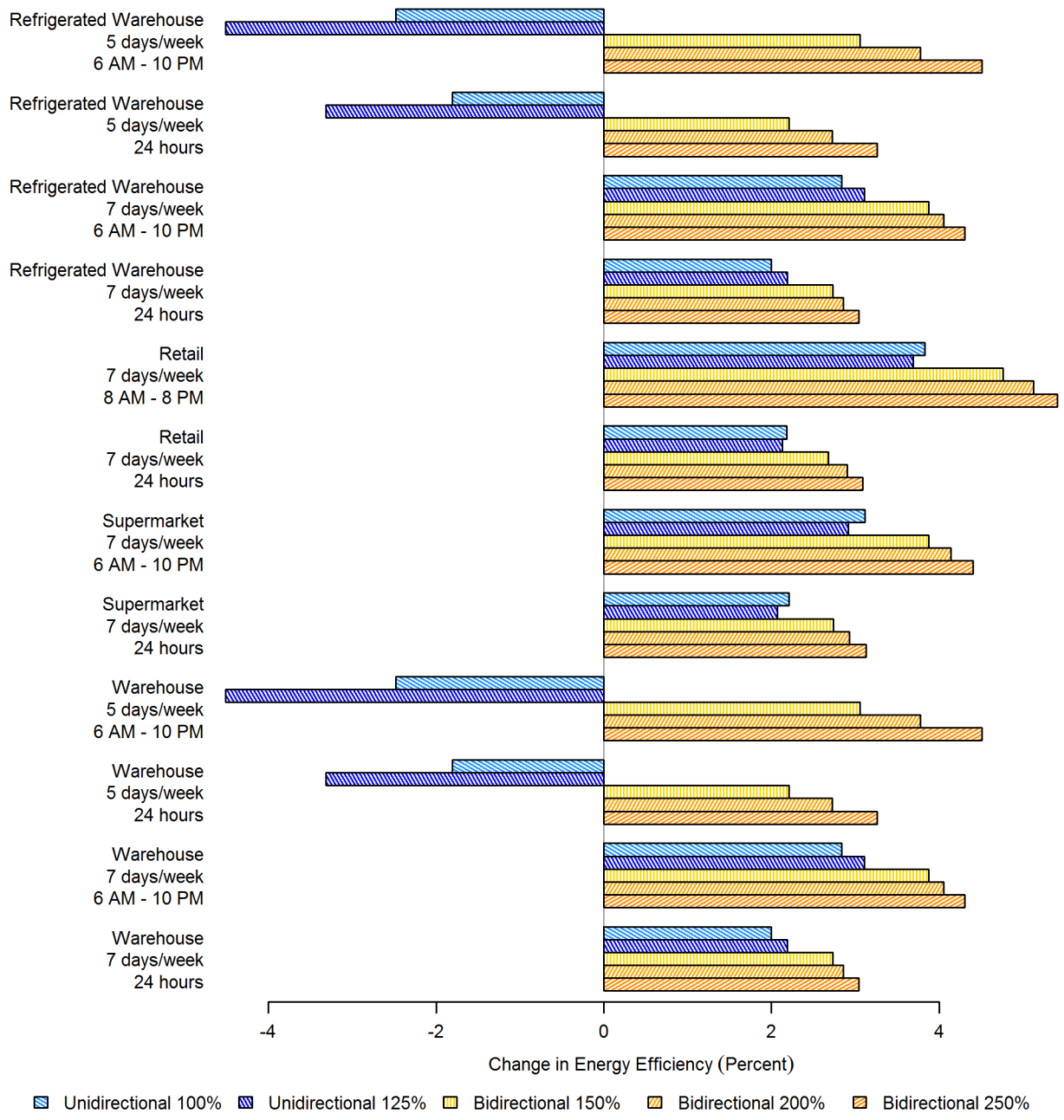

Figure 8. Analysis results—Average change in lighting system energy efficiency
Bosch DCMG compared to AC Baseline (%)

Because the primary efficiency gain of the Bosch DCMG over the AC baseline is the reduction of loss associated with PV-to-load energy transfer, lighting system energy efficiency gains are largest for analysis cases where the ratio of PV energy to grid energy is largest. Thus, gains are larger for buildings with daily operating schedules and for systems with larger PV array sizes. Converter and PV array sizing mismatch have a secondary effect, with well-sized systems (supermarkets, retail stores) performing slightly better than poorly sized systems (warehouses).

As with change in grid energy intensity, the results sets for the two warehouse types are identical because the refrigerated and non-refrigerated warehouses use the same lighting system design.

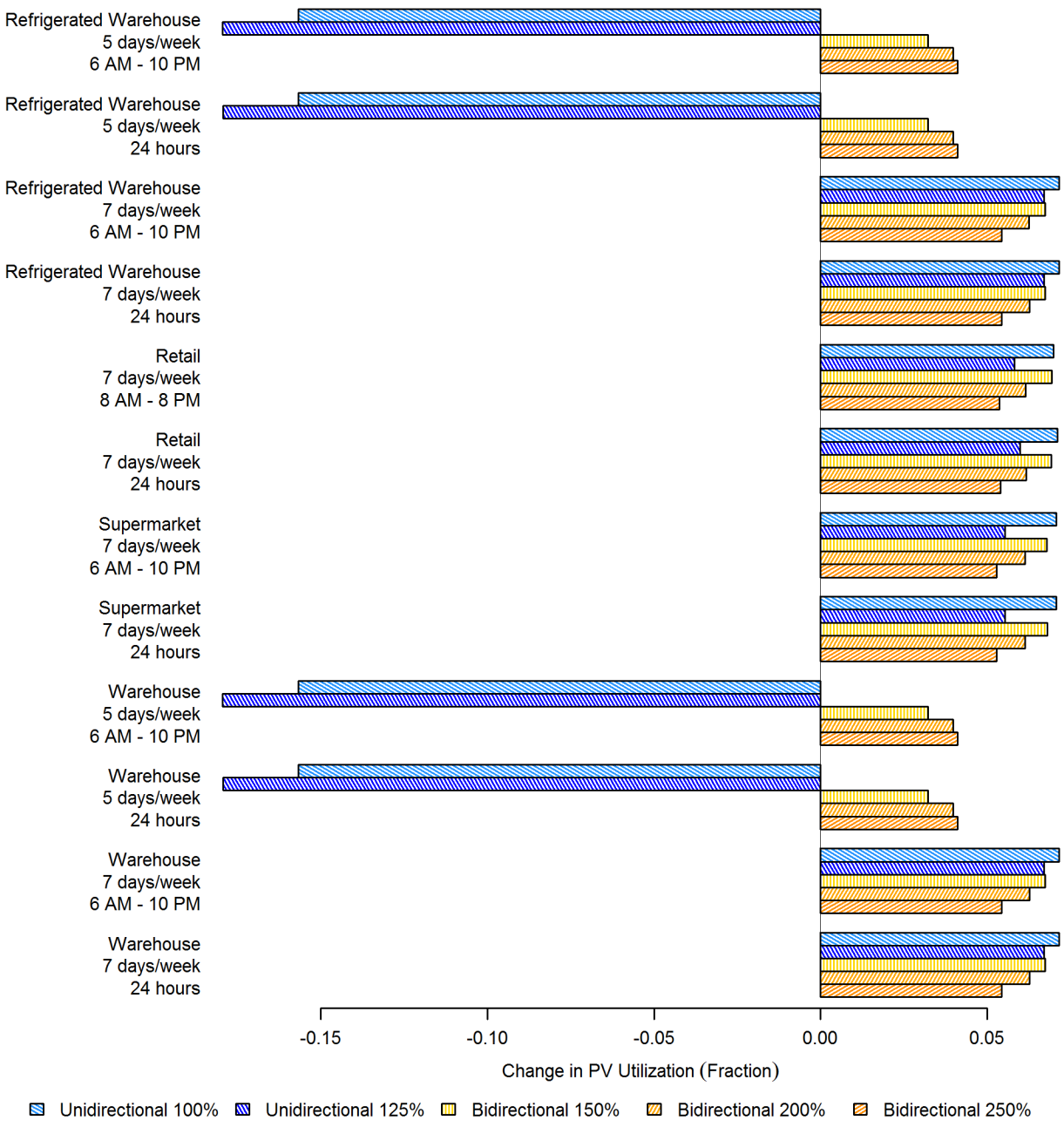

Figure 9. Analysis results—Average change in PV utilization fraction
Bosch DCMG compared to AC Baseline (fraction)

Excluding buildings operating five days per week, the increase in PV utilization for the Bosch DCMG compared to the AC baseline was similar for all building types and operating schedules. The warehouse cases exhibited slightly less PV curtailment due to their undersized PV arrays, but this reduction in curtailment had a negligible effect on overall PV utilization. PV utilization fraction decreased with nominal array size. For the Bosch unidirectional DCMG with 125% nominal array scaling factor, this reduction is attributable to increase PV curtailment. For the Bosch bidirectional DCMG, the reduction is attributable to the lower efficiency of exporting energy to the grid versus using it locally in the DC lighting system.

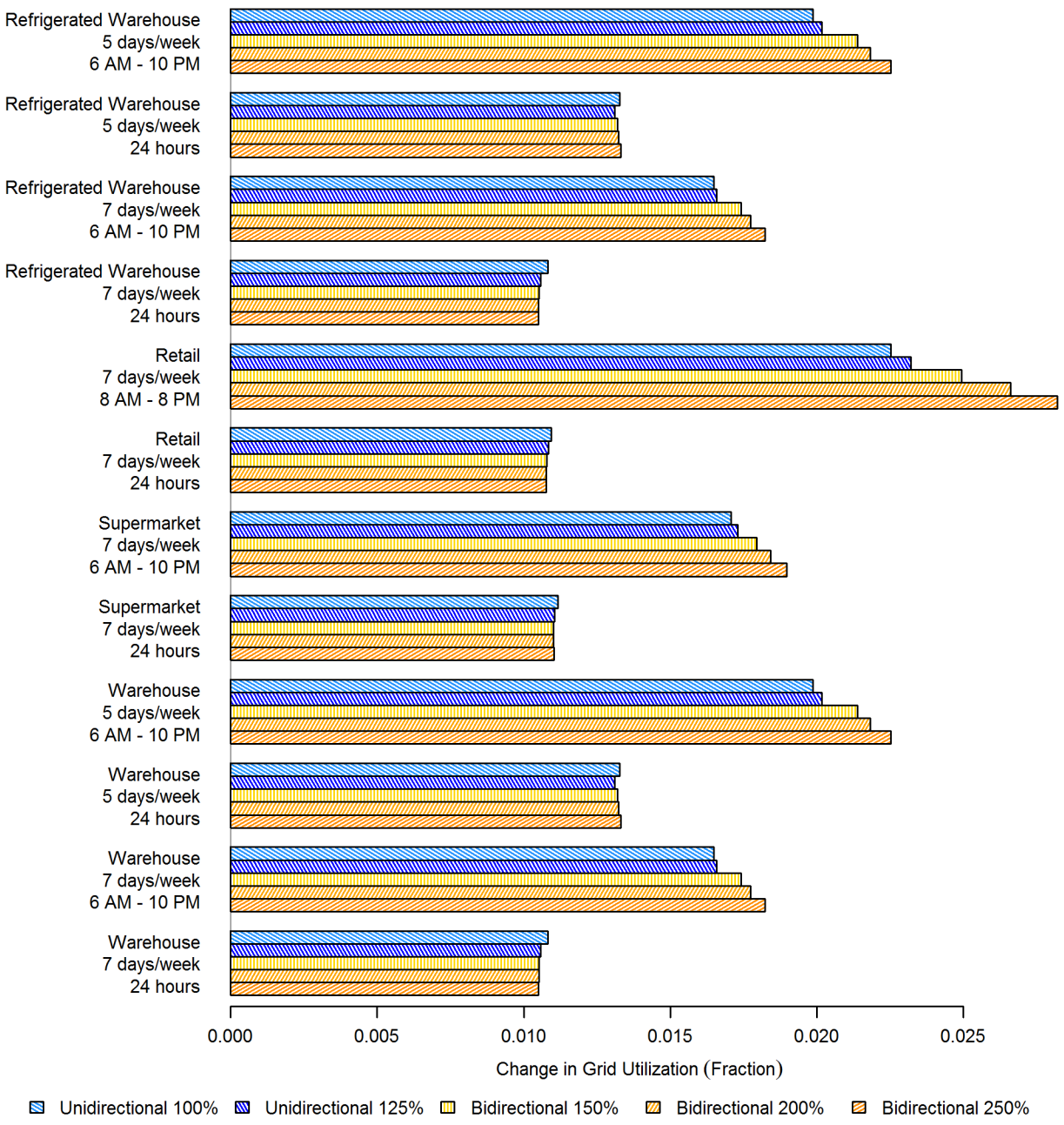

Figure 10. Analysis results—Average change in grid utilization fraction
Bosch DCMG compared to AC Baseline (fraction)

Of the four performance metrics specific to the lighting system, the grid utilization fraction changed the least. Change in grid utilization fraction results from a higher efficiency conversion path for grid energy in the Bosch DCMG compared to the AC baseline. Interestingly, the increase in grid utilization fraction was greatest for buildings with daily operating schedules. This may be because the efficiency difference between the AC and DC LED drivers is most pronounced at low load, as occurs overnight (when lights are assumed dimmed to 10% output).

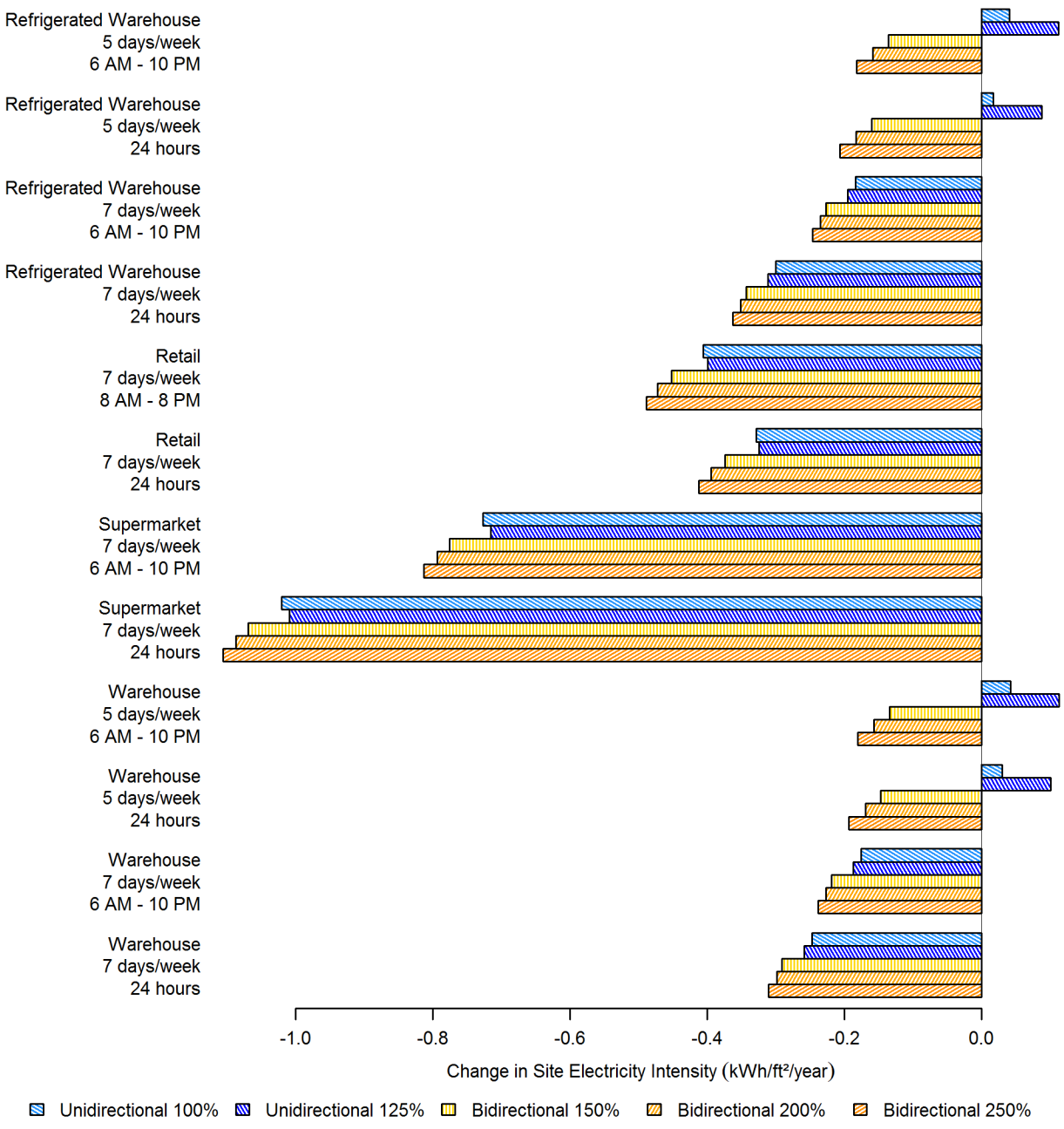

Figure 11. Analysis results—Average change in site electricity intensity
Bosch DCMG compared to AC Baseline (kWh/ft^2/year)

Change in site total electricity intensity, which includes Bosch DCMG direct and indirect savings, varies significantly by building type. Building types with greater cooling load experience greater energy reductions associated with the higher energy efficiency of the DC LED driver. Electricity reduction for supermarkets was particularly high because the DC LED driver reduced load for both the space cooling system and the open case refrigeration system. However, electricity reduction for refrigerated warehouses was smaller than expected. This is because the refrigeration system in the refrigerated warehouse models interacted only minimally with the lighting system; see discussion in Section 3.3 for details.

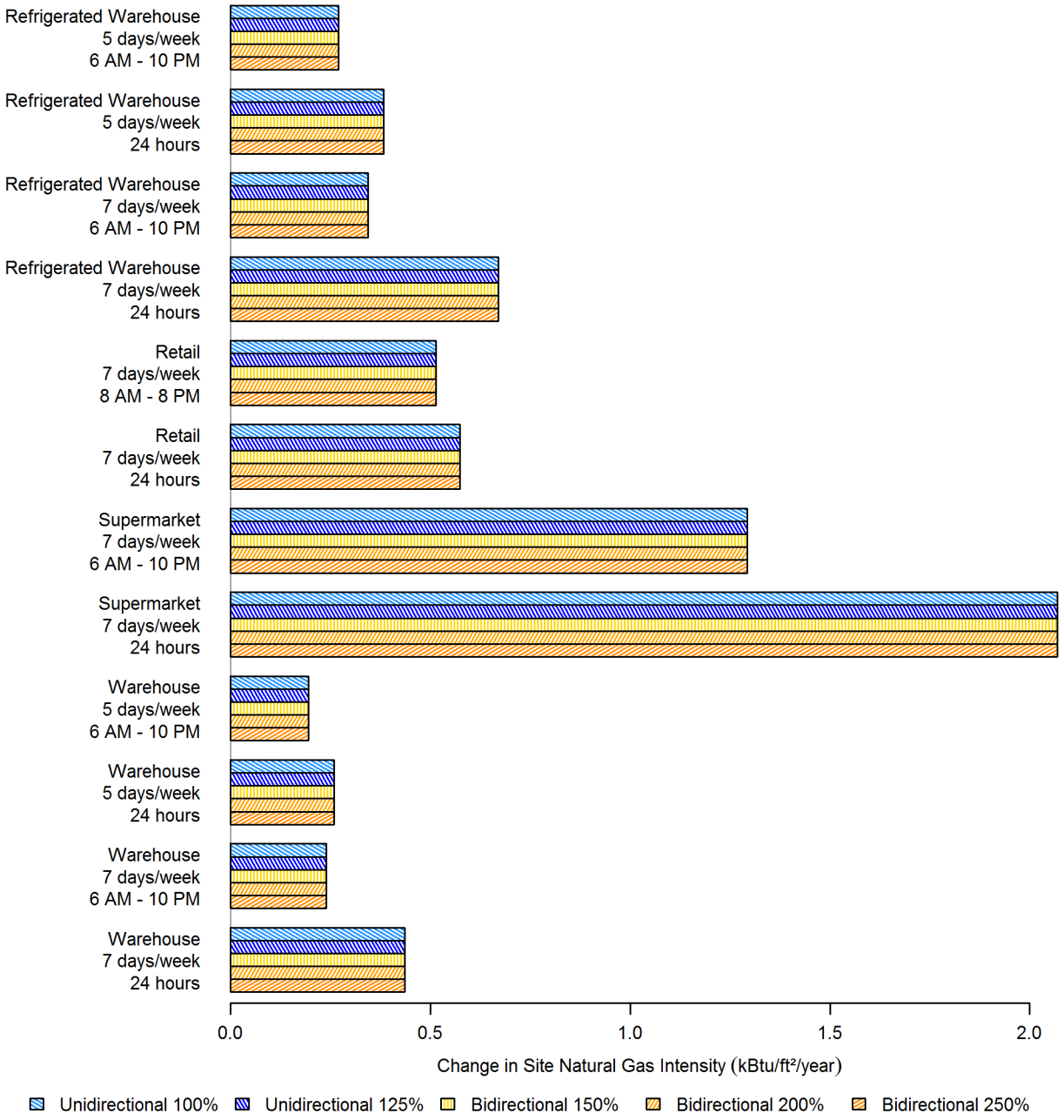

Figure 12. Analysis results—Average change in site natural gas intensity
Bosch DCMG compared to AC Baseline (kBtu/ft^2/year)

The Bosch DCMG's reduction in internal heat gains increased heating load (natural gas consumption) for all building types. Since internal heat gains are related only to LED driver efficiency, PV array size had no impact on the site natural gas intensity. Site natural gas increases were higher for building types with larger average LPD and longer operating hours. Natural gas impacts were much larger than expected for supermarkets; see discussion in Section 3.3.

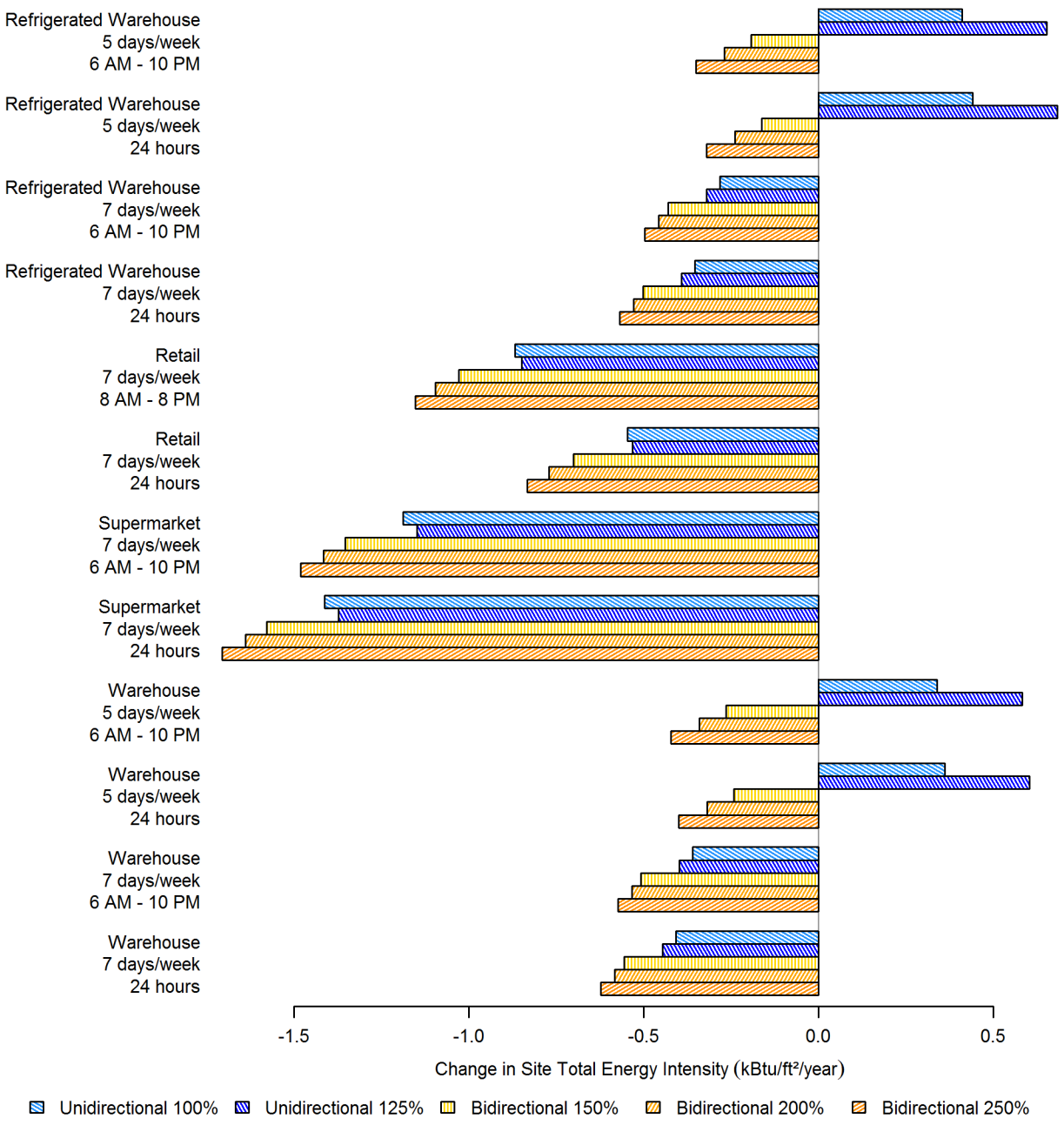

Figure 13. Analysis results—Average change in site total energy intensity
Bosch DCMG compared to AC Baseline (kBtu/ft^2/year)

The site total energy intensity impact combines Bosch DCMG electricity effects (direct and indirect) and natural gas effects into a single metric. The site energy savings are therefore greater for systems with larger PV arrays. The Bosch DCMG saved site energy for all buildings with seven days per week operation. Savings were greatest for supermarkets due to the significant reduction of open case refrigeration load.

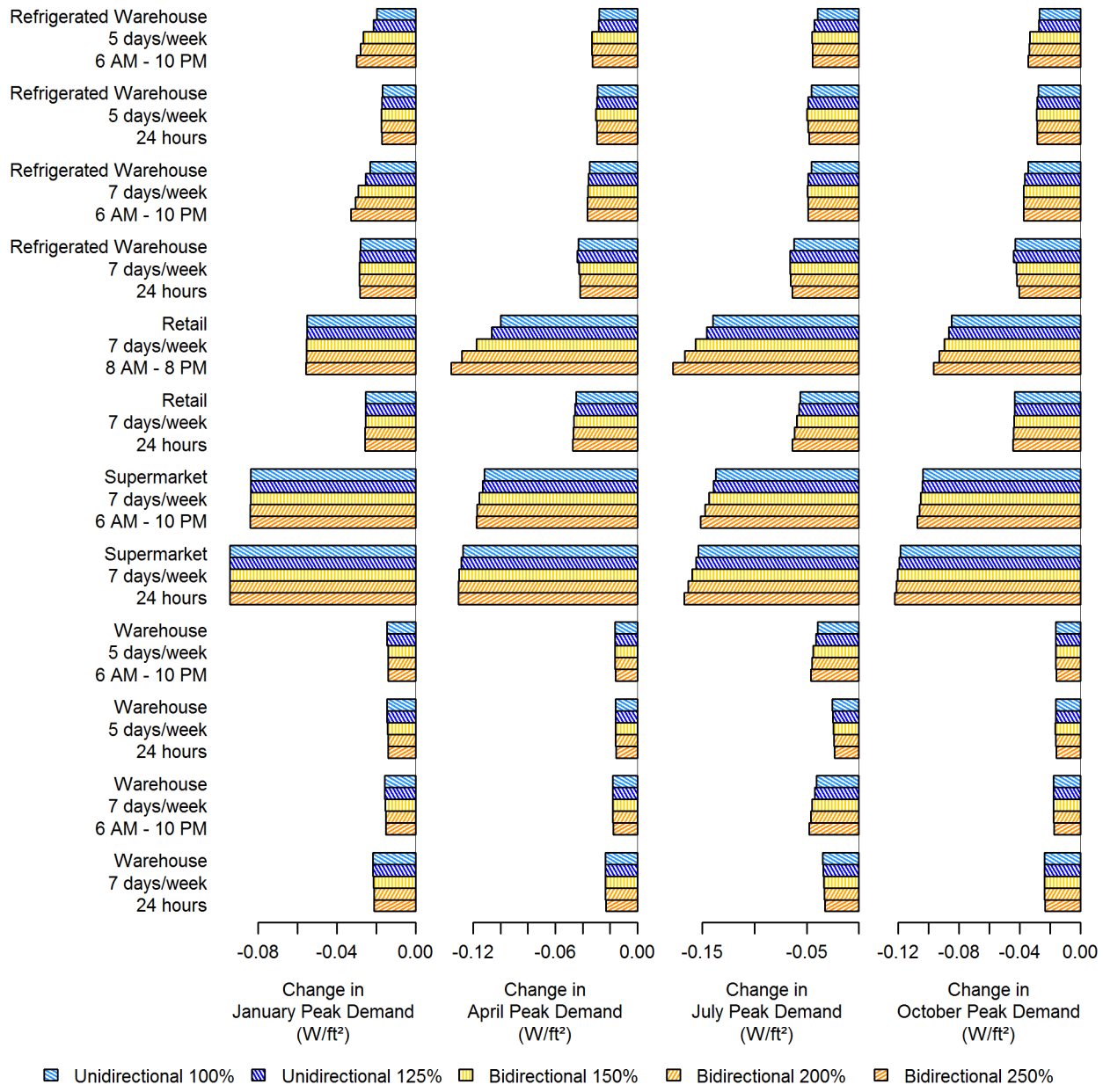

Figure 14. Analysis results—Average change in site monthly peak electricity demand
Bosch DCMG compared to AC Baseline (W/ft^2)

Because the underlying simulations produce hourly output, the peak electricity demand analysis is based on hourly data rather than the customary 15 minute interval. On average, the Bosch DCMG reduced site peak electricity demand in all months of the year, with the greatest reductions in the summer months. Reductions were greater for buildings with larger lighting systems and larger indirect impacts on cooling energy. For buildings with daily operating schedules, average peak demand reduction also exhibited a slight correlation with PV array size. Section 3.3.2 provides additional discussion and caveats related to the demand analysis.

3.2 Performance Maps

The performance of the Bosch DCMG compared to the AC baseline varied significantly by geographic location. This section presents selected performance maps for the warehouse building type that illustrate key trends from the analysis. Additional maps are provided electronically; see Appendix E for details.

In general, most metrics for the Bosch DCMG showed the greatest performance gains in warm, sunny climates. The primary exception was the PV utilization fraction, which showed the greatest performance gains in cool, cloudy climates, most likely because traditional PV inverters in such climates operate more often at inefficient part-load ratios. Peak electricity demand reduction also varied significantly with location, month of the year, building type, and building operating schedule. The greatest peak demand reduction occurred in the summer months.

Figures 15, 16, and 17 display the changes in the lighting system, site energy, and site demand metrics, respectively, for the warehouse building type, 6 a.m.–10 p.m. operation, seven days per week, using the Bosch unidirectional DCMG with a 100% nominal array scaling factor. The system energy efficiency, PV utilization fraction, and grid utilization fraction performance gains shown are typical of the seven days per week analysis cases examined.

For comparison, Figure 18 displays changes in the lighting system metrics for the five days per week version of the same case. Weekend PV curtailment in the five days per week case severely degrades the Bosch DCMG performance compared to the AC baseline. Similarly, Figure 19 displays changes in lighting system metrics for the warehouse building type, 6 a.m.–10 p.m. operation, seven days per week, using the Bosch unidirectional DCMG with a 125% nominal array scaling factor. The array oversizing causes significant PV curtailment and lowers the PV utilization fraction compared to the 100% case.

Finally, for reference, Figures 20–22 display changes in the performance metrics for the same case with the Bosch bidirectional DCMG system type and a 150% nominal array scaling factor. The map is typical of the Bosch bidirectional DCMG results for the 150%, 200%, and 250% nominal array scaling factors across all building types. The metrics for the Bosch bidirectional DCMG are overall very similar to the Bosch unidirectional DCMG.

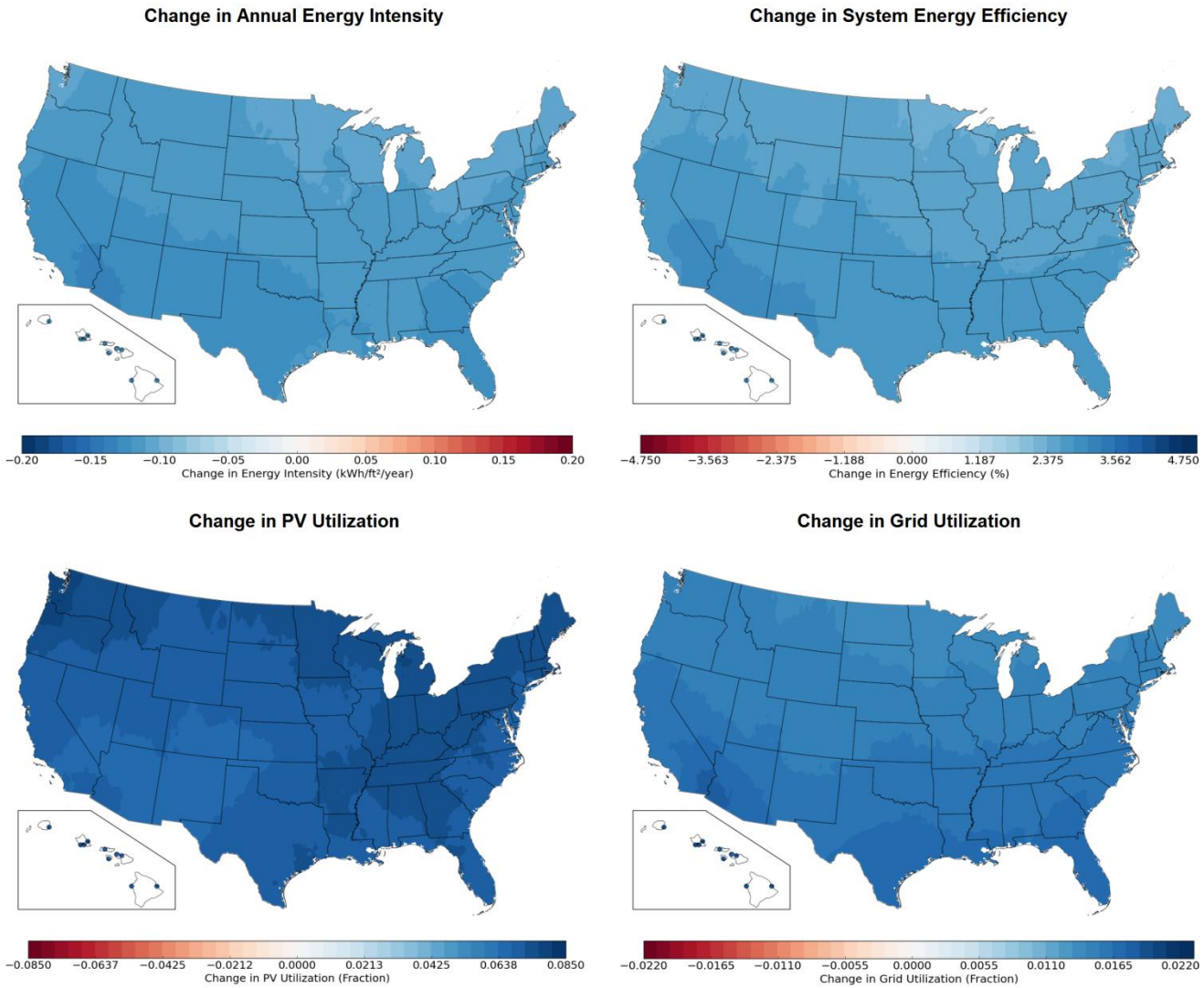

Figure 15. Performance comparison maps for lighting system metrics: Warehouse, 6 a.m.–10 p.m. operation, 7 days/week, unidirectional DCMG, 100% nominal array scaling factor
Bosch DCMG compared to AC baseline

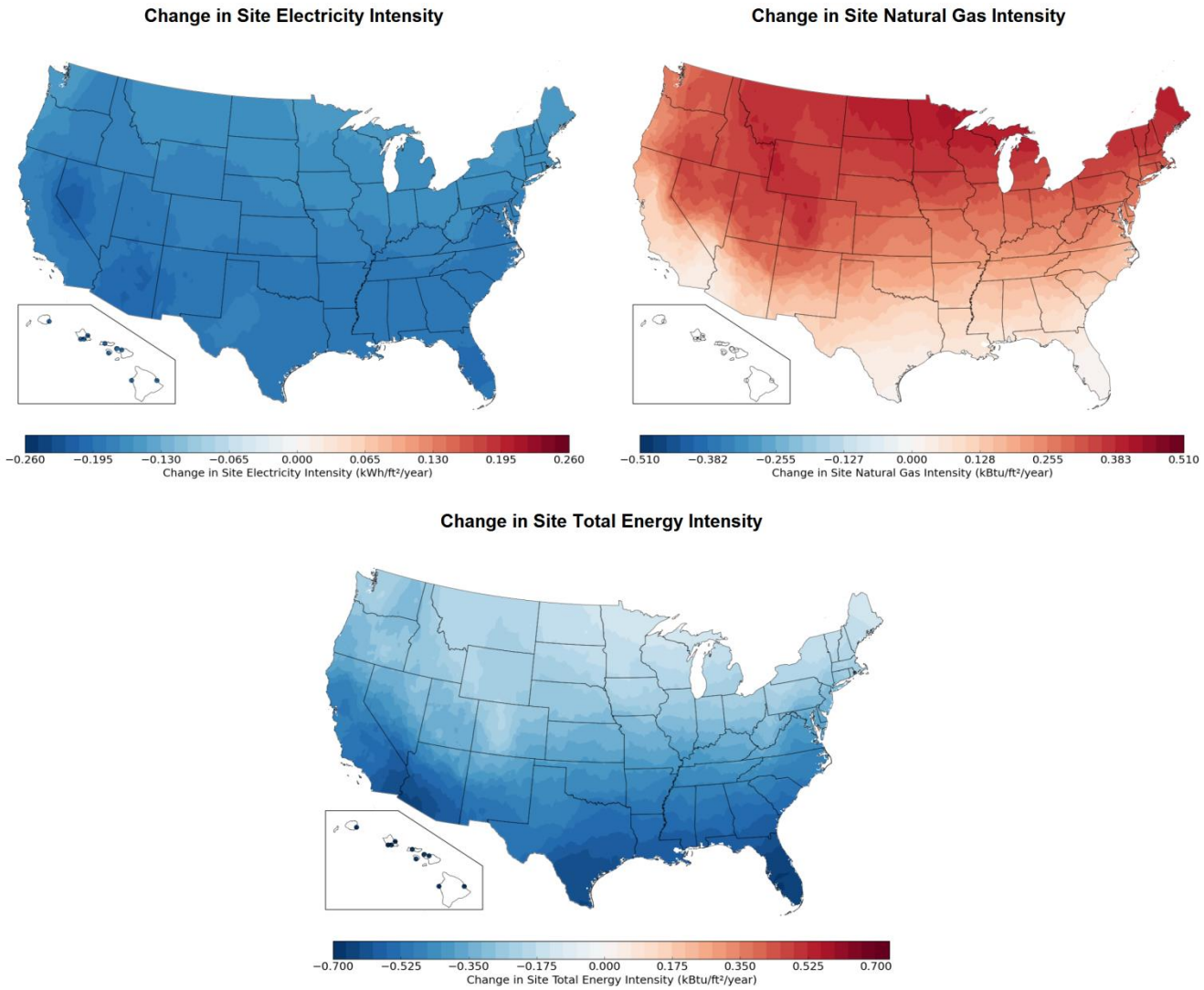

Figure 16. Performance comparison maps for site energy metrics:
Warehouse, 6 a.m.–10 p.m. operation, 7 days/week, unidirectional DCMG, 100% nominal array scaling factor
Bosch DCMG compared to AC baseline

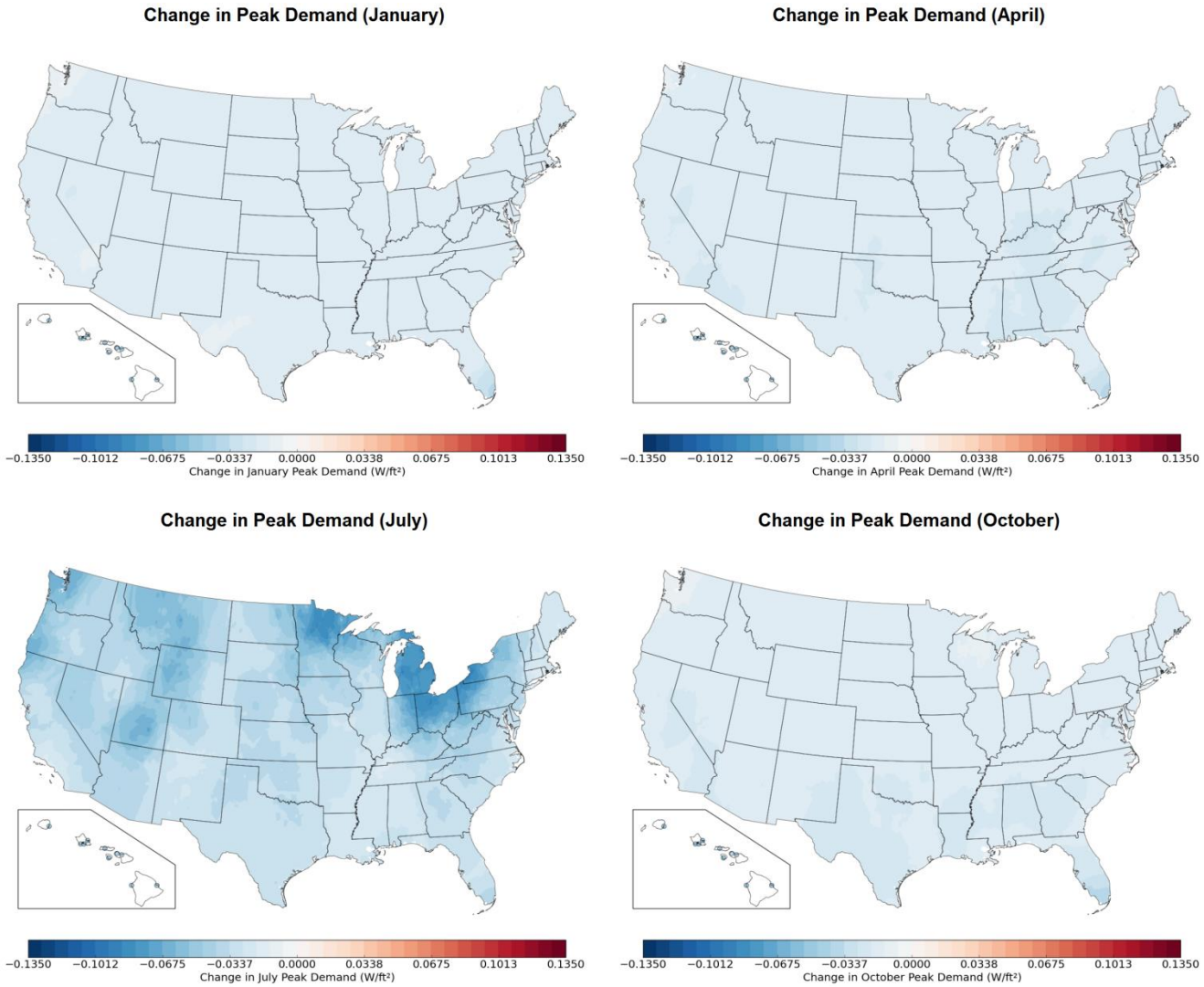

Figure 17. Performance comparison maps for site monthly peak electricity demand: Warehouse, 6 a.m.–10 p.m. operation, 7 days/week, unidirectional DCMG, 100% nominal array scaling factor
Bosch DCMG compared to AC baseline

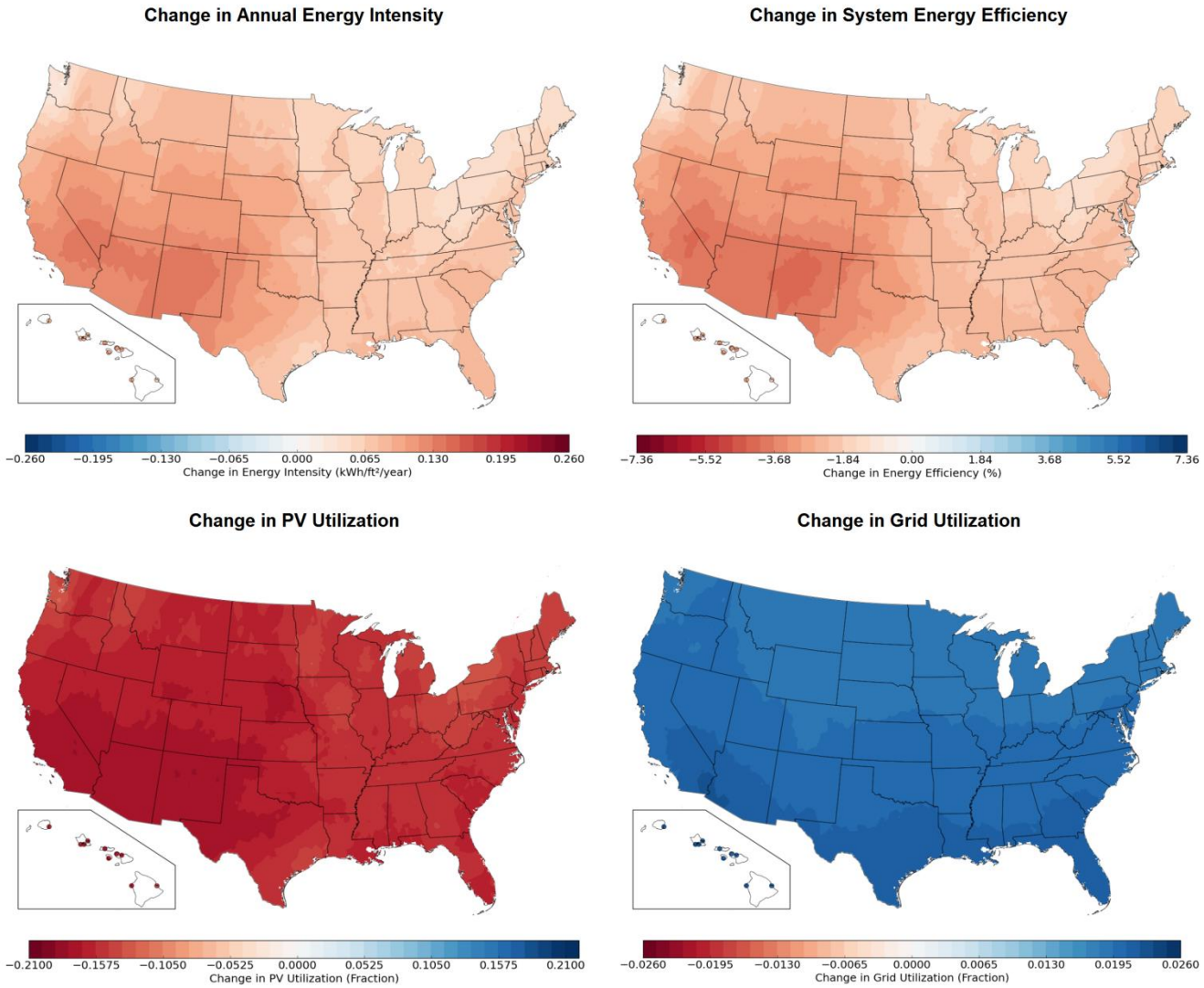

Figure 18. Performance comparison maps for lighting system metrics: Warehouse, 6 a.m.–10 p.m. operation, 5 days/week, unidirectional DCMG, 100% nominal array scaling factor
Bosch DCMG compared to AC baseline

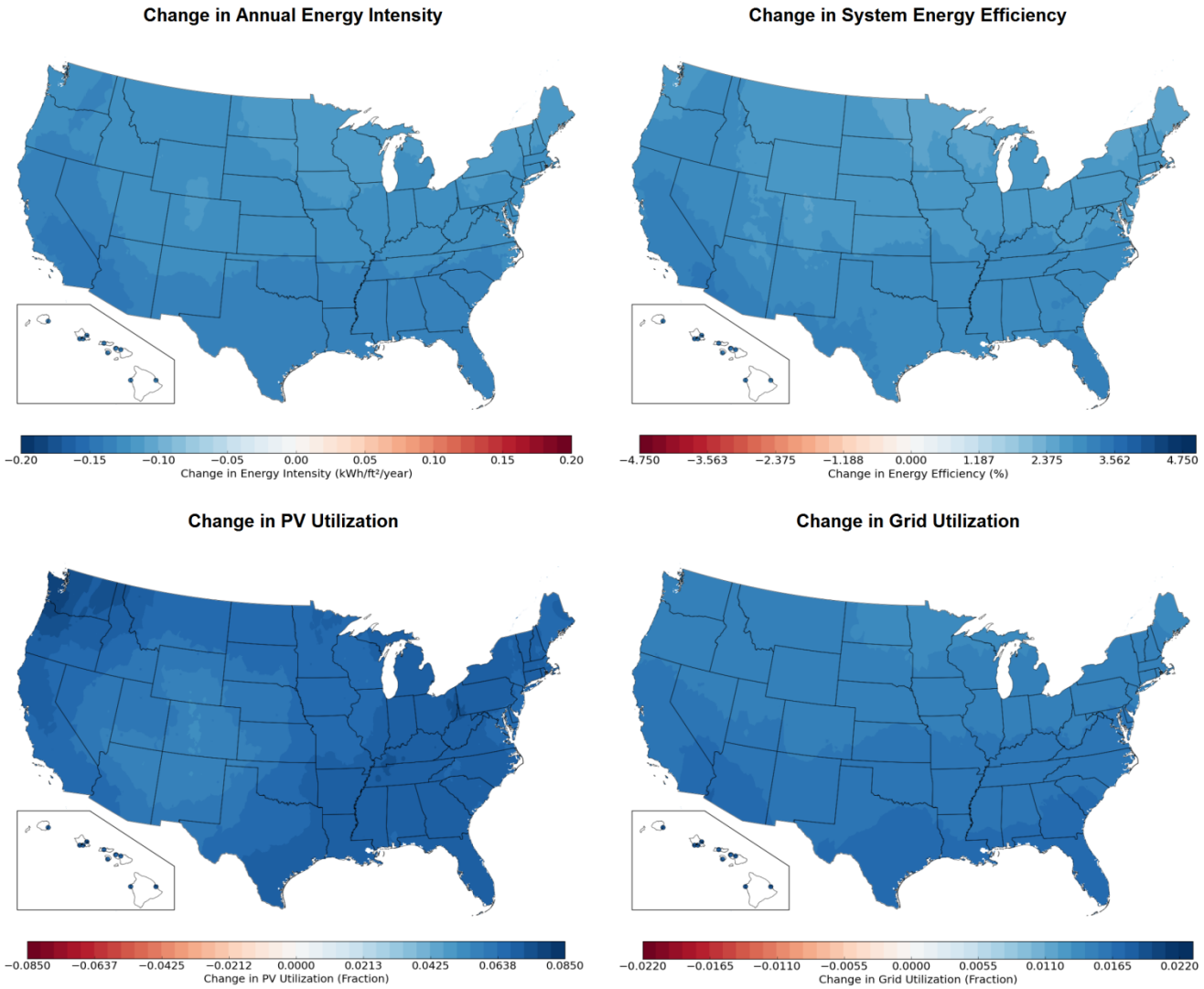

Figure 19. Performance comparison maps for lighting system metrics: Warehouse, 6 a.m.–10 p.m. operation, 7 days/week, unidirectional DCMG, 125% nominal array scaling factor
Bosch DCMG compared to AC baseline

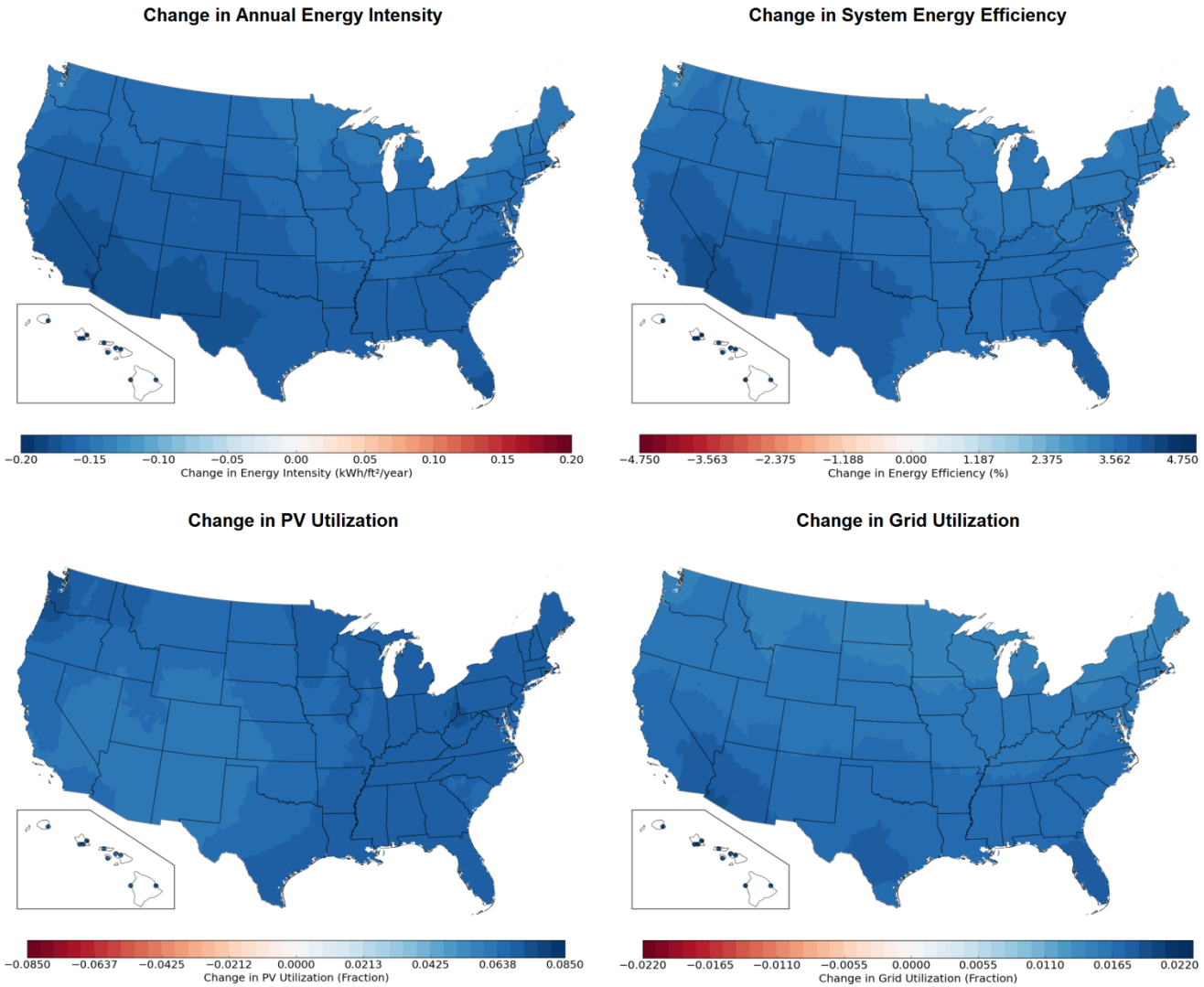

Figure 20. Performance comparison maps for lighting system metrics: Warehouse, 6 a.m.–10 p.m. operation, 7 days/week, bidirectional DCMG, 150% nominal array scaling factor
Bosch DCMG compared to AC baseline

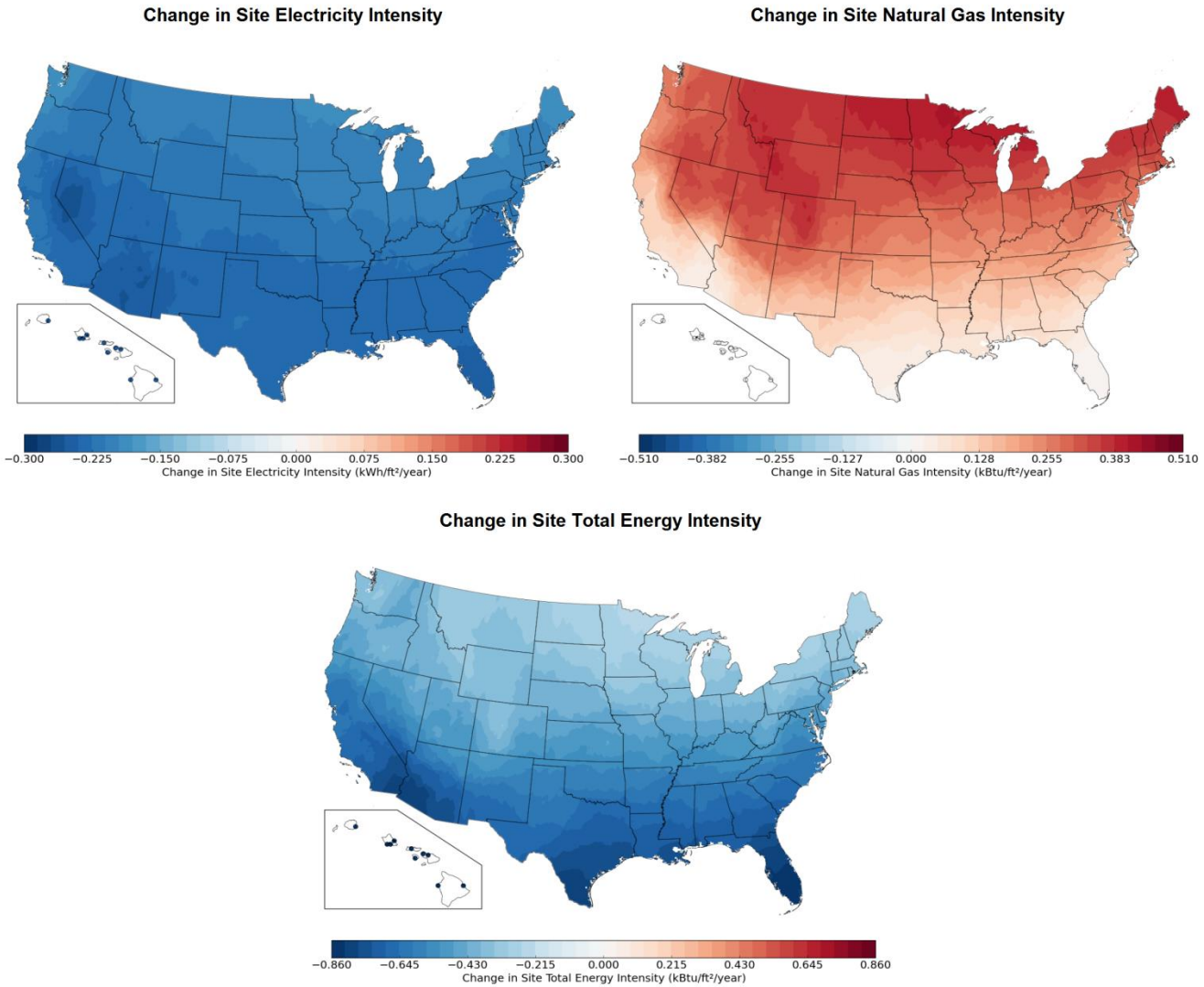

Figure 21. Performance comparison maps for site energy metrics: Warehouse, 6 a.m.–10 p.m. operation, 7 days/week, bidirectional DCMG, 150% nominal array scaling factor
Bosch DCMG compared to AC baseline

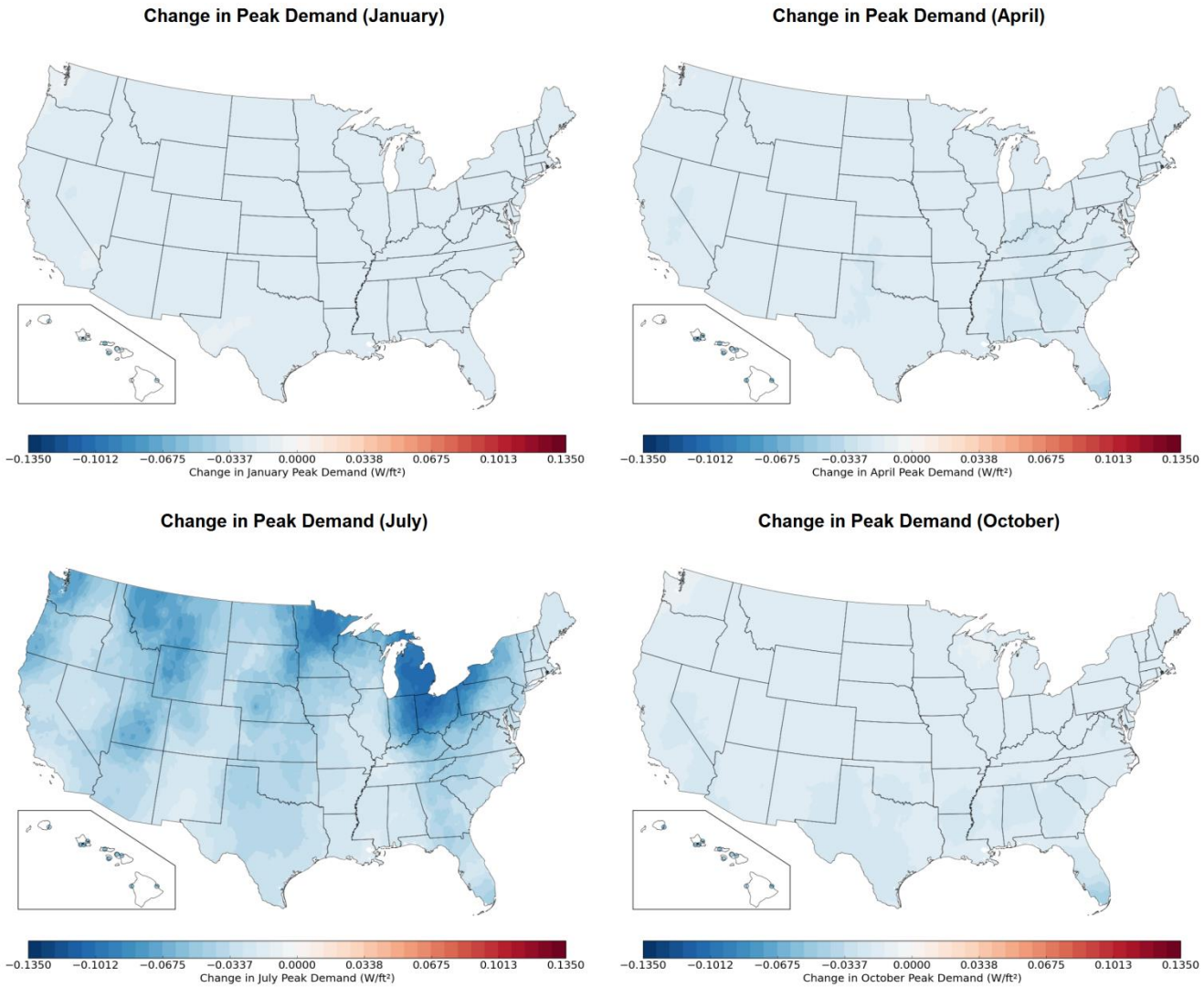

Figure 22. Performance comparison maps for site monthly peak electricity demand: Warehouse, 6 a.m.–10 p.m. operation, 7 days/week, bidirectional DCMG, 150% nominal array scaling factor
Bosch DCMG compared to AC baseline

3.3 Discussion

Two key insights from the analysis are that

1. The Bosch unidirectional DCMG performs very poorly for buildings with fewer than seven days per week operation, and
2. Oversizing the PV array for the Bosch unidirectional DCMG significantly reduces DCMG performance.

In both cases, the performance degradation is due to PV curtailment that occurs when PV generation exceeds the local DC load. These results illustrate the potential benefit of energy storage for the Bosch unidirectional DCMG—energy storage would enable greater performance for intermittent loads and/or oversized PV systems without the need for a bidirectional converter and associated utility interconnection agreement. The remainder of the discussion in this section pertains to the high performing system configurations (seven days per week operation and/or use of bidirectional converters).

The site energy impact metrics provide an interesting case study. For many analysis cases, the reduction in cooling energy exceeded the reduction in lighting system energy by a factor of five to 10, resulting in substantially greater site energy savings than the Bosch DCMG alone delivered. The site electricity savings were greatest in warmer climate zones (see performance maps in Section 3.2). This seemingly counterintuitive result stems from the electrical behavior of the Bosch DCMG: the Bosch DCMG shifts a significant portion of the energy associated with grid-to-load energy transfer outside the conditioned space. Therefore, the reduction in internal heat gains to the building conditioned space is significantly larger than the net savings of the Bosch DCMG considered as a whole. By extension, the ratio of cooling energy savings to lighting system energy savings is much larger than the typical value of 0.3 dictated by conventional wisdom.

The supermarket building type had the greatest site electricity savings because the reduction in internal heat gains significantly reduced refrigeration load in addition to reducing cooling load: the open refrigeration cases in the supermarket model are highly sensitive to changes in space internal gains. Conversely, the refrigeration load in the refrigerated warehouse model was insensitive to the lighting system efficiency because the refrigeration system is modeled as a large walk-in cooler which is thermally isolated from the lighting system. In this respect, the model may not reflect real refrigerated warehouses, in which the lights are located within the coolers themselves. This is a limitation of the modeling approach and is a recommendation for future work.

During heating months, the reduction in internal gains from the lighting system resulted in increased natural gas consumption for heating for most cases analyzed. (The remaining cases saw no net increase in natural gas consumption; in no cases did natural gas consumption decrease.) The increase in natural gas consumption over the AC baseline was greatest in colder climate zones. However, in the majority of cases, the reduction in cooling energy was greater than the increase in heating energy, particularly for southern coastal regions.

Natural gas consumption increased much more for supermarkets than for the other building types; the increase was significantly greater than the change in internal heat gains alone would

suggest. Although the exact cause is difficult to determine from the model results, the increase is most likely a product of the complex interactions between the building internal gains, the open refrigerated cases, and the heating load.

In a small handful of cases (less than 0.2% of simulations), the increase in natural gas consumption fully offset the lighting system performance gains from the Bosch DCMG such that the site total energy intensity *increased* very slightly for the Bosch DCMG system type. This behavior occurred at two types of sites:

1. Cold climate sites with very large heating loads (for example, Leadville, Colorado)
2. Cool but relatively mild climate sites with moderate heating loads such that the marginal impact of the heat gains from the lighting system is significant (for example, Crescent City, California).

Such cases were extreme outliers, however.

One important caveat for the site impact metrics is that they are all based on the assumption that the Bosch gateway converters will be located outside of the conditioned space (for instance, on a rooftop) and therefore do not contribute heat to the space. NREL made this assumption because this arrangement is typical of traditional AC systems, in which the PV inverters are located on the rooftop or within a dedicated electrical room with separate ventilation systems. If the gateway converters are installed within the conditioned space, then the additional heat gains from the gateway converters would significantly alter the site energy metrics. A corollary of this observation is that it may be beneficial to install the gateway converters in conditioned space in particularly cold climates in order to make use of their waste heat.

3.3.1 Model Validation

The analysis results predict annual increases in PV utilization fraction approximately 3% lower than the upper end of the range of instantaneous energy savings that Bosch has observed at existing DCMG pilot sites in Plymouth, Michigan, and Charlotte, North Carolina. There are several possible reasons for the discrepancy:

1. The performance metrics modeled for this report are annual metrics, not instantaneous metrics. It is expected that the annual average will be somewhat lower than the best observed instantaneous differences in PV utilization. In the simulation output, NREL observed gains in PV utilization of up to 20% at some time steps. However, the simulated annual PV utilization fraction for the 100% nominal array scaling factor was only approximately 7% better for the Bosch DCMG than the AC baseline for these two sites across all building types.
2. The annual performance metrics include the impact of non-ideal operating conditions, in particular PV curtailment. PV curtailment lowered the PV utilization fraction by an average of 0.005 (0.5%); see the analysis in Section 3.3.4.
3. In addition, the Bosch DCMG model used in this study includes conservative assumptions that slightly favor the AC baseline; see section 2.2.3.

4. The existing Bosch DCMG pilots serve induction lights rather than LED lights, so driver efficiencies may differ. Because the existing pilot sites are not instrumented to measure DC-side driver output, this hypothesis could not be explored in detail.

Although some time series power data for the pilot sites have been recorded, comprehensive data including weather measurements are not available. For this reason, NREL could not perform a detailed verification of the model using measured data.

3.3.2 Demand Analysis

Peak electricity demand savings varied significantly by month of the year, building type, operating schedule, and geographic location. Supermarkets had the greatest absolute peak demand savings, with average savings exceeding 0.15 W/ft^2 during the summer months. Retail stores had the greatest relative savings, with average savings approaching 5% of peak demand in some months of the year (Figure 23).

Geographical variation in peak demand savings exhibited strong dependence on building type and operating schedule. Figures 24–27 illustrate this effect for each of the four building types using the July peak demand maps.[9]

[9] Note the difference in color bar scale for each individual map.

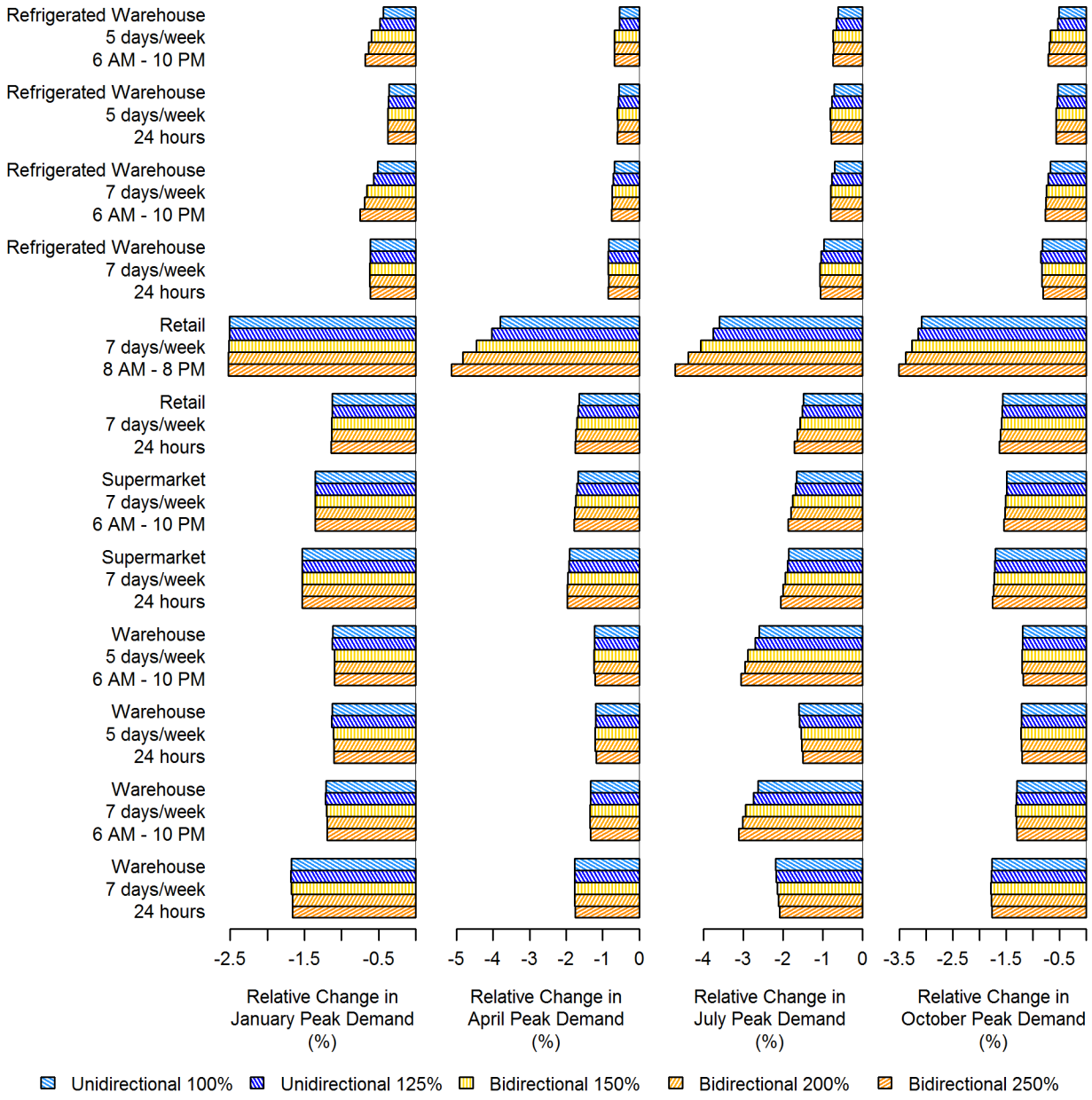

Figure 23. Average relative change in site monthly peak electricity demand
Bosch DCMG compared to AC Baseline (%)

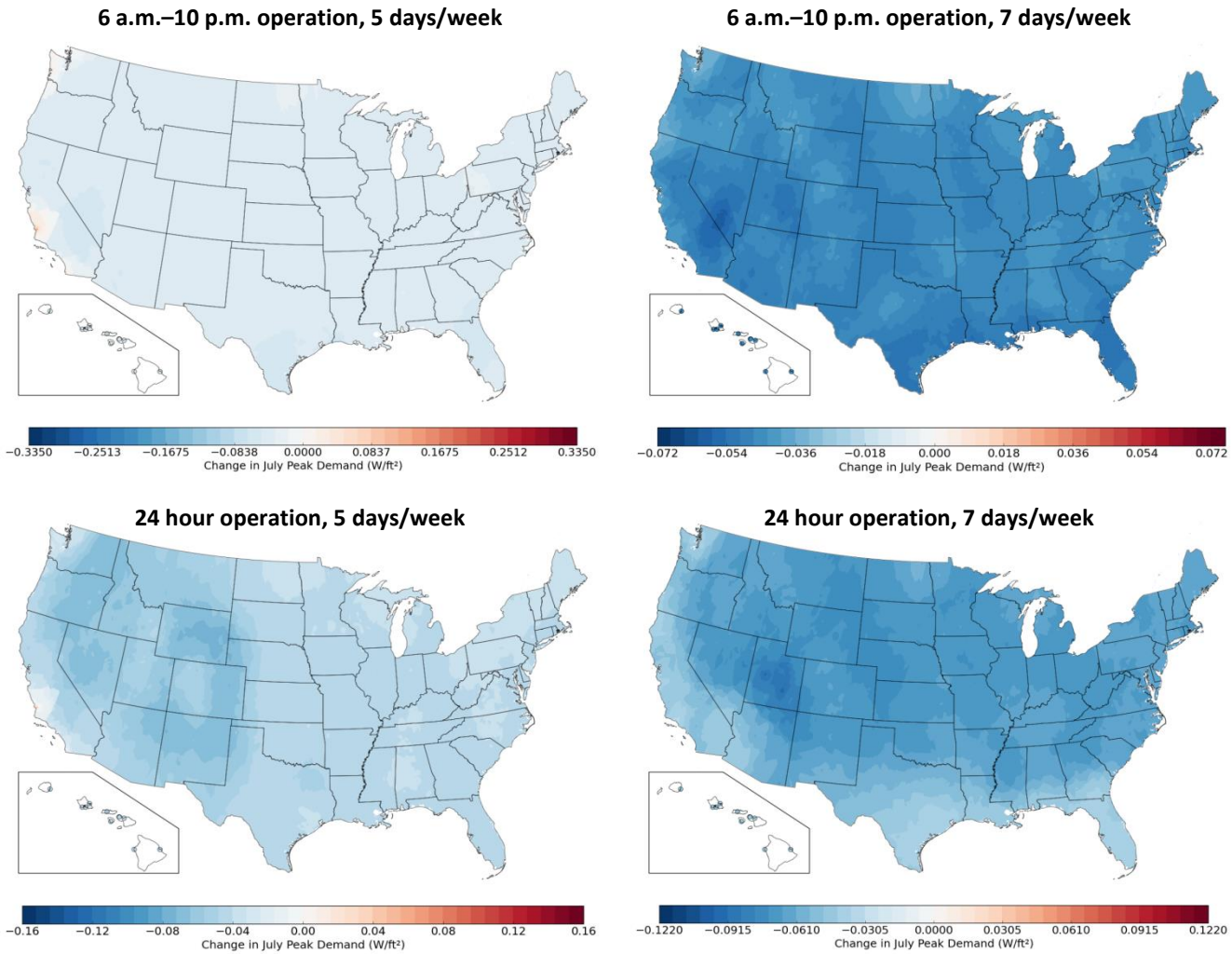

Figure 24. Selected performance comparison maps for July peak demand: Refrigerated warehouse, unidirectional DCMG, 100% nominal array scaling factor
Bosch DCMG compared to AC baseline

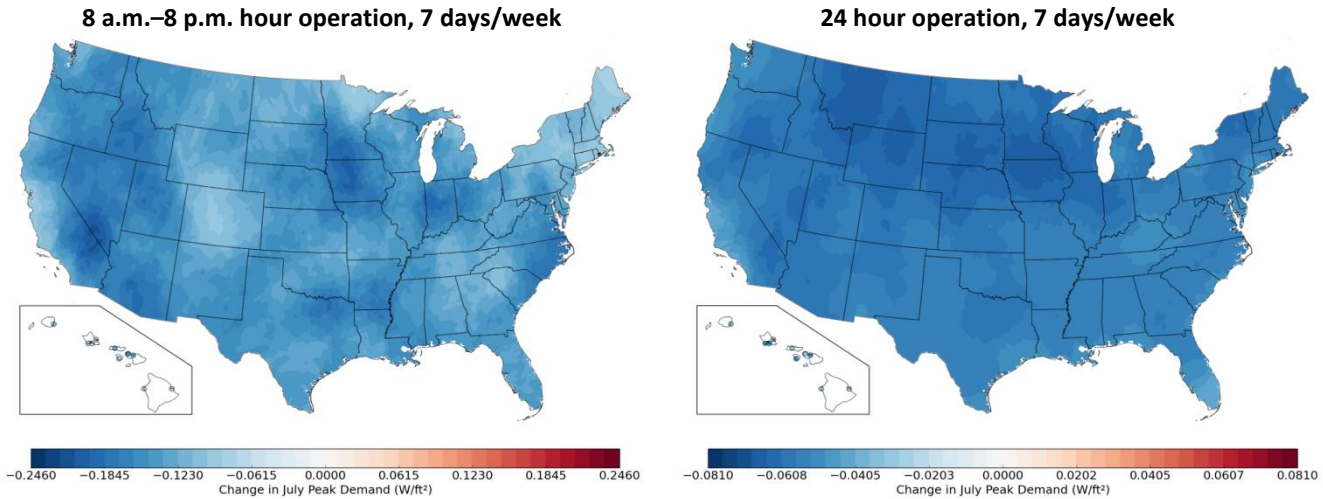

Figure 25. Selected performance comparison maps for July peak demand: Retail, unidirectional DCMG, 100% nominal array scaling factor
Bosch DCMG compared to AC baseline

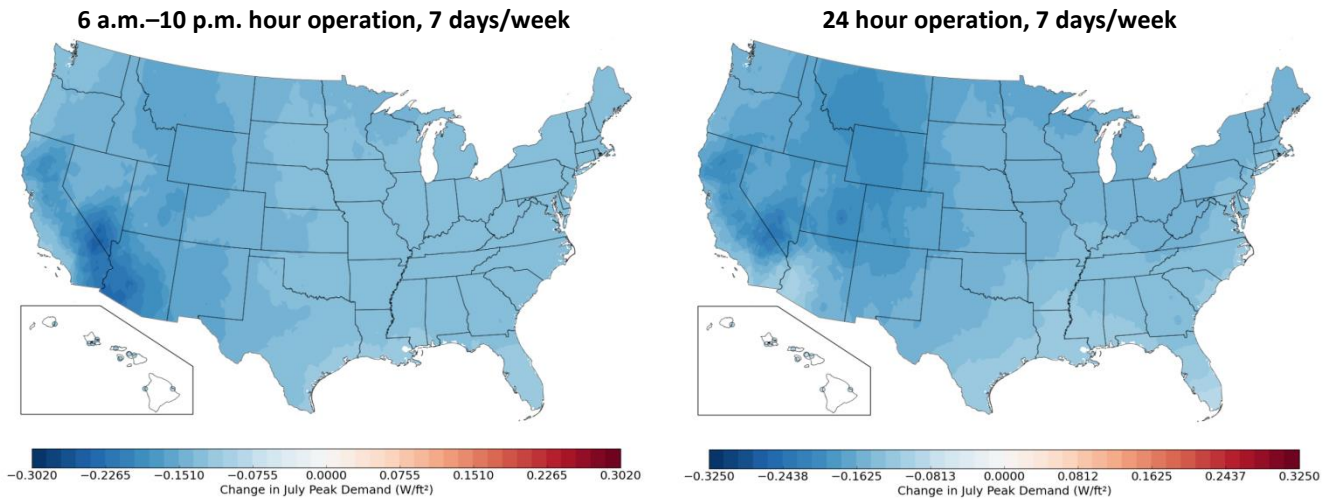

Figure 26. Selected performance comparison maps for July peak demand: Supermarket, unidirectional DCMG, 100% nominal array scaling factor
Bosch DCMG compared to AC baseline

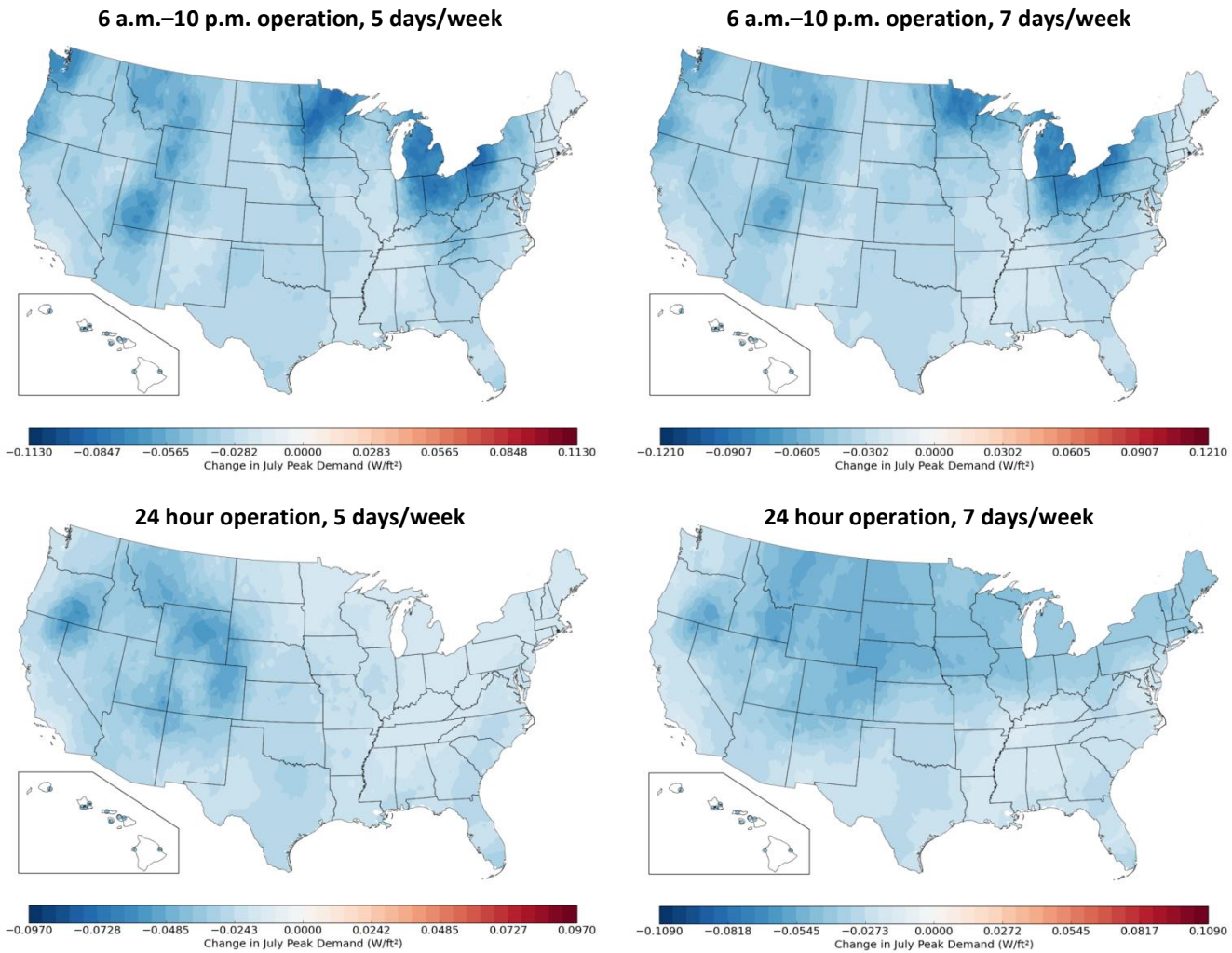

Figure 27. Selected performance comparison maps for July peak demand: Warehouse, unidirectional DCMG, 100% nominal array scaling factor
Bosch DCMG compared to AC baseline

In the vast majority of cases, the Bosch DCMG reduced peak demand compared to the AC baseline. However, in small minority of simulations (less than 0.2% of all cases), peak demand increased for the Bosch DCMG in at least one month of the year. This phenomenon primarily occurred for refrigerated warehouse cases with 5 days/week operation (Figure 28).

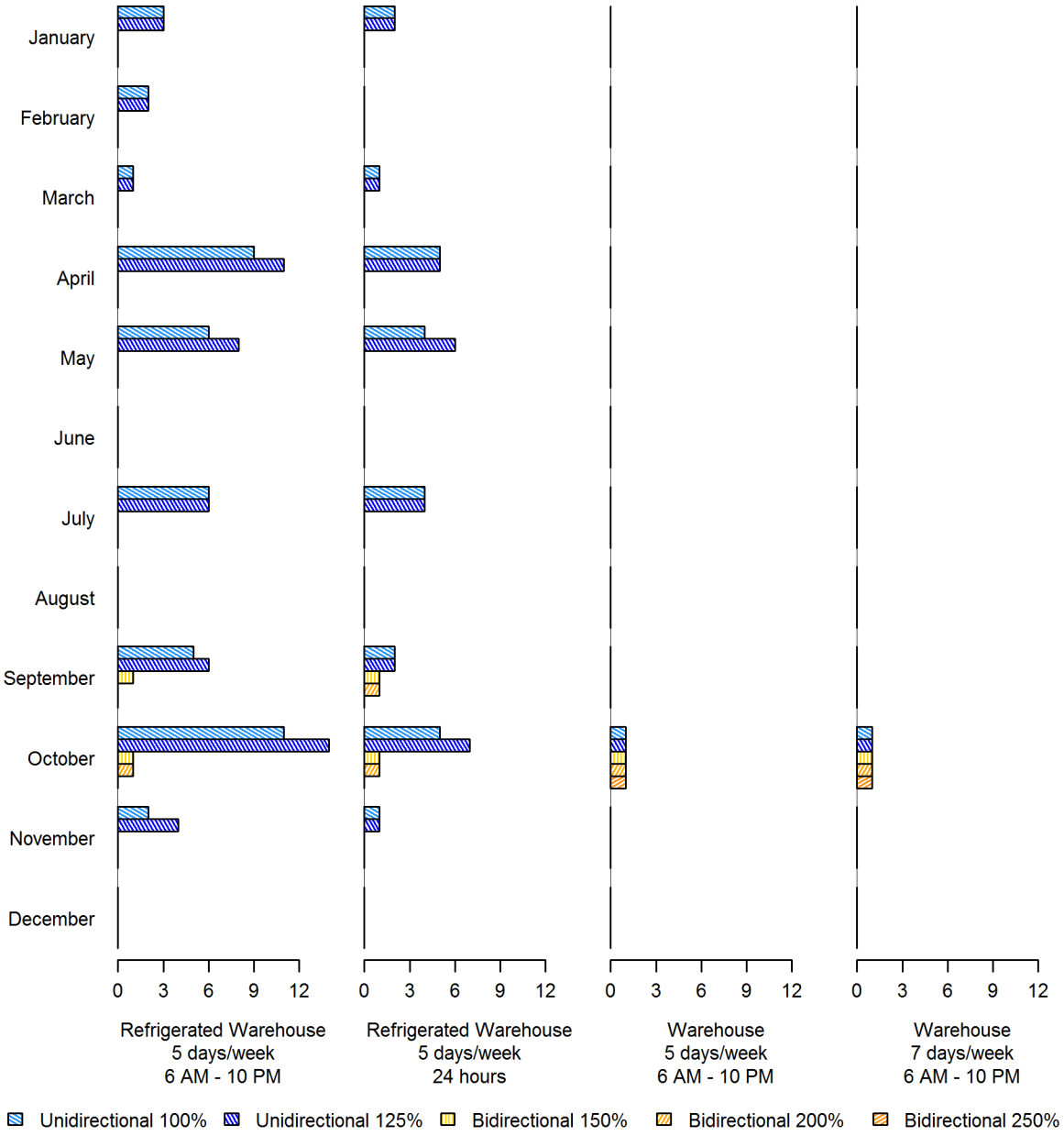

Figure 28. Number of simulations in which peak electricity demand increased
Bosch DCMG compared to AC Baseline[10]

[10] Building types and operating schedules excluded from the plot had no instances in which peak electricity demand increased for the Bosch DCMG compared to the AC baseline.

The cases in which peak electricity demand increased fall into three categories:

1. The peak demand increase was negligible and attributable to slight differences in the simulation of cooling energy consumption between the Bosch DCMG and AC baseline simulations.
2. The peak demand day occurred on a weekend when the Bosch DCMG experienced PV curtailment that did not occur in the AC baseline, causing overall load to increase.
3. Weekend curtailment in the Bosch DCMG case caused the peak demand day to shift to a different day than in the AC baseline.

Figures 29–31 show examples for each case. Note the PV curtailment in Figures 30 and 31.

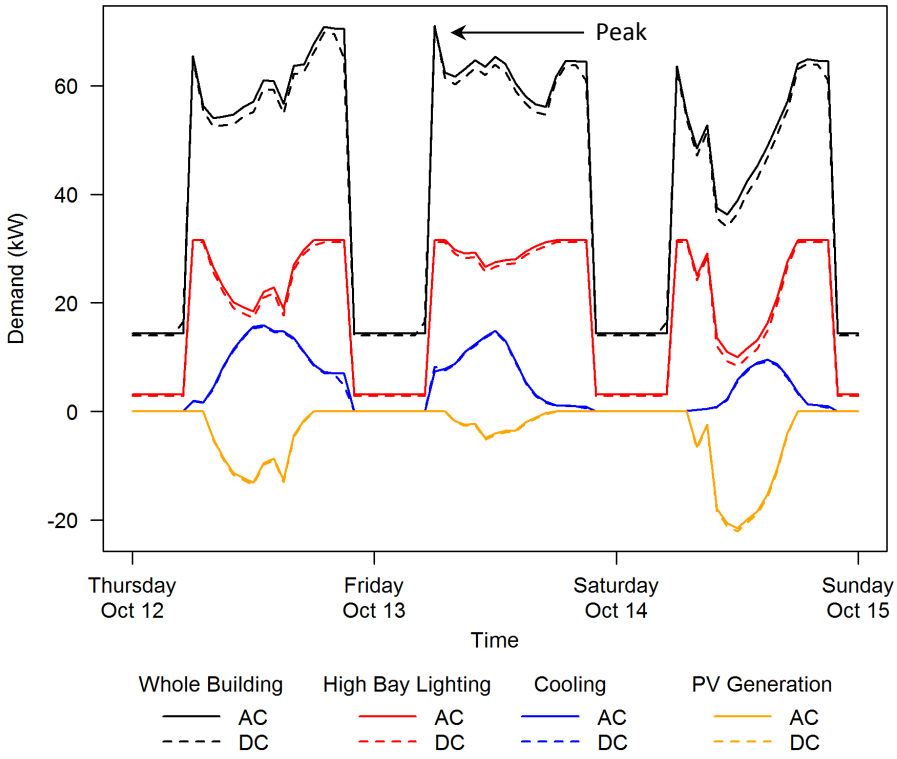

Figure 29. Example of peak demand increase due to increase in cooling energy
Warehouse, 6 a.m.–10 p.m. operation, 7 days/week, unidirectional DCMG,
100% nominal array scaling factor in New Orleans, LA

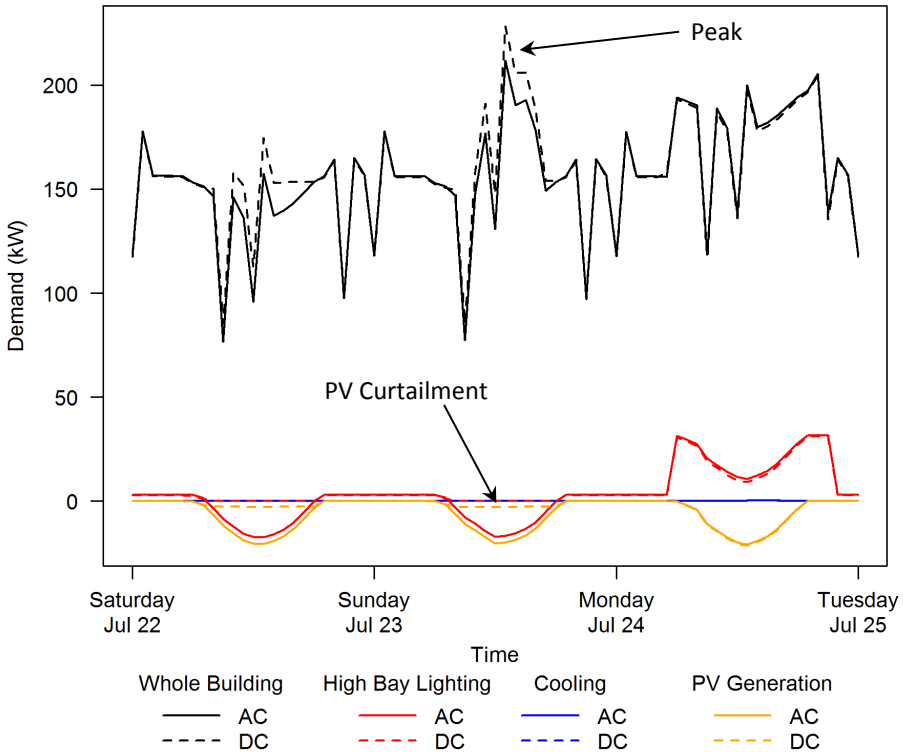

Figure 30. Example of peak demand increase due to same-day PV curtailment
Refrigerated warehouse, 6 a.m.–10 p.m. operation, 5 days/week, unidirectional DCMG, 100% nominal array scaling factor in San Luis county, CA

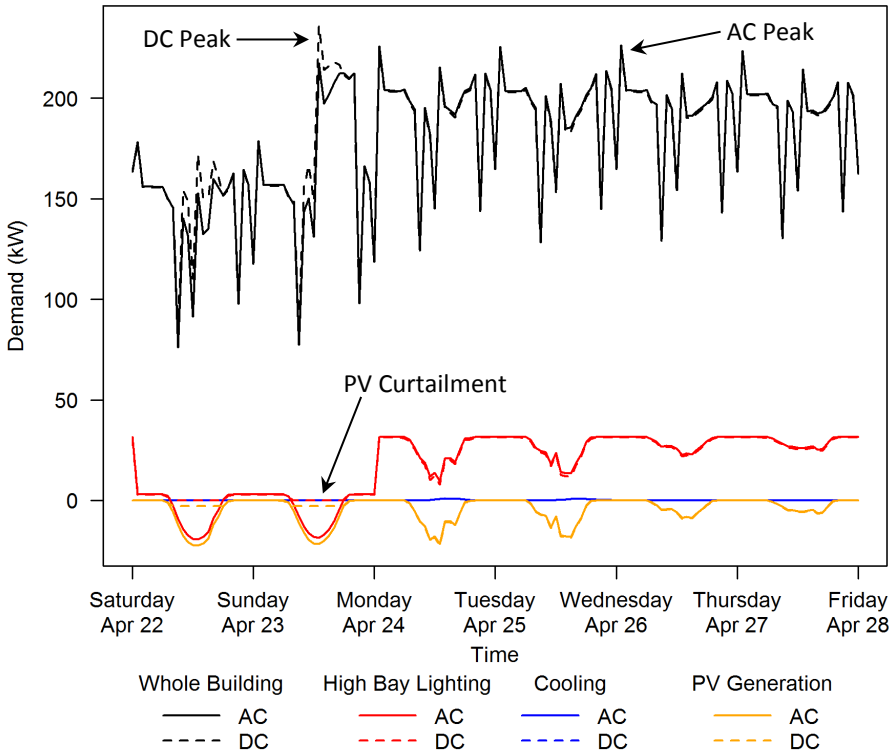

Figure 31. Example of peak demand increase due to different-day PV curtailment
Refrigerated warehouse, 6 a.m.–10 p.m. operation, 5 days/week, unidirectional DCMG, 100% nominal array scaling factor in Lynchburg, VA

NREL's demand analysis has some caveats pertaining to accuracy. EnergyPlus is not necessarily designed to precisely predict peak demand. In particular, the HVAC models used in the Commercial Reference Building Models rely on performance curves with part load ratios rather than explicit equipment cycling; this approach can fail to capture peak demand events produced by concurrent operation of HVAC equipment. In addition, the simulations used an hourly time step rather than the customary 15 minute averaging interval used by electric utilities to determine peak demand charges. However, given that the same assumptions and limitations apply equally to the AC baseline and Bosch DCMG models, the *difference* between the AC baseline and Bosch DCMG should be considered a more reliable metric than the absolute peak demand value of either case independently.

3.3.3 Uncertainty Analysis

The analysis combines results from three different modeling environments, each with associated uncertainty:

1. *Building models (EnergyPlus):* Although the Commercial Reference Building Models are heavily reviewed and have characteristics typical of real buildings, the models' energy performance nevertheless reflects the particular mechanical systems and equipment types specified in the design. Therefore, given the variety of mechanical systems specified in actual buildings, the models provide illustrative results only; they should not be used alone to predict performance gains for any specific building.

Uncertainty in the building models contributes to uncertainty in the DCMG analysis in two ways: uncertainty in the exact LPD scales the total lighting power for both the AC baseline and DCMG system types, and uncertainty in the HVAC system types and performance affects the impact of the lighting system on the whole building energy performance. The former has little impact on the comparison of the AC and DC systems, as scaling in the connected lighting load scales energy consumption in both systems and does not significantly alter Bosch DCMG performance. Conversely, the HVAC interactions have a strong impact on the site energy metrics. The site metrics should therefore be considered qualitatively less certain than the high bay lighting system metrics.

2. *PV models (SAM):* The PV models are not a significant source of uncertainty. First, SAM's flate-plate PV modeling engine is well-validated for commercial-scale systems—Freeman et al. (2013) report root-mean-squared errors under 5% for hourly energy data for most of the case studies considered. Second, predicted DC PV generation is identical for the AC baseline and Bosch DCMG, so any error scales both results. Changes in system loss for both the AC baseline and Bosch DCMG in response to small changes in the hourly generation are negligible.
3. *Electric power distribution system models (MATLAB):* The primary source of uncertainty in the electric power distribution system loss model is the quality of fit for the power loss in each system converter. Bias in the modeled converter losses also biases the comparison metrics between the AC baseline and Bosch DCMG systems. For several of the converters modeled for this analysis, there is significant uncertainty in the fitted model due to anomalies or measurement jitter (see Appendix C).

Because of the complexity of the converter models, direct calculation of the uncertainty was not possible. Instead, NREL performed a numerical uncertainty analysis for the retail building type in order to explore the impact of converter modeling error on Bosch DCMG performance claims. NREL examined eight scenarios for the retail building type:

- *Two DCMG types:* unidirectional with a 100% nominal array scaling factor and bidirectional with a 150% nominal array scaling factor
- *Two operating schedules:* 8 a.m.–8 p.m. and 24 hours/day
- *Two locations:* Phoenix, Arizona (a very sunny climate) and Seattle, Washington (a very cloudy climate).

For each case, NREL perturbed each converter model individually by introducing a bias in the modeled power loss equal to the standard error in the fitted power loss presented in Table C-3. For each perturbation, NREL generated a single simulation output and calculated the corresponding change in each of the lighting system performance metrics: energy intensity, energy efficiency, PV utilization fraction, and grid utilization fraction. This approach provided an estimate of the sensitivity of each metric with respect to the modeled converter power loss.[11]

[11] Because the modeled converter loss is biased in the same direction at every time step, this approach yields a worst-case estimate of the sensitivity. In practice, an unbiased model, such as the least-squares models used to fit converter loss, should average near-zero bias over many samples assuming normally distributed inputs. In other

In a linear system, the total variance in a calculation output is the sum of the variances with respect to each individual uncertain variable. Because the sensitivity analysis perturbed each uncertain variable (the various converter losses) by its corresponding standard error, the sensitivity analysis outputs provide an estimate of the transformed standard error for each metric. The estimate of the total variance is

$$\sigma^2 = \sum_i (x_0 - x_i)^2,$$

in which x_0 is the unperturbed metric and x_i represents the perturbed metric for each converter i. Although the converter power loss and performance metric calculations are nonlinear, the previous equation nevertheless provides a qualitative estimate of the overall uncertainty in each metric.

Using this approach, NREL estimated the total variance σ^2 and standard error σ for each metric under the eight scenarios described above. Tables 5–8 summarize the estimated standard errors and corresponding 95% confidence intervals for the true difference in each metric between the AC baseline and Bosch DCMG cases. Even with considerable uncertainty in some individual converter models, the uncertainty bands in the system metrics are sufficiently small to justify the claim that the Bosch DCMG significantly outperforms the AC baseline in all eight scenarios. Because of the similarity of the metrics across all the analysis cases, this result is also likely to be true for the other building types, locations, and operating schedules.

The uncertainty analysis conclusions depend on the assumption that the data used to fit the converter models accurately characterizes converter operation under real-world conditions, that is, that the mean and standard deviation in the power loss are similar to what would be encountered in the field. As discussed in Section 3.3.1, this may not be true for the converters selected for the analysis. NREL recommends that future work include calibration of the converter models using field measurements.

words, when summed over the entire year as is done in the metric calculations, the average error in converter loss should be approximately zero, which greatly mitigates the uncertainty.

Table 5. Uncertainty Analysis for Retail Building Type—Change in Grid Energy Intensity Compared to AC Baseline (kWh/ft^2/year)

DCMG Type	Array Size	Operating Schedule		Location	Value	Standard Error	95% Confidence Interval
Unidirectional	100%	8 a.m.–8 p.m.	7 days/week	Phoenix, AZ	−0.22	0.025	−0.27 to −0.17
				Seattle, WA	−0.18	0.026	−0.23 to −0.13
		24 hours/day	7 days/week	Phoenix, AZ	−0.22	0.029	−0.28 to −0.16
				Seattle, WA	−0.18	0.030	−0.24 to −0.13
Bidirectional	150%	8 a.m.–8 p.m.	7 days/week	Phoenix, AZ	−0.27	0.025	−0.31 to −0.22
				Seattle, WA	−0.22	0.025	−0.27 to −0.17
		24 hours/day	7 days/week	Phoenix, AZ	−0.27	0.028	−0.33 to −0.22
				Seattle, WA	−0.22	0.029	−0.28 to −0.17

Table 6. Uncertainty Analysis for Retail Building Type—Change in System Energy Efficiency Compared to AC Baseline (%)

DCMG Type	Array Size	Operating Schedule		Location	Value	Standard Error	95% Confidence Interval
Unidirectional	100%	8 a.m.–8 p.m.	7 days/week	Phoenix, AZ	4.38%	0.519%	3.37% to 5.40%
				Seattle, WA	3.64%	0.529%	2.60% to 4.67%
		24 hours/day	7 days/week	Phoenix, AZ	2.49%	0.331%	1.84% to 3.14%
				Seattle, WA	2.06%	0.340%	1.40% to 2.73%
Bidirectional	150%	8 a.m.–8 p.m.	7 days/week	Phoenix, AZ	5.38%	0.503%	4.39% to 6.36%
				Seattle, WA	4.43%	0.518%	3.42% to 5.45%
		24 hours/day	7 days/week	Phoenix, AZ	3.04%	0.318%	2.42% to 3.67%
				Seattle, WA	2.50%	0.331%	1.86% to 3.15%

Table 7. Uncertainty Analysis for Retail Building Type—Change in PV Utilization Fraction Compared to AC Baseline (fraction)

DCMG Type	Array Size	Operating Schedule		Location	Value	Standard Error	95% Confidence Interval
Unidirectional	100%	8 a.m.–8 p.m.	7 days/week	Phoenix, AZ	0.068	0.0029	0.062 to 0.073
				Seattle, WA	0.079	0.0033	0.072 to 0.085
		24 hours/day	7 days/week	Phoenix, AZ	0.068	0.0029	0.062 to 0.073
				Seattle, WA	0.078	0.0032	0.072 to 0.085
Bidirectional	150%	8 a.m.–8 p.m.	7 days/week	Phoenix, AZ	0.066	0.0026	0.061 to 0.071
				Seattle, WA	0.076	0.0029	0.070 to 0.081
		24 hours/day	7 days/week	Phoenix, AZ	0.067	0.0025	0.061 to 0.075
				Seattle, WA	0.075	0.0027	0.070 to 0.081

Table 8. Uncertainty Analysis for Retail Building Type—Change in Grid Utilization Fraction Compared to AC Baseline (fraction)

DCMG Type	Array Size	Operating Schedule		Location	Value	Standard Error	95% Confidence Interval
Unidirectional	100%	8 a.m.–8 p.m.	7 days/week	Phoenix, AZ	0.027	0.0069	0.013 to 0.040
				Seattle, WA	0.021	0.0062	0.009 to 0.033
		24 hours/day	7 days/week	Phoenix, AZ	0.012	0.0037	0.005 to 0.020
				Seattle, WA	0.011	0.0036	0.004 to 0.018
Bidirectional	150%	8 a.m.–8 p.m.	7 days/week	Phoenix, AZ	0.030	0.0083	0.014 to 0.047
				Seattle, WA	0.023	0.0067	0.010 to 0.036
		24 hours/day	7 days/week	Phoenix, AZ	0.012	0.0037	0.005 to 0.019
				Seattle, WA	0.011	0.0036	0.004 to 0.018

3.3.4 Curtailment Analysis

Among factors analyzed, PV curtailment caused the largest reductions in performance for the Bosch unidirectional DCMG. Weekend curtailment makes the Bosch unidirectional DCMG poorly suited for buildings that do not have continuous daily operation. In addition, although PV system oversizing does allow the PV system to fully meet the lighting load more often, it also causes significant curtailment during peak irradiance conditions.

Even buildings with continuous operations shut down occasionally. In the analysis, NREL modeled three shutdowns per year during major holidays (Thanksgiving, Christmas, and New Year's Day) for buildings with seven days per week operation. NREL found that in approximately one third of all seven days per week, 100% nominal array scaling factor simulations that experience curtailment, low load conditions during these three holidays accounted for 100% of total annual PV energy curtailed. In another one-third of the simulations, holiday curtailment accounts for at least half of the total annual PV energy curtailed. Overall, PV curtailment attributable to holiday operation ranged from 0.0% to approximately 0.8% of total annual PV production, with greater curtailment in sunnier locations.

These results illustrate the benefit of a bidirectional system—simply having the ability to export may avoid up to 0.8% lost annual energy due to curtailment. Alternatively, the results indicate the potential benefit of energy storage even for otherwise well-designed system. However, at curtailment levels below 1.0%, it is unlikely that the additional cost associated with adding bidirectional conversion or energy storage could be justified solely by eliminating curtailment.

4 Conclusion

NREL performed a simulation analysis of Robert Bosch LLC's DC microgrid platform for a variety of building types and operating conditions. The analysis results demonstrate that for buildings with continuous daily operation (seven days per week) the Bosch DCMG significantly improves the energy performance of the Bosch high bay LED lighting system compared to an AC baseline with equivalent LED light fixtures. The Bosch DCMG improved the fraction of PV energy that performs useful work from approximately 0.90 for the AC baseline to approximately 0.97 for the Bosch DCMG and improved lighting system annual energy efficiency from approximately 92% for the AC baseline to approximately 95% for the Bosch DCMG, with small variations in response to design parameters and operating conditions.

In addition, the Bosch DCMG indirectly benefits buildings by reducing cooling load and, if applicable, refrigeration load compared to the AC baseline. The Bosch DCMG reduces cooling load in two ways: it reduces overall waste energy from the lighting system and it shifts a portion of the waste energy from conditioned to unconditioned space. The reductions were most significant in hot, humid climates. Conversely, the loss of waste heat in the winter increased site natural gas consumption compared to the AC baseline, with the greatest increases in cold climates. In nearly all locations, the net indirect impact of the Bosch DCMG on site HVAC energy was a reduction of site energy compared to the AC baseline, with the strongest reductions in hot, humid, and sunny climates. The Bosch DCMG also reduced building monthly peak electricity demand in nearly all cases. The magnitude of this reduction varied significantly by building type, operating schedule, time of year, and geographic location.

The Bosch bidirectional DCMG, which allows export of surplus PV energy, performed well for all array sizes, building types, and building operating schedules. In contrast, the Bosch unidirectional DCMG performed well only for system designs and building operating schedules that did not result in significant curtailment of PV production; the Bosch unidirectional DCMG did not perform well for buildings with five days per week operation or buildings with significantly oversized PV systems relative to the connected lighting load.

More broadly, this analysis supports the larger body of evidence that DC distribution systems in commercial buildings can produce significant energy savings.[12] In principle, building-scale DC microgrids are not limited to lighting products. The energy savings are worth investigating for other DC load types, including telecommunication equipment, variable frequency motor drives, and consumer electronic loads.

4.1 Recommended Future Work

This analysis raised several key questions that NREL recommends as topics for future research. These include:

1. *Is the DCMG energy model valid for real systems?* Due to budgetary constraints, time constraints, and a lack of available data, NREL did not perform a detailed verification of the Bosch DCMG energy model as part of this analysis. NREL recommends

[12] See, for instance, the analysis provided in (Savage, Nordhaus, and Jamieson 2010) and (AlLee and Tschudi 2012) and the case studies documented by Nextek Power Systems (http://www.nextekpower.com/case-studies).

performing a detailed model validation study in the future in order to both increase model fidelity and increase community confidence in the energy savings predictions. The study should include converter model calibration and validation using independent data sets.

2. *Can a simpler DCMG model accurately predict energy savings?* For the analysis, NREL used high-fidelity models which required multiple modeling environments and significant computation time. However, the predicted savings were remarkably similar to the rough estimate developed in Section 1.2. Development and validation of a simple, computationally-efficient model would allow rapid estimates of energy savings, enabling streamlined tools for customer interaction, such as website calculators.
3. *Are the indirect benefits of the Bosch DCMG for refrigerated warehouses greater than the model used in this analysis suggests?* Given the limitations of the way the lighting system interacts with the refrigerated cases in the refrigerated warehouse model used in this analysis, the model results may not accurately predict the indirect energy benefits of using high efficiency DC drivers for refrigerated warehouse lighting systems. If refrigerated warehouses are of specific interest, NREL recommends that future work include development of a more sophisticated refrigerated warehouse model that properly applies lighting load heat gains directly to the refrigeration system. However, modifying EnergyPlus to properly model this interaction will be difficult and time consuming, so this may be a lower priority task.
4. *What is the technical potential of DC distribution in general?* This analysis focused on Bosch's DCMG platform and anticipated product offerings. Therefore, NREL intentionally limited the analysis to LED lighting systems and included non-ideal effects, such as converter size mismatch, that can be overcome with engineering design optimization. However, an analysis that treats DC distribution systems of this type in a broader context would be of general interest. Such an analysis could predict DC distribution benefits for more technologies and could analyze potential savings using implementation-agnostic methods.

Addressing these questions will foster greater confidence in the energy benefits of Bosch's DCMG platform and of DC distribution in general as well as further the DC power technology industry and research communities' understanding of DC systems.

References

AlLee, G., Tschudi, W. (2012). "Edison Redux: 380 Vdc Brings Reliability and Efficiency to Sustainable Data Centers." *IEEE Power and Energy Magazine* (10:6); pp. 50-59.

Deru, M., et al. (2011). *U.S. Department of Energy Commercial Reference Building Models of the National Building Stock.* NREL/TP-5500-46861. Golden, CO: National Renewable Energy Laboratory. Accessed Mar. 18, 2015: http://www.nrel.gov/docs/fy11osti/46861.pdf

EMerge Alliance. (2012). *EMerge Alliance Occupied Space Standard Version 1.1.* San Ramon, CA: EMerge Alliance.

EnergyPlus Energy Simulation Software, Version 8.1. (2013). Washington, D.C.: U.S. Department of Energy. Accessed Dec. 8, 2014: http://apps1.eere.energy.gov/buildings/energyplus/

Frank, S., Rebennack, S. (2015). "Optimal design of mixed AC-DC distribution systems for commercial buildings: A Nonconvex Generalized Benders Decomposition approach." *European Journal of Operational Research* (242:3), pp. 710-729.

Freeman, J., Whitmore, J., Kaffine, L., Blair, N., Dobos, A. P. (2013). *System Advisor Model: Flat Plate Photovoltaic Performance Modeling Validation Report.* NREL/TP-6A20-60204. Golden, CO: National Renewable Energy Laboratory. Accessed Jan. 27, 2015: http://www.nrel.gov/docs/fy14osti/60204.pdf

"Inverter Performance Test Summaries." (2015). California Energy Commission. Accessed: Jan. 27, 2015: http://www.gosolarcalifornia.ca.gov/equipment/inverter_tests/summaries/

Judkoff, R., Neymark, J. (1995). *International Energy Agency Building Energy Simulation Test (BESTEST) and Diagnostic Method.* NREL/TP-472-6231. Golden, CO: National Renewable Energy Laboratory. Accessed Mar. 18, 2015: http://www.nrel.gov/docs/legosti/old/6231.pdf

King, D. L., Gonzalez, S., Galbraith, G. M., Boyson, W. E. (2007). *Performance Model for Grid-Connected Photovoltaic Inverters.* SAND2007-5036. Albuquerque, NM: Sandia National Laboratories. Accessed Mar. 18, 2015: http://prod.sandia.gov/techlib/access-control.cgi/2007/075036.pdf

Lopez, A. (2011). *U.S. TMY3 Boundaries (PDF).* Golden, CO: National Renewable Energy Laboratory. Accessed Mar. 18, 2015: http://en.openei.org/w/index.php?title=File:NREL-tmy3-boundary-01.pdf

MATLAB Release 2014b. (2014). Software. Natick, MA: The MathWorks, Inc.

Sannino, A., Postiglione, G., Bollen, M. H. (2003). "Feasibility of DC network for commercial facilities." *IEEE Transactions on Industry Applications* (39:5), pp. 1499-1507.

Savage, P., Nordhaus, R. R., Jamieson, S. (2010). DC Microgrids: Benefits and Barriers. In L. Parker, R. Maxwell, B. Gentry, M. Wilder, R. Saines, J. Cameron (Eds.), *From Silos to Systems:*

Issues in Clean Energy & Climate Change. New Haven, CT: Yale School of Forestry & Environmental Studies, pp. 51-66. Accessed Jan. 27, 2015: http://environment.research.yale.edu/publication-series/climate_change/5981

System Advisor Model Version 2014.11.24 (SAM 2014.11.24). (2014). Software. Golden, CO: National Renewable Energy Laboratory. Accessed Dec. 8, 2014: https://sam.nrel.gov/

Whitaker, J. (2015). "Basemap Matplotlib Toolkit 1.0.8 documentation." Accessed Jan. 27, 2015: http://matplotlib.org/basemap/

Wilcox, S., Marion, W. (2008). *User Manual for TMY3 Data Sets.* NREL/TP-581-43156. Golden, CO: National Renewable Energy Laboratory. Accessed Mar. 18, 2015: http://www.nrel.gov/docs/fy08osti/43156.pdf

Appendix A: Building Model Inputs and Assumptions

This appendix provides details for the building models described in Section 2.2.1, including input data and modeling assumptions.

Refrigerated Warehouse

The Commercial Reference Building warehouse model best represents non-refrigerated warehouses. To develop the refrigerated warehouse model, NREL added a large walk-in freezer to the bulk storage zone and a large walk-in cooler to the fine storage zone of the Commercial Reference Building warehouse model. In reality, a refrigerated warehouse is itself a large walk-in cooler/freezer (with the walls exposed directly to the outdoors). However, in the interest of expediency, the approximation of inserting walk-in boxes inside the warehouse is sufficient for understanding lighting load.

In the NREL-developed model, the walk-in freezer and cooler comprised the entire volume of the bulk storage and fine storage zones, respectively. To determine the load, NREL assumed a load of 15 Btu/h per square foot of exposed surface for each walk-in and that the refrigerant would be R-404a.[13] The model includes two compressor racks: a low-temperature rack for the walk-in freezer and a medium temperature rack for the walk-in cooler. Each rack is matched to air-cooled condensers assuming a total heat of rejection multipliers based on the design temperature (Table A-1 and Table A-2). These multipliers scale the size of the condenser based on the design temperature.

Table A-1. Assumed Low Temperature Heat Rejection Multipliers Based on Design Temperature

Design Temperature	Multiplier	Design Temperature	Multiplier
65°F	1.38	100°F	1.60
70°F	1.42	105°F	1.63
75°F	1.44	110°F	1.65
80°F	1.48	115°F	1.70
85°F	1.51	120°F	1.73
90°F	1.55	125°F	1.76
95°F	1.58		

[13] NREL made these assumptions in the interest of expediency given a limited time and budget for refrigerated warehouse model development.

Table A-2. Assumed Medium Temperature Heat Rejection Multipliers Based on Design Temperature

Design Temperature	Multiplier	Design Temperature	Multiplier
65°F	1.18	100°F	1.31
70°F	1.20	105°F	1.33
75°F	1.22	110°F	1.35
80°F	1.24	115°F	1.37
85°F	1.26	120°F	1.39
90°F	1.28	125°F	1.41
95°F	1.30		

NREL assumed off-cycle defrost that operates twice a day. The walk-in freezer has defrost start times of 9 a.m. and 9 p.m. with 45 minute duration and a five minute drip down. The walk-in cooler has defrost start times of 1 a.m. and 1 p.m. with one hour duration and no drip-down time. Lastly, NREL used a 6.25% door open schedule from 6 a.m. to 10 p.m. that is pre-encoded in the EnergyPlus walk-in cooler object; this schedule was deemed adequate for the analysis.

Operating Hours, Schedules, and Holidays

For this study, NREL greatly simplified the schedules for lighting, occupancy, and plug loads within the reference building models. NREL uses a simplified schedule approach to better investigate the impact of operating schedules on the Bosch high bay lighting technology, which typically operates in either an on or an off state (dimming is limited). The list below shows the operating hours that NREL investigated for each building type:

- Stand-alone retail
    - Occupied from 8 a.m. to 8 p.m. 7 days/week
    - Occupied 24 hours/day, 7 days/week.
- Supermarket
    - Occupied from 6 a.m. to 10 p.m. 7 days/week
    - Occupied 24 hours/day, 7 days/week.
- Warehouse (both refrigerated and non-refrigerated)
    - Occupied from 6 a.m. to 10 p.m. 5 days/week
    - Occupied from 6 a.m. to 10 p.m. 7 days/week
    - Occupied 24 hours/day, 5 days/week
    - Occupied 24 hours/day, 7 days/week.

NREL modified the following non-binary schedules to match these operating hours: plug load schedules, lighting schedules, occupancy schedules, and thermostat set points. There are many binary (on/off) schedules in the models that control equipment such as outdoor air dampers; such

schedules are "on" when the building is occupied and "off" when the building is unoccupied. The plug load, lighting, and occupancy schedules, however, are specified as a fraction of peak load (connected load). NREL adjusted the fractions schedules as follows:

- *Plug loads:* 0.8 during occupied hours, 0.2 during unoccupied hours
- *Lighting:* 1.0 during occupied hours, 0.1 during unoccupied hours
- *Occupancy:* 0.8 during occupied hours, 0.0 during unoccupied hours.

The thermostat set points for all models are 70°F (heating) and 75°F (cooling) during occupied hours, 60°F (heating) and 86°F (cooling) during unoccupied hours. Finally, a few of the models have zones that are semi-conditioned (not cooled, heated only to 55°F). For these zones, the thermostat schedules remain as originally specified in the Reference Building Model.

In the different operating hours listed above, there are both 5 day/week and 7 day/week operating schedules. For 5 day/week operation, there are 10 annual holidays; for 7 day/week operation, there are 3 annual holidays (Table A-3). During a holiday in the simulation, all schedules take their unoccupied value for the entire day.

Table A-3. Assumed Holidays for 5 Day/Week and 7 Day/Week Operating Schedules

Holiday	Date	5 day/week	7 day/week
New Year's Day	January 1	✓	✓
MLK Day	Third Monday in January	✓	
Presidents' Day	Third Monday in February	✓	
Memorial Day	Last Monday in May	✓	
Independence Day	July 4	✓	
Labor Day	First Monday in September	✓	
Columbus Day	Second Monday in October	✓	
Veterans Day	November 11	✓	
Thanksgiving	Fourth Thursday in November	✓	✓
Christmas	December 25	✓	✓

Location-Specific Modifications

For each geographic location, NREL made the following modifications to each model based on the TMY3 climate data:

- Set site-specific latitude, longitude, time zone, and elevation.
- Changed floor construction in all models to use F-Factors (F-0.73) from ASHRAE Standard 90.1-2004 rather than estimating location-specific ground temperatures.

(Determining the monthly average ground temperature for each of the 554 locations would be too time-consuming.)

- Set the design day information for sizing HVAC equipment and refrigeration condensers.
- Estimated water mains temperatures based on annual average outdoor air temperature and the maximum difference in monthly average outdoor air temperature. The outdoor air temperature values were taken directly from the STAT file that comes packaged with the EnergyPlus EPW weather file; EnergyPlus uses an internal algorithm to derive water mains temperatures from these data.

Sixty locations did not include design day information with the TMY3 weather data. For these locations, NREL used design day data from the nearest neighbor site with similar elevation in the same climate zone.

Lighting Power Densities

As a starting point, NREL selected the maximum LPD for each zone allowed by ASHRAE 90.1-2013. The values range from 0.58 W/ft² for bulk storage to 1.44 W/ft² for sales areas. The LPDs in the standard were derived using typical source type and efficacy, coefficient of utilization, and light loss factors for each space type. Fixture descriptions for the typical lighting design are:

- *Retail display space:* U-shaped fluorescent 2 ft by 2 ft recessed troffer
- *Storage space:* Linear fluorescent industrial strip fixture
- *Lobby:* Compact fluorescent downlight.

For this study, NREL applied identical assumptions to develop lighting designs for the different space types used in the retail, supermarket, and warehouse models, which is consistent with the approach used in the standard. (However, NREL did not address the impact of accent or other specialty lighting that is discussed in the standard as the LPD impact is minimal.) NREL approximated the typical fluorescent fixture efficacy by sampling real products that match the ASHRAE 90.1-2013 description. NREL used the higher end of the efficacy range found to represent a conservative energy savings case when replaced by LED, although the variation in efficacy among products was not wide.

To estimate the LED replacement fixture efficacy, NREL again sampled real products that could serve as a replacement in a field demonstration. To determine fixture selection, NREL assumed that the following characteristics remain constant:

- Occupant need (illuminance criteria)
- Room characteristics (room surface color, shape, etc.)
- Environment-related light loss factors (space temperature, room and luminaire dirt depreciation, etc.).[14]

Given these criteria, NREL selected replacement fixtures based on comparable lumen output (accounting for improved lumen maintenance of LED sources) and distribution. NREL used the

[14] The impact of these characteristics is negligible compared to the variability in efficacy among LED fixtures surveyed.

lower end of the efficacy range found to represent a conservative energy savings case when compared to a typical fluorescent fixture (ASHRAE 90.1-2013 allowance), although the variation in efficacy among LED products was not wide.

NREL computed the efficacy ratio for each replacement and used the ratio to derive a reduction multiplier for zone LPD. The resulting multipliers range from 0.73 for the retail spaces to 0.92 for the storage spaces (Table 3). The range shows that strip fixtures already have a high efficacy and therefore offer less opportunity for lighting type related energy savings than retail space replacement. These results assume that the LED replacement fixture for the retail space has high visual quality (e.g., glare mitigation). This assumption was not thoroughly examined and could impact the practicality of the energy savings potential demonstrated by the LPD multiplier.

Appendix B: Photovoltaic Model Inputs and Assumptions

This appendix documents the modeling approach and assumptions used to develop the PV array models described in Section 2.2.2.

PV Array Sizing

For each combination of building type and PV array scaling factor, the target array size equals the connected (peak) high bay lighting load multiplied by the scaling factor. This philosophy extends from the sizing criteria for the current unidirectional Bosch DCMG prototype, in which the PV array is sized to never exceed the lighting load (representing a scaling factor of 1.0). Table B-1 displays the resulting array size targets.

Table B-1. Target PV Array Sizes for Each Building Type and Array Scaling Factor

Building Type	Connected Lighting Load	*Target PV Array Size for Each Array Scaling Factor*				
		100%	125%	150%	200%	250%
Retail	96,022 W	96,022 W	120,028 W	144,034 W	192,045 W	240,056 W
Supermarket	43,143 W	43,143 W	53,929 W	64,715 W	86,286 W	107,858 W
Warehouse	31,517 W	31,517 W	39,396 W	47,275 W	63,033 W	78,792 W

For each target in Table B-1, NREL developed a baseline array design using SolarWorld SW 270 monocrystalline PV modules (270 W) and ABB/Power-One PVI-10.0-I PV inverters (480 V, 10 kW) using the following process:

1. *String sizing:* NREL sized each array string to yield a nominal maximum power point string voltage as close as possible to 350 V (the nominal Bosch DCMG voltage and the optimal string voltage for the PVI-10.0-I inverter). For the selected PV panels, this yielded a string size of 11, a nominal voltage of 339.9 V, and a nominal string wattage of 2,992 W.
2. *Modules per inverter:* NREL selected the greatest number of strings that can be simultaneously paralleled within a limit up to 1.1 the DC input capacity of the selected inverter. The maximum DC to AC ratio of 1.1 was derived from SAM modeling defaults. For the selected inverter/panel combination, this yielded three strings per panel, for a nominal array size per panel of 8,976 W (33 panels) and an actual DC to AC ratio of 0.898.
3. *Total array size and number of inverters:* Using building blocks of 8,976 W nominal, NREL then computed the derated array size and corresponding number of inverters that meets the target array size from Table B-1. For the unidirectional cases (100% and 125%), NREL sized the array such that it did not exceed the target, that is, NREL rounded the number of inverters down. This was done to minimize the potential for excessive curtailment of PV generation. For the bidirectional cases (150%, 200%, and

250%), NREL rounded to the nearest whole inverter. NREL assumed a derating factor of 0.9556, consistent with SAM defaults.

Table B-2 displays the nominal array sizes resulting from this process. (Derated array sizes are 0.9556 times the nominal sizes.) Table B-3 displays the resulting mismatch (with respect to the derated array sizes).

Table B-2. Actual PV Array Sizes for Each Building Type and Array Scaling Factor

Building Type	*Actual PV Array Size for Each Array Scaling Factor*				
	100%	125%	150%	200%	250%
Retail	98,736 W	116,688 W	152,592 W	197,472 W	251,328 W
Supermarket	44,880 W	53,856 W	71,808 W	89,760 W	116,688 W
Warehouse	26,928 W	35,904 W	53,856 W	62,832 W	80,784 W

Table B-3. PV Array Size Mismatch for Each Building Type and Array Scaling Factor

Building Type	*PV Array Size Mismatch for Each Array Scaling Factor*				
	100%	125%	150%	200%	250%
Retail	−1.7%	−7.1%	1.2%	−1.7%	0.0%
Supermarket	−0.6%	−4.6%	6.0%	−0.6%	3.4%
Warehouse	−18.4%	−12.9%	8.9%	−4.7%	−2.0%

Array mismatch ranges from −18.4% to 8.9%, depending on the building type and scaling factor. The warehouse cases had the smallest target array sizes and therefore the experienced the worst mismatch. Some array mismatch is unavoidable when using discrete inverter and panel string sizes, but selection of a smaller baseline inverter would have improved the mismatch. NREL elected not to change the baseline inverter because the 10 kW model selected is a better match to the anticipated converter size and efficiency of Bosch's DCMG products (see Appendix C).

Table B-4 displays the number of inverters. The number of PV panels per system equals 33 times the number of inverters.

Table B-4. Number of PV Inverters for Each Building Type and Array Scaling Factor

Building Type	*Number of Inverters for Each Array Scaling Factor*				
	100%	125%	150%	200%	250%
Retail	11	13	17	22	28
Supermarket	5	6	8	10	13
Warehouse	3	4	6	7	9

Location-Specific Models

NREL implemented a seed model for each array in SAM using the string size, number of inverters, and total array size developed above. From the seed models, NREL generated PV models for each geographic location by making the following modifications:

- Set site-specific latitude, longitude, time zone, and elevation
- Modify array tilt angle to match the latitude (to the nearest 5° increment)
- Load site-specific weather data from the corresponding TMY3 file.

Appendix C: Electricity Distribution Efficiency Model Inputs and Assumptions

This appendix documents the modeling approach and assumptions used to develop the AC baseline and Bosch DCMG electric power distribution system models described in Section 2.2.3.

Converter Models

NREL fitted converter models for the analysis from publicly available data (California Energy Commission 2015) and using measured and simulated characterization data supplied by Bosch (Table C-1, Table C-2).

Table C-1. Converters Selected for AC Baseline Models

Converter	Manufacturer/Model	Power Rating	Data Source
PV inverter	ABB/Power-One PVI-10.0-I	10 kW	CEC Inverter Database
AC LED driver	Inventronics 200 W	204 W	Lab Measurements (supplied by Bosch)

Table C-2. Converters Selected for Bosch DCMG Models

Converter	Manufacturer/Model	Power Rating	Data Source
Gateway rectifier (AC/DC)	Emerson 15 kW	15 kW	Lab Measurements (supplied by Bosch)
Gateway inverter (DC/AC)	ABB/Power-One PVI-10.0-I	10 kW	CEC Inverter Database
DC LED driver	Bosch proprietary	200 W	Simulation (supplied by Bosch)

NREL developed models of the form given in Section 2.2.3 for each converter:

- Output-referenced models for the PV inverter, gateway rectifier, gateway inverter, and DC LED driver
- Input-referenced models for the gateway inverter and AC LED driver.

The AC LED driver model excluded voltage terms β_4–β_6, as voltages on both side of the converter are assumed to be approximately constant (and, in any case, voltage data was not available). The PV inverter and gateway inverter models are the same; Bosch intends to use the ABB/Power-One PVI-10.0-I or a similarly performing inverter model in the Bosch DCMG bidirectional gateway. For the gateway inverter, NREL used the input-referenced models in most circumstances but used the output-referenced model when curtailment occurred. The two models matched within 0.1% in all instances when PV curtailment occurred.

Table C-3 summarizes the error metrics for the power loss model and, by extension, the efficiency model for each converter. The power loss error metrics are given in per-unit (pu); that is, as a ratio with respect to the rated power of the converter. No power loss models have an inherent bias because all model coefficients were determined using linear least squares. The

efficiency models are derived from the power loss models and display some bias due to the nonlinearity of the transformation. However, NREL used the power loss model in all calculations; the uncertainty in the efficiency model is provided for reference only.

Table C-3. Error Metrics for Converter Models Used in the Analysis

	Power Loss		*Efficiency*	
Converter	**Bias Error**	**Standard Error**	**Bias Error**	**Standard Error**
PV inverter	0.0000 pu	0.0006 pu	0.00%	0.14%
AC LED driver	0.0000 pu	0.0024 pu	0.21%	1.06%
Gateway rectifier (AC/DC)	0.0000 pu	0.0021 pu	−0.06%	1.46%
Gateway inverter (DC/AC)	0.0000 pu	0.0006 pu	0.00%	0.14%
DC LED driver	0.0000 pu	0.0012 pu	−0.01%	0.26%

Figures C-1 through C-4 display the fitted efficiency model for each converter. (The ABB/Power-One PVI-10.0-I model applies to both the AC baseline PV inverter and the Bosch DCMG gateway inverter.) Two key pieces of information are required in order to adequately interpret the plots:

1. For converter models which include voltage effects, the fitted model plots show only the nominal, minimum, and maximum voltages used in model fitting to reduce clutter in the plot.[15] In some cases, this approach makes the model appear slightly biased due to poor performance at extreme voltages. However, the residual error plots display all data points, including for voltages not shown in the fitted model plots.
2. The efficiency models and plots are derived nonlinearly from the loss models and plots, and are not necessarily unbiased. However, NREL used the fitted power loss models directly in all calculations; the derived efficiency models are for reference only.

[15] The three separate curves are presented for subsets of the fitted data for visualization purposes; there is only a single underlying model for all three curves.

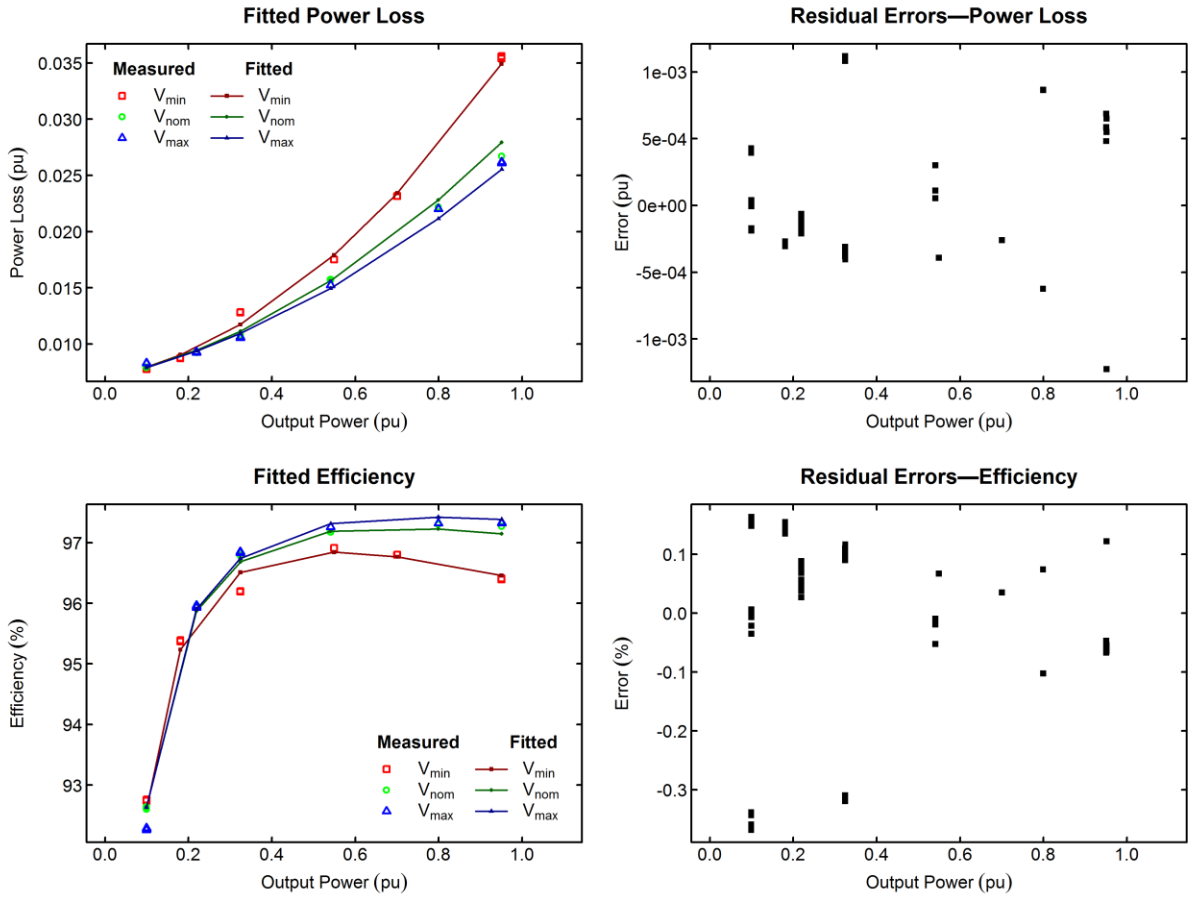

Figure C-1. Fitted model for ABB/Power-One PVI-10.0-I PV inverter

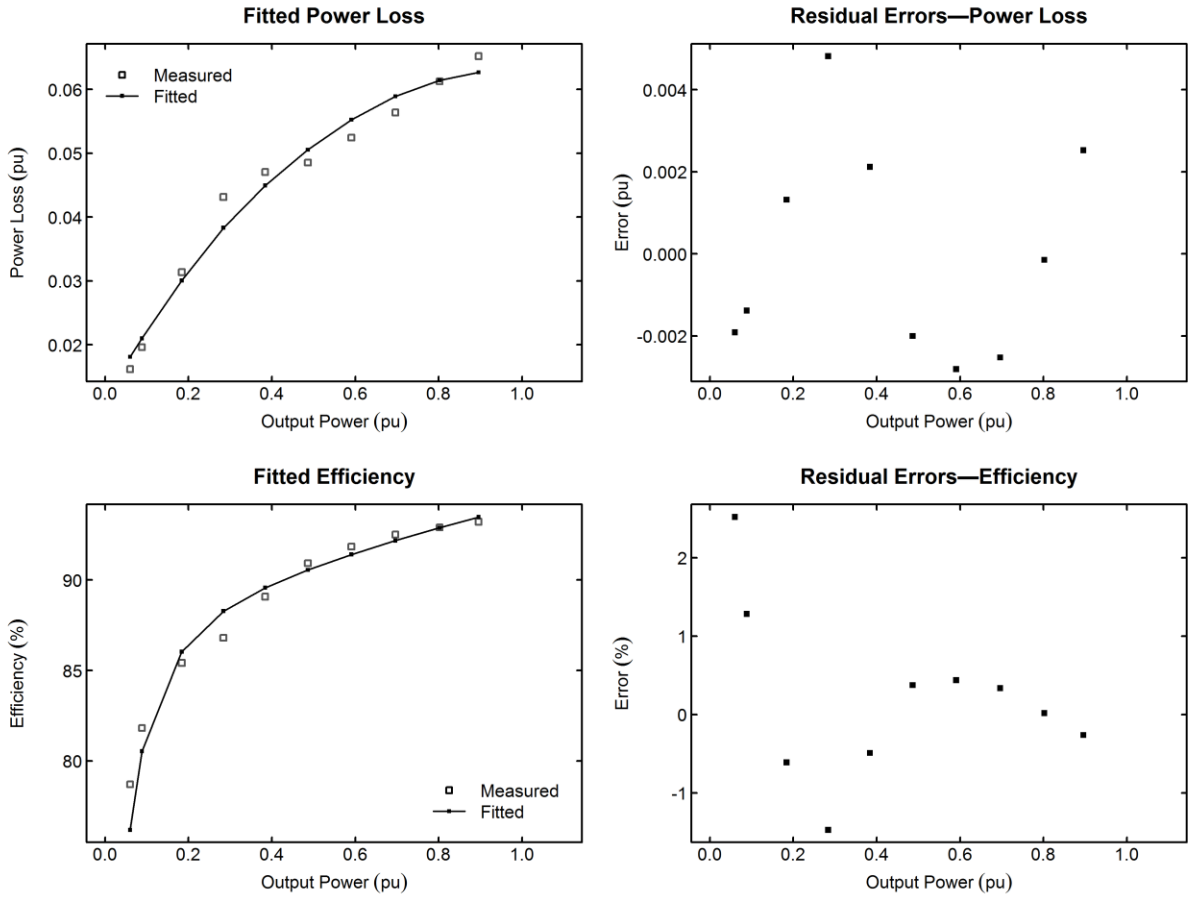

Figure C-2. Fitted model for Inventronics 200 W AC LED driver

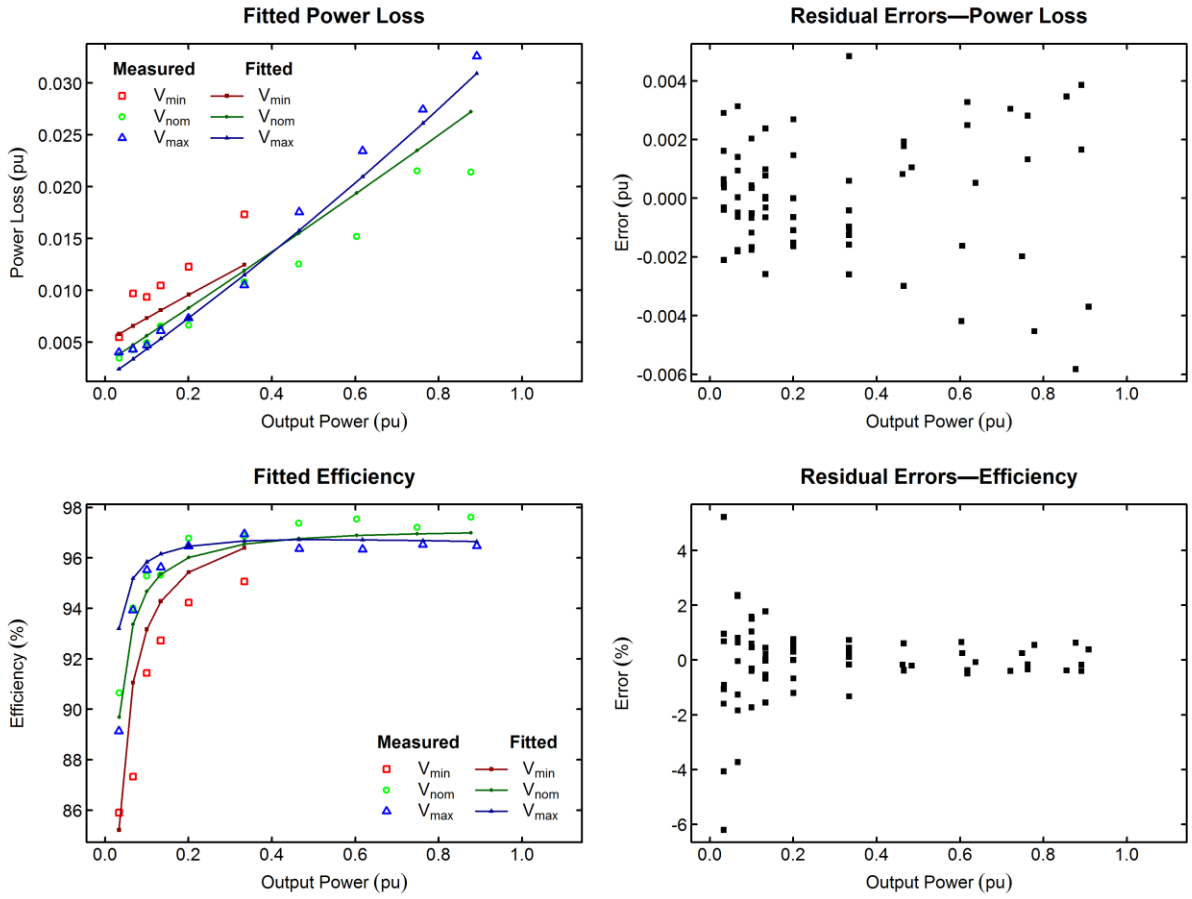

Figure C-3. Fitted model Emerson 15 kW gateway rectifier

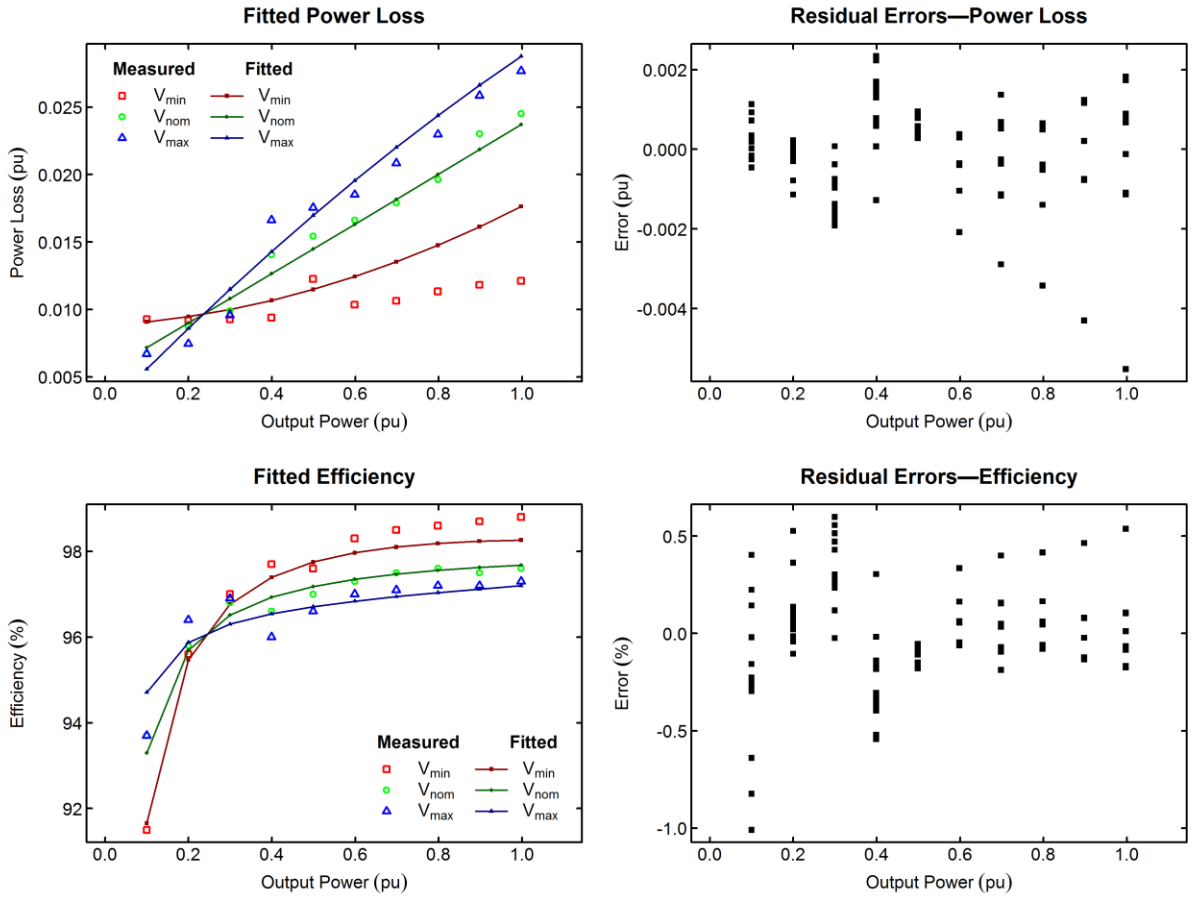

Figure C-4. Fitted model for Bosch DC LED driver

There is noticeable scatter in the Emerson 15 kW gateway rectifier model; this may indicate noisy measurements or an unknown forcing function (such as ambient temperature). This scatter reduces model the quality of the model fit. In addition, both the AC and DC LED driver models display dips in efficiency around 30% to 40% loading; these anomalies reduce the quality of fit for the corresponding converter models. However, the driver models are reasonably accurate for both high and low loads at typical operating voltage, which are the load levels used in the analysis (see Appendix A).

Bosch DCMG Sizing

As described in Section 2.2.3, NREL determined the number and nominal size of the Bosch DCMG gateway rectifiers based on the connected DC load and the DC array size. Because the connected load for each building did not perfectly align with the rectifier sizing increment, this process resulted in oversized rectifier configurations (significantly so in the warehouse case). Table C-4 displays the Bosch DCMG gateway rectifier sizing.

Table C-4. Gateway Rectifier Sizing

Building Type	Connected DC Load	Gateway Rectifier Size	Number of Gateways	Total Rectifier Size	Percent Oversize
Retail	93,142 W	60,000 W	2	120,000 W	25.0%
Supermarket	41,849 W	45,000 W	1	45,000 W	4.3%
Warehouse	30,571 W	45,000 W	1	45,000 W	42.8%

For the Bosch bidirectional DCMG analysis cases (150%, 200%, and 250% PV array scaling factors), the number of inverters is sized to the difference between the connected DC load (Table C-4) and the PV array size (Table B-2). Table C-5 displays the resulting system sizing.

Table C-5. DCMG Gateway Inverter Capacity for Each Building Type and Array Scaling Factor

Building Type	Number of Inverters per Gateway			Total Inverter Capacity		
	150%	200%	250%	150%	200%	250%
Retail	3	6	8	60,000 W	120,000 W	160,000 W
Supermarket	3	5	8	30,000 W	50,000 W	80,000 W
Warehouse	3	4	6	30,000 W	40,000 W	60,000 W

Appendix D: Analysis Summary Tables

Tables D-1 through D-11 (following pages) summarize the performance of the Bosch DCMG relative to the AC baseline for the seven performance metrics presented in Section 2.3. The data are the same as presented graphically in Figures 7–14.

Table D-1. Analysis Results—Average Change in System Grid Energy Intensity for Bosch DCMG Compared to AC Baseline (kWh/ft^2/year)

Building Type	Operating Schedule		Change in Grid Energy Intensity by Case				
			100%	125%	150%	200%	250%
Refrigerated Warehouse	6 a.m.–10 p.m.	5 days/week	0.08	0.15	−0.10	−0.12	−0.14
Refrigerated Warehouse	6 a.m.–10 p.m.	7 days/week	−0.12	−0.13	−0.16	−0.17	−0.18
Refrigerated Warehouse	24 hours/day	5 days/week	0.08	0.15	−0.10	−0.12	−0.14
Refrigerated Warehouse	24 hours/day	7 days/week	−0.12	−0.13	−0.16	−0.17	−0.18
Retail	8 a.m.–8 p.m.	7 days/week	−0.19	−0.18	−0.24	−0.26	−0.27
Retail	24 hours/day	7 days/week	−0.19	−0.19	−0.24	−0.26	−0.28
Supermarket	6 a.m.–10 p.m.	7 days/week	−0.20	−0.19	−0.25	−0.27	−0.28
Supermarket	24 hours/day	7 days/week	−0.20	−0.19	−0.25	−0.26	−0.28
Warehouse	6 a.m.–10 p.m.	5 days/week	0.08	0.15	−0.10	−0.12	−0.14
Warehouse	6 a.m.–10 p.m.	7 days/week	−0.12	−0.13	−0.16	−0.17	−0.18
Warehouse	24 hours/day	5 days/week	0.08	0.15	−0.10	−0.12	−0.14
Warehouse	24 hours/day	7 days/week	−0.12	−0.13	−0.16	−0.17	−0.18

Table D-2. Analysis Results—Average Change in System Energy Efficiency for Bosch DCMG Compared to AC Baseline (%)

Building Type	Operating Schedule		*Change in System Energy Efficiency by Case*				
			100%	**125%**	**150%**	**200%**	**250%**
Refrigerated Warehouse	6 a.m.–10 p.m.	5 days/week	−2.48%	−4.51%	3.06%	3.77%	4.51%
Refrigerated Warehouse	6 a.m.–10 p.m.	7 days/week	2.84%	3.10%	3.88%	4.05%	4.30%
Refrigerated Warehouse	24 hours/day	5 days/week	−1.81%	−3.32%	2.21%	2.73%	3.26%
Refrigerated Warehouse	24 hours/day	7 days/week	2.00%	2.19%	2.73%	2.86%	3.04%
Retail	8 a.m.–8 p.m.	7 days/week	3.83%	3.69%	4.76%	5.13%	5.41%
Retail	24 hours/day	7 days/week	2.18%	2.13%	2.68%	2.90%	3.09%
Supermarket	6 a.m.–10 p.m.	7 days/week	3.12%	2.92%	3.87%	4.14%	4.40%
Supermarket	24 hours/day	7 days/week	2.21%	2.07%	2.74%	2.93%	3.12%
Warehouse	6 a.m.–10 p.m.	5 days/week	−2.48%	−4.51%	3.06%	3.77%	4.51%
Warehouse	6 a.m.–10 p.m.	7 days/week	2.84%	3.10%	3.88%	4.05%	4.30%
Warehouse	24 hours/day	5 days/week	−1.81%	−3.32%	2.21%	2.73%	3.26%
Warehouse	24 hours/day	7 days/week	2.00%	2.19%	2.73%	2.86%	3.04%

Table D-3. Analysis Results—Average Change in PV Utilization Fraction for Bosch DCMG Compared to AC Baseline (fraction)

Building Type	Operating Schedule		*Change in PV Utilization Fraction by Case*				
			100%	**125%**	**150%**	**200%**	**250%**
Refrigerated Warehouse	6 a.m.–10 p.m.	5 days/week	−0.157	−0.179	0.032	0.040	0.041
Refrigerated Warehouse	6 a.m.–10 p.m.	7 days/week	0.072	0.067	0.067	0.063	0.054
Refrigerated Warehouse	24 hours/day	5 days/week	−0.157	−0.179	0.032	0.040	0.041
Refrigerated Warehouse	24 hours/day	7 days/week	0.072	0.067	0.067	0.063	0.054
Retail	8 a.m.–8 p.m.	7 days/week	0.070	0.058	0.069	0.062	0.054
Retail	24 hours/day	7 days/week	0.071	0.060	0.069	0.062	0.054
Supermarket	6 a.m.–10 p.m.	7 days/week	0.071	0.055	0.068	0.061	0.053
Supermarket	24 hours/day	7 days/week	0.071	0.055	0.068	0.061	0.053
Warehouse	6 a.m.–10 p.m.	5 days/week	−0.157	−0.179	0.032	0.040	0.041
Warehouse	6 a.m.–10 p.m.	7 days/week	0.072	0.067	0.067	0.063	0.054
Warehouse	24 hours/day	5 days/week	−0.157	−0.179	0.032	0.040	0.041
Warehouse	24 hours/day	7 days/week	0.072	0.067	0.067	0.063	0.054

Table D-4. Analysis Results—Average Change in Grid Utilization Fraction for Bosch DCMG Compared to AC Baseline (fraction)

Building Type	Operating Schedule		*Change in Grid Utilization Fraction by Case*				
			100%	125%	150%	200%	250%
Refrigerated Warehouse	6 a.m.–10 p.m.	5 days/week	0.020	0.020	0.021	0.022	0.023
Refrigerated Warehouse	6 a.m.–10 p.m.	7 days/week	0.016	0.017	0.017	0.018	0.018
Refrigerated Warehouse	24 hours/day	5 days/week	0.013	0.013	0.013	0.013	0.013
Refrigerated Warehouse	24 hours/day	7 days/week	0.011	0.011	0.011	0.011	0.011
Retail	8 a.m.–8 p.m.	7 days/week	0.023	0.023	0.025	0.027	0.028
Retail	24 hours/day	7 days/week	0.011	0.011	0.011	0.011	0.011
Supermarket	6 a.m.–10 p.m.	7 days/week	0.017	0.017	0.018	0.018	0.019
Supermarket	24 hours/day	7 days/week	0.011	0.011	0.011	0.011	0.011
Warehouse	6 a.m.–10 p.m.	5 days/week	0.020	0.020	0.021	0.022	0.023
Warehouse	6 a.m.–10 p.m.	7 days/week	0.016	0.017	0.017	0.018	0.018
Warehouse	24 hours/day	5 days/week	0.013	0.013	0.013	0.013	0.013
Warehouse	24 hours/day	7 days/week	0.011	0.011	0.011	0.011	0.011

Table D-5. Analysis Results—Average Change in Site Electricity Intensity for Bosch DCMG Compared to AC Baseline (kWh/ft^2/year)

Building Type	Operating Schedule		*Change in Site Electricity Intensity by Case*				
			100%	125%	150%	200%	250%
Refrigerated Warehouse	6 a.m.–10 p.m.	5 days/week	0.04	0.11	−0.14	−0.16	−0.18
Refrigerated Warehouse	6 a.m.–10 p.m.	7 days/week	−0.18	−0.19	−0.23	−0.23	−0.25
Refrigerated Warehouse	24 hours/day	5 days/week	0.02	0.09	−0.16	−0.18	−0.21
Refrigerated Warehouse	24 hours/day	7 days/week	−0.30	−0.31	−0.34	−0.35	−0.36
Retail	8 a.m.–8 p.m.	7 days/week	−0.41	−0.40	−0.45	−0.47	−0.49
Retail	24 hours/day	7 days/week	−0.33	−0.32	−0.37	−0.39	−0.41
Supermarket	6 a.m.–10 p.m.	7 days/week	−0.73	−0.72	−0.78	−0.79	−0.81
Supermarket	24 hours/day	7 days/week	−1.02	−1.01	−1.07	−1.09	−1.11
Warehouse	6 a.m.–10 p.m.	5 days/week	0.04	0.11	−0.13	−0.16	−0.18
Warehouse	6 a.m.–10 p.m.	7 days/week	−0.18	−0.19	−0.22	−0.23	−0.24
Warehouse	24 hours/day	5 days/week	0.03	0.10	−0.15	−0.17	−0.19
Warehouse	24 hours/day	7 days/week	−0.25	−0.26	−0.29	−0.30	−0.31

Table D-6. Analysis Results—Average Change in Site Natural Gas Intensity for Bosch DCMG Compared to AC Baseline (kBtu/ft^2/year)

Building Type	Operating Schedule		*Change in Site Natural Gas Intensity by Case*				
			100%	125%	150%	200%	250%
Refrigerated Warehouse	6 a.m.–10 p.m.	5 days/week	0.27	0.27	0.27	0.27	0.27
Refrigerated Warehouse	6 a.m.–10 p.m.	7 days/week	0.34	0.34	0.34	0.34	0.34
Refrigerated Warehouse	24 hours/day	5 days/week	0.38	0.38	0.38	0.38	0.38
Refrigerated Warehouse	24 hours/day	7 days/week	0.67	0.67	0.67	0.67	0.67
Retail	8 a.m.–8 p.m.	7 days/week	0.51	0.51	0.51	0.51	0.51
Retail	24 hours/day	7 days/week	0.57	0.57	0.57	0.57	0.57
Supermarket	6 a.m.–10 p.m.	7 days/week	1.29	1.29	1.29	1.29	1.29
Supermarket	24 hours/day	7 days/week	2.07	2.07	2.07	2.07	2.07
Warehouse	6 a.m.–10 p.m.	5 days/week	0.19	0.19	0.19	0.19	0.19
Warehouse	6 a.m.–10 p.m.	7 days/week	0.24	0.24	0.24	0.24	0.24
Warehouse	24 hours/day	5 days/week	0.26	0.26	0.26	0.26	0.26
Warehouse	24 hours/day	7 days/week	0.44	0.44	0.44	0.44	0.44

Table D-7. Analysis Results—Average Change in Site Total Energy Intensity for Bosch DCMG Compared to AC Baseline (kBtu/ft^2/year)

Building Type	Operating Schedule		*Change in Site Total Energy Intensity by Case*				
			100%	125%	150%	200%	250%
Refrigerated Warehouse	6 a.m.–10 p.m.	5 days/week	0.41	0.65	−0.19	−0.27	−0.35
Refrigerated Warehouse	6 a.m.–10 p.m.	7 days/week	−0.28	−0.32	−0.43	−0.46	−0.50
Refrigerated Warehouse	24 hours/day	5 days/week	0.44	0.68	−0.16	−0.24	−0.32
Refrigerated Warehouse	24 hours/day	7 days/week	−0.35	−0.39	−0.50	−0.53	−0.57
Retail	8 a.m.–8 p.m.	7 days/week	−0.87	−0.85	−1.03	−1.10	−1.15
Retail	24 hours/day	7 days/week	−0.55	−0.53	−0.70	−0.77	−0.83
Supermarket	6 a.m.–10 p.m.	7 days/week	−1.19	−1.15	−1.35	−1.42	−1.48
Supermarket	24 hours/day	7 days/week	−1.41	−1.37	−1.58	−1.64	−1.71
Warehouse	6 a.m.–10 p.m.	5 days/week	0.34	0.58	−0.26	−0.34	−0.42
Warehouse	6 a.m.–10 p.m.	7 days/week	−0.36	−0.40	−0.51	−0.53	−0.57
Warehouse	24 hours/day	5 days/week	0.36	0.60	−0.24	−0.32	−0.40
Warehouse	24 hours/day	7 days/week	−0.41	−0.45	−0.56	−0.58	−0.62

Table D-8. Analysis Results—Average Change in January Peak Electricity Demand for Bosch DCMG Compared to AC Baseline (W/ft^2)

Building Type	Operating Schedule		*Change in Peak Electricity Demand by Case*				
			100%	125%	150%	200%	250%
Refrigerated Warehouse	6 a.m.–10 p.m.	5 days/week	−0.020	−0.021	−0.026	−0.028	−0.030
Refrigerated Warehouse	6 a.m.–10 p.m.	7 days/week	−0.023	−0.025	−0.029	−0.030	−0.033
Refrigerated Warehouse	24 hours/day	5 days/week	−0.017	−0.017	−0.017	−0.017	−0.017
Refrigerated Warehouse	24 hours/day	7 days/week	−0.028	−0.028	−0.029	−0.028	−0.028
Retail	8 a.m.–8 p.m.	7 days/week	−0.055	−0.055	−0.055	−0.055	−0.056
Retail	24 hours/day	7 days/week	−0.025	−0.025	−0.026	−0.026	−0.026
Supermarket	6 a.m.–10 p.m.	7 days/week	−0.084	−0.084	−0.084	−0.084	−0.084
Supermarket	24 hours/day	7 days/week	−0.094	−0.094	−0.094	−0.094	−0.094
Warehouse	6 a.m.–10 p.m.	5 days/week	−0.014	−0.015	−0.014	−0.014	−0.014
Warehouse	6 a.m.–10 p.m.	7 days/week	−0.016	−0.016	−0.015	−0.015	−0.015
Warehouse	24 hours/day	5 days/week	−0.015	−0.015	−0.014	−0.014	−0.014
Warehouse	24 hours/day	7 days/week	−0.022	−0.022	−0.021	−0.021	−0.021

Table D-9. Analysis Results—Average Change in April Peak Electricity Demand for Bosch DCMG Compared to AC Baseline (W/ft^2)

Building Type	Operating Schedule		*Change in Peak Electricity Demand by Case*				
			100%	125%	150%	200%	250%
Refrigerated Warehouse	6 a.m.–10 p.m.	5 days/week	−0.028	−0.028	−0.033	−0.033	−0.033
Refrigerated Warehouse	6 a.m.–10 p.m.	7 days/week	−0.035	−0.036	−0.036	−0.036	−0.036
Refrigerated Warehouse	24 hours/day	5 days/week	−0.029	−0.029	−0.030	−0.030	−0.029
Refrigerated Warehouse	24 hours/day	7 days/week	−0.043	−0.044	−0.043	−0.042	−0.042
Retail	8 a.m.–8 p.m.	7 days/week	−0.100	−0.107	−0.118	−0.128	−0.136
Retail	24 hours/day	7 days/week	−0.045	−0.045	−0.046	−0.047	−0.047
Supermarket	6 a.m.–10 p.m.	7 days/week	−0.112	−0.113	−0.115	−0.117	−0.118
Supermarket	24 hours/day	7 days/week	−0.128	−0.129	−0.130	−0.131	−0.131
Warehouse	6 a.m.–10 p.m.	5 days/week	−0.016	−0.016	−0.016	−0.016	−0.016
Warehouse	6 a.m.–10 p.m.	7 days/week	−0.018	−0.018	−0.018	−0.018	−0.017
Warehouse	24 hours/day	5 days/week	−0.016	−0.016	−0.016	−0.016	−0.015
Warehouse	24 hours/day	7 days/week	−0.023	−0.023	−0.023	−0.023	−0.023

Table D-10. Analysis Results—Average Change in July Peak Electricity Demand for Bosch DCMG Compared to AC Baseline (W/ft^2)

Building Type	Operating Schedule		*Change in Peak Electricity Demand by Case*				
			100%	125%	150%	200%	250%
Refrigerated Warehouse	6 a.m.–10 p.m.	5 days/week	−0.040	−0.043	−0.045	−0.044	−0.044
Refrigerated Warehouse	6 a.m.–10 p.m.	7 days/week	−0.045	−0.049	−0.049	−0.049	−0.049
Refrigerated Warehouse	24 hours/day	5 days/week	−0.046	−0.049	−0.049	−0.048	−0.048
Refrigerated Warehouse	24 hours/day	7 days/week	−0.062	−0.066	−0.066	−0.065	−0.064
Retail	8 a.m.–8 p.m.	7 days/week	−0.140	−0.146	−0.156	−0.167	−0.178
Retail	24 hours/day	7 days/week	−0.056	−0.057	−0.059	−0.062	−0.064
Supermarket	6 a.m.–10 p.m.	7 days/week	−0.137	−0.139	−0.143	−0.147	−0.151
Supermarket	24 hours/day	7 days/week	−0.153	−0.156	−0.160	−0.163	−0.167
Warehouse	6 a.m.–10 p.m.	5 days/week	−0.040	−0.041	−0.044	−0.045	−0.046
Warehouse	6 a.m.–10 p.m.	7 days/week	−0.040	−0.042	−0.045	−0.046	−0.047
Warehouse	24 hours/day	5 days/week	−0.025	−0.025	−0.024	−0.024	−0.023
Warehouse	24 hours/day	7 days/week	−0.035	−0.034	−0.034	−0.033	−0.033

Table D-11. Analysis Results—Average Change in October Peak Electricity Demand for Bosch DCMG Compared to AC Baseline (W/ft^2)

Building Type	Operating Schedule		*Change in Peak Electricity Demand by Case*				
			100%	125%	150%	200%	250%
Refrigerated Warehouse	6 a.m.–10 p.m.	5 days/week	−0.027	−0.028	−0.033	−0.034	−0.034
Refrigerated Warehouse	6 a.m.–10 p.m.	7 days/week	−0.035	−0.037	−0.037	−0.037	−0.038
Refrigerated Warehouse	24 hours/day	5 days/week	−0.028	−0.028	−0.029	−0.029	−0.028
Refrigerated Warehouse	24 hours/day	7 days/week	−0.043	−0.044	−0.042	−0.042	−0.040
Retail	8 a.m.–8 p.m.	7 days/week	−0.085	−0.086	−0.090	−0.093	−0.097
Retail	24 hours/day	7 days/week	−0.043	−0.044	−0.044	−0.044	−0.045
Supermarket	6 a.m.–10 p.m.	7 days/week	−0.104	−0.104	−0.105	−0.106	−0.107
Supermarket	24 hours/day	7 days/week	−0.118	−0.119	−0.120	−0.121	−0.122
Warehouse	6 a.m.–10 p.m.	5 days/week	−0.016	−0.016	−0.016	−0.016	−0.016
Warehouse	6 a.m.–10 p.m.	7 days/week	−0.018	−0.018	−0.018	−0.018	−0.017
Warehouse	24 hours/day	5 days/week	−0.016	−0.017	−0.017	−0.016	−0.016
Warehouse	24 hours/day	7 days/week	−0.024	−0.024	−0.024	−0.024	−0.023